
LN's

Endless

Chemistry Notes



Art:

Kira, by @Ekkoberry

C12. CHEMICAL DATA AND STANDARDS	616
12.1. Practical Chemistry in the Laboratory	616
12.2. Chemical Data	621
12.3. General Nomenclature of Organic Compounds	631
C13. PHYSICAL CHEMISTRY	633
13.1. Atomic Structure and Quantum Chemistry	633
13.2. Crystallography and Solid State Chemistry	651
13.3. Theory of Kinetics, Energetics and Thermodynamics	670
13.4. Solutions and Heterogeneous Equilibria	683
13.5. Electrochemistry	697
13.6. Acid-Base Chemistry	721
C14. SURFACE AND PARTICLE CHEMISTRY	728
14.1. Catalysis	728
14.2. Separation Processes and Chemical Engineering	732
14.3. Colloids and Nanoparticle Chemistry	744
C15. INORGANIC AND ENVIRONMENTAL CHEMISTRY	754
15.1. Metallurgy	754
15.2. Earth Science, Geochemistry and Physical Geography	762
15.3. Reactions of Inorganic Compounds	775
15.4. Periodicity Trends	786
15.5. Coordination and Organometallic Chemistry	788
C16. ORGANIC AND BIOCHEMISTRY	803
16.1. Bonding and Forces in Organic Molecules	803
16.2. Structure of Organic Molecules	813
16.3. Synthetic Organic Chemistry	818
16.4. Analytical Methods in Chemistry and Molecular Biology	842
16.5. Polymers and Biochemistry	858

C12. CHEMICAL DATA AND STANDARDS

12.1. Practical Chemistry in the Laboratory

12.1.1. Hazard Pictograms

GHS hazard symbols found on chemical substance containers include:



Toxic



Health Hazard



Flammable



Irritant



Oxidising Agent

Compressed
Gas

Explosive

Environmental
Hazard

Corrosive

Common symbols for other hazards include:



Biohazard



Radioactive

Non-ionising
Radiation

Electrocution



Lasers

Chemical
Weapon

Hot Surface



Forklifts



Trip Hazard

Explosive
AtmosphereEntrapment by
MachineryMagnetic
Fields

12.1.2. Risk Assessments

Regulations regarding workplace safety are location dependent. In the UK, the HSE (Health and Safety Executive) sets the regulations. The most important laws for substances are the **CoSHH** (Control of Substances Hazardous to Health) regulations.

Evaluating Risks: determine the extent to which a risk needs to be mitigated

		Severity of potential harm		
		Slightly harmful	Harmful	Extremely harmful
Likelihood of harm occurring	Highly unlikely	Trivial	Tolerable	Moderate
	Unlikely	Tolerable	Moderate	Substantial
	Likely	Moderate	Substantial	Intolerable

Mitigating Risks: the hierarchy of controls. From 'most effective' to 'least effective', consider, in order:

<p>1. Elimination Remove the hazard entirely by redesigning the activity or experiment</p>	<ul style="list-style-type: none"> Work at height eliminated for window cleaning by using long-handled cleaning equipment used from the ground
<p>2. Substitution Replace the hazard with a safer alternative</p>	<ul style="list-style-type: none"> Nanoparticles bought in paste form rather than powder to prevent exposure by inhalation Lower power of laser used Lower concentration of hazardous substance bought to reduce severity Less harmful pesticide used
<p>3. Engineering Controls Use of physical guards to separate people from the hazards</p>	<ul style="list-style-type: none"> Fixed guards for moving parts of machinery (lathes) Trip guards over cables on the floor, handrails and footplates on stairs Screens for lasers and radioactive substance use Remote operation (other room) for X-ray generators Fume cupboards, glove boxes and general ventilation Isolators for electrical safety Pressure relief valves on pressure vessels (to avoid explosion) Sprinklers in place to deal with fires (reduce consequences)
<p>4. Administrative Controls Use of regulations and training to change the way people work around the hazard</p>	<ul style="list-style-type: none"> Access to high-risk rooms or machinery restricted to people with training Standard operating/safe working procedure put in place Permit to work issued for high-risk work (e.g. on roofs) Emergency response plan in place (e.g. for spillages or fires) Validation protocols used for biological safety cabinets/autoclaves Maintenance, examination and testing of equipment in place to ensure all working to correct safety standards (e.g. fume cupboard testing) Exposure time restricted (e.g. work with noisy machinery)
<p>5. Personal Protective Equipment (PPE)</p>	<ul style="list-style-type: none"> Eye protection when using chemicals even in a fume cupboard, because splashes to the eye cannot be entirely ruled out Cotton lab coat with poppers (not buttons) and nitrile gloves when using chemicals – special gloves for use with hydrofluoric acid

12.1.3. Chemical Safety in Chemistry Laboratories

All chemicals have some degree of risk attached to their use. It is important that before any work is started a risk assessment is carried out.

Assessing Risk of Chemical Substances

All chemicals have a CAS number (e.g. acetone: #67-64-1), which can be searched to find its material safety data sheet (MSDS). The MSDS contains useful information for compiling a risk assessment, including sections **2) hazard precautionary statements** (including GHS pictograms, signal words 'Warning' or 'Danger', and H&P statements found online [here](#) and [here](#)), 4) first-aid measures, 5) fire-fighting measures, 6) accidental release measures, 8) occupational exposure limits, 9) physical and chemical properties, 10) stability/reactivity and compatibility, and 11) toxicological data including carcinogenicity and mutagenicity.

Control Measures in the Chemistry Lab

Best practices: always keep your work area(s) clean and tidy, clean up spills immediately, ensure all eyewash stations, emergency showers, fire extinguishers and exits are unobstructed and accessible, keep only materials you require for your work in your work area (everything else should be stored safely out of the way and not on the floor), any equipment that requires air flow or ventilation to prevent overheating should always be kept clear, handle glassware with caution, never eat or drink in the lab, do not apply cosmetics or touch your face, mouth or eyes, wear lab coat, safety glasses, long hair tied back, gloves, long trousers and enclosed shoes, avoid lone working, report near-misses and accidents to appropriate personnel immediately.

Fume cupboards: a partial containment enclosure designed to protect against airborne contaminants (chemical fumes, gases, chemical aerosols). The fume cupboard is ventilated by an induced flow of air through an adjustable working opening (the sash) which also offers the user some degree of mechanical protection against splashes of substances and flying particles.

DSEAR (Dangerous Substances and Explosive Atmosphere Regulations): risk assessments for solvents, paints, varnishes, flammable gases and LPG, dusts from machining, sanding, foodstuffs, pressurised gases and substances corrosive to metals. Ensure at least one element in the 'fire triangle' is eliminated: fuel, oxygen and heat.

Chemical storage and disposal: pay attention to shelf life, store in cupboards below head height, use drip trays, use vented caps, minimise exposure to heat/light, and check that existing waste disposal streams are suitable for each chemical used.

Emergencies: fire alarms, fire drills, carbon monoxide alarms, evacuation procedures, first-aid kits, spill kits, eye-wash stations, burn kits.

SOPs (Safe Operating Procedures): specialised protocols for particularly hazardous chemicals or activities e.g. hydrofluoric acid, piranha solution, fuming nitric acid.

12.1.4. Biological Safety in Biolabs

Biological agents are microorganisms (e.g. bacteria, viruses, moulds), cell cultures, or human endoparasites which may cause infection, allergy, toxicity or any other hazard to human health. Routes of infection can include ingestion, inhalation, instillation (eyes) or percutaneous (skin). Biohazards differ from chemical hazards in that there is no 'dose-response' relationship: even a tiny amount of contact can have serious consequences. Therefore, containment procedures are stricter when working with biological agents.

Biohazards are classed into the following hazard groups (1-4). An appropriate containment level (CL) for the biolab is required to handle such a hazard e.g. CL2 can handle groups 1 and 2.

1. Unlikely to cause disease to humans e.g. disabled *E. Coli*.
2. Potential to cause disease and spread, prophylaxis/treatment available e.g. *Streptococcus*.
3. Severe risk of disease and spreading, prophylaxis/treatment available e.g. Hepatitis B.
4. Severe risk of disease and spreading, prophylaxis/treatment **not** available e.g. Ebola.

Containment level	Cell line types	Facilities
CL1	<ul style="list-style-type: none"> well characterised, authenticated cell lines of human or primate origin low risk of endogenous infection with a biological agent presenting no apparent harm to laboratory tested for the most serious pathogens. 	<ul style="list-style-type: none"> impervious & resistant surfaces, easy to clean autoclave on site door closed during work observation window disinfection stations dedicated bins for contaminated solid waste sharps bins validated inactivation of liquid waste
CL2	<ul style="list-style-type: none"> finite or continuous cell lines/strains of human or primate origin not fully characterised or authenticated, except where there is a high risk of endogenous biological agents, e.g. blood-borne viruses. 	<ul style="list-style-type: none"> negative pressure if possible, microbiological safety cabinet (class II MSC with HEPA filter) access restricted side or back fastening lab coats, appropriate gloves, spill trays specified decontamination procedures control aerosol dissemination safe storage of biological agents

Higher CL biolabs (CL3, CL4) work with cell lines with endogenous biological agents or cells that have been deliberately infected, or primary cells from blood or lymphoid cells of human or simian origin, and have highly specialised working procedures.

Special facilities are required for working with live animals, which is prohibited entirely for great apes (human subjects are out of scope, requiring informed consent), and with restrictions for cats, dogs, fetuses and embryos. Ethical approval is required for working with human or animal tissue (surgical specimens or cadavers). Special risk assessments are required for working with genetically modified organisms (GMOs), where the recipient organism, inserted gene, donor and vector must be documented.

12.1.5. Common Equipment used in Chemistry

Glassware:

- **Small solutions:** test tube, boiling tube, Thiele tube
- **Large solutions:** beaker, graduated cylinder, conical/Erlenmeyer flask, volumetric flask, round-bottomed flask, Florence flask, Kjeldahl flask, pear-shaped flask, retort flask, Schlenk flask, Straus flask, Buchner flask
- **Funnels:** separating funnel, dropping funnel, filter funnel, thistle funnel
- **Columns and condensers:** burette, Liebig condenser, Graham condenser, Friedrichs condenser, distilling column, Claisen flask, Soxhlet extractor, chromatography column
- **Transferring solutions:** pipette, micropipette, capillary tube/melting point tube, gas syringe, graduated pipette, volumetric pipette

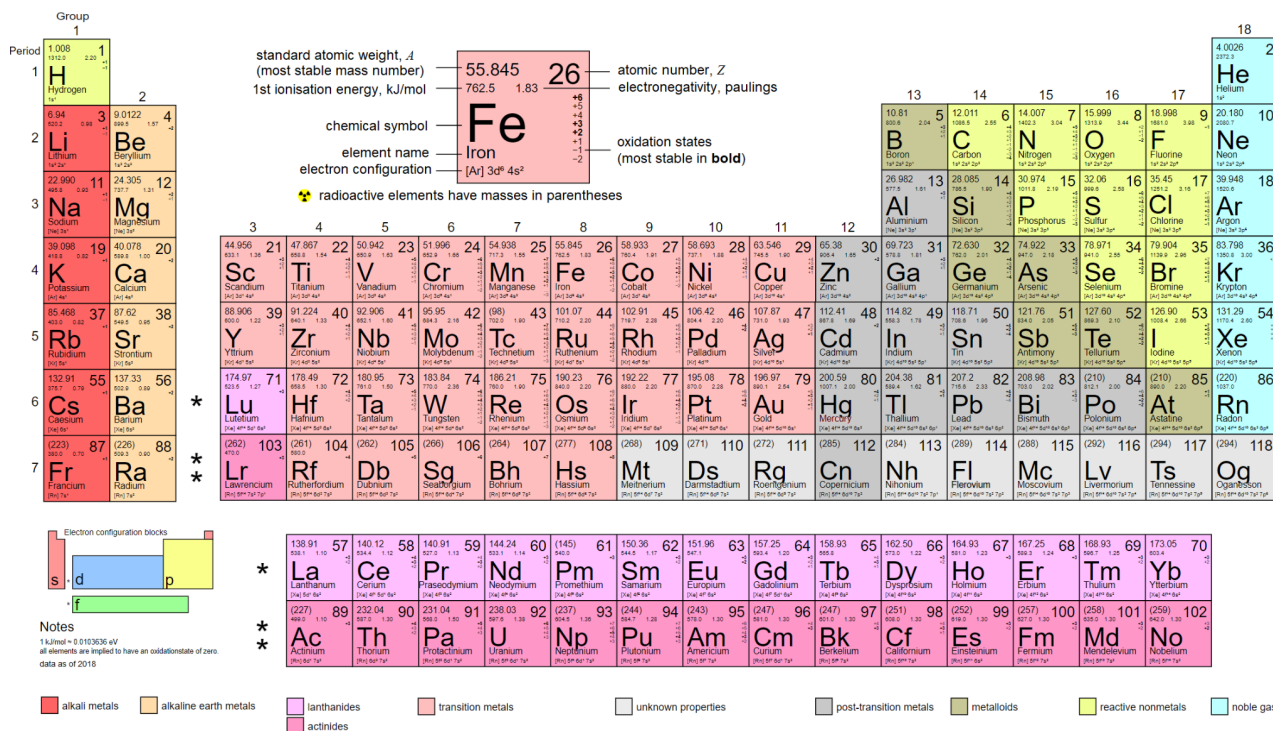
Apparatus:

- **Heating:** Bunsen burner, water bath
- **Holding:** retort stand (clamp, stand and boss), test tube rack

12.1.6. Common Experimental Procedures used in Chemistry

12.2. Chemical Data

12.2.1. The Periodic Table of Elements



Groupings and Classification of Elements

- Group 1 (1): Alkali Metals (Li, Na, K, Rb, Cs, Fr)
- Group 2 (2): Alkaline Earth Metals (Be, Mg, Ca, Sr, Ba, Ra)
- Groups (3)-(12): Transition Metals (excludes lanthanides and actinides)
- Group 5 (15): Pnictogens (N, P, As, Sb, Bi, Mc)
- Group 6 (16): Chalcogens (O, S, Se, Te, Po, Lv)
- Group 7 (17): Halogens (F, Cl, Br, I, At, Ts)
- Group 0 (18): Noble Gases (He, Ne, Ar, Kr, Xe, Rn, Og)

- Period 6, f-block: lanthanides
- Period 7, f-block: actinides
- Period 7, d/p-block: transactinides

- Platinoids (noble metals): Ru, Rh, Pd, Os, Ir, Pt
- Metalloids (semimetals): B, Si, Ge, As, Sb, Te, Po, At
- Poor metals: Al, Ga, In, Sn, Tl, Pb, Bi

12.2.2. Chemical Properties of Elements

Z		Electron Configuration	Atomic Radius (pm)	1st Ionisation Energy (kJ mol ⁻¹)	1st Electron Affinity (kJ mol ⁻¹)	Electronegativity (Paulings)
1	H	1s ¹	25	1312.0	72.769	3.04
2	He	1s ²	120	2372.3	-48	-
3	Li	[He] 2s ¹	145	520.2	59.632	2.17
4	Be	[He] 2s ²	105	899.5	-48	2.42
5	B	[He] 2s ² 2p ¹	85	800.6	26.989	3.04
6	C	[He] 2s ² 2p ²	70	1086.5	121.776	3.15
7	N	[He] 2s ² 2p ³	65	1402.3	-6.8	3.56
8	O	[He] 2s ² 2p ⁴	60	1313.9	140.976	3.78
9	F	[He] 2s ² 2p ⁵	50	1681.0	328.165	4.00
10	Ne	[He] 2s ² 2p ⁶	160	2080.7	-116	-
11	Na	[Ne] 3s ¹	180	495.8	52.867	2.15
12	Mg	[Ne] 3s ²	150	737.7	-40	2.39
13	Al	[Ne] 3s ² 3p ¹	125	577.5	41.762	2.52
14	Si	[Ne] 3s ² 3p ²	110	786.5	134.0684	2.82
15	P	[Ne] 3s ² 3p ³	100	1011.8	72.037	3.16
16	S	[Ne] 3s ² 3p ⁴	100	999.6	200.4101	3.44
17	Cl	[Ne] 3s ² 3p ⁵	100	1251.2	348.575	3.50
18	Ar	[Ne] 3s ² 3p ⁶	71	1520.6	-96	-
19	K	[Ar] 4s ¹	220	418.8	48.383	2.07
20	Ca	[Ar] 4s ²	180	589.8	2.37	2.20
21	Sc	[Ar] 4s ² 3d ¹	160	633.1	17.3076	2.35
22	Ti	[Ar] 4s ² 3d ²	140	658.8	7.289	2.23
23	V	[Ar] 4s ² 3d ³	135	650.9	50.911	2.08
24	Cr	[Ar] 4s ¹ 3d ⁵	140	652.9	65.217 2	2.12
25	Mn	[Ar] 4s ² 3d ⁵	140	717.3	-50	2.20
26	Fe	[Ar] 4s ² 3d ⁶	140	762.5	14.785	2.32
27	Co	[Ar] 4s ² 3d ⁷	135	760.4	63.8979	2.34
28	Ni	[Ar] 4s ² 3d ⁸	135	737.1	111.65	2.32
29	Cu	[Ar] 4s ¹ 3d ¹⁰	135	745.5	119.235	2.86
30	Zn	[Ar] 4s ² 3d ¹⁰	135	906.4	-58	2.26
31	Ga	[Ar] 4s ² 3d ¹⁰ 3p ¹	130	578.8	29.0581	2.43
32	Ge	[Ar] 4s ² 3d ¹⁰ 3p ²	125	762	118.9352	2.79
33	As	[Ar] 4s ² 3d ¹⁰ 3p ³	115	947.0	77.65	3.15
34	Se	[Ar] 4s ² 3d ¹⁰ 3p ⁴	115	941.0	194.9587	3.37
35	Br	[Ar] 4s ² 3d ¹⁰ 3p ⁵	115	1139.9	324.5369	3.45
36	Kr	[Ar] 4s ² 3d ¹⁰ 3p ⁶		1350.8	-96	-

Continued:

Z		Electron Configuration	Atomic Radius (pm)	1st Ionisation Energy (kJ mol ⁻¹)	1st Electron Affinity (kJ mol ⁻¹)	Electronegativity (Paulings)
37	Rb	[Kr] 5s ¹	235	403	46.884	2.07
38	Sr	[Kr] 5s ²	200	549.5	5.023	2.13
39	Y	[Kr] 5s ² 4d ¹	180	600	30.035	2.52
40	Zr	[Kr] 5s ² 4d ²	155	640.1	41.806	2.05
41	Nb	[Kr] 5s ¹ 4d ⁴	145	652.1	88.516	2.59
42	Mo	[Kr] 5s ¹ 4d ⁵	145	684.3	72.097	2.47
43	Tc	[Kr] 5s ² 4d ⁵	135	702	53	2.82
44	Ru	[Kr] 5s ¹ 4d ⁷	130	710.2	100.950	2.68
45	Rh	[Kr] 5s ¹ 4d ⁸	135	719.7	110.27	2.65
46	Pd	[Kr] 4d ¹⁰	140	804.4	54.24	2.70
47	Ag	[Kr] 5s ¹ 4d ¹⁰	160	731	125.862	2.88
48	Cd	[Kr] 5s ² 4d ¹⁰	155	867.8	-68	2.36
49	In	[Kr] 5s ² 4d ¹⁰ 4p ¹	155	558.3	37.043	2.29
50	Sn	[Kr] 5s ² 4d ¹⁰ 4p ²	145	708.6	107.298 4	2.68
51	Sb	[Kr] 5s ² 4d ¹⁰ 4p ³	145	834	101.059	3.05
52	Te	[Kr] 5s ² 4d ¹⁰ 4p ⁴	140	869.3	190.161	3.14
53	I	[Kr] 5s ² 4d ¹⁰ 4p ⁵	140	1008.4	295.1531	3.20
54	Xe	[Kr] 5s ² 4d ¹⁰ 4p ⁶		1170.4	-77	-
55	Cs	[Xe] 6s ¹	260	375.7	45.505	1.97
56	Ba	[Xe] 6s ²	215	502.9	13.954	2.02
57	La	[Xe] 6s ² 5d ¹	195	538.1	53.795	2.49
58	Ce	[Xe] 6s ² 5d ¹ 4f ¹	185	534.4	57.9067	2.61
59	Pr	[Xe] 6s ² 4f ³	185	527	10.539	2.24
60	Nd	[Xe] 6s ² 4f ⁴	185	533.1	9.406	2.11
61	Pm	[Xe] 6s ² 4f ⁵	185	540	12.45	2.24
62	Sm	[Xe] 6s ² 4f ⁶	185	544.5	15.63	1.90
63	Eu	[Xe] 6s ² 4f ⁷	185	547.1	11.2	1.81
64	Gd	[Xe] 6s ² 5d ¹ 4f ⁷	180	593.4	20.5	2.40
65	Tb	[Xe] 6s ² 4f ⁹	175	565.8	12.670	2.29
66	Dy	[Xe] 6s ² 4f ¹⁰	175	573	1.45	2.07
67	Ho	[Xe] 6s ² 4f ¹¹	175	581	32.61	2.12
68	Er	[Xe] 6s ² 4f ¹²	175	589.3	30.10	2.02
69	Tm	[Xe] 6s ² 4f ¹³	175	596.7	99	2.03
70	Yb	[Xe] 6s ² 4f ¹⁴	175	603.4	-1.93	1.78
71	Lu	[Xe] 6s ² 4f ¹⁴ 5d ¹	175	523.5	23.04	2.68

Continued:

Z		Electron Configuration	Atomic Radius (pm)	1st Ionisation Energy (kJ mol ⁻¹)	1st Electron Affinity (kJ mol ⁻¹)	Electronegativity (Paulings)
72	Hf	[Xe] 6s ² 4f ¹⁴ 5d ²	155	658.5	17.18	2.01
73	Ta	[Xe] 6s ² 4f ¹⁴ 5d ³	145	761	31.7301	2.32
74	W	[Xe] 6s ² 4f ¹⁴ 5d ⁴	135	770	78.76	2.42
75	Re	[Xe] 6s ² 4f ¹⁴ 5d ⁵	135	760	5.8273	2.59
76	Os	[Xe] 6s ² 4f ¹⁴ 5d ⁶	130	840	104.0	2.72
77	Ir	[Xe] 6s ² 4f ¹⁴ 5d ⁷	135	880	150.9	2.79
78	Pt	[Xe] 6s ¹ 4f ¹⁴ 5d ⁹	135	870	205.041	2.98
79	Au	[Xe] 6s ¹ 4f ¹⁴ 5d ¹⁰	135	890.1	222.747	2.81
80	Hg	[Xe] 6s ² 4f ¹⁴ 5d ¹⁰	150	1007.1	-48	2.92
81	Tl	[Xe] 6s ² 4f ¹⁴ 5d ¹⁰ 6p ¹	190	589.4	30.8804	2.26
82	Pb	[Xe] 6s ² 4f ¹⁴ 5d ¹⁰ 6p ²	180	715.6	34.4183	2.62
83	Bi	[Xe] 6s ² 4f ¹⁴ 5d ¹⁰ 6p ³	160	703	90.924	2.69
84	Po	[Xe] 6s ² 4f ¹⁴ 5d ¹⁰ 6p ⁴	190	812.1	136	2.85
85	At	[Xe] 6s ² 4f ¹⁴ 5d ¹⁰ 6p ⁵	202	899	233.087	3.04
86	Rn	[Xe] 6s ² 4f ¹⁴ 5d ¹⁰ 6p ⁶	200	1037	-68	-
87	Fr	[Rn] 7s ¹	270	393	46.89	2.01
88	Ra	[Rn] 7s ²	215	509.3	9.648 5	2.15
89	Ac	[Rn] 7s ² 6d ¹	195	499	33.77	2.22
90	Th	[Rn] 7s ² 6d ²	180	587	58.633	2.62
91	Pa	[Rn] 7s ² 6d ¹ 5f ²	180	568	53.03	2.33
92	U	[Rn] 7s ² 6d ¹ 5f ³	175	597.6	30.390	2.45
93	Np	[Rn] 7s ² 6d ¹ 5f ⁴	175	604.5	45.85	2.35
94	Pu	[Rn] 7s ² 5f ⁶	175	584.7	-48.33	2.22
95	Am	[Rn] 7s ² 5f ⁷	175	578	9.93	2.28
96	Cm	[Rn] 7s ² 6d ¹ 5f ⁷	176	581	27.17	2.31
97	Bk	[Rn] 7s ² 5f ⁹		598	-165.24	2.08
98	Cf	[Rn] 7s ² 5f ¹⁰		608	-97.31	2.18
99	Es	[Rn] 7s ² 5f ¹¹		619	-28.60	2.29
100	Fm	[Rn] 7s ² 5f ¹²		629	33.96	2.38
101	Md	[Rn] 7s ² 5f ¹³		636	93.91	2.47
102	No	[Rn] 7s ² 5f ¹⁴		639	-223.22	2.06
103	Lr	[Rn] 7s ² 5f ¹⁴ 7p ¹		479	-30.04	2.10

Properties of transactinide elements are not well established and are primarily theoretical.

12.2.3. Bond Enthalpy and Bond Length Data

Bond enthalpies (energies) E [kJ mol^{-1}] and bond lengths L [$\text{pm} = 0.001 \text{ nm}$] are given. Values are averaged over a large number of chemical compounds.

Hydrogen Boron Carbon Metalloids N, P, As, Sb O, S, Se Halogens Noble Gases

Bond	E	L	Bond	E	L	Bond	E	L	Bond	E	L	Bond	E	L
H-H	432	74	C-C	346	154	Si-Si	222	233	N-N	167	145	O-O	142	148
H-B	389	119	C=C	602	134	Si-N	355		N=N	418	125	O=O	494	121
H-C	411	109	C≡C	835	120	Si-O	452	163	N≡N	942	110	O-F	190	142
H-Si	318	148	C-Si	318	185	Si-S	293	200	N-O	201	140	S=O	522	143
H-Ge	288	153	C-Ge	238	195	Si-F	565	160	N=O	607	121	S-S (S_8)	226	205
H-Sn	251	170	C-Sn	192	216	Si-Cl	381	202	N-F	283	136	S=S	425	149
H-N	386	101	C-Pb	130	230	Si-Br	310	215	N-Cl	313	175	S-F	284	156
H-P	322	144	C-N	305	147	Si-I	234	243	P-P	201	221	S-Cl	255	207
H-As	247	152	C=N	615	129	Ge-Ge	188	241	P-O	335	163	Se-Se	172	
H-O	459	96	C≡N	887	116	Ge-N	257		P=O	544	150	Se=Se	272	215
H-S	363	134	C-P	264	184	Ge-F	470	168	P=S	335	186	F-F	155	142
H-Se	276	146	C-O	358	143	Ge-Cl	349	210	P-F	490	154	Cl-Cl	240	199
H-Te	238	170	C=O	799	120	Ge-Br	276	230	P-Cl	326	203	Br-Br	190	228
H-F	565	92	C≡O	1072	113	Ge-I	212		P-Br	264		I-I	148	267
H-Cl	428	127	C-B	356	160	Sn-F	414		P-I	184		At-At	116	
H-Br	362	141	C-S	272	182	Sn-Cl	323	233	As-As	146	243	I-O	201	
H-I	295	161	C=S	573	160	Sn-Br	273	250	As-O	301	178	I-F	273	191
B-B	293		C-F	485	135	Sn-I	205	270	As-F	484	171	I-Cl	208	232
B-O	536		C-Cl	327	177	Pb-F	331		As-Cl	322	216	I-Br	175	
B-F	613		C-Br	285	194	Pb-Cl	243	242	As-Br	458	233	Kr-F (KrF_2)	50	190
B-Cl	456	175	C-I	240	228	Pb-Br	201		As-I	200	254	Xe-O	84	175
B-Br	377					Pb-I	142	279	Sb-Sb	121		Xe-F	130	195
B-B	293								Sb-F	440				
									Sb-Cl (SbCl_5)	248				
									Sb-Cl (SbCl_3)	315	232			

12.2.4. Thermochemical Data

Standard Enthalpy of Formation and Standard Entropy

($\Delta_f H^\circ$ [kJ mol⁻¹]: standard enthalpy of formation, S° [J mol⁻¹ K⁻¹]: standard entropy)

Solids				Solids			
Substance	Formula	$\Delta_f H^\circ$	S°	Substance	Formula	$\Delta_f H^\circ$	S°
carbon (diamond)	C (s)	1.90	2.4	potassium	K (s)	0	64.7
carbon (graphite)	C (s)	0	5.7	sodium chloride	NaCl (s)	-411.1	72.1
polystyrene*	(CH ₂) _n (s)	-28.5	25	potassium chloride	KCl (s)	-436.7	82.6
lithium fluoride	LiF (s)	-146.2	35.7	iodine	I ₂ (s)	0	116.1
silicon dioxide	SiO ₂ (s)	-911	41.5	glucose	C ₆ H ₁₂ O ₆ (s)	-1273.3	209.2
calcium	Ca (s)	0	41.6	xenon hexafluoride	XeF ₆ (s)	-294	210.4
sodium	Na (s)	0	51.5	sucrose	C ₁₂ H ₂₂ O ₁₁ (s)	-2221.2	392.4
magnesium fluoride	MgF ₂ (s)	-1124.2	57.2				
Liquids				Liquids			
Substance	Formula	$\Delta_f H^\circ$	S°	Substance	Formula	$\Delta_f H^\circ$	S°
water	H ₂ O (l)	-285.8	70.0	ethanoyl chloride	CH ₃ COCl (l)	-272	200.8
mercury	Hg (l)	0	75.9	cyclohexane	C ₆ H ₁₂ (l)	-157.7	204.0
hydrogen peroxide	H ₂ O ₂ (l)	-187.8	109.6	carbon tetrachloride	CCl ₄ (l)	-95.6	214.4
methanol	CH ₃ OH (l)	-238.4	127.2	silicon tetrachloride	SiCl ₄ (l)	-687.0	239.7
bromine	Br ₂ (l)	0	152.2	sulfur trioxide	SO ₃ (l)	-395.8	256.8
ethanoic acid	CH ₃ COOH (l)	-483.5	158.0	<i>n</i> -hexane	C ₆ H ₁₄ (l)	-198.7	296.1
ethanol	C ₂ H ₅ OH (l)	-276.2	159.9	isooctane**	C ₈ H ₁₈ (l)	-259.3	328.0
benzene	C ₆ H ₆ (l)	49.0	173.3	<i>n</i> -heptane	C ₇ H ₁₆ (l)	-224.4	328.6
Gases				Gases			
Substance	Formula	$\Delta_f H^\circ$	S°	Substance	Formula	$\Delta_f H^\circ$	S°
helium	He (g)	0	126.2	phosphine	PH ₃ (g)	5	210
hydrogen	H ₂ (g)	0	130.7	nitric oxide	NO (g)	90.3	210.8
hydrogen chloride	HCl (g)	-92.3	186.9	carbon dioxide	CO ₂ (g)	-393.5	213.8
methane	CH ₄ (g)	-74.9	188.7	ethene	C ₂ H ₄ (g)	52.5	219.3
water	H ₂ O (g)	-241.8	188.8	chlorine	Cl ₂ (g)	0	223.1
nitrogen	N ₂ (g)	0	191.6	ethane	C ₂ H ₆ (g)	-84.0	229.6
ammonia	NH ₃ (g)	-45.9	192.8	sulfur dioxide	SO ₂ (g)	-296.8	248.2
carbon monoxide	CO (g)	-110.5	197.7	iodine	I ₂ (g)	62.4	260.7
fluorine	F ₂ (g)	0	202.8	propane	C ₃ H ₈ (g)	-104.7	269.9
oxygen	O ₂ (g)	0	205.2	butane	C ₄ H ₁₀ (g)	-125.6	310.2

* polystyrene: value per (CH₂) monomer. $\Delta_f H^\circ$ varies up to $\pm 2\%$ due to crystallinity (HDPE has the slightly more exothermic $\Delta_f H^\circ$).

** isooctane = 2,2,4-trimethylpentane.

Standard Enthalpy of Combustion

($\Delta_c H^\ominus$ [kJ mol⁻¹]: standard enthalpy of combustion, per mole of fuel, dry basis)

Fuel	Combusted Product	$\Delta_c H^\ominus$ [kJ mol ⁻¹]
hydrogen	H ₂ O (l)	-285.8
carbon monoxide	CO ₂ (g)	-283.0
carbon (graphite)	CO ₂ (g)	-292.5
sulfur	SO ₂ (g)	-296.8
magnesium	MgO (s)	-601.6
polyethylene*	n CO ₂ (g) + n H ₂ O (l)	-651
methanol	CO ₂ (g) + 2 H ₂ O (l)	-726.1
methane	CO ₂ (g) + 2 H ₂ O (l)	-890.7
acetylene	2 CO ₂ (g) + H ₂ O (l)	-1301.1
ethanol	CO ₂ (g) + 3 H ₂ O (l)	-1366.8
ethene	2 CO ₂ (g) + 2 H ₂ O (l)	-1411.2
ethane	2 CO ₂ (g) + 3 H ₂ O (l)	-1560.7
glucose	6 CO ₂ (g) + 6 H ₂ O (l)	-2840
phosphorus (red)	P ₄ O ₁₀ (s)	-2967
phosphorus (white)	P ₄ O ₁₀ (s)	-2984
benzene	6 CO ₂ (g) + 3 H ₂ O (l)	-3267
trinitrotoluene	7 CO ₂ (g) + 5/2 H ₂ O (l) + 3/2 N ₂ (g)	-3406
cyclohexane	6 CO ₂ (g) + 6 H ₂ O (l)	-3930
isooctane	8 CO ₂ (g) + 9 H ₂ O (l)	-5461

* polystyrene: value per (CH₂) monomer. $\Delta_c H^\ominus$ varies up to $\pm 0.1\%$ due to crystallinity (LDPE has the slightly more exothermic $\Delta_c H^\ominus$).

Phase Change Enthalpy and Entropy

(T_m [K]: melting point or freezing point,

T_b [K]: boiling point,

$\Delta_{fus}H^\ominus$ [kJ mol⁻¹]: molar latent heat of fusion,

$\Delta_{vap}H^\ominus$ [kJ mol⁻¹]: molar latent heat of vaporisation,

$\Delta_{fus}S^\ominus$ [J mol⁻¹ K⁻¹]: molar entropy change of fusion,

$\Delta_{vap}S^\ominus$ [J mol⁻¹ K⁻¹]: molar entropy change of vaporisation)

Substance	Formula	T_m	T_b	$\Delta_{fus}H^\ominus$	$\Delta_{vap}H^\ominus$	$\Delta_{fus}S^\ominus$	$\Delta_{vap}S^\ominus$
water	H ₂ O	273.2	373.2	6.01	40.68	22.0	118.89
ethanol	C ₂ H ₅ OH	159.1	351.5	4.9	42.3	31	109.67
ammonia	NH ₃	195.3	239.7	5.65	23.35	29.83	97.41
propene	C ₃ H ₆	88.0	225.6	3.0	18.4	34.2	81.7
aluminium	Al	933.5	2473	8.66	307.6	9.28	124.4
xenon hexafluoride	XeF ₆	322.4	348.8	5.74	47.75	17.8	136.9

$$\text{Specific latent heat of phase change, } L \text{ [J g}^{-1}\text{]} = \frac{\text{Molar latent heat } \Delta H^\ominus = T \Delta S^\ominus \text{ [J mol}^{-1}\text{]}}{\text{Molar mass } M_r \text{ [g mol}^{-1}\text{]}}$$

'Trouton's Rule': $\Delta_{vap}S^\ominus$ is typically 85-88 J K⁻¹ mol⁻¹ for a wide range of liquids.

Hydrogen-bonded liquids have higher values.

Enthalpy of Hydration of Ions: $X^+(g) \rightarrow X^+(aq)$ ($\Delta_{hyd}H^\ominus$ [kJ mol⁻¹]: standard enthalpy of hydration)

Cations:

Anions:

	$\Delta_{hyd}H^\ominus$		$\Delta_{hyd}H^\ominus$		$\Delta_{hyd}H^\ominus$		$\Delta_{hyd}H^\ominus$		$\Delta_{hyd}H^\ominus$		$\Delta_{hyd}H^\ominus$
H ⁺	-1091	Cu ⁺	-593	Ba ²⁺	-1309	Pt ²⁺	-2100	Y ³⁺	-4105	F ⁻	-524
Li ⁺	-520	Ag ⁺	-473	Ti ²⁺	1862	Zn ²⁺	-2047	Ga ³⁺	-4701	Cl ⁻	-378
Na ⁺	-406	Au ⁺	-615	Cr ²⁺	-1908	Cd ²⁺	-1809	In ³⁺	-4118	Br ⁻	-348
K ⁺	-320	NH ₄ ⁺	-307	Mn ²⁺	-1851	Hg ²⁺	-1829	Tl ³⁺	-4108	I ⁻	-308
Rb ⁺	-296	Be ²⁺	-2484	Fe ²⁺	-1950	Sn ²⁺	-1554	Cr ³⁺	-4563	NO ₃ ⁻	-314
Cs ⁺	-264	Mg ²⁺	-1926	Co ²⁺	-2010	Pb ²⁺	-1485	Fe ³⁺	-4429	OH ⁻	-460
In ⁺	-344	Ca ²⁺	-1579	Ni ²⁺	-2096	Al ³⁺	-4680	Co ³⁺	-4653		
Tl ⁺	-328	Sr ²⁺	-1446	Cu ²⁺	-2099	Sc ³⁺	-3930				

Enthalpy of Solution of Ionic Substances: $X_aY_b(s) \rightarrow aX^+(aq) + bY^-(aq)$ ($\Delta_{sol}H^\ominus$ [kJ mol⁻¹]: standard enthalpy of solution)

Cation	Anion				
	fluoride (F ⁻)	chloride (Cl ⁻)	bromide (Br ⁻)	iodide (I ⁻)	hydroxide (OH ⁻)
lithium (Li ⁺)	4.7	-37.0	-48.8	-63.3	-23.6
sodium (Na ⁺)	0.9	3.9	-0.6	-7.5	-44.5
potassium (K ⁺)	-17.7	17.2	19.9	20.3	-57.6
ammonium (NH ₄ ⁺)	-1.2	14.8	16.8	13.7	—
silver (Ag ⁺)	-22.5	65.5	84.4	112.2	—
magnesium (Mg ²⁺)	-17.7	-160.0	-185.6	-213.2	2.3
calcium (Ca ²⁺)	11.5	-81.3	-103.1	-119.7	-16.7

Cation	Anion			
	nitrate (NO ₃ ⁻)	acetate (CH ₃ COO ⁻)	carbonate (CO ₃ ²⁻)	sulfate (SO ₄ ²⁻)
lithium (Li ⁺)	-2.5	—	-18.2	-29.8
sodium (Na ⁺)	20.5	-17.3	-26.7	2.4
potassium (K ⁺)	34.9	-15.3	-30.9	23.8
ammonium (NH ₄ ⁺)	25.7	-2.4	—	6.6
silver (Ag ⁺)	22.6	—	22.6	17.8
magnesium (Mg ²⁺)	-90.9	—	-25.3	-91.2
calcium (Ca ²⁺)	-19.2	—	-13.1	-18.0

12.2.5. Higher Ionisation Energies (up to Krypton): $X^{(n-1)+}(\text{g}) \rightarrow X^{n+}(\text{g}) + e^{-}$ [kJ mol⁻¹]

Z	Atom	1st	2nd	3rd	4th	5th	6th	7th	8th
1	H	1312.0							
2	He	2372.3	5250.5						
3	Li	520.2	7298.1	11,815.0					
4	Be	899.5	1757.1	14,848.7	21,006.6				
5	B	800.6	2427.1	3659.7	25,025.8	32,826.7			
6	C	1086.5	2352.6	4620.5	6222.7	37,831	47,277.0		
7	N	1402.3	2856	4578.1	7475.0	9444.9	53,266.6	64,360	
8	O	1313.9	3388.3	5300.5	7469.2	10,989.5	13,326.5	71,330	84,078.0
9	F	1681.0	3374.2	6050.4	8407.7	11,022.7	15,164.1	17,868	92,038.1
10	Ne	2080.7	3952.3	6122	9371	12,177	15,238.90	19,999.0	23,069.5
11	Na	495.8	4562	6910.3	9543	13,354	16,613	20,117	25,496
12	Mg	737.7	1450.7	7732.7	10,542.5	13,630	18,020	21,711	25,661
13	Al	577.5	1816.7	2744.8	11,577	14,842	18,379	23,326	27,465
14	Si	786.5	1577.1	3231.6	4355.5	16,091	19,805	23,780	29,287
15	P	1011.8	1907	2914.1	4963.6	6273.9	21,267	25,431	29,872
16	S	999.6	2252	3357	4556	7004.3	8495.8	27,107	31,719
17	Cl	1251.2	2298	3822	5158.6	6542	9362	11,018	33,604
18	Ar	1520.6	2665.8	3931	5771	7238	8781	11,995	13,842
19	K	418.8	3052	4420	5877	7975	9590	11,343	14,944
20	Ca	589.8	1145.4	4912.4	6491	8153	10,496	12,270	14,206
21	Sc	633.1	1235.0	2388.6	7090.6	8843	10,679	13,310	15,250
22	Ti	658.8	1309.8	2652.5	4174.6	9581	11,533	13,590	16,440
23	V	650.9	1414	2830	4507	6298.7	12,363	14,530	16,730
24	Cr	652.9	1590.6	2987	4743	6702	8744.9	15,455	17,820
25	Mn	717.3	1509.0	3248	4940	6990	9220	11,500	18,770
26	Fe	762.5	1561.9	2957	5290	7240	9560	12,060	14,580
27	Co	760.4	1648	3232	4950	7670	9840	12,440	15,230
28	Ni	737.1	1753.0	3395	5300	7339	10,400	12,800	15,600
29	Cu	745.5	1957.9	3555	5536	7700	9900	13,400	16,000
30	Zn	906.4	1733.3	3833	5731	7970	10,400	12,900	16,800
31	Ga	578.8	1979.3	2963	6180				
32	Ge	762	1537.5	3302.1	4411	9020			
33	As	947.0	1798	2735	4837	6043	12,310		
34	Se	941.0	2045	2973.7	4144	6590	7880	14,990	
35	Br	1139.9	2103	3470	4560	5760	8550	9940	18,600
36	Kr	1350.8	2350.4	3565	5070	6240	7570	10,710	12,138

12.3. General Nomenclature of Organic Compounds

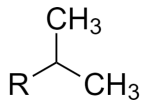
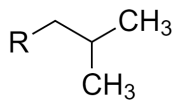
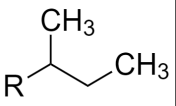
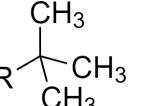
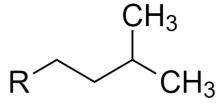
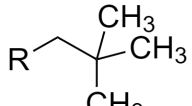
12.3.1. Alkane Chain Names

Prefixes for straight chains:

- Add -yl for an alkane substituent.
- Add -ane for the longest alkane chain with no other substituents.

<i>n</i>	1	2	3	4	5	6	7
	meth- (Me)	eth- (Et)	prop- (Pr)	but- (Bu)	pent-	hex-	hept-
<i>n</i>	8	9	10	11	12	13	14
	oct-	non-	dec-	undec-	dodec-	tridec-	tetradec-
<i>n</i>	15	16	17	18	19	20	21
	pentadec-	hexadec-	heptadec-	octadec-	nonadec-	icos-	unicos-

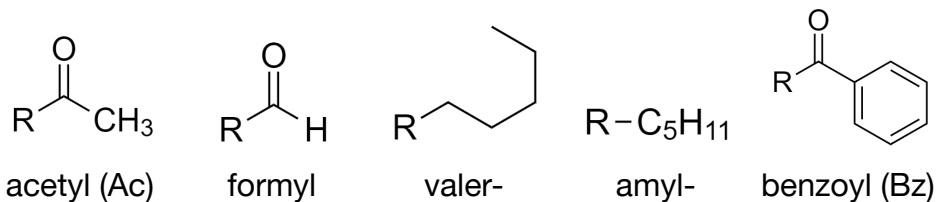
Common prefixes and IUPAC equivalents for branched chains:

					
isoprop- (iPr)	isobut- (iBu)	sec-but- (sBu)	tert-but- (tBu)	isopent-	neopent-
isoprop-	2-methylprop-	butan-2-	tert-but-	3-methylbut-	2,2-dimethylprop-

When ordering substituent names alphabetically,

- iso and cyclo prefixes **are** included.
- all other prefixes (*sec*, *tert*, *neo*, *di*, *tri*, *tetra*...) are **not** included; order by the base name.

Other unofficial names:



12.3.2. Functional Group Names and Priorities

Colour key: hydrocarbon, halogen, oxygen, nitrogen, sulfur, phosphorus

Naming key (top to bottom): functional group name; suffix (highest priority); prefix (lower priority)

Alkane -ane	Alkene -ene	Alkyne -yne	Arene -yl benzene phenyl-	Haloalkane halo-	Alcohol -ol hydroxy-	Aldehyde -al oxo-	Ketone -one oxo-	Carboxylic Acid -oic acid carboxy-	Acid Anhydride -oic anhydride alkyloxycarbonyl-
Acyl Halide -oyl halide chlorocarbonyl-	Ester -yl -oate alkoxycarbonyl-	Ether -oxy -ane -oxy -yl-	Epoxide -ene oxide oxiranyl-	Amine -amine amino-	Amide -amide carbamoyl-	Nitrate -nitrate nitrooxy-	Nitrite -nitrite nitrosooxy-	Nitrile -nitrile cyano-	Nitro nitro-
Nitroso nitroso-	Imine -imine alkylimino-	Imide -imide alkylcarbonyl-	Azide azido-	Cyanate -yl cyanate cyanato-	Isocyanate -yl isocyanate isocyanato-	Azo Compound azo-	Thiol -thiol mercapto-	Sulfide -yl sulfane alkylthio-	Disulfide disulfide alkyldisulfanyl-
Sulfoxide sulfoxide -ylsulfinyl-	Sulfone sulfone -ylsulfonyl-	Sulfinic Acid -sulfinic acid sulfino-	Sulfonic Acid -sulfonic acid sulfo-	Sulfonate -yl sulfonate oxysulfonyl-	Thiocyanate thiocyanate thiocyanato-	Isothiocyanate isothiocyanate isothiocyanato-	Thial thial thioformyl-	Thioketone thione thioyl-	Phosphine -yl phosphine phosphanyl
Oxime -one oxime hydroxyimino-	Hydrazone -ylidene hydrazine hydrazineylidene-	Acetal -oxy-	Hemiacetal -oxy -ol -oxy- hydroxy-	Ketal -oxy -alkoxy -oxy-	Hemiketal -oxy -ol -oxy- hydroxy-	Phosphonic Acid -phosphonic acid phospho-	Phosphinic Acid -phosphinic acid phosphino-	Phosphonate -yl phosphonate -oxyphosphonyl-	Sulfonamide N-alkyl -sulfonamide N- -sulfamoyl-

Naming priority order (not exhaustive):

(Highest priority: suffix) Carboxylic Acid > Sulfonic Acid > Ester > Acyl Halide > Amide > Nitrile > Aldehyde > Ketone > Alcohol > Thiol > Amine > Arene > Alkene > Alkyne > **Alkane** > Haloalkane > Ether > Azide > Nitro (Lowest priority: prefix)

C13. PHYSICAL CHEMISTRY

13.1. Atomic Structure and Quantum Chemistry

13.1.1. History of Molecular Theory and Atomic Theory

- In ~450 BC (Ancient Greece), Empedocles claimed all matter was composed of four **fundamental elements** (earth, fire, air, water) as continuous substances, as well as a fifth element permeating the space outside of Earth (quintessence; the luminiferous aether). There were also similar ideas in ancient China and India regarding fundamental elements.
- In ~400 BC, Democritus proposed '**atomism**', the concept that every substance is made of indivisible parts ('atomos'). The concept of the aether was retained, passed on by Aristotle. Atomism was developed further in ~300 BC by Epicurus. In ~50 BC (Ancient Rome), Lucretius brought back atomism. After the fall of the Roman Empire, Western thought on matter regressed and did not develop in any significant way until the late Renaissance.

During the Islamic Golden Age, alchemy (mysticism and proto-chemistry) was developed, with the fundamental 'principles' including sulfur, mercury and salt. Alchemy was considered more an art than a science, and was widely practised throughout Asia and spread to Europe in the late Middle Ages under scholasticism. The majority of thought in these times concerned metaphysics (e.g. souls, existence) and not matter. Many writers (Dante, Chaucer) considered alchemy to be fraudulent and/or nonsensical. In the 17th century (the Scientific Revolution), Newton, Gassendi, Boyle, Descartes and Lemery tried to rationalise properties of matter. They considered atoms to have different shapes and hook together, modifying Democritus' atomism to create corpuscular theory, which considered light to be made of particles (corpuscles). In the 18th century, the phlogiston theory was created to explain combustion and corrosion, and disproved in the 1770s with the discovery of oxygen by Lavoisier.

- **1803: Dalton's model** considered atoms as hard spheres in different forms (elements), that atoms can join together to form compounds, and that chemical reactions involve rearranging the atoms. In 1811, Avogadro considered gases as lots of molecules made of small numbers of atoms, building on Bernoulli's kinetic theory of gases, reconciling it with Gay-Lussac's law. By the 1830s, the molecular formulas of many simple molecules had been correctly identified. In 1871, Mendeleev's periodic table of elements was published, recognising periodicity and predicting properties. In 1887, the Michelson-Morley experiment disproved the existence of the luminiferous aether.
- **1904: Thompson's 'plum pudding' model**, proposed after his discovery of the electron with cathode ray tube experiments in 1897, with atoms as a large positively charged body with small negative electrons distributed inside.
- **1911: Rutherford's 'nuclear' model**, proposed after his discovery of the proton with his alpha particle scattering experiment, with a small positive nucleus and electrons around.
- **1913: Bohr's 'planetary model'**, proposed the electrons orbit in shells.

- **1916: Lewis' octet rule**, provided a rationale for the Lewis structure of covalent molecules.
- **1926: Quantum mechanics**, developed by de Broglie, Heisenberg, Schrödinger and Born, gave rise to the quantum model of the atom, with electrons as probability density clouds occupying orbitals around the nucleus.
- **1928: Dirac** formulated **quantum electrodynamics**, combining the quantum model with Einstein's special relativity, describing electrons as fundamental particles with **spin**.
- **1929:** Bethe and van Vleck developed **crystal field theory** to describe bonding in metal-inorganic complexes using the concepts of atomic orbital theory.
- **1931:** Pauling developed **hybridisation theory** to describe bonding in molecules.
- **1932:** Hund, Mulliken and Hückel developed **molecular orbital theory**, describing covalent bonds as in-phase and antiphase overlaps between atomic or hybridised orbitals. In the same year, Chadwick discovered neutrons in the nucleus, completing the nuclear model.
- **1933:** Pauling developed **resonance bonding** in terms of quantum superposition. Soviet scientists rejected this theory until the late 1950s due to their Marxist-Leninist philosophy, seeing resonance and quantum phenomena as anti-materialist and anti-deterministic, criticising it as metaphysical.
- **1957:** Griffith and Orgel developed **ligand field theory**, applying the techniques of molecular orbital theory to crystal field theory, accurately describing the bonding in organometallic compounds.
- **1964:** Gell-Mann and Zweig proposed that protons and neutrons are composed of **quarks** with deep inelastic scattering experiments. The quark model was incorporated into Dirac's quantum field theory.

13.1.1. Types of Structures due to Bonding

	Ionic	Covalent	Metallic
Solid	<ul style="list-style-type: none"> • Regular ion lattice with a repeating unit cell containing ions of opposite charges. • High melting point, electrical insulator, often soluble in water. 	<ul style="list-style-type: none"> • Simple molecular (e.g. CO₂ (s), H₂O (s)): low melting point, weak VdW intermolecular forces. • Giant covalent (e.g. diamond (C), SiO₂ (s)): very high melting point, electrical insulator or semiconductor. • Polymer (e.g. polyethylene, BeCl₂ (s)): medium melting point, strong VdW IMFs. 	<ul style="list-style-type: none"> • Regular ion lattice surrounded by a sea of delocalised electrons. • High electrical and thermal conductivity, variable melting point, high density, shiny (lustrous), sonorous.
Liquid	<ul style="list-style-type: none"> • Freely moving ions with strong IMFs. • Electrical conductor. 	<ul style="list-style-type: none"> • Freely moving molecules with strong IMFs. 	<ul style="list-style-type: none"> • Freely moving ions with delocalised electrons. • Electrical conductor.
Gas	<ul style="list-style-type: none"> • Single neutral molecules and small clusters. • All ionic properties lost. 	<ul style="list-style-type: none"> • Freely moving molecules with weak IMFs. • No distinctive properties. 	<ul style="list-style-type: none"> • Single neutral atoms and small molecule clusters. • All metallic properties lost.

13.1.2. Lewis Dot Structures

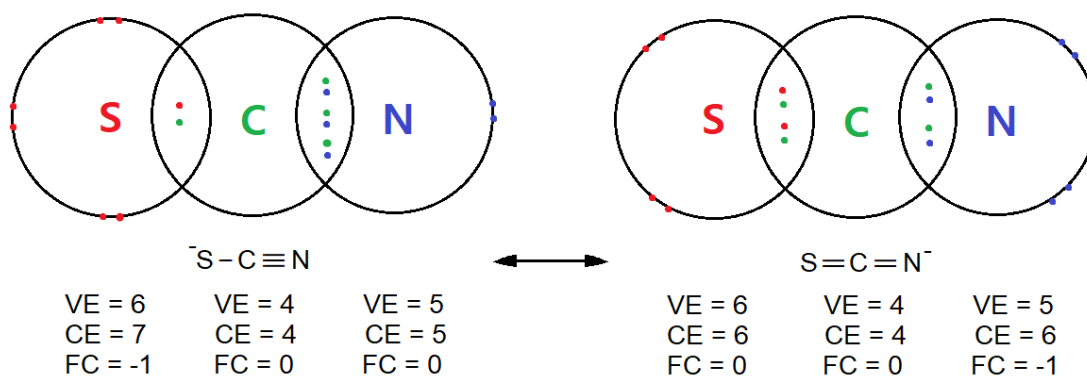
Valence electrons: $VE = \text{group number of atom}$

Contributed electrons: $CE = \text{nonbonding electrons} + \text{donated electrons}$

Donated electrons: 1 per single bond, 2 per double bond, 2 per dative covalent bond

Formal charge: $FC = VE - CE$

Lewis Dot example: the resonance forms of the thiocyanate anion (SCN^-)



Lewis dot structures are usually only valid for atoms up to Period 3 (allowing for expanded octets in e.g. P (10 e⁻) and S (12 e⁻)), and are a highly simplified depiction of bonding.

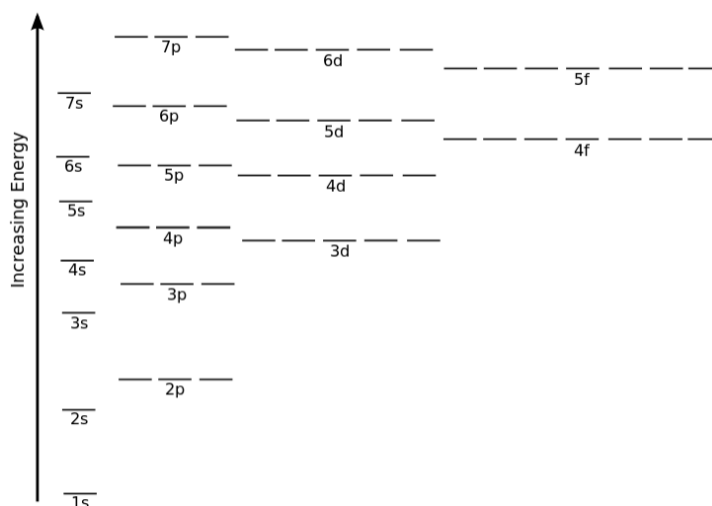
13.1.3. Predicted Ground-State Electron Configurations

- **Aufbau principle:** electrons occupy the orbitals with the lowest energy before the orbitals with higher energy. The usual order is:

$1s \rightarrow 2s \rightarrow 2p \rightarrow 3s \rightarrow 3p \rightarrow 4s \rightarrow 3d \rightarrow 4p \rightarrow 5s \rightarrow 4d \rightarrow 5p \rightarrow 6s \rightarrow 4f \rightarrow 5d \rightarrow 6p \rightarrow 7s \rightarrow 5f \rightarrow 6d \rightarrow 7p.$

- **Hund's rule:** every suborbital is singly occupied before any orbital in the sublevel is doubly occupied.
- **Pauli exclusion principle:** two electrons with the same spin cannot occupy the same suborbital.

From these three observations, the ground-state electron configurations of neutral atoms follows from the lowest unoccupied energy level in the following diagram:



The main exceptions to this rule are neutral Cu, Cr, Ag, Au, Pd and Mo atoms: see Section 11.2.1. for the electron configurations of all atoms. This is often due to the additional exchange energy of a half-full or full d orbital.

The noble gases [He], [Ne], [Ar], [Kr], [Xe], [Rn] end in $1s^2$, $2p^6$, $3p^6$, $4p^6$, $5p^6$, $6p^6$ respectively.

When a transition metal is ionised, electrons are removed from the valence s orbital before the valence d orbital.

13.1.4. Quantum Numbers

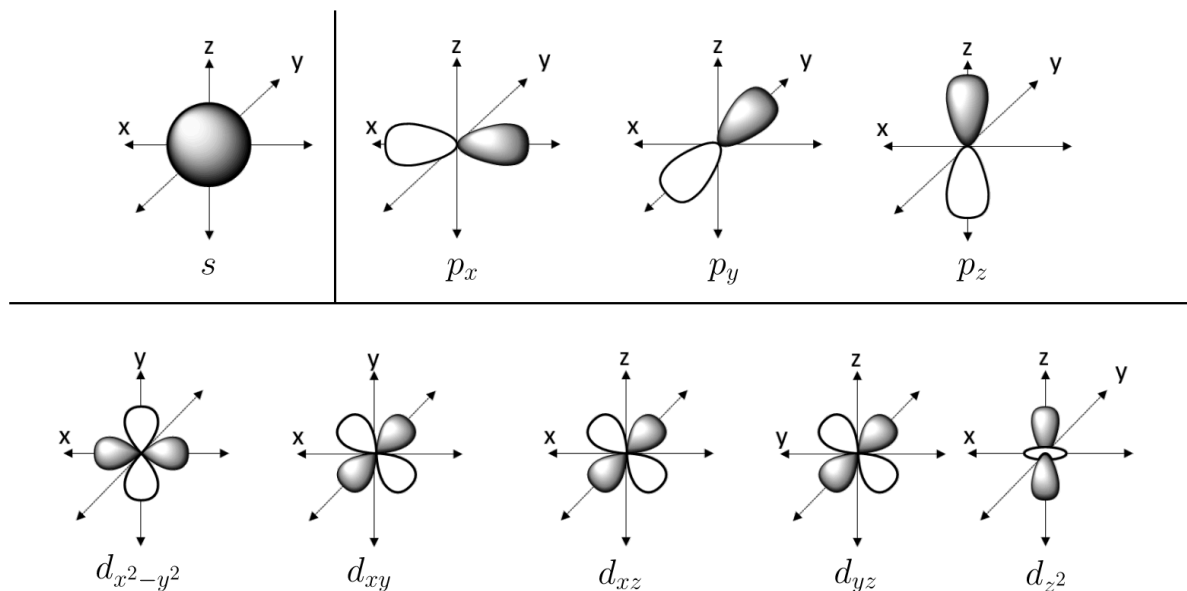
An electron can be described with four quantum numbers (n, l, m_l, m_s):

- Principal quantum number, n : the period, or equivalent Bohr model orbit.
- Azimuthal (angular momentum) quantum number, l : the type of orbital.
 $l = 0$ is an s -orbital, $l = 1$ is a p -orbital, $l = 2$ is a d -orbital, $l = 3$ is an f -orbital.
- Magnetic quantum number, m_l or m : the sub-orbital, with $-l \leq m_l \leq l$.
- Spin quantum number, m_s : represents spin-up or spin-down, with $m_s = \pm \frac{1}{2}$.

12.1.5. Shapes and Designations of Atomic s , p and d -orbitals

The shades represent opposing phases of the wavefunction for the atomic orbital.

The z -axis is taken as the internuclear axis when bond formation occurs.




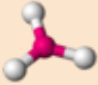
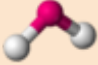
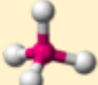
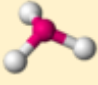
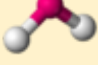
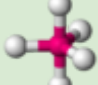
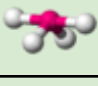
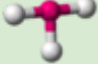

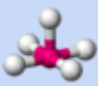
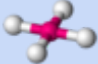
The magnetic quantum numbers of these orbitals are

$$\begin{array}{cccccc}
 p_z: m_l = 0, & p_x: m_l = 1, & p_y: m_l = -1 & & & \\
 d_z: m_l = 0, & d_{xz}: m_l = 1, & d_{yz}: m_l = -1, & d_{xy}: m_l = 2, & d_{x^2-y^2}: m_l = -2 &
 \end{array}$$


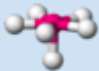
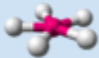


For the field splitting of d -orbitals in transition metal complexes, see Section 15.4.1.

13.1.6. Molecular Geometry, Hybridisation and the VSEPR Theory

The bonding in covalent molecules is predicted by VSEPR (valence shell electron pair repulsion) theory. Some of the valence atomic orbitals (s , p , d) on a single atom can be combined into a set of degenerate hybrid atomic orbitals (sp , sp^2 , ...), which can then form covalent bonds with other orbitals.

Atoms	Lone pairs	Electron domains (hybridisation)	Shape (point group)	Ideal bond angles	Examples	Image
2	0	2 (sp)	linear ($D_{\infty h}$)	180°	CO ₂ , BeF ₂	
3	0	3 (sp^2)	trigonal planar (D_{3h})	120°	BF ₃ , SO ₃	
2	1		bent (C_{2v})	120° (119°)	SO ₂	
4	0	4 (sp^3)	tetrahedral (T_d)	109.47°	CH ₄ , MnO ₄ ⁻	
3	1		trigonal pyramidal (C_{3v})	109.47° (106.8°)	NH ₃ , ClO ₃ ⁻	
2	2		bent (C_{2v})	109.47° (104.48°)	H ₂ O	
5	0	5 (sp^3d)	trigonal bipyramidal (D_{3h})	90°, 120°	PCl ₅ , Fe(CO) ₅	
4	1		seesaw (C_{2v})	180°, 120°, 90°	SF ₄ , AsF ₄ ⁻	
3	2		T-shaped (C_{2v})	90°, 180°	ClF ₃	
6	0	6 (sp^3d^2)	octahedral (O_h)	90°, 180°	SF ₆ , Mo(CO) ₆	
5	1		square pyramidal (C_{4v})	90°	BrF ₅ , MnCl ₅ ²⁻	
4	2		square planar (D_{4h})	90°, 180°	XeF ₄ , PtCl ₄ ²⁻	

For higher numbers of atoms, more complex geometries are:

Atoms	Lone pairs	Electron domains (hybridisation)	Shape (point group)	Ideal bond angles	Examples	Image
7	0	7 (sp^3d^3)	pentagonal bipyramidal (D_{5h})	$90^\circ, 72^\circ, 180^\circ$	IF_7, ZrF_7^{3-}	
6	1		pentagonal pyramidal (C_{5v})	$72^\circ, 90^\circ, 144^\circ$	$XeOF_5^-, IOF_5^{2-}$	
5	2		pentagonal planar (D_{5h})	$72^\circ, 144^\circ$	IF_5^{2-}	
8	0	8 (sp^3d^4)	square antiprismatic (D_{4d})	$70.5^\circ, 99.6^\circ, 109.5^\circ$	TaF_8^{3-}	
9	0	9 (sp^3d^5)	tricapped trigonal prismatic (D_{3h})	$90^\circ, 120^\circ$	$ReH_9^{2-}, Th(H_2O)_9^{4+}$	

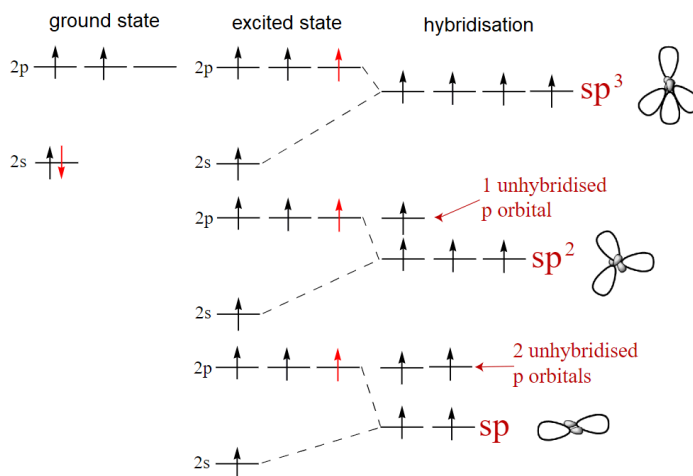
The presence of lone pairs on an atom reduces the bond angles. Bonding pairs repel less strongly:

$$LP-LP > LP-BP > BP-BP$$

There is a reduction in bond angle by about 2.5° per lone pair (very approximate).

Note: the point groups are not unique to a particular geometry and are only true when the groups surrounding the central atom are identical.

Conceptual Formation of sp , sp^2 and sp^3 Hybrid Atomic Orbitals: e.g. for carbon.



13.1.7. Bohr Model for Hydrogenic Atoms

The Bohr model has electrons in orbits around the nucleus analogous to planets around the Sun.

- Orbit radius, $r_n = \frac{a_0 n^2}{Z}$
- Orbit speed, $v_n = \frac{e^2}{2\epsilon_0 \hbar} \frac{Z}{n}$
- Orbit angular momentum, $L_n = \frac{nh}{2\pi} = \hbar n$
- Kinetic energy, $T_n = \frac{Z^2 e^2}{8\pi\epsilon_0 a_0 n^2}$
- Potential energy, $V_n = -\frac{Z^2 e^2}{4\pi\epsilon_0 a_0 n^2}$
- Total energy, $E_n = -\frac{Z^2 e^2}{8\pi\epsilon_0 a_0 n^2}$

(Z : nuclear charge (H = 1, He⁺ = 2, Li²⁺ = 3...), $m_e = 9.109 \times 10^{-31}$ kg: electron rest mass, $h = 6.63 \times 10^{-34}$ J s: Planck's constant, $\hbar = 1.06 \times 10^{-34}$: reduced Planck's constant, $|e| = 1.61 \times 10^{-19}$ C: electron charge, $a_0 = 5.292 \times 10^{-11}$ m: Bohr radius, $\epsilon_0 = 8.854 \times 10^{-12}$ C N⁻¹ m⁻²: vacuum permittivity.)

Line spectrum of hydrogen: the lines in the emission spectra can be divided into the Lyman series ($n \rightarrow 1$), Balmer series ($n \rightarrow 2$), Paschen series ($n \rightarrow 3$), Brackett series ($n \rightarrow 4$), Pfund series ($n \rightarrow 5$) and Humphreys series ($n \rightarrow 6$), in which the electron falls from a higher state to the state shown.

Direct de-excitation from state n_2 to state n_1 shows at line wavelength (Rydberg's formula):

$$\frac{1}{\lambda} = \frac{\Delta E}{hc} = Z^2 R_\infty \left(\frac{1}{n_1^2} - \frac{1}{n_2^2} \right) \quad (R_\infty = 1.097 \times 10^7 \text{ m}^{-1}: \text{Rydberg constant})$$

When an electron in the excited state n_2 de-excites to state n_1 , there are a maximum of $\frac{\Delta n (\Delta n + 1)}{2}$ emission lines due to intermediate transitions (where $\Delta n = n_2 - n_1$).

In X-ray experiments, the shells $n = 1, 2, 3$ are denoted K, L, M respectively.

The Bohr model is a significant oversimplification for multi-electron atoms. The electron shells are considered to have 2, 8, 8, 18, 18, 32, 32... electrons, in that order.

13.1.8. Quantum Model for Hydrogenic Atoms

The time-independent Schrodinger equation (TISE) for a one-electron atom (hydrogen-like) is:

$$\hat{H}\Psi = E\Psi, \quad \hat{H} = -\frac{\hbar^2}{2\mu}\nabla^2 + V, \quad V = \frac{Ze^2}{4\pi\epsilon_0 r}, \quad \mu = \frac{m_e m_{nucleus}}{m_e + m_{nucleus}}$$

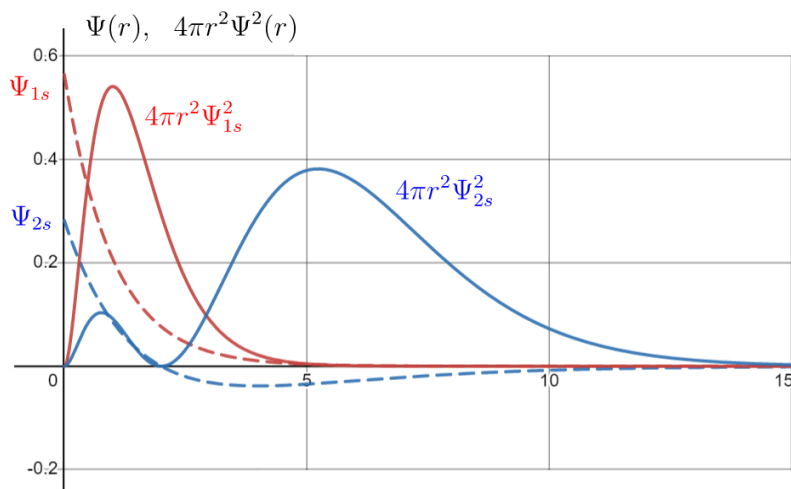
(E : energy of a state, $\Psi(\mathbf{r})$: wavefunction of a state.) The solution for Ψ with \mathbf{r} in spherical coordinates (r, θ, ϕ) is separable (radial: polynomial with exponential decay; angular: spherical harmonic) and is given by:

$$\Psi_{nlm}(r, \theta, \phi) = \underbrace{\sqrt{\frac{4(n-l-1)!}{(a_0^*)^3 n^4 (n+l)!}}}_{\text{normalisation constant}} \times \underbrace{\rho^l e^{-\frac{1}{2}\rho} L_{n-l-1}^{2l+1}(\rho)}_{\text{radial dependence}} \times \underbrace{Y_l^m(\theta, \phi)}_{\text{angular dependence}}$$

($a_0^* = m_e a_0 / \mu$: reduced Bohr radius, $\rho = 2r / n a_0^*$: dimensionless radial coordinate, L : generalised Laguerre polynomial (Section 1.7.12), Y_l^m : spherical harmonic (Section 1.7.17).)

The corresponding energy eigenvalues (energy levels) are $E_n = \frac{-m_e e^4}{32\pi^2 \epsilon_0^2 \hbar^2} \frac{1}{n^2} \approx \frac{-13.6 \text{ eV}}{n^2}$.

Plots of the 1s and 2s Wavefunctions for Hydrogenic Atoms



The quantity $4\pi r^2 |\Psi|^2$ is the radial probability density function.

$$1s : \Psi_{1,0,0} = \pi^{-1/2} a_0^{-3/2} e^{-r/a_0}$$

Maximum of $4\pi r^2 \Psi_{1s}^2$ is at $r = a_0$.

$$\frac{r}{a_0} \quad 2s : \Psi_{2,0,0} = \frac{1}{4} \pi^{-1/2} a_0^{-3/2} \left(2 - \frac{r}{a_0} \right) e^{-r/(2a_0)}$$

Node of $4\pi r^2 \Psi_{2s}^2$ is at $r = 2a_0$.

- The s orbitals ($l = 0$) are spherical, with radial nodes and alternating phases between them.
- The p orbitals ($l = 1$) are axial, with one nodal plane and opposite phases on each side of the plane.
- Number of radial nodes = $n - l - 1$. Number of angular nodes (nodal planes) = l .
- The higher orbitals have more complex geometries.

13.1.9. Quantum Model for Multi-Electron Atoms

For a system of n electrons, the wavefunction is a function of $3n$ spatial variables e.g. the spherical coordinates $(r_1, \theta_1, \phi_1, r_2, \theta_2, \phi_2, \dots, r_n, \theta_n, \phi_n)$. The Hamiltonian is

$$\hat{H} = \underbrace{-\frac{\hbar^2}{2\mu} \sum_{i=1}^n \nabla_i^2}_{\text{kinetic energy}} - \underbrace{\sum_{i=1}^n \frac{Ze^2}{4\pi\epsilon_0 r_i}}_{\text{nuclear attraction potential energy}} + \underbrace{\sum_{i=1}^{n-1} \sum_{j=i+1}^n \frac{e^2}{4\pi\epsilon_0 r_{ij}}}_{\text{mutual repulsion potential energy}}$$

∇_i^2 is the Laplacian operator with respect to only the coordinates of electron i :

$$\nabla_i^2 = \frac{1}{r_i^2 \sin \theta_i} \left[\sin \theta_i \frac{\partial}{\partial r_i} \left(r_i^2 \frac{\partial}{\partial r_i} \right) + \frac{\partial}{\partial \theta_i} \left(\sin \theta_i \frac{\partial}{\partial \theta_i} \right) + \frac{1}{\sin \theta_i} \frac{\partial^2}{\partial \phi_i^2} \right]$$

and r_{ij} is the distance between electron i and electron j :

$$r_{ij} = \sqrt{r_i^2 + r_j^2 - 2r_i r_j (\cos \theta_i \cos \theta_j + \sin \theta_i \sin \theta_j \cos(\phi_i - \phi_j))}$$

13.1.10. Linear Combinations of Atomic Orbitals (LCAO)

A common simplification to multi-electron or polynuclear species is the LCAO approximation. Under this assumption, a molecular orbital (MO) can be formed by combining atomic orbitals (AOs) in either constructive or destructive interference:

$$\Psi^{(MO)} = \sum_n c_n \psi^{(AO)} \quad \text{i.e. a linear superposition of atomic orbitals.}$$

The collection of AOs used to form an MO is the 'basis set'. The coefficients c_n can be found by variational methods to minimise the energy of each electron. Hybridised atomic orbitals can also be expressed in this way (e.g. $\Psi^{(sp^3)} = \frac{1}{2}(\psi^{(s)} \pm \psi^{(p_x)} \pm \psi^{(p_y)} \pm \psi^{(p_z)})$).

For binary homonuclear species, $|c_1| = |c_2|$ (equal sharing of electrons):

$$\Psi_{MO} = \frac{1}{\sqrt{2(1+S)}} (\psi_1^{(AO)} + \psi_2^{(AO)}) \quad \text{and} \quad \Psi_{MO^*} = \frac{1}{\sqrt{2(1-S)}} (\psi_1^{(AO)} - \psi_2^{(AO)})$$

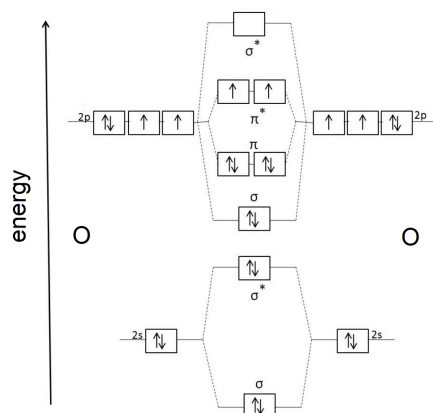
(bonding: constructive interference) (anti-bonding: destructive interference)

where $S = \int_V \psi_1^{(AO)} \psi_2^{(AO)} dV$ is the overlap integral, bounded by $0 \leq S \leq 1$.

13.1.11. Molecular Orbital Theory

Atomic orbitals (AOs, potentially hybridised) on two nearby atoms can interact. The resulting molecular orbital (MO) can be considered a linear superposition of a bonding MO and an antibonding MO, where the AOs interfere constructively and destructively respectively.

- When AOs interact directly (e.g. s orbitals, sp^n hybrid orbitals, axial p orbitals), the resulting MOs are sigma (σ and σ^*)
- When AOs interact laterally (e.g. lateral p orbitals), the resulting MOs are pi (π and π^*).



Example: MO diagram for diatomic oxygen (O_2)

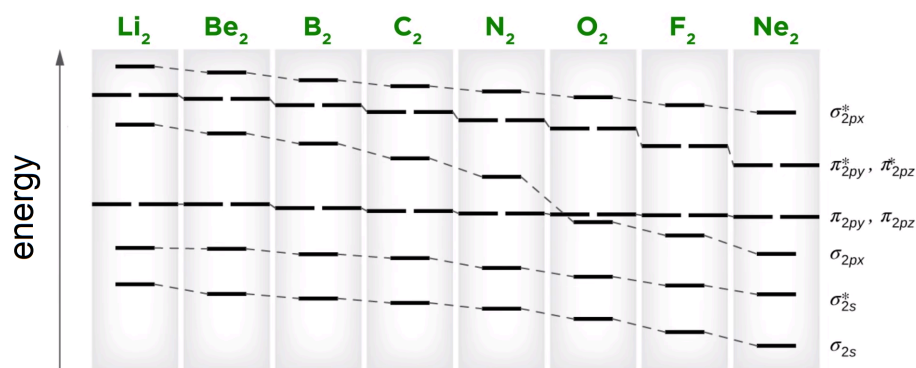
Each O atom has valence configuration $2s^2 2p^4$.

The $2p_z$ AOs interfere directly to form σ_{2p} and σ^*_{2p} .

The $2p_x$ and $2p_y$ AOs interfere laterally to form π_{2p} and π^*_{2p} .

(The $2s$ AOs also form σ_{2s} and σ^*_{2s} , but these are both fully filled and so cancel out i.e. do not contribute to bond order.)

s - p Mixing in Period 2 Homonuclear Diatomic Molecules



When the s and p AOs have similar energies, the resulting σ_{2s} and σ_{2p} interfere such that σ_{2p} becomes less stable.

For less electronegative atoms (Li...N), the resulting $\sigma_{2p} > \pi_{2p}$, leading to a different order of MO filling.

$$\text{Bond order} = \frac{\# \text{ bonding } e^- - \# \text{ antibonding } e^-}{2} \quad (1: \text{ single}, 2: \text{ double}, 3: \text{ triple})$$

For the application of MO theory to d orbitals, see Ligand Field Theory (LFT, Section 15.5.14.)

13.1.12. Magnetic Properties of Matter

Materials may respond to external magnetic field \mathbf{B} by creating an internal magnetisation \mathbf{M} which may act in the same or opposite direction.

- If $\mathbf{B} = 0$ produces $\mathbf{M} = 0$, then the material is an induced magnet.
- If $\mathbf{B} = 0$ produces $\mathbf{M} > 0$, then the material is a permanent magnet (ferromagnetic).

Iron, cobalt, nickel, ruthenium and many rare-earth alloys are ferromagnetic at room temperature. These elements have a microstructure of magnetic domains in which all electron spins are aligned to produce a large unidirectional magnetisation (below the Curie temperature). For more information / data on magnetic materials, see Section 8.6.

For the relationships between \mathbf{B} , \mathbf{H} , \mathbf{M} and μ , see Section 8.1.1. The two modes of induced magnetism are:

	Diamagnetic	Paramagnetic
Electron configuration	No unpaired electrons	At least one unpaired electron
Spin alignment with external magnetic field \mathbf{B}	Anti-parallel to \mathbf{B} ($-1 \leq \chi_v < 0$)	Parallel to \mathbf{B} ($\chi_v > 0$)
Reaction to magnets	Weakly repelled	Attracted
Effect on field lines of \mathbf{B}	Field bends away from material	Field bends towards material

Magnetic susceptibility: $\chi_v = \frac{\text{internal magnetisation}}{\text{applied magnetic field}} = \frac{M}{H} = \mu_r - 1.$

Molar susceptibility: $\chi_m = \frac{M_r}{\rho} \chi_v$

Superconductors are perfectly diamagnetic with $\chi = -1$ below the critical temperature and expel the magnetic field completely (Meissner effect).

13.1.13. Symmetry Adapted Linear Combinations (SALCs) of Atomic Orbitals

Molecular orbitals for polyatomic molecules can be deduced using projection operators to account for the symmetry about a central atom. For the character tables of point groups, see Section 13.2.10.

1. Determine the point group. (If linear, use D_{2h} / C_{2v} instead as it is simpler.)
2. Assign the x - y - z axes. z is the principal axis. If nonlinear, y points to the outer atom.
3. Find reducible representation Γ of outer atom orbitals (moves: 0, symmetric: +1, antisymmetric: -1)
4. Use the character table to find the irreducible representation Γ of outer atom orbitals (SALCs).

Example: SALCs of the water molecule (H_2O). H_2O belongs to the C_{2v} point group. Assign the z -axis as principal axis (C_2 symmetry) so that the molecule lies in the x - z plane. The character table for C_{2v} contains the symmetries $\{E, C_2^z, \sigma^{xz}, \sigma^{yz}\}$. Consider the counts of each symmetry applied to each atomic orbital:

Hydrogen $1s$ orbital:

Reducible representation:

$$\Gamma = \{E: 2, C_2: 0, \sigma^{xz}: 2, \sigma^{yz}: 0\}$$

Irreducible representation:

$$\Gamma_{2\text{H},1s} = 1 A_1 \oplus 1 B_1.$$

Oxygen $2s$ orbital:

Reducible representation

$$\Gamma = \{E: 1, C_2: 1, \sigma^{xz}: 1, \sigma^{yz}: 1\}$$

Irreducible representation

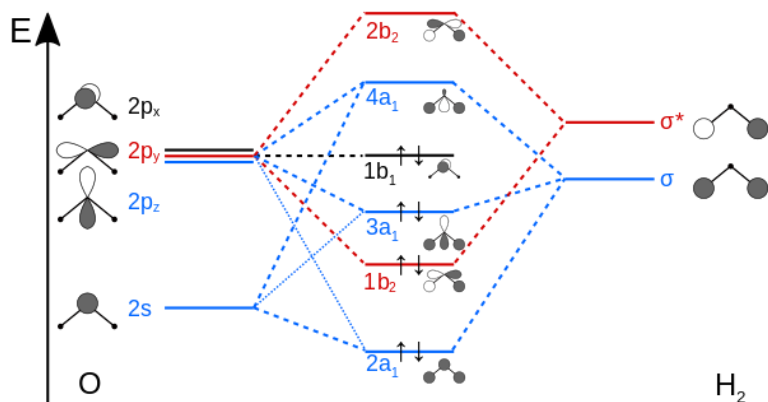
$$\Gamma_{\text{O},2s} = 1 A_1.$$

Oxygen $2p$ orbital:

From the character table, these are by definition:

$$A_1 (p_z), B_1 (p_x), B_2 (p_y).$$

Orbitals with the same symmetry now interact, splitting into bonding and antibonding to form the MO diagram.

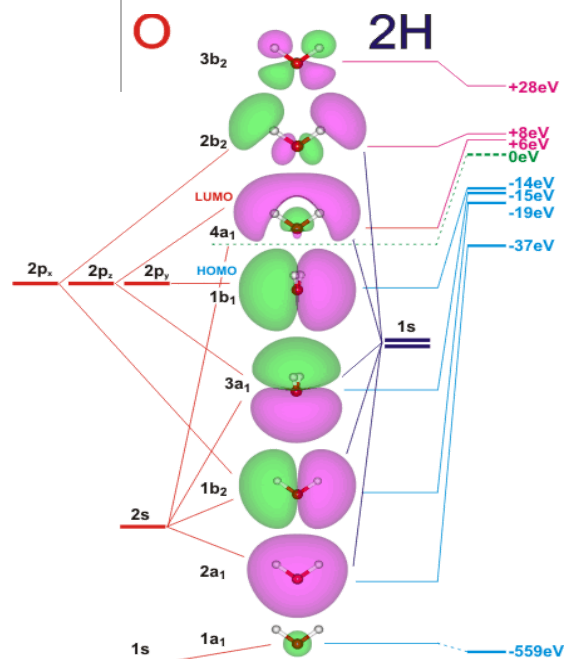


SALC-predicted MO diagram of water

(HOMO: $1b_1$, nonbonding; LUMO: $4a_1$, anti-bonding)

$1b_1$ acts as the main 'lone pair' (hydrogen bond acceptor) can be considered the second lone pair.

This applies in the ideal gas phase (energies are shifted and broadened slightly into bands in liquid water/ice).



True MOs and energy levels of water (computed with Hartree-Fock DFT)

but $2a_1$

13.1.14. Huckel's Method

13.1.15. Angular Overlap Method

13.1.15. Density Functional Theory (DFT)

DFT is a computational algorithm used to determine the electron density of a system across space. It effectively approximates the solution to the Schrodinger equation for large quantum systems e.g. interacting molecules, large molecules, nanoparticles, network solids, for which molecular dynamics simulations are prohibitively computationally expensive.

Hohenberg-Kohn Theorems:

1. The external potential and total energy are unique functionals of electron density.
2. The functional corresponding to the system's ground state energy gives the lowest energy if and only if the input density is the true ground-state density.

Kohn-Sham Equations: the electrons are approximated as non-interacting, instead modifying the potential function to account for the changes. The equations modelling the fictitious system are:

$$\left(-\frac{\hbar^2}{2m} \nabla^2 + v_{\text{eff}}(\mathbf{r}) \right) \varphi_i(\mathbf{r}) = \varepsilon_i \varphi_i(\mathbf{r}).$$

Schrodinger equation

$$\rho(\mathbf{r}) = \sum_i^N |\varphi_i(\mathbf{r})|^2.$$

Electron density

($\varphi_i(\mathbf{r})$): wavefunction for Kohn-Sham orbital, given by a Slater determinant)

Exchange-correlation functional: used to approximate the $E'_{xc}[n]$ term in the energy density functional (n : electron density per unit volume).

$$\begin{aligned} E[n] &= E_{\text{kin,KS}}[n] + E_{\text{Coul}}[n] + E_{\text{ext}}[n] + (E_{\text{kin}}[n] - E_{\text{kin,KS}}[n]) + E_{\text{xc}}[n] \\ &= 2 \sum_{i=1}^{N_{\text{el}}/2} \int \psi_i^*(\mathbf{r}) \left(-\frac{1}{2} \nabla^2 \right) \psi_i(\mathbf{r}) d\mathbf{r} + E_{\text{Coul}}[n] + E_{\text{ext}}[n] + E'_{\text{xc}}[n] \end{aligned}$$

The EC functionals can be written in terms of the energy per electron, $E'_{xc}[n] = \int n(\mathbf{r}) \varepsilon_{xc}[n(\mathbf{r})] d\mathbf{r}$.

Local density approximation (LDA): $E'_{xc}[n] = E_x[n] + E_c[n]$, where $E_x[n] = C \int n(\mathbf{r})^{4/3} d\mathbf{r}$.

A variety of expressions for $E_c[n]$ exist (e.g. VWN, VWN5, CAPZ), and should be chosen suitably depending on the type of computation, which may contain empirically-derived parameters.

13.1.16. Classical Computational Chemistry (Molecular Dynamics)

While quantum mechanics must be considered for atomic-scale simulation, for larger systems this is typically infeasible. A classical alternative to DFT is molecular dynamics.

A molecular dynamics simulation produces a trajectory of states \mathbf{x} at time steps t . Useful information is obtained by computing an observable quantity $A(\mathbf{x})$.

Monte Carlo Simulation

In Monte Carlo simulation, the aim is to create a stochastic process that tends to the Boltzmann distribution, as fast as possible and compute observables as averages over phase space. Dynamical evolution of system variables does not correspond to real dynamics in any way. It is not suitable for studying non-equilibrium and other time-dependent phenomena.

- Transition probability: $p(j \rightarrow i) = \min\{1, e^{-\frac{E_i - E_j}{kT}}\}$, then apply the Metropolis-Hastings algorithm (Section 5.4.10).
- Time-averaged value of an observable A : $\bar{A} \approx \frac{1}{Z} \int A(x) e^{-\frac{E(x)}{kT}} dx \approx \int_0^\tau A(x_{Langevin}(t)) dt$

Error Analysis in Correlated Time Series of Observables

- Time-averaged value of an observable A : $\bar{A} = \frac{1}{\tau} \int_0^\tau A(x(t)) dt = \frac{1}{N} \sum_{i=1}^N A(x(t_i))$
- Normalised autocorrelation: $\rho(\tau) = C(\tau)/C(0)$, where C is the autocorrelation of A given by $C(\tau) = E[(A(t) - \bar{A})(A(t + \tau) - \bar{A})]$, and $C(0) = \text{Var}[A]$.
- Exponential autocorrelation time: if $|\rho(\tau)| \leq e^{-\tau/\tau_0}$ then $\tau_0^{exp} = \lim_{\tau \rightarrow \infty} \sup\{\frac{-\tau}{\ln|\rho(\tau)|}\}$.

Measurements separated by at least $\sim 10 \tau_0^{exp}$ are uncorrelated (independent). This can be used to set a 'burn-in' period of a simulation after setting initial conditions, where the system equilibrates before collecting data.

- Variance of mean observable: $\text{Var}[\bar{A}] = 2\tau_0^{int} \times \frac{C(0)}{N}$, where $\tau_0^{int} = \frac{1}{2} + \sum_{k=1}^{\infty} \rho(\tau_k)$.

To reduce noise effects, compute smallest M such that $M \geq 10 \hat{\tau}_0^{int}$ ($\hat{\tau}_0^{int} = \frac{1}{2} + \sum_{k=1}^M \rho(\tau_k)$).

LAMMPS is a package written in C++ that can use an OPLS force model (bond stretching + bending + torsion + electrostatics + Lennard-Jones VdW), commonly used for high-speed classical molecular dynamics.

13.2. Crystallography and Solid State Chemistry

13.2.1. Unit Cells of Some Simple Crystal Structures

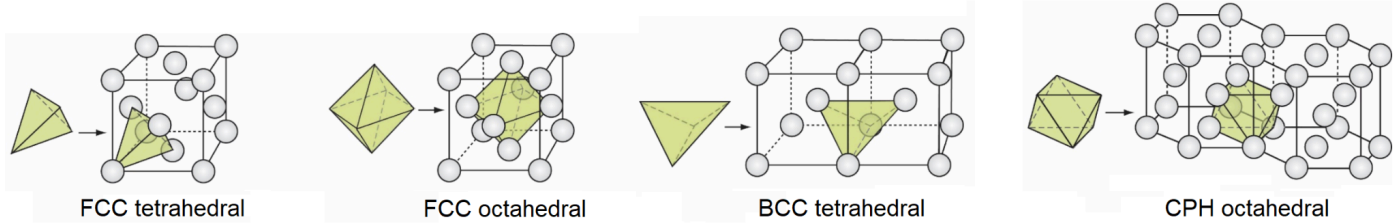
Unit Cell (green: close-packed planes)			
Name	FCC Face-Centred Cubic	BCC Body-Centred Cubic	CPH (HCP) Close-Packed Hexagonal
Atoms	4	2	6
Coordination Number	12	8	12
Packing Fraction	$\frac{\sqrt{2}\pi}{6} \approx 74\%$	$\frac{\sqrt{3}\pi}{8} \approx 68\%$	$\frac{\sqrt{2}\pi}{6} \approx 74\%$
Atomic radius in terms of lattice constant(s)	$r = \frac{\sqrt{2}}{4}a \approx 0.354a$	$r = \frac{\sqrt{3}}{4}a \approx 0.433a$	$r = \frac{1}{2}a = \frac{\sqrt{6}}{8}c \approx 0.306c$
Cell Volume	$V = 16\sqrt{2}r^3$	$V = \frac{64\sqrt{3}}{9}r^3$	$V = 24\sqrt{2}r^3$

Some common particular structures are:

- **Diamond Cubic (DC):** an FCC lattice with either four (1:1) or eight (1:2) of the tetrahedral voids occupied. Notable cases: zinc blende / sphalerite (ZnS), fluorites (CaF₂), antifluorites (Na₂O, Li₂O), Si and Ge, diamond (C), silicon carbide (SiC).
- **Corundum:** a CPH lattice with four (2:3) of the octahedral voids occupied. Notable cases: metal(III) oxides (Al₂O₃, Fe₂O₃, Cr₂O₃)
- **Halite:** two FCC lattices of each atom (1:1), alternating along any edge. Notable cases: rock salt (NaCl).
- **Primitive Cubic BCC:** a simple cubic structure with the single body-centre position occupied (1:1). Notable cases: caesium chloride (CsCl).

13.2.2. Voids in Simple Lattices

Only FCC, BCC and CPH are given here. For other lattices, see Section 12.2.7.



Voids in an FCC Lattice, per unit cell with monatomic radius R :

- 8 regular tetrahedral voids, with $\frac{r}{R} = \sqrt{\frac{3}{2}} - 1 \approx 0.225$, coordination number 4, with centroids at $\{\frac{1}{2} \pm \frac{1}{4}, \frac{1}{2} \pm \frac{1}{4}, \frac{1}{2} \pm \frac{1}{4}\}$.
- 4 regular octahedral voids, with $\frac{r}{R} = \sqrt{2} - 1 \approx 0.414$, coordination number 6, with centroids at $\{\frac{1}{2}, \frac{1}{2}, \frac{1}{2}\}, \{0, 0, \frac{1}{2}\}$, etc.

Voids in a BCC lattice, per unit cell with monatomic radius R :

- 12 irregular (distorted) tetrahedral voids, with $\frac{r}{R} = \sqrt{\frac{5}{3}} - 1 \approx 0.290$, coordination number 2, with a centroid at $\{\frac{1}{2}, 0, \frac{1}{4}\}$, etc.
- 6 irregular (distorted) octahedral voids, with $\frac{r}{R} = \frac{2\sqrt{3}-3}{3} \approx 0.155$, coordination number 2, with a centroids at $\{\frac{1}{2}, \frac{1}{2}, 0\}$ and $\{\frac{1}{2}, 0, 0\}$ (among others).

Voids in a CPH lattice, per unit cell with monatomic radius R :

- 12 regular tetrahedral voids, with $\frac{r}{R} = \sqrt{\frac{3}{2}} - 1 \approx 0.225$, coordination number 4, with centroids at $\{0, 0, \frac{3}{8}\}, \{0, 0, \frac{5}{8}\}, \{\frac{2}{3}, \frac{1}{3}, \frac{1}{8}\}$ and $\{\frac{2}{3}, \frac{1}{3}, \frac{7}{8}\}$ (among others).
- 6 regular octahedral voids, with $\frac{r}{R} = \sqrt{2} - 1 \approx 0.414$, coordination number 6, with centroids at $\{\frac{1}{3}, \frac{2}{3}, \frac{1}{4}\}$ and $\{\frac{1}{3}, \frac{2}{3}, \frac{3}{4}\}$ (among others).

13.2.3. Crystallographic Defects

Point Defects:

- **Schottky defect:** vacancy of equal numbers of cation and anion lattice positions.
- **Frenkel defect:** displacement of an ion at a lattice position to an interstitial position.
- **Metal excess defect:** replacement of an anion lattice position with an unpaired electron (F-centre). The electron absorbs light in the visible spectrum, giving colour.
- **Metal deficiency defect:** vacancy of a cation lattice position, balanced by cations in higher oxidation states.

Line Defects:

- **Edge dislocation:** an extra half-plane of atoms.
The line vector is perpendicular to the Burgers vector.
- **Screw dislocation:** a fork in the lattice.
The line vector is parallel to the Burgers vector.
- **Mixed dislocation:** a combination of edge and screw dislocations.
The line vector is at an acute angle to the Burgers vector.

Plane and Bulk Defects:

- Areas: Grain boundaries, Twin boundaries,
- Volumes: Cracks, Pores, Precipitates.

13.2.4. Defect Reactions

Kröger-Vink notation for point defects: A_S^C where

- A is the entity symbol (atomic element symbol, or v = vacancy, e = electron, h = hole),
- S is the substituted entity symbol (atomic element symbol, or i = interstitial site),
- C is the real or effective charge (\bullet = positive, $/$ = negative, \times = zero)

Defect reactions for fully ionised point defects of metal oxides M_aO_b are:

Schottky disorder	$0 \Rightarrow v_M^{\frac{2b}{a}/} + \frac{b}{a} v_O^{\bullet\bullet}$ balanced = metal vacancy + oxygen vacancy
Frenkel disorder	$M_M^{\times} + v_i^{\times} \Rightarrow v_M^{\frac{2b}{a}/} + M_i^{\frac{2b}{a}\bullet}$ metal atom + interstitial void = metal vacancy + interstitial metal
Anti-Frenkel disorder	$O_O^{\times} + v_i^{\times} \Rightarrow v_O^{\bullet\bullet} + O_i^{//}$ oxygen atom + interstitial void = oxygen vacancy + interstitial oxygen
Intrinsic electronic ionisation	$0 \Rightarrow e' + h^{\bullet}$ balanced = conduction band electron + valence band hole
Oxygen excess	$\frac{1}{2} O_2(g) + v_i^{\times} \Rightarrow O_i^{//} + 2 h^{\bullet}$ $O_2(g) + \text{interstitial void} = \text{interstitial oxygen} + \text{valence holes}$
Oxygen deficiency	$O_O^{\times} \Rightarrow v_O^{\bullet\bullet} + 2 e' + \frac{1}{2} O_2(g)$ oxygen atom = oxygen vacancy + conduction electrons + $O_2(g)$
Metal excess	$M_M^{\times} + \frac{b}{a} O_O^{\times} + v_i^{\times} \Rightarrow M_i^{\frac{2b}{a}\bullet} + \frac{2b}{a} e' + \frac{b}{2a} O_2(g)$ metal atom + oxygen atom + interstitial void = interstitial metal + conduction electrons + $O_2(g)$
Metal deficiency	$\frac{b}{2a} O_2(g) \Rightarrow v_M^{\frac{2b}{a}/} + \frac{b}{a} O_O^{\times} + \frac{2b}{a} h^{\bullet}$ $O_2(g) = \text{metal vacancy} + \text{oxygen atom} + \text{valence hole}$

Doping of ionic compounds: either form defects with opposite effective charge, or consume defects of same effective charge. Examples:

- Doping of $Ni_{1-x}O$ with Li_2O :

$$Li_2O(s) + 2 v_{Ni}^{//} \Rightarrow 2 Li_{Ni}' + O_O^{\times}$$
 or, in the presence of oxygen:

$$Li_2O(s) + \frac{1}{2} O_2(g) \Rightarrow 2 Li_{Ni}' + 2 O_O^{\times} + 2 h^{\bullet}$$
- Doping of ZrO_{2-y} with Y_2O_3 :

$$Y_2O_3(s) \Rightarrow 2 Y_{Zr}' + v_O^{\bullet\bullet} + 3 O_O^{\times}$$
- Doping of $LaScO_3$ with CaO :

$$CaO(s) + \frac{1}{2} Sc_2O_3 \Rightarrow Ca_{La}' + Sc_{Sc}^{\times} + \frac{5}{2} O_O^{\times} + \frac{1}{2} v_O^{\bullet\bullet}$$
- Doping of LaF_{3-x} with EuF_2 :

$$EuF_2(s) \Rightarrow Eu_{La}' + v_F^{\bullet} + F^{-}$$

13.2.5. Kinetics and Thermodynamics of Defect Reactions

Defect activity (site fraction): $a_{A_S^c} = \frac{[A_S^c]}{[S]}$. Equilibrium constant, $K = \prod_i a_i^{v_i}$.

Note that terms such as $a_{Zn_{Zn}^x} = \frac{[Zn_{Zn}^x]}{[Zn]} \approx 1$ and can be neglected from the expression.

For electronic defects, use $a_{e'} = \frac{n}{N_c}$ and $a_{h\cdot} = \frac{p}{N_v}$ (N : state density in conduction / valence bands)

Thermodynamics: $K = \exp\left(\frac{-\Delta G^\ominus}{RT}\right) = \exp\left(\frac{\Delta S_{vib}^\ominus}{R}\right) \exp\left(\frac{-\Delta H^\ominus}{RT}\right)$

Conventional electronic 'equilibrium' constant: $K' = [e'][h\cdot] = np = N_c N_v \exp\left(\frac{-E_g}{RT}\right)$.

Other common conventional simplifications: scale $a_{O_2(g)}$ as $\frac{p_{O_2}}{1 \text{ bar}}$, scale $a_{e'}$, $a_{h\cdot} = n, p$.

Brouwer diagram: plot of $\log n$ against $\log p_{O_2}$, typically a straight line.

Example reaction: $0 \Rightarrow v_M^{2n/} + n v_O^{\bullet\bullet}$, activities are constrained by:

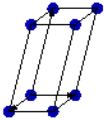
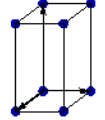
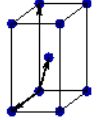
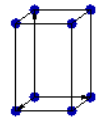
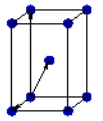
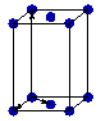
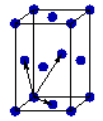
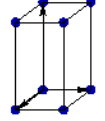
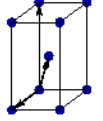
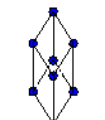
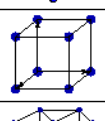
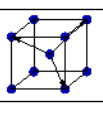
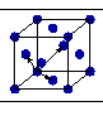
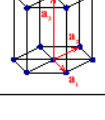
Electroneutrality: $n [v_O^{\bullet\bullet}] = [v_M^{2n/}]$ since net charge remains constant

Site balance: $[v_M^{2n/}] + [M_M^x] = [M] = \text{const.}$ and $[v_O^{\bullet\bullet}] + [O_O^x] = [O] = \text{const.}$

Therefore $K = [v_M^{2n/}][v_O^{\bullet\bullet}]^n \Rightarrow K = n [v_O^{\bullet\bullet}]^{n+1} \Rightarrow [v_O^{\bullet\bullet}] = \left(\frac{K}{n}\right)^{1/(n+1)}$.

13.2.6. Bravais Lattices

The Bravais lattices fall into seven main classes:

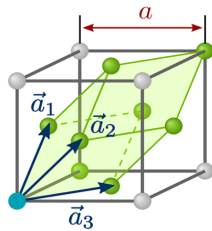
	Sides, Angles	Simple (Primitive, P)	Body Centred (I)	Base Centred (C)	Face Centred (F)
Triclinic	$a \neq b \neq c$ $\alpha \neq \beta \neq \gamma$				
Monoclinic	$a \neq b \neq c$ $\beta = \gamma = 90^\circ$, $\alpha \neq 90^\circ$				
Orthorhombic	$a \neq b \neq c$ $\alpha = \beta = \gamma = 90^\circ$				
Tetragonal	$a = b \neq c$ $\alpha = \beta = \gamma = 90^\circ$				
Trigonal	$a = b = c$ $\alpha = \beta = \gamma < 120^\circ$				
Cubic	$a = b = c$ $\alpha = \beta = \gamma = 90^\circ$				
Hexagonal	$a = b \neq c$ $\alpha = 120^\circ$ $\beta = \gamma = 90^\circ$				

13.2.7. Reciprocal Lattices and Brillouin Zones

Wigner-Seitz Primitive Unit Cell: a new unit cell with reduced size based on Voronoi partitioning. The Wigner-Seitz primitive unit cell is the Voronoi tessellation (regions closest to each lattice point: Section 2.3.15) of a given set of lattice points. It is the smallest possible unit cell choice. It can be constructed as the region enclosed by the perpendicular bisector planes to all nearest-neighbour lattice points. Primitive cubic → cubic; BCC → truncated octahedron; FCC → rhombic dodecahedron.

Reciprocal space (k-space): for a given Bravais lattice, define a set of primitive translation vectors $\{\mathbf{a}_1, \mathbf{a}_2, \mathbf{a}_3\}$ such that any lattice point in the Bravais lattice can be written in the form $\mathbf{r} = m\mathbf{a}_1 + n\mathbf{a}_2 + o\mathbf{a}_3$ where (m, n, o) are integers. The corresponding reciprocal lattice is composed of translation vectors $\{\mathbf{b}_1, \mathbf{b}_2, \mathbf{b}_3\}$ (or labelled $\{\mathbf{k}_x, \mathbf{k}_y, \mathbf{k}_z\}$ in quantum mechanics with spatial frequency and momentum as the Fourier transform of position), where:

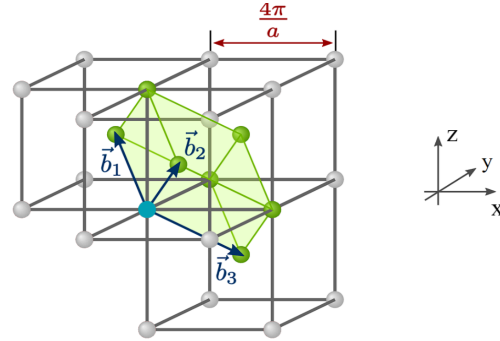
$$\mathbf{b}_1 = \frac{2\pi}{V}(\mathbf{a}_2 \times \mathbf{a}_3), \quad \mathbf{b}_2 = \frac{2\pi}{V}(\mathbf{a}_3 \times \mathbf{a}_1), \quad \mathbf{b}_3 = \frac{2\pi}{V}(\mathbf{a}_1 \times \mathbf{a}_2), \quad V = |\mathbf{a}_1 \cdot (\mathbf{a}_2 \times \mathbf{a}_3)|: \text{unit cell volume}$$



Bravais lattice:

FCC, lattice spacing a

Primitive translation vectors: $\{\mathbf{a}_1, \mathbf{a}_2, \mathbf{a}_3\}$

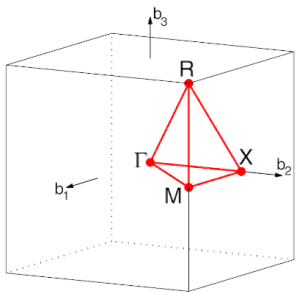


Reciprocal lattice:

BCC, lattice spacing $4\pi/a$

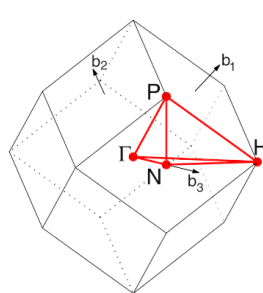
Primitive translation vectors: $\{\mathbf{b}_1, \mathbf{b}_2, \mathbf{b}_3\}$

First Brillouin Zones: Wigner-Seitz unit cell of the **reciprocal** (wavenumber) lattice unit cell. The Brillouin zone indicates the periodicity of the lattice as a function of direction. More isotropic lattices have more spherical Brillouin zones. The **irreducible Brillouin zone (IBZ)** is a smaller unit cell that exploits more symmetries, shown in red below. The n th Brillouin zone is constructed using the n th nearest neighbours in constructing the WS unit cell instead of the nearest.



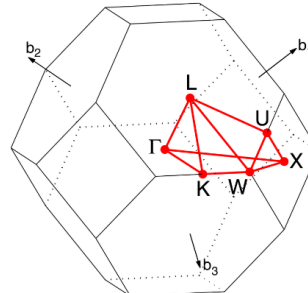
Primitive Cubic

Reciprocal lattice: cubic
First Brillouin zone: cube



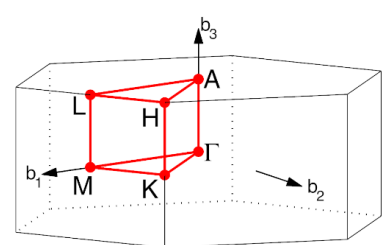
Body-centred Cubic (BCC)

Reciprocal lattice: FCC
First Brillouin zone: rhombic dodecahedron



Face-centred Cubic (FCC)

Reciprocal lattice: BCC
First Brillouin zone: truncated octahedron



Primitive Hexagonal (HCP)

Reciprocal lattice: HCP
First Brillouin zone: hexagonal prism

13.2.8. Miller Indices, k -Space and X-ray Diffraction of Lattices

Consider a coordinate system with axes parallel to the basis vectors $\{\mathbf{a}_1, \mathbf{a}_2, \mathbf{a}_3\}$ of a Bravais lattice. Let the lengths of a unit cell along these directions be $\{a, b, c\}$.

Miller index notation: the notation $[hkl]$ can, depending on context, represent either:

- the **plane** intersecting the three axes at positions $\left[\frac{a}{h}, \frac{b}{k}, \frac{c}{l}\right]$ along each axis. A Miller index is taken as zero if the plane is parallel to the axis i.e. intersects at infinity. A Miller index is represented with an overbar if it intersects at a negative ordinate e.g. $-1 \rightarrow \bar{1}$.
- the **line** which passes through the origin and has direction vector $[h, k, l]$, which is a normal vector to the above plane.

Spacing between adjacent parallel planes $[hkl]$ in adjacent unit cells: $\frac{1}{d^2} = \frac{h^2}{a^2} + \frac{k^2}{b^2} + \frac{l^2}{c^2}$

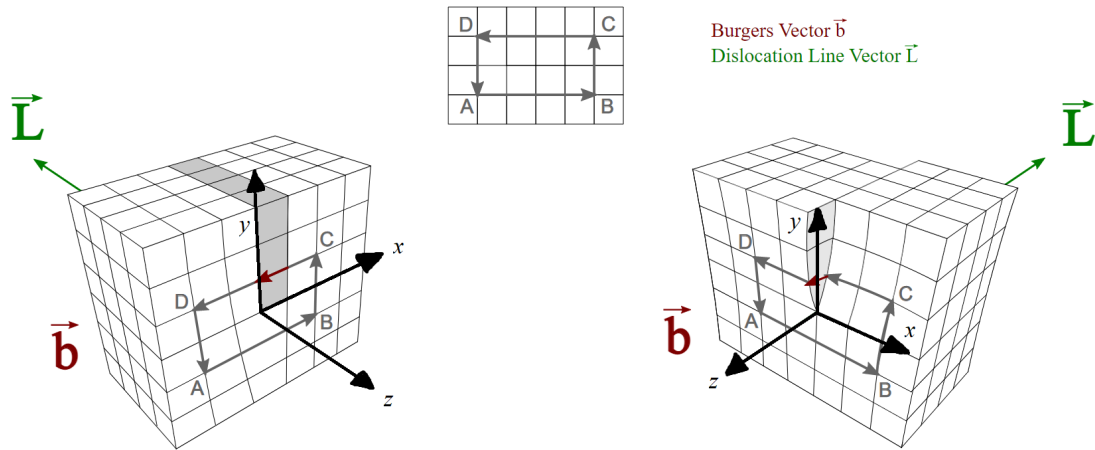
Vector equation of planes: $\mathbf{r} \cdot \left[\frac{h}{a}, \frac{k}{b}, \frac{l}{c}\right] = 1$. (see also Section 2.4.6.)

Symmetry-adapted extension to HCP lattices: use four basis vectors so that the plane $[hkl]$ in $\{\mathbf{a}, \mathbf{b}, \mathbf{d}\}$ space becomes $[hkil]$ in $\{\mathbf{a}, \mathbf{b}, \mathbf{c}, \mathbf{d}\}$ space, where $i = -(h + k)$, and \mathbf{c} is the third vector in the hexagonal plane such that $(\mathbf{a}, \mathbf{b}, \mathbf{c})$ are separated by 120° and $\mathbf{c} \perp \mathbf{d}$. In this new basis, all symmetry-related planes and lines have Miller indices which are permutations, like the cubic lattices.

X-Ray Diffractometry: diffraction pattern has peaks at the reciprocal lattice points

- Bragg's law of diffraction: $n\lambda = 2d \sin \theta$
(n : order of diffraction, λ : beam wavelength, θ : glancing angle of incidence)
- Laue equations: $\Delta \mathbf{k} \cdot \mathbf{a}_1 = 2\pi h$; $\Delta \mathbf{k} \cdot \mathbf{b}_2 = 2\pi k$; $\Delta \mathbf{k} \cdot \mathbf{c}_3 = 2\pi l$
($\Delta \mathbf{k} = \mathbf{k}_{\text{out}} - \mathbf{k}_{\text{in}}$: scattering vector / transferred wavevector, such that the X-ray can be represented as $\mathbf{E}(\mathbf{x}, t) = \mathbf{E}_0 \cos(\omega t - \mathbf{k} \cdot \mathbf{x} + \varphi)$.)

13.2.9. Stress Fields due to Dislocations



Edge Dislocation ($\mathbf{b} = -a \mathbf{i}$)

Screw Dislocation ($\mathbf{b} = a \mathbf{k}$)

$$\sigma_{xx} = - \frac{Gby(3x^2 + y^2)}{2\pi(1 - \nu)(x^2 + y^2)^2}$$

$$\sigma_{yy} = - \frac{Gby(x^2 - y^2)}{2\pi(1 - \nu)(x^2 + y^2)^2}$$

$$\sigma_{zz} = \frac{Gby}{\pi(1 - \nu)(x^2 + y^2)^2}$$

$$\tau_{xy} = \tau_{yx} = - \frac{Gbx(x^2 - y^2)}{2\pi(1 - \nu)(x^2 + y^2)^2}$$

$$\tau_{xz} = \tau_{zx} = \tau_{yz} = \tau_{zy} = 0$$

$$\tau_{xz} = \tau_{zx} = \frac{Gby}{2\pi(x^2 + y^2)} = \frac{Gb \sin \theta}{2\pi r}$$

$$\tau_{yz} = \tau_{zy} = \frac{Gbx}{2\pi(x^2 + y^2)} = \frac{Gb \cos \theta}{2\pi r}$$

$$\sigma_{xx} = \sigma_{yy} = \sigma_{zz} = \tau_{xy} = \tau_{yx} = 0$$

(ν : Poisson's ratio, G : shear modulus)

compressive stresses for $y > 0$ and
tensile stresses for $y < 0$

For macroscopic results involving dislocations, including external stress fields, see Section 6.6.1.

13.2.10. Crystallographic Point Group Notation (Schönflies Notation)

A point group identifies the ways to transform a molecule or crystal lattice such that the overall arrangement of the atoms is unchanged.

Symmetry elements and operations:

Element	Symbol	Operation
Identity (all space)	E	Do nothing
Mirror Plane (plane)	σ	Reflection (σ_h : plane of highest order rotation, σ_v : plane containing highest order rotational axis, σ_d : vertical plane cutting bonds only)
Proper Rotation Axis (line)	C_n	Proper Rotation (n : rotation by $360^\circ/n$)
Improper Rotation Axis (line)	S_n	Improper Rotation / Rotoinversion ($S_n^{(m)}$ rotation followed by reflection σ_h)
Inversion Centre (point)	i	Inversion (i.e. S_2)

Symmetry species (Γ)

Mulliken symbol	Description	Mulliken symbol	Description
A	Symmetric with respect to principal axis	g	Symmetric to inversion
B	Antisymmetric with respect to principal axis	u	Antisymmetric to inversion
E	Doubly degenerate	X'	Symmetric to σ_h
T	Triply degenerate	X''	Antisymmetric to σ_h
X_1	Symmetric to C_2 rotation perpendicular to principal axis		
X_2	Antisymmetric to the C_2 rotation perpendicular to principal axis		

13.2.11. Character Tables for Point Groups

The point groups are generated by the quotient of the space groups by the Bravais lattices.

$n = 2$ point groups:

C_i	E	i	
A_g	1	1	$R_x; R_y; R_z \quad x^2; y^2; z^2; xy; xz; yz$
A_u	1	-1	$x; y; z$

C_s	E	σ_h	
A'	1	1	$x; y \quad R_z \quad x^2; y^2; z^2; xy$
A''	1	-1	$z \quad R_x; R_y \quad xz; yz$

C_2	E	C_2^z	
A	1	1	$z \quad R_z \quad x^2; y^2; z^2; xy$
B	1	-1	$x; y \quad R_x; R_y \quad xz; yz$

C_{2v}	E	C_2^z	σ^{xz}	σ^{yz}	
A_1	1	1	1	1	$z \quad x^2; y^2; z^2$
A_2	1	1	-1	-1	$R_z \quad xy$
B_1	1	-1	1	-1	$x \quad R_y \quad xz$
B_2	1	-1	-1	1	$y \quad R_x \quad yz$

C_{2h}	E	C_2^z	i	σ^{xy}	
A_g	1	1	1	1	$R_z \quad x^2; y^2; z^2; xy$
B_g	1	-1	1	-1	$R_x; R_y \quad xz; yz$
A_u	1	1	-1	-1	z
B_u	1	-1	-1	1	$x; y$

D_2	E	C_2^z	C_2^y	C_2^x	
A	1	1	1	1	$x^2; y^2; z^2$
B_1	1	1	-1	-1	$z \quad R_z \quad xy$
B_2	1	-1	1	-1	$y \quad R_y \quad xz$
B_3	1	-1	-1	1	$x \quad R_x \quad yz$

D_{2d}	E	$2S_4$	C_2^z	$2C_2'$	$2\sigma_d$	
A_1	1	1	1	1	1	$x^2 + y^2; z^2$
A_2	1	1	1	-1	-1	R_z
B_1	1	-1	1	1	-1	$x^2 - y^2$
B_2	1	-1	1	-1	1	$z \quad xy$
E	2	0	-2	0	0	$(x, y) \quad (R_x, R_y) \quad (xz, yz)$

D_{2h}	E	C_2^z	C_2^y	C_2^x	i	σ^{xy}	σ^{xz}	σ^{yz}	
A_g	1	1	1	1	1	1	1	1	$x^2; y^2; z^2$
B_{1g}	1	1	-1	-1	1	1	-1	-1	$R_z \quad xy$
B_{2g}	1	-1	1	-1	1	-1	1	-1	$R_y \quad xz$
B_{3g}	1	-1	-1	1	1	-1	-1	1	$R_x \quad yz$
A_u	1	1	1	1	-1	-1	-1	-1	
B_{1u}	1	1	-1	-1	-1	-1	1	1	z
B_{2u}	1	-1	1	-1	-1	1	-1	1	y
B_{3u}	1	-1	-1	1	-1	1	1	-1	x

$n = 3$ point groups:

C_3	E	C_3	C_3^2	$\omega = \exp(2\pi i/3)$
A	1	1	1	$z \quad R_z \quad x^2 + y^2; z^2$
$E \left\{ \right.$	1	ω	ω^2	$x - iy \quad R_x - iR_y \quad xz - iyz; x^2 + 2ixy - y^2$
	1	ω^2	ω	$x + iy \quad R_x + iR_y \quad xz + iyz; x^2 - 2ixy - y^2$

C_{3v}	E	$2C_3$	$3\sigma_v$	
A_1	1	1	1	$z \quad x^2 + y^2; z^2$
A_2	1	1	-1	R_z
E	2	-1	0	$(x, y) \quad (R_x, R_y) \quad (xz, yz); (x^2 - y^2, 2xy)$

D_3	E	$2C_3$	$3C_2$	
A_1	1	1	1	$x^2 + y^2; z^2$
A_2	1	1	-1	$z \quad R_z$
E	2	-1	0	$(x, y) \quad (R_x, R_y) \quad (xz, yz); (x^2 - y^2, 2xy)$

D_{3d}	E	$2C_3$	$3C_2$	i	$2S_6$	$3\sigma_d$	
A_{1g}	1	1	1	1	1	1	$x^2 + y^2; z^2$
A_{2g}	1	1	-1	1	1	-1	R_z
E_g	2	-1	0	2	-1	0	$(R_x, R_y) \quad (xz, yz); (x^2 - y^2, 2xy)$
A_{1u}	1	1	1	-1	-1	-1	
A_{2u}	1	1	-1	-1	-1	1	z
E_u	2	-1	0	-2	1	0	(x, y)

D_{3h}	E	$2C_3$	$3C_2$	σ_h	$2S_3$	$3\sigma_v$	
A_1'	1	1	1	1	1	1	$x^2 + y^2; z^2$
A_2'	1	1	-1	1	1	-1	R_z
E'	2	-1	0	2	-1	0	$(x, y) \quad (x^2 - y^2, 2xy)$
A_1''	1	1	1	-1	-1	-1	
A_2''	1	1	-1	-1	-1	1	z
E''	2	-1	0	-2	1	0	$(R_x, R_y) \quad (xz, yz)$

$n = 4$ point groups:

C_{4v}	E	$2C_4$	C_4^2	$2\sigma_v$	$2\sigma_d$	
A_1	1	1	1	1	1	z $x^2 + y^2; z^2$
A_2	1	1	1	-1	-1	R_z
B_1	1	-1	1	1	-1	$x^2 - y^2$
B_2	1	-1	1	-1	1	xy
E	2	0	-2	0	0	(x, y) (R_x, R_y) (xz, yz)

Note: The σ_v planes in C_{4v} coincide with the xz and yz planes.

\mathcal{D}_{4h}	E	$2C_4$	C_4^2	$2C_2$	$2C_2'$	i	$2S_4$	σ_h	$2\sigma_v$	$2\sigma_d$	
A_{1g}	1	1	1	1	1	1	1	1	1	1	$x^2 + y^2; z^2$
A_{2g}	1	1	1	-1	-1	1	1	1	-1	-1	R_z
B_{1g}	1	-1	1	1	-1	1	-1	1	1	-1	$x^2 - y^2$
B_{2g}	1	-1	1	-1	1	1	-1	1	-1	1	xy
E_g	2	0	-2	0	0	2	0	-2	0	0	(R_x, R_y) (xz, yz)
A_{1u}	1	1	1	1	1	-1	-1	-1	-1	-1	z
A_{2u}	1	1	1	-1	-1	-1	-1	-1	1	1	
B_{1u}	1	-1	1	1	-1	-1	1	-1	-1	1	
B_{2u}	1	-1	1	-1	1	-1	1	-1	1	-1	
E_u	2	0	-2	0	0	-2	0	2	0	0	(x, y)

Note: The C_2 axes in \mathcal{D}_{4h} coincide with the x and y axes, and the σ_v planes with the xz and yz planes.

 $n = 5$ point groups:

Note that the quantities $\eta_{\pm} \equiv \frac{1}{2}(\sqrt{5} \pm 1)$ satisfy $\eta_{\pm}^2 = 1 \pm \eta_{\pm}$ and $\eta_+ \eta_- = 1$.

C_{5v}	E	$2C_5$	$2C_5^2$	$5\sigma_v$	$\eta_{\pm} = \frac{1}{2}(\sqrt{5} \pm 1)$
A_1	1	1	1	1	z $x^2 + y^2; z^2$
A_2	1	1	1	-1	R_z
E_1	2	η_-	$-\eta_+$	0	(x, y) (R_x, R_y) (xz, yz)
E_2	2	$-\eta_+$	η_-	0	$(x^2 - y^2, 2xy)$

\mathcal{D}_5	E	$2C_5$	$2C_5^2$	$5C_2$	$\eta_{\pm} = \frac{1}{2}(\sqrt{5} \pm 1)$
A_1	1	1	1	1	$x^2 + y^2; z^2$
A_2	1	1	1	-1	z R_z
E_1	2	η_-	$-\eta_+$	0	(x, y) (R_x, R_y) (xz, yz)
E_2	2	$-\eta_+$	η_-	0	$(x^2 - y^2, 2xy)$

\mathcal{D}_{5d}	E	$2C_5$	$2C_5^2$	$5C_2$	i	$2S_{10}^3$	$2S_{10}$	$5\sigma_d$	$\eta_{\pm} = \frac{1}{2}(\sqrt{5} \pm 1)$
A_{1g}	1	1	1	1	1	1	1	1	$x^2 + y^2; z^2$
A_{2g}	1	1	1	-1	1	1	1	-1	R_z
E_{1g}	2	η_-	$-\eta_+$	0	2	η_-	$-\eta_+$	0	(R_x, R_y) (xz, yz)
E_{2g}	2	$-\eta_+$	η_-	0	2	$-\eta_+$	η_-	0	$(x^2 - y^2, 2xy)$
A_{1u}	1	1	1	1	-1	-1	-1	-1	z
A_{2u}	1	1	1	-1	-1	-1	-1	1	
E_{1u}	2	η_-	$-\eta_+$	0	-2	$-\eta_-$	η_+	0	(x, y)
E_{2u}	2	$-\eta_+$	η_-	0	-2	η_+	$-\eta_-$	0	

\mathcal{D}_{5h}	E	$2C_5$	$2C_5^2$	$5C_2$	σ_h	$2S_5$	$2S_5^3$	$5\sigma_v$	$\eta_{\pm} = \frac{1}{2}(\sqrt{5} \pm 1)$
A_1'	1	1	1	1	1	1	1	1	$x^2 + y^2; z^2$
A_2'	1	1	1	-1	1	1	1	-1	R_z
E_1'	2	η_-	$-\eta_+$	0	2	η_-	$-\eta_+$	0	(x, y)
E_2'	2	$-\eta_+$	η_-	0	2	$-\eta_+$	η_-	0	$(x^2 - y^2, 2xy)$
A_1''	1	1	1	1	-1	-1	-1	-1	z
A_2''	1	1	1	-1	-1	-1	-1	1	
E_1''	2	η_-	$-\eta_+$	0	-2	$-\eta_-$	η_+	0	(R_x, R_y) (xz, yz)
E_2''	2	$-\eta_+$	η_-	0	-2	η_+	$-\eta_-$	0	

$n = 6$ point groups:

C_{6v}	E	$2C_6$	$2C_6^2$	C_6^3	$3\sigma_v$	$3\sigma_d$	
A_1	1	1	1	1	1	1	z $x^2 + y^2; z^2$
A_2	1	1	1	1	-1	-1	R_z
B_1	1	-1	1	-1	1	-1	
B_2	1	-1	1	-1	-1	1	
E_1	2	1	-1	-2	0	0	(x,y) (R_x, R_y) (xz, yz)
E_2	2	-1	-1	2	0	0	$(x^2 - y^2, 2xy)$

D_6	E	$2C_6$	$2C_6^2$	C_6^3	$3C_2$	$3C_2'$	
A_1	1	1	1	1	1	1	$x^2 + y^2; z^2$
A_2	1	1	1	1	-1	-1	z R_z
B_1	1	-1	1	-1	1	-1	
B_2	1	-1	1	-1	-1	1	
E_1	2	1	-1	-2	0	0	(x,y) (R_x, R_y) (xz, yz)
E_2	2	-1	-1	2	0	0	$(x^2 - y^2, 2xy)$

D_{6h}	E	$2C_6$	$2C_6^2$	C_6^3	$3C_2$	$3C_2'$	i	$2S_3$	$2S_6$	σ_h	$3\sigma_d$	$3\sigma_v$	
A_{1g}	1	1	1	1	1	1	1	1	1	1	1	1	$x^2 + y^2; z^2$
A_{2g}	1	1	1	1	-1	-1	1	1	1	1	-1	-1	R_z
B_{1g}	1	-1	1	-1	1	-1	1	-1	1	-1	1	-1	
B_{2g}	1	-1	1	-1	-1	1	1	-1	1	-1	-1	1	
E_{1g}	2	1	-1	-2	0	0	2	1	-1	-2	0	0	(R_x, R_y) (xz, yz)
E_{2g}	2	-1	-1	2	0	0	2	-1	-1	2	0	0	$(x^2 - y^2, 2xy)$
A_{1u}	1	1	1	1	1	1	-1	-1	-1	-1	-1	-1	
A_{2u}	1	1	1	1	-1	-1	-1	-1	-1	-1	1	1	z
B_{1u}	1	-1	1	-1	1	-1	-1	1	-1	1	-1	1	
B_{2u}	1	-1	1	-1	-1	1	-1	1	-1	1	1	-1	
E_{1u}	2	1	-1	-2	0	0	-2	-1	1	2	0	0	(x,y)
E_{2u}	2	-1	-1	2	0	0	-2	1	1	-2	0	0	

Cubic symmetry:

T	E	$4C_3$	$4C_3^2$	$3C_2$	$\omega = \exp(2\pi i/3)$
A_1	1	1	1	1	$x^2 + y^2 + z^2$
E {	1	ω	ω^2	1	$z^2 + \omega^2 x^2 + \omega y^2$
	1	ω^2	ω	1	$z^2 + \omega x^2 + \omega^2 y^2$
T_2	3	0	0	-1	(x,y,z) (R_x, R_y, R_z) (yz, xz, xy)

T_d	E	$8C_3$	$3C_2$	$6S_4$	$6\sigma_d$	
A_1	1	1	1	1	1	$x^2 + y^2 + z^2$
A_2	1	1	1	-1	-1	
E	2	-1	2	0	0	$((2z^2 - x^2 - y^2), \sqrt{3}(x^2 - y^2))$
T_1	3	0	-1	1	-1	(R_x, R_y, R_z)
T_2	3	0	-1	-1	1	(x,y,z) (yz, xz, xy)

O	E	$8C_3$	$3C_2^2$	$6C_4$	$6C_2$	
A_1	1	1	1	1	1	$x^2 + y^2 + z^2$
A_2	1	1	1	-1	-1	
E	2	-1	2	0	0	$((2z^2 - x^2 - y^2), \sqrt{3}(x^2 - y^2))$
T_1	3	0	-1	1	-1	(x,y,z) (R_x, R_y, R_z)
T_2	3	0	-1	-1	1	(xz, xy, yz)

O_h	E	$8C_3$	$3C_2^2$	$6C_4$	$6C_2$	i	$8S_6$	$3\sigma_h$	$6S_4$	$6\sigma_d$	
A_{1g}	1	1	1	1	1	1	1	1	1	1	$x^2 + y^2 + z^2$
A_{2g}	1	1	1	-1	-1	1	1	1	-1	-1	
E_g	2	-1	2	0	0	2	-1	2	0	0	$((2z^2 - x^2 - y^2), \sqrt{3}(x^2 - y^2))$
T_{1g}	3	0	-1	1	-1	3	0	-1	1	-1	(R_x, R_y, R_z)
T_{2g}	3	0	-1	-1	1	3	0	-1	-1	1	(xz, xy, yz)
A_{1u}	1	1	1	1	1	-1	-1	-1	-1	-1	
A_{2u}	1	1	1	-1	-1	-1	-1	-1	1	1	
E_u	2	-1	2	0	0	-2	1	-2	0	0	
T_{1u}	3	0	-1	1	-1	-3	0	1	-1	1	(x,y,z)
T_{2u}	3	0	-1	-1	1	-3	0	1	1	-1	

Icosahedral symmetry:

I_h	E	$12C_5$	$12C_5^2$	$20C_3$	$15C_2$	i	$12S_{10}^3$	$12S_{10}$	$20S_6$	15σ	$\eta_{\pm} = \frac{1}{2}(\sqrt{5} \pm 1)$
A_g	1	1	1	1	1	1	1	1	1	1	$x^2 + y^2 + z^2$
T_{1g}	3	η_+	$-\eta_-$	0	-1	3	η_+	$-\eta_-$	0	-1	(R_x, R_y, R_z)
T_{2g}	3	$-\eta_-$	η_+	0	-1	3	$-\eta_-$	η_+	0	-1	
G_g	4	-1	-1	1	0	4	-1	-1	1	0	
H_g	5	0	0	-1	1	5	0	0	-1	1	$(\sqrt{\frac{1}{12}}(2z^2 - x^2 - y^2), \frac{1}{2}(x^2 - y^2), xz, xy, yz)$
A_u	1	1	1	1	1	-1	-1	-1	-1	-1	
T_{1u}	3	η_+	$-\eta_-$	0	-1	-3	$-\eta_+$	η_-	0	1	(x,y,z)
T_{2u}	3	$-\eta_-$	η_+	0	-1	-3	η_-	$-\eta_+$	0	1	
G_u	4	-1	-1	1	0	-4	1	1	-1	0	
H_u	5	0	0	-1	1	-5	0	0	1	-1	

Linear symmetry:

$C_{\infty v}$	E	$2C^z(\alpha)$	\dots	$\infty\sigma_v$	
Σ^+ (A_1)	1	1	\dots	1	z $x^2 + y^2; z^2$
Σ^- (A_2)	1	1	\dots	-1	R_z
Π (E_1)	2	$2\cos\alpha$	\dots	0	(x,y) (R_x, R_y) (xz, yz)
Δ (E_2)	2	$2\cos 2\alpha$	\dots	0	$(x^2 - y^2, 2xy)$
Φ (E_3)	2	$2\cos 3\alpha$	\dots	0	
\dots	\dots	\dots	\dots	\dots	

$D_{\infty h}$	E	$2C^z(\alpha)$	\dots	$\infty\sigma_v$	i	$2S^z(\alpha)$	\dots	∞C_2	
Σ_g^+ (A_{1g})	1	1	\dots	1	1	1	\dots	1	$x^2 + y^2; z^2$
Σ_g^- (A_{2g})	1	1	\dots	-1	1	1	\dots	-1	R_z
Π_g (E_{1g})	2	$2\cos\alpha$	\dots	0	2	$-2\cos\alpha$	\dots	0	(R_x, R_y) (xz, yz)
Δ_g (E_{2g})	2	$2\cos 2\alpha$	\dots	0	2	$2\cos 2\alpha$	\dots	0	$(x^2 - y^2, 2xy)$
Φ_g (E_{3g})	2	$2\cos 3\alpha$	\dots	0	2	$-2\cos 3\alpha$	\dots	0	
\dots	\dots	\dots	\dots	\dots	\dots	\dots	\dots	\dots	
Σ_u^+ (A_{1u})	1	1	\dots	1	-1	-1	\dots	-1	z
Σ_u^- (A_{2u})	1	1	\dots	-1	-1	-1	\dots	1	
Π_u (E_{1u})	2	$2\cos\alpha$	\dots	0	-2	$2\cos\alpha$	\dots	0	(x,y)
Δ_u (E_{2u})	2	$2\cos 2\alpha$	\dots	0	-2	$-2\cos 2\alpha$	\dots	0	
Φ_u (E_{3u})	2	$2\cos 3\alpha$	\dots	0	-2	$2\cos 3\alpha$	\dots	0	
\dots	\dots	\dots	\dots	\dots	\dots	\dots	\dots	\dots	

13.2.12. Tables for Descent in Symmetry

C_{2v}	C_2	C_s (E, σ^{xz})	C_s (E, σ^{yz})
A_1	A	A'	A'
A_2	A	A''	A''
B_1	B	A'	A''
B_2	B	A''	A'

D_{3h}	C_{3v}	C_{2v} ($\sigma_h \rightarrow \sigma^{xz}$)	C_s (E, σ_h)	C_s (E, σ_v)
A'_1	A_1	A_1	A'	A'
A'_2	A_2	B_2	A'	A''
E'	E	$A_1 \oplus B_2$	$2A'$	$A' \oplus A''$
A''_1	A_2	A_2	A''	A''
A''_2	A_1	B_1	A''	A'
E''	E	$A_2 \oplus B_1$	$2A''$	$A' \oplus A''$

$D_{\infty h}$ (x,y,z) \rightarrow	C_{2v} (x,z,y)
Σ_g^+	A_1
Σ_g^-	B_1
Π_g	$A_2 \oplus B_2$
Δ_g	$A_1 \oplus B_1$
\dots	\dots
Σ_u^+	B_2
Σ_u^-	A_2
Π_u	$A_1 \oplus B_1$
Δ_u	$A_2 \oplus B_2$
\dots	\dots

$O(3)$	O_h	T_d
S_g	A_{1g}	A_1
P_g	T_{1g}	T_1
D_g	$E_g \oplus T_{2g}$	$E \oplus T_2$
F_g	$A_{2g} \oplus T_{1g} \oplus T_{2g}$	$A_2 \oplus T_1 \oplus T_2$
G_g	$A_{1g} \oplus E_g \oplus T_{1g} \oplus T_{2g}$	$A_1 \oplus E \oplus T_1 \oplus T_2$
\dots	\dots	\dots
S_u	A_{1u}	A_2
P_u	T_{1u}	T_2
D_u	$E_u \oplus T_{2u}$	$E \oplus T_1$
F_u	$A_{2u} \oplus T_{1u} \oplus T_{2u}$	$A_1 \oplus T_2 \oplus T_1$
G_u	$A_{1u} \oplus E_u \oplus T_{1u} \oplus T_{2u}$	$A_2 \oplus E \oplus T_2 \oplus T_1$
\dots	\dots	\dots

13.2.13. Reduction of Representation and Products of Group Operations

Reduction of Representation: If $\Gamma = a_1\Gamma^{(1)} \oplus a_2\Gamma^{(2)} \oplus \dots \oplus a_n\Gamma^{(n)}$ then

$$a_k = \frac{1}{h} \sum_R \chi^{(k)}(R)^* \chi(R)$$

($\chi(R)$: character of the operation R in the representation Γ , $\chi^{(k)}(R)$: character of the operation R in the representation $\Gamma^{(k)}$, h : number of elements in the group)

Projection Operators: The projection operator for representation $\Gamma^{(k)}$ is

$$\mathcal{P}^{(k)} = \frac{n_k}{h} \sum_R \chi^{(k)}(R)^* R.$$

The projected function $\mathcal{P}^{(k)}f$ (obtained by applying $\mathcal{P}^{(k)}$ to any function f) is either zero or a component for the basis for $\Gamma^{(k)}$.

Direct Products: In general, $\chi^{\Gamma \otimes \Gamma'}(R) = \chi^\Gamma(R) \chi^{\Gamma'}(R)$ and if the resulting representation is reducible it can be reduced in the usual way. Alternatively the following rules can be applied:

- Treat g/u and $'/'$ symmetry separately. For groups with an inversion centre,

$$g \otimes g = u \otimes u = g \quad \text{and} \quad g \otimes u = u.$$

- For groups with a horizontal plane σ_h but no inversion centre, the notation $'$ and $''$ denotes symmetry and antisymmetry with respect to σ_h . Then,

$$' \otimes ' = '' \otimes '' = ' \quad \text{and} \quad ' \otimes '' = ''.$$

- Direct products involving non-degenerate representations are easily worked out from the character table. The product of any A or B with any E is an E , and likewise the product of any A or B with any T is a T . In the cubic groups T_d , O and O_h ,

$$E \otimes E = A_1 \oplus A_2 \oplus E$$

$$E \otimes T_1 = E \otimes T_2 = T_1 \oplus T_2$$

$$T_1 \otimes T_1 = T_2 \otimes T_2 = A_1 \oplus E \oplus T_1 \oplus T_2$$

$$T_1 \otimes T_2 = A_2 \oplus E \oplus T_1 \oplus T_2$$

See the next page for direct products in axial groups.

Direct Products in Axial Groups: For products of E_i with E_j in the axial groups, the rules are more complicated. If there is only one E representation, apart from g/u or $'/'$ labels, it should be considered as E_1 . The order n of the principal axis is usually obvious e.g. 5 for D_{5h} - **but** for D_{md} with m even, $n = 2m$ (because D_{md} has an S_{2m} axis when m is even).

- For $E_i \otimes E_i$:
 - If E_{2i} exists then $E_i \otimes E_i = A_1 \oplus A_2 \oplus E_{2i}$
 - Otherwise, if $4i = n$ then $E_i \otimes E_i = A_1 \oplus A_2 \oplus B_1 \oplus B_2$
 - Otherwise $E_i \otimes E_i = A_1 \oplus A_2 \oplus E_{|2i-n|}$

- For $E_i \otimes E_j$ with $i \neq j$:
 - If E_{i+j} exists then $E_i \otimes E_j = E_{|i-j|} \oplus E_{i+j}$
 - If $2(i+j) = n$ then $E_i \otimes E_j = E_{|i-j|} \oplus B_1 \oplus B_2$
 - Otherwise $E_i \otimes E_j = E_{|i-j|} \oplus E_{|i+j-n|}$

(If there is only one A representation, apart from g/u and $'/'$ labels, read A_1 and A_2 above as A , and likewise for B .)

Antisymmetrised Squares:

The antisymmetric component of $E \otimes E$ or $E_i \otimes E_i$ is always A_2 .

In the cubic groups, the antisymmetric component of $T_1 \otimes T_1$ and $T_2 \otimes T_2$ is always T_1 .

13.2.14. Identification of IR-active and Raman-active Bonds

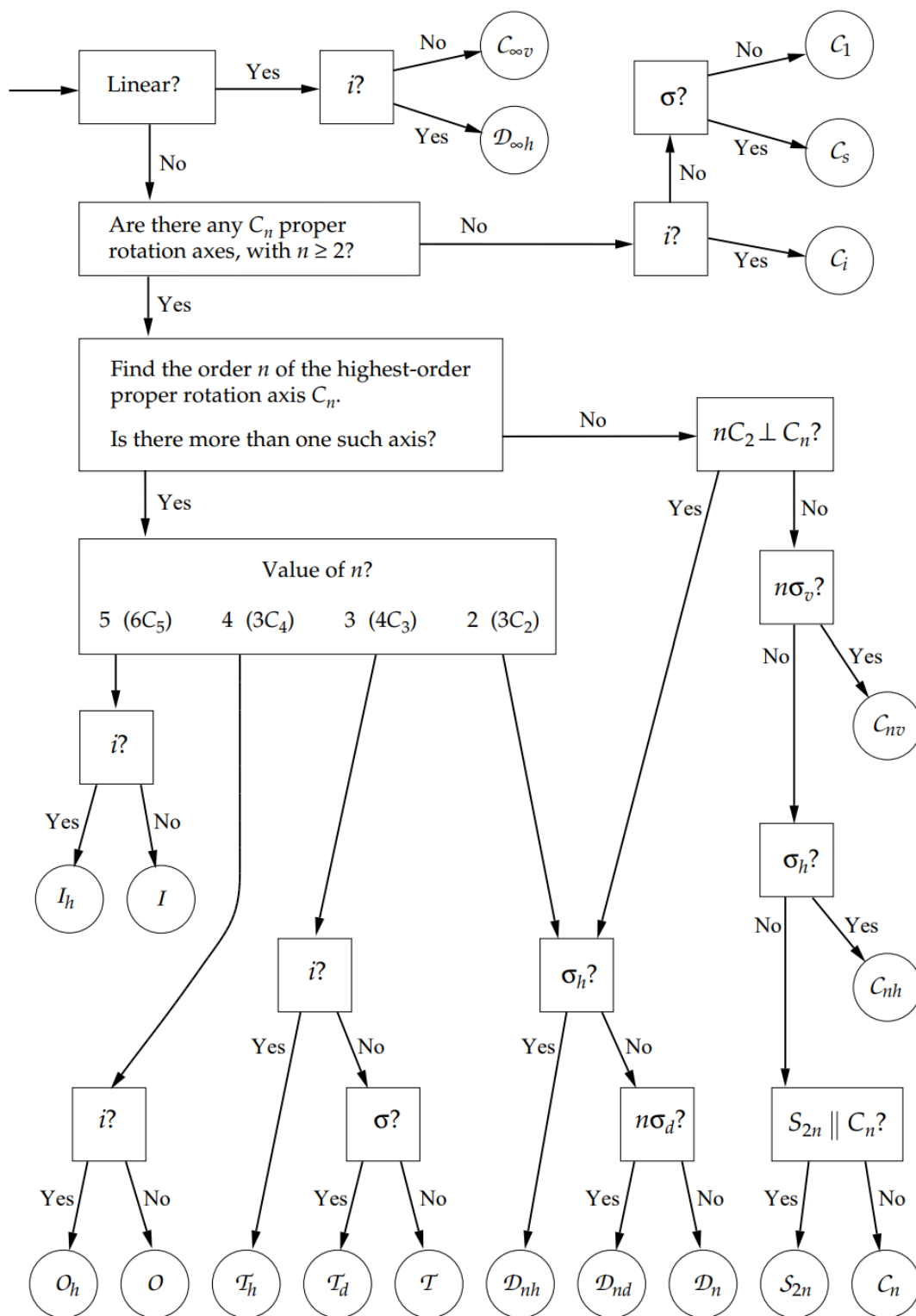
If a vibration results in the change in the molecular dipole moment, it is **IR-active**. In the character table, the vibrational modes that are IR-active are those with symmetry of the x , y and z axes (**linear terms**).

If a vibration results in a change in the molecular polarisability, it is **Raman active**. In the character table, the vibrational modes that are Raman-active are those with symmetry of any of the binary products xy , xz , yz , x^2 , y^2 , z^2 (**quadratic terms**) or a linear combination of binary products (e.g. $x^2 - y^2$).

For the IR absorbance wavenumber table, see Section 15.4.3.

13.2.15. Point Group Classification Flow Chart From Geometry

For the names of the common molecular geometries and their associated point groups, see Section 12.1.8.



13.2.16. Common Space Groups and their Equipoints

Graphic symbol	Num. symbol	Graphic symbol	Num. symbol
None	1		$\bar{1}$
	2		$2/m$
	2_1		$2_1/m$
	3		$\bar{3}$
	3_1		$\bar{4}$
	3_2		$4/m$
	4		$4_2/m$
	4_1		$\bar{6}$
	4_2		$6/m$
	4_3		$6_3/m$
	6		m
	6_1		a,b,c
	6_2		a,b,c
	6_3		n
	6_4		d
	6_5		d

The space groups comprise all rigid transformation operations, including translations. There are a total of 230 distinct space groups. The Hermann-Mauguin notation describes the lattices and some generators of the group.

Screw axis n_m : a symmetry group comprising C_n followed by a translation m/n of a unit cell parallel to the C_n axis. The rotation is defined anticlockwise when viewed down the screw axis (so that the translation moves the molecule towards the viewer).

Glide plane g : a symmetry group comprising σ followed by a translation by $1/2$ of a unit cell parallel to the plane

Enantiomorphs: screw axes with different handedness (e.g. 4_1 (right) and 4_3 (left)), which can occur when the individual species are enantiomers.

General Equivalent Positions (GEPs) and Special Equivalent Positions (SEPs)

Space Group $P2_1$: (primitive monoclinic, 2_1 screw axis along b)

- GEPs: 2, at (x_n, y_n, z_n) and $(-x_n, \frac{1}{2} + y_n, -z_n)$.
- SEPs: None.

Space Group $P2_1/c$: (with perpendicular c -glide)

- GEPs: 4, at (x_n, y_n, z_n) , $(-x_n, \frac{1}{2} + y_n, \frac{1}{2} - z_n)$, $(x_n, \frac{1}{2} - y_n, \frac{1}{2} + z_n)$, $(-x_n, -y_n, -z_n)$.
- SEPs: 4 pairs:

2 at $(0, 0, 0)$ and $(0, \frac{1}{2}, \frac{1}{2})$;	2 at $(0, 0, \frac{1}{2})$ and $(0, \frac{1}{2}, 0)$;
2 at $(\frac{1}{2}, 0, 0)$ and $(\frac{1}{2}, \frac{1}{2}, \frac{1}{2})$;	2 at $(\frac{1}{2}, \frac{1}{2}, 0)$ and $(\frac{1}{2}, 0, \frac{1}{2})$.

Space Group $P2_12_12_1$: (primitive orthorhombic, layers parallel to (010) planes)

- GEPs: 4, at (x_n, y_n, z_n) , $(-x_n, \frac{1}{2} + y_n, \frac{1}{2} - z_n)$, $(\frac{1}{2} + x_n, \frac{1}{2} - y_n, -z_n)$, $(\frac{1}{2} - x_n, -y_n, \frac{1}{2} + z_n)$.
- SEPs: None.

For the Bravais lattices and applications to XRD, see Sections 12.2.5-6.

13.3. Theory of Kinetics, Energetics and Thermodynamics

13.3.1. Macroscopic Kinetic Theory of Gases

Physical constants:

- Ideal gas constant: $\bar{R} = 8.314 \text{ J mol}^{-1} \text{ K}^{-1}$
- Avogadro's number: $N_A = 6.022 \times 10^{23} \text{ mol}^{-1}$
- Boltzmann constant: $k_B = \bar{R} / N_A = 1.3806 \times 10^{-23} \text{ J K}^{-1}$

Ideal Gases:

Macroscopic ideal gas law: $pV = n\bar{R}T$ or $pV = mRT$ or $pv = RT$ or $p = \rho RT$

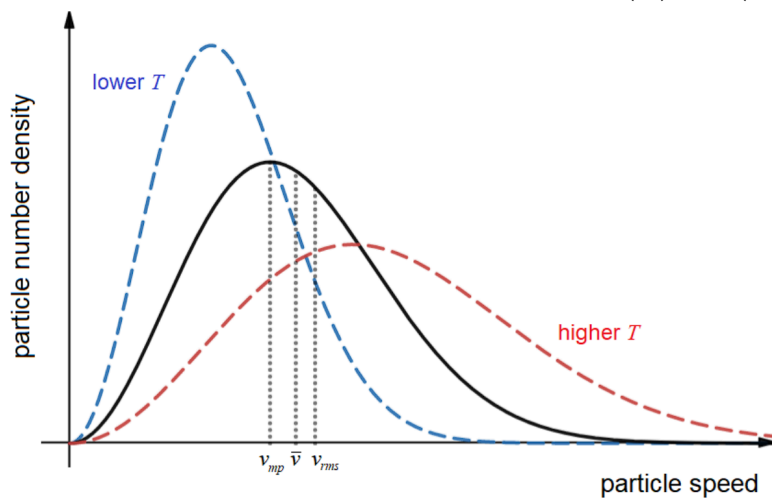
(p [Pa]: pressure, V [m^3]: volume, n [mol]: moles, T [K]: temperature, m [kg]: mass, R [$\text{J kg}^{-1} \text{ K}^{-1}$]
 $= \frac{\bar{R} [\text{J mol}^{-1} \text{ K}^{-1}]}{M_r [\text{kg mol}^{-1}]}$: mass gas constant, v [$\text{m}^3 \text{ kg}^{-1}$] = $\frac{V}{m} = \frac{1}{\rho}$: specific volume, ρ [kg m^{-3}]: density)

13.3.2. Microscopic Kinetic Theory of Gases

Microscopic ideal gas law: $pV = Nk_B T$ ($N = \frac{n}{N_A}$: number of particles)

Maxwell-Boltzmann Distribution: probabilistic distribution of particle speeds

Maxwell-Boltzmann distribution: $f_v(v) = \left(\frac{2}{\pi}\right)^{1/2} \left(\frac{m}{k_B T}\right)^{3/2} v^2 \exp\left(-\frac{mv^2}{2k_B T}\right)$ (m : particle mass)



Mode particle speed: $v_{mp} = \sqrt{\frac{2k_B T}{m}}$

Mean particle speed: $\bar{v} = \sqrt{\frac{8k_B T}{\pi m}}$

RMS particle speed: $v_{rms} = \sqrt{\frac{3k_B T}{m}}$

Macro RMS speed: $pV = \frac{1}{3}Nm(v_{rms})^2$

Mean particle kinetic energy \bar{E}_k :

$$\bar{E}_k = \frac{3}{2}k_B T = \frac{1}{2}m(v_{rms})^2 \quad (3 \text{ dof})$$

The x , y and z components of the particle velocities and momenta are all identical and independent Normal distributions: $v_x \sim N(0, k_B T / m)$.

13.3.3. Statistical Mechanics (Microscopic Thermodynamics)

Statistical mechanics assumes isolated ergodic systems at thermal equilibrium, for which each accessible microscopic state is equally likely (equipartition theorem). When two systems of different temperature are allowed to exchange energy (but not mass), they will reach the same temperature at thermal equilibrium.

- Number of microstates at a given energy: $\Omega(E)$
- For equilibrium systems A and B: $\Omega(E_A, E_B) = \Omega_A(E_A) \Omega_B(E_B)$
- Boltzmann configurational entropy: $\ln \Omega = \ln \Omega_A(E_A) + \ln \Omega_B(E - E_A)$
- Most likely state is observed: $\frac{\partial(\ln \Omega)}{\partial E_A} = 0 \Rightarrow \frac{\partial(\ln \Omega_A(E_A))}{\partial E_A} = \frac{\partial(\ln \Omega_B(E_B))}{\partial E_B} = \frac{1}{kT} = \beta$

If the states of A are $\{x\}$ and the states of B are $\{y\}$ then

- The joint probability distribution $p(x, y)$ is uniform; $p(x) = \sum_y p(x, y)$ is proportional to $\Omega_B(E_B)$.
- For a large system B ($E_B \gg E_A$), it follows that $p(x) = \frac{1}{Z} e^{-\beta E_A}$ ($Z = \sum_x e^{-\beta E_A}$: partition function)
- Total internal energy: $U = \int E(x) p(x) dx = - \frac{\partial(\ln Z)}{\partial \beta}$.

13.3.3. Properties of Gases and Gas Mixtures

Assumptions in the ideal gas model: point gas particles, elastic collisions, no inter-particle forces, large separation between particles.

Special Cases of the Ideal Gas Law:

- Boyle's law: for constant T , pV is constant.
- Charles' law: for constant p , VT^{-1} is constant.
- Gay-Lussac's law: for constant V , pT^{-1} is constant.
- Avogadro's law: for constant p and T , nV^{-1} is constant.

Effusion of Ideal Gases: diffusional flux through a hole smaller than the mean free path

Relative rates of efflux: $\frac{r_1}{r_2} = \sqrt{\frac{\rho_2}{\rho_1}} = \sqrt{\frac{M_2}{M_1}} \Leftrightarrow \rho r^2$ and Mr^2 are constant (Graham's law)

(r [mol s^{-1}]: rate of diffusion out of hole, ρ [kg m^{-3}]: gas density, M [kg mol^{-1}]: gas molar mass.)

Partial Pressure in a Gas Mixture

For a mixture containing n_i moles of gaseous species i , with total pressure P and total moles of particles N , the partial pressure p_i of species i is

$$p_i = \frac{n_i}{N} \times P \quad \Leftrightarrow \quad \frac{p_i}{P} = \frac{n_i}{N} \quad (\text{Dalton's law})$$

Many other state variables of mixtures can be partitioned in this way e.g. enthalpy, entropy, internal energy.

Degrees of Freedom for Polyatomic Gases

	DOF, f (including vibrational)	
Monatomic (He, Ne, Ar, ...):	3	(3 translational, 0 rotational, 0 vibrational)
Diatomic (H_2 , O_2 , HCl):	6	(3 translational, 2 rotational, 1 vibrational)
Triatomic, linear (CO_2):	9	(3 translational, 2 rotational, 4 vibrational)
Triatomic, nonlinear (H_2O):	9	(3 translational, 3 rotational, 3 vibrational)

Mean energy per degree of freedom = $\frac{\bar{E}}{f} = \frac{1}{2}k_B T$ (equipartition theorem)

Isobaric specific heat capacity per degree of freedom = $\frac{c_p}{f} = \frac{1}{2}R$

Adiabatic constant = $\gamma = 1 + \frac{2}{f} = \frac{c_p}{c_v}$

Note: if $300 \text{ K} < T < 600 \text{ K}$, then the vibrational mode is inactive and should **not** be counted in per-degree-of-freedom basis calculations.

13.3.4. Non-Ideal Gases

Van der Waals equation of state for non-ideal gases: $\left(p + \frac{an^2}{V^2}\right)(V - bn) = n\bar{R}T$

a represents attractive forces. $b = \frac{16}{3}N_A n\pi r^3$ represents the volume occupied by the molecules (r : radius of molecules)

Compressibility factor: $Z = \frac{pV}{nRT} = 1 + \left(b - \frac{a}{RT}\right)V^{-1} + b^2V^{-2} + b^3V^{-3} + \dots$ ($Z = 1$: ideal)

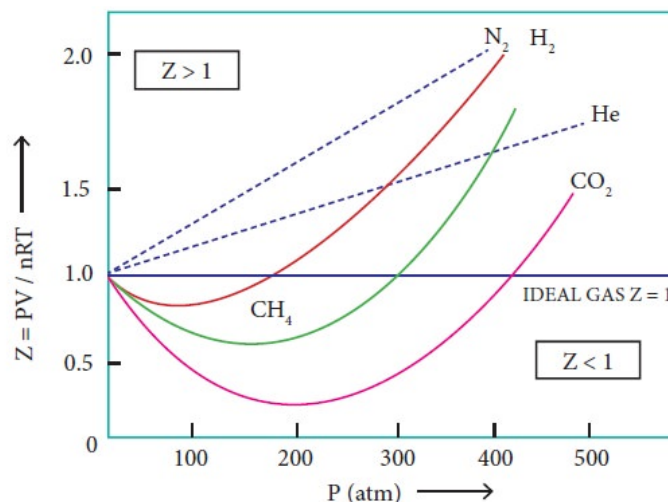
Fugacity: $f = p \exp\left(\frac{bp}{RT}\right) = p \exp\left(\frac{bnZ}{V}\right)$ ($f \rightarrow p$ as $Z \rightarrow 1$)

Activity coefficient: $\phi = \frac{f}{p} = e^{bp/\bar{R}T}$

Van der Waals constants for some gases. Note pressure units are in atm.

Substance	a [L ² atm / mol ²]	b [L / mol]	Substance	a [L ² atm / mol ²]	b [L / mol]
He	0.0341	0.02370	Cl ₂	6.49	0.0562
Ne	0.211	0.0171	H ₂ O	5.46	0.0305
Ar	1.34	0.0322	CH ₄	2.25	0.0428
Kr	2.32	0.0398	CO	1.51	0.0399
Xe	4.19	0.0510	CO ₂	3.59	0.0427
Rn	6.60	0.0624	CCl ₄	20.4	0.1383
N ₂	1.39	0.0391	NH ₃	4.23	0.0371
H ₂	0.244	0.0266	C ₂ H ₆	5.56	0.0638
O ₂	1.36	0.0318	C ₂ H ₄	4.61	0.0582

Variation of compressibility factor Z with pressure for some gases:

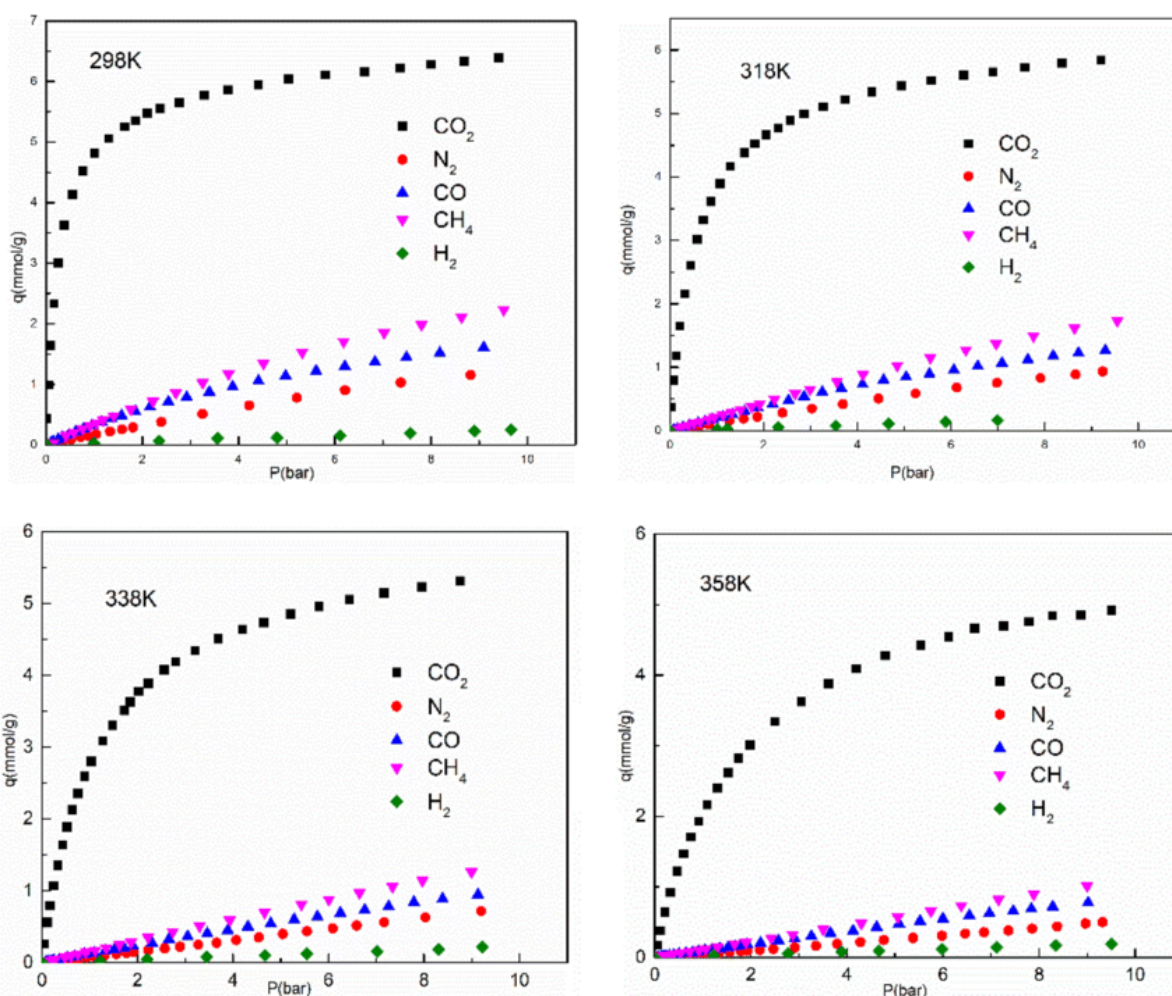


13.3.5. Freundlich Adsorption Isotherms

The extent of adsorption, $\frac{x}{m} = \frac{\text{mass (or moles) of adsorbate}}{\text{mass of adsorbent}}$, varies with pressure p at a particular temperature given by the power-law relationship:

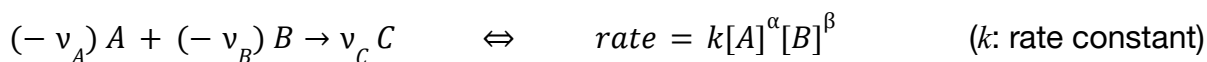
$$\frac{x}{m} = k p^{1/n} \quad n \approx 1 \text{ for } P \ll p_0; \quad n \rightarrow \infty \text{ for } P \gg p_0$$

Isotherms for adsorption of CO₂, N₂, CO, CH₄ and H₂ on NaY zeolite are shown at 298 K, 318 K, 338 K and 358 K, given in mmol adsorbate per gram adsorbent.



13.3.6. Rate Equations

Elementary reactions have rate equations in the form of a product of reactant concentrations:



Notes: (v : stoichiometric coefficient, which is **negative** for reactants)

- For elementary reactions (single step mechanism), $\alpha = -v_A$ and $\beta = -v_B$ (law of mass action).
- The overall order of reaction is $\alpha + \beta$.
- For multistep reactions, the orders may differ from the stoichiometric ratios.
- Only species in the rate limiting step of the mechanism may appear in the rate equation.
- For a homogeneous catalyst, the catalyst may appear in the rate equation.
- Note that heterogeneous catalysts (and macromolecular e.g. enzyme-catalysed) do not obey a power-law expression: for details of their kinetics see Section 13.3.4.

In differential form, the rate equations form a system of first-order nonlinear ODEs:

$$r = \frac{d[C]}{dt} = k[A]^\alpha[B]^\beta = \frac{v_C}{v_A} \frac{d[A]}{dt} = \frac{v_C}{v_B} \frac{d[B]}{dt}, \text{ initial conditions } [A]_0, [B]_0 \text{ at } t = 0$$

The system can be uncoupled into an ODE in each species by substituting from the similarity

relation $\frac{[X] - [X]_0}{[Y] - [Y]_0} = \frac{v_X}{v_Y}$ where X and Y are any two species.

Order n	ODE	Solution (integrated rate law)	Half-life $t_{1/2}$	Characteristic kinetic plot	Slope of plot	Units of k
0	$\frac{d[A]}{dt} = -k$	$[A] = [A]_0 - kt$	$\frac{[A]_0}{2k}$	$[A]$ vs t	$-k$	$\text{mol dm}^{-3} \text{s}^{-1}$
1	$\frac{d[A]}{dt} = -k[A]$	$[A] = [A]_0 e^{-kt}$	$\frac{\ln 2}{k}$	$\ln [A]$ vs t	$-k$	s^{-1}
2	$\frac{d[A]}{dt} = -k[A]^2$	$[A] = \frac{[A]_0}{1 + k[A]_0 t}$	$\frac{1}{k[A]_0}$	$1/[A]$ vs t	k	$\text{mol}^{-1} \text{dm}^3 \text{s}^{-1}$
3	$\frac{d[A]}{dt} = -k[A]^3$	$[A] = \frac{[A]_0}{\sqrt{1 + 2k[A]_0^2 t}}$	$\frac{3}{2k[A]_0}$	$1/(2[A]^2)$ vs t	k	$\text{mol}^{-2} \text{dm}^6 \text{s}^{-1}$

13.3.7. Reaction Kinetics and Transition State Theory

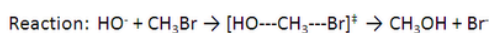
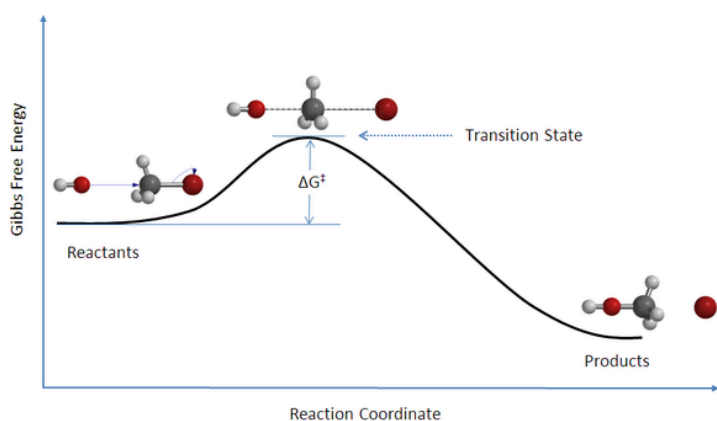
Arrhenius Equation: For a wide variety of physical and chemical processes (chemical reactions, diffusion, crystal nucleation rate, crystal growth rate, etc), the rate constant k is

$$\text{rate constant, } k = A \exp\left(-\frac{E_a}{RT}\right) \Leftrightarrow \ln k = \ln A - \frac{E_a}{RT}$$

(A : constant pre-exponential factor, E_a : activation energy, $\exp(-E_a/RT)$: fraction of the particle ensemble with the required activation energy.)

The A -factor accounts for steric effects (collision theory) and represents the rate which would occur if the kinetic barrier E_a was nonexistent.

Transition State Theory: quasi-equilibrium between reactants and intermediate state



Van 't Hoff equation: $\frac{d(\ln K)}{dT} = \frac{\Delta_r H^\ominus}{RT^2}$

Integrated: $K = K^\ominus \exp\left[\frac{\Delta_r H^\ominus}{R}\left(\frac{1}{T^\ominus} - \frac{1}{T}\right)\right]$

Transition thermodynamics:

$$\Delta G^\ddagger = \Delta H^\ddagger - T \Delta S^\ddagger \quad (\Delta H^\ddagger = E_a)$$

Eyring equation:

$$k = \frac{\kappa k_B T}{h} \exp\left(-\frac{\Delta G^\ddagger}{RT}\right)$$

(κ : transmission coefficient, $h = 6.63 \times 10^{-34}$ J s: Planck's constant)

13.3.8. Reaction Thermodynamics

Absolute values of thermodynamic potentials based on the state functions (Q : heat absorbed by the system, W : work done by the system, P : pressure, V : volume, S : entropy, T : temperature) are:

- Internal Energy: $U = Q - W$ (1st law of thermodynamics)
- Enthalpy: $H = U + PV$
- Gibbs Energy: $G = H - TS = U + PV - TS$
- Helmholtz Free Energy: $A = U - TS = G - PV$

Incremental changes are:

$$dU = T dS - P dV, \quad dH = T dS + V dP, \quad dG = V dP - S dT, \quad dA = -P dV - S dT$$

Isothermal $\rightarrow dT = 0$; isobaric $\rightarrow dP = 0$; isochoric $\rightarrow dV = 0$; adiabatic $\rightarrow dQ = 0$,
isentropic $\rightarrow dS = 0$; reversible $\rightarrow dG = 0$; isenthalpic $\rightarrow dH = 0$.

Under isobaric conditions, $W = P \Delta V$ and $Q = \Delta H$ ($\Delta H < 0$: exothermic; $\Delta H > 0$: endothermic)

Total entropy never decreases: $\Delta S_{\text{universe}} = \Delta S + \Delta S_{\text{surroundings}} \geq 0$ (2nd law of thermodynamics)

Entropy increase of the surroundings: $\Delta S_{\text{surroundings}} = -\frac{\Delta H}{T}$

Gibbs spontaneity criterion: $\Delta G = \Delta H - T \Delta S \leq 0$ (if isobaric and isothermal)

Helmholtz spontaneity criterion: $\Delta A = \Delta U - T \Delta S \leq 0$ (if isochoric and isothermal)

Gibbs Free Energy: for an isothermal, isobaric process (assumed in a reaction):

$$\Delta G = \Delta H - T \Delta S.$$

$\Delta G = 0 \rightarrow$ system at dynamic equilibrium (reversible).

$\Delta G < 0 \rightarrow$ spontaneous (exergonic); $\Delta G > 0 \rightarrow$ nonspontaneous (endergonic).

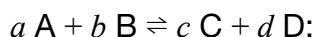
	$\Delta S > 0$	$\Delta S < 0$
$\Delta H > 0$	spontaneous only at high T	never spontaneous
$\Delta H < 0$	always spontaneous	spontaneous only at low T

Spontaneity temperature: $\Delta G = 0$ when $T = \frac{\Delta H}{\Delta S}$.

For Ellingham diagrams, see Section 15.1.3.

13.3.9. Equilibrium Thermodynamics

Basic Principles of Equilibria: for a reversible chemical system at dynamic equilibrium



- The forward rate is $r_1 = k_1[A]^p[B]^q$ (p, q : orders of reaction, k_1 : forward rate constant)
- The reverse rate is $r_{-1} = k_{-1}[C]^r[D]^s$ (r, s : orders of reaction, k_{-1} : reverse rate constant)
- The forward and reverse rates are equal: $r_1 = r_{-1}$.
- The amounts of each species remain constant in time.

Le Chatelier's principle: when conditions change, the equilibrium shifts to oppose the change.

Equilibrium Constant: defined as $K^\ominus = \frac{\{C\}^c\{D\}^d}{\{A\}^a\{B\}^b} = \frac{k_1}{k_{-1}}$ where $\{X\}$ is the activity of X.

In the strict sense, K and $\{X\}$ are all dimensionless. K is independent of pressure and reaction mechanism (e.g. use of catalyst). K_c uses concentrations. K_p uses partial pressures.

Activity of Species in Heterogeneous Media

Solutions: For a dissolved species X, the activity is $\{X\} = \frac{\gamma_X}{c^\ominus} [X]$, where:

- $[X]$ is the concentration of X in units of mol dm^{-3} , defined as $[X] = n_X / V$
- c^\ominus is the standard concentration, a constant ($c^\ominus = 1 \text{ mol dm}^{-3}$).
- γ_X is the activity coefficient (between 0 and 1). Often assumed that $\gamma_X \approx 1$ for $[X] \ll 1$.

Gases: For a gaseous species X, the activity (dimensionless fugacity) is $\{X\} = \frac{f_X}{p^\ominus} = \frac{\phi_X}{p^\ominus} p_X$, where:

- f_X is the fugacity of X in units of bar, defined as $d\mu_X = RT d(\ln f_X)$ (μ_X : chemical potential of X)
- p^\ominus is the standard pressure, a constant ($p^\ominus = 1 \text{ bar}$).
- ϕ_X is the fugacity coefficient (between 0 and 1). For ideal gases, $\phi_X = 1$.
- p_X is the partial pressure of X in units of bar, defined as $p_X = (n_X / n_{\text{tot,g}}) \times P_{\text{tot,g}}$

Pure liquids and undissolved solids: assumed to have $\{X\} = 1$ (exact at $p = 1 \text{ bar}$).

Free Energy at Equilibrium: net free energy change is zero at equilibrium

Standard Gibbs free energy change (for the forward reaction) is $\Delta G^\ominus = -RT \ln K$.

Non-equilibrium free energy change (for the forward reaction) is $\Delta G = \Delta G^\ominus + RT \ln \zeta$

(In general, the reaction quotient ζ (Section 13.3.10) is used. At equilibrium, $\zeta = K$, so $\Delta G = 0$.)

13.3.10. Chemical Potential and Reaction Quotient

Chemical Potential

The chemical potential μ is defined such that (N : number of particles):

$$dU = T dS - P dV + \sum \mu dN, \quad dG = -S dT + V dP + \sum \mu dN$$

For an isothermal and isobaric process, $dG = \sum \mu dN$.

For a binary mixture AB at equilibrium: $n_A d\mu_A + n_B d\mu_B = 0$ (Gibbs-Duhem equation)

Reaction Quotient

For a system of reactants and products $a A + b B \rightleftharpoons c C + d D$, **not** necessarily having reached equilibrium, the reaction quotient ξ is

$$\xi = \frac{\{C\}^c \{D\}^d}{\{A\}^a \{B\}^b} \quad \text{where } \{X\} = \text{activity of species X.}$$

- For solids and liquids, $\{X\} = 1$ i.e. can be omitted from the formula.
- For gases and aqueous phases, $\{X\}$ is as defined in Section 13.3.9.

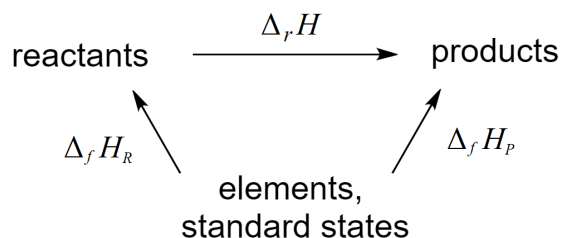
The equilibrium value of ξ is the (concentration) equilibrium constant K_c .

- If $\xi < K_c$ then the equilibrium shifts right.
- If $\xi > K_c$ then the equilibrium shifts left.

13.3.11. Hess's Law

Since enthalpy is a thermodynamic state function, the energy change in a chemical reaction is independent of the route taken. By drawing a 'Hess triangle', the energy changes can be considered like vectors: going along the arrow takes the value shown, while going against the arrow means the negative of the value shown. Values are added head to tail to find the total energy change for a given route.

Typical simple application: enthalpies of reaction given standard values.



Enthalpy of reaction: $\Delta_r H = \Delta_f H_P - \Delta_f H_R$ (change = products - reactants)

Entropy of reaction: $\Delta_r S = S_P - S_R$ (change = products - reactants)

Bond enthalpy: $\Delta_r H = \sum_R \Delta_{bond} H - \sum_P \Delta_{bond} H$ (change = bonds broken - bonds made)

Bond enthalpies, as listed in the table in Section 12.2.3, are positive for bond dissociation.

Enthalpies of reaction to non-standard states must account for enthalpies of vaporisation or fusion using additional steps.

13.3.12. Standard Enthalpy Changes and Experimental Lattice Enthalpies

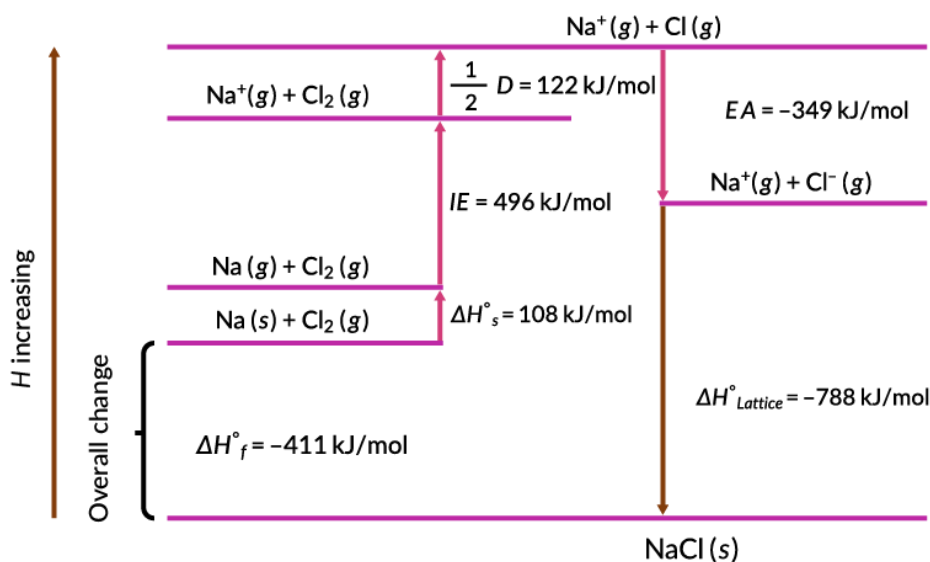
In the definitions, standard states are denoted with $^\ominus$. Standard enthalpies are defined as

- Enthalpy of Reaction ($\Delta_{rxn} H^\ominus$): reactants $^\ominus \rightarrow$ products $^\ominus$ (mole basis must be specified)
- Enthalpy of Formation ($\Delta_f H^\ominus$): elements $^\ominus \rightarrow$ substance $^\ominus$ (1 mole)
- Enthalpy of Solution ($\Delta_{sol} H^\ominus \approx 0$): substance $^\ominus$ (s) (1 mole) \rightarrow substance $^\ominus$ (aq)
- Enthalpy of Combustion ($\Delta_c H^\ominus < 0$): substance $^\ominus$ (1 mole) + x O₂ \rightarrow products $^\ominus$
- Enthalpy of Atomisation ($\Delta_{at} H^\ominus > 0$): substance $^\ominus \rightarrow$ atoms (g) (1 mole)
- Enthalpy of Sublimation ($\Delta_{sub} H^\ominus > 0$): substance $^\ominus \rightarrow$ substance (g) (1 mole)
- Enthalpy of Hydration ($\Delta_{hyd} H^\ominus < 0$): ions (g) (1 mole) \rightarrow ions (aq)
- (First) Enthalpy of Ionisation ($\Delta_{ion} H^\ominus > 0$): substance (g) (1 mole) \rightarrow cation (g) + e⁻
- Enthalpy of Bond Dissociation ($\Delta_{bond} H^\ominus > 0$): covalent bonds (g) (1 mole) \rightarrow radicals or atoms
- (First) Electron affinity ($\Delta_{ea} H^\ominus > 0$): substance (g) (1 mole) + e⁻ \rightarrow anion (g)
- Enthalpy of Lattice formation ($\Delta_{lat} H^\ominus < 0$): ions (g) \rightarrow ionic solid $^\ominus$ (1 mole)

A Born-Haber cycle can be used to calculate unknown enthalpies from standard values.

Born-Haber cycles cannot be used to predict lattice enthalpies involving polyatomic ions.

Solution, Lattice formation and Hydration: $\Delta_{sol} H = \Delta_{hyd} H - \Delta_{lat} H$; see also Section 13.3.8.



Born-Haber Cycle for NaCl

Experimentally-determined lattice enthalpy of formation involves standard state formation, sublimation, ionisation, bond breaking, electron affinity

13.3.13. Theoretical Enthalpy of Lattice Dissociation from Perfect Ionic Model

The Born-Landé equation, based on assuming perfectly electrostatic interactions between point ions with complete lattice crystallinity, gives:

$$\Delta_{lat}H = \frac{N_A M z_1 z_2 e^2}{4\pi\epsilon_0 r_0} \left(1 - \frac{1}{n}\right) = \frac{1.389 \times 10^{-4} \times (1 - 1/n) M z_1 z_2}{r_1 + r_2} \text{ [J mol}^{-1}\text{]}$$

(N_A : Avogadro's constant, M : Madelung constant, (z_1, z_2) : charge on ions, e : charge on electron, ϵ_0 : vacuum permittivity, r : inter-ionic (lattice) spacing, n : Born parameter)

The Madelung constant M is lattice geometry dependent (weighted distance to every ion):

lattice	ZnS	NaCl	CsCl	TiO ₂	CaF ₂	Al ₂ O ₃
M	1.64132	1.74756	1.76267	2.408	2.51939	4.17186

The Born parameter n represents repulsion. It can be estimated from the period of the ion:

Period	2 [He]	3 [Ne]	4 [Ar]	5 [Kr]	6 [Xe]	7 [Rn]
n	5	7	9	10	12	12

Differences between the theoretical and experimental lattice enthalpies indicate a degree of covalent character in the lattice (incomplete charge polarisation). This typically occurs when the constituent ions have 1) a small difference in electronegativity and/or 2) low polarising power (soft acids or soft bases; low charge density). The theoretical value typically underestimates the experimental value. The values are typically within 10% for an electronegativity difference of more than 1 Paulings, and within 1% for an electronegativity difference of more than 2 Paulings.

For a table of electronegativities, see Section 12.2.4. For HSAB theory, see Section 15.5.16.

13.4. Solutions and Heterogeneous Equilibria

13.4.1. Molarity, Molality and Normality

(m : mass of solute A, M : mass of solvent B, $M_{r(X)}$: relative molecular mass of X (g mol^{-1}), ρ : mass density, V : volume of solvent (dm^3), ν_A : stoichiometric coefficient when A reacts with 1 mole of a given substance)

- Moles: $n_A = \frac{m}{M_{r(A)}}$, $n_B = \frac{M}{M_{r(B)}}$ [mol]
- Molarity: $c = \frac{n_A}{V_B} = \frac{\rho_B n_A}{M}$ [$\text{mol dm}^{-3} = \text{M (molar)}$]
- Molality: $b = \frac{n_A}{M} = \frac{n_A}{\rho_B V_B}$ [mol kg^{-1} (molal)]
- Normality: $N = \frac{n_A \times (\text{reactive units of A})}{V_B}$ [$\text{Eq L}^{-1} = \text{N (equivalents per litre)}$]
- Weight and Volume fractions: $w/v \% = \frac{m [\text{g}]}{V_A + V_B [\text{ml}]} \times 100\%$ (grams of solute in 100 ml solution)
 $v/v \% = \frac{V_A}{V_A + V_B} \times 100\%$ (volume fraction)
 $w/w \% = \frac{m}{M + m} \times 100\%$ (mass fraction = weight fraction)

Conversion between b and c : $\frac{c}{b} = \rho_B - \frac{M_{r(A)}}{1000} c$ (further from proportional if M_r is large)

Note that $1 \text{ dm}^3 = 1 \text{ L} = 1000 \text{ ml} = 1000 \text{ cm}^3$. The density of water is $1 \text{ kg dm}^{-3} = 1 \text{ g ml}^{-1}$, so molarity and molality have approximately the same numerical value in the above units.

The product of moles of A with its number of reactive units is the 'mole equivalent' of A.

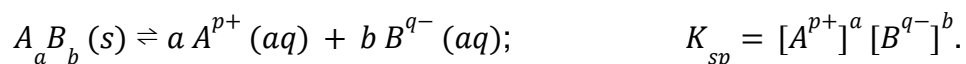
Making Solutions

Example: magnetic polymer solution of 10 wt% polystyrene and 30 wt% iron oxide in a 1000 μL binary solvent of (85 v/v% DMF + 15 v/v% acetone):

- To make the solvent, mix 850 μL DMF with 150 μL acetone in a glass vial.
- Measure the mass of the solvent. Suppose that the solvent mass is found to be 894 mg.
- The mass of polystyrene to be added is $\frac{0.1}{1 - (0.1 + 0.3)} \times 894 \text{ mg} = 149 \text{ mg}$.
- The mass of iron oxide to be added is $\frac{0.3}{1 - (0.1 + 0.3)} \times 894 \text{ mg} = 447 \text{ mg}$.
- The total mass of the system is then 1490 mg.

13.4.2. Ionic Solubility Products and Precipitation from Solution

A solute $A_a B_b$ dissolves in a solvent to give ions A^{p+} and B^{q-} in an equilibrium given by



For non-binary solutes, the solubility equilibrium constant is defined similarly: ignore solids, include only aqueous species. For strong (fully soluble) electrolytes, $K_{sp} \rightarrow \infty$.

For a pure solute, $\frac{[A^{p+}]}{[B^{q-}]} = \frac{a}{b}$. The limiting solubility is $[A_a B_b] = \left(a^a b^b \times K_{sp} \right)^{1/(a+b)}$.

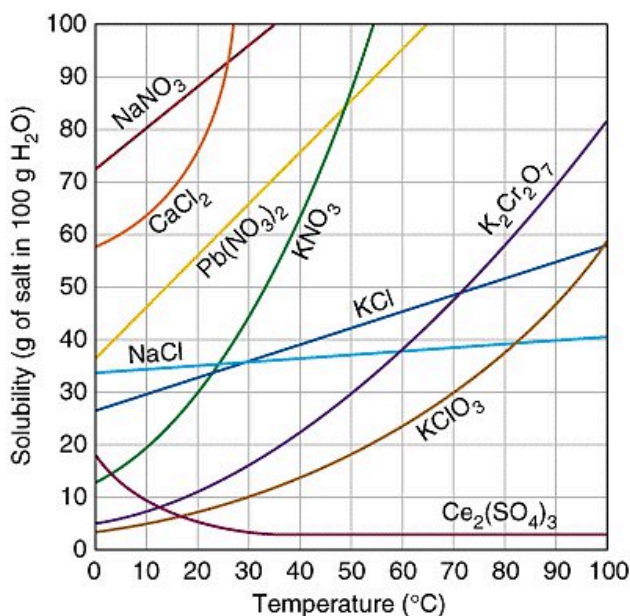
The solubility limit will be reached and precipitation will occur if the reaction quotient $Q \geq K_{sp}$.

Selective precipitation: in a saturated mixture, the least soluble precipitate will form predominantly.

Common ion effect: adding an ion to a solution promotes precipitation with that ion.

Relation to thermodynamics: $\Delta G_{sol}^{\ominus} = -RT \ln K_{sp}$ where $\Delta G_{sol}^{\ominus} = \Delta H_{sol}^{\ominus} - T \Delta S_{sol}^{\ominus}$.

Solubility Data for Soluble Ionic Substances



Solubility limit for salts in water at varying temperatures (x : g salt per 100 g water).

$$x \text{ [g salt per 100 g water]} = \frac{10x}{M_r \text{ [g/mol]}} \text{ mol dm}^{-3}$$

For an aqueous salt A_aB_b ,

$$\text{Solubility product: } K_{sp} = \frac{1}{a^a b^b} \left(\frac{\rho(T) \text{ [kg m}^{-3}\text{]} x}{100 M_r \text{ [g/mol]}} \right)^{(a+b)}$$

(M_r : salt molecular mass, $\rho(T)$: water density at temp)

Solubility Data for Sparingly Soluble Ionic Substances

Table of values of K_{sp} in $(\text{mol dm}^{-3})^{a+b}$ in water at 25 °C (listed in A-Z by compound name):

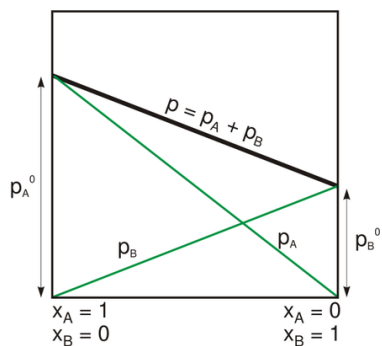
Al(OH) ₃	1.8×10^{-5}	CaC ₂ O ₄	2.7×10^{-9}	Fe(OH) ₂	8.0×10^{-16}	MgNH ₄ PO ₄	2.5×10^{-13}	Ag ₃ AsO ₄	1.0×10^{-22}	Tl(OH) ₃	6.3×10^{-46}
AlPO ₄	6.3×10^{-19}	Ca ₃ (PO ₄) ₂	2.0×10^{-29}	FeS*	6×10^{-19}	Mg ₃ (AsO ₄) ₂	2×10^{-20}	AgN ₃	2.8×10^{-9}	Sn(OH) ₂	1.4×10^{-28}
BaCO ₃	5.1×10^{-9}	CaSO ₄	9.1×10^{-6}	FeAsO ₄	5.7×10^{-21}	MgCO ₃	3.5×10^{-8}	AgBr	5.0×10^{-13}	SnS*	1×10^{-26}
BaCrO ₄	1.2×10^{-10}	CaSO ₃	6.8×10^{-8}	Fe ₄ [Fe(CN) ₆] ₃	3.3×10^{-41}	MgF ₂	3.7×10^{-8}	AgCl	1.8×10^{-10}	ZnCO ₃	1.4×10^{-11}
BaF ₂	1.0×10^{-6}	Cr(OH) ₂	2×10^{-16}	Fe(OH) ₃	4×10^{-38}	Mg(OH) ₂	1.8×10^{-11}	Ag ₂ CrO ₄	1.1×10^{-12}	Zn(OH) ₂	1.2×10^{-17}
Ba(OH) ₂	5×10^{-3}	Cr(OH) ₃	6.3×10^{-31}	FePO ₄	1.3×10^{-22}	MgC ₂ O ₄	8.5×10^{-5}	AgCN	1.2×10^{-16}	ZnC ₂ O ₄	2.7×10^{-8}
BaSO ₄	1.1×10^{-10}	CoCO ₃	1.4×10^{-13}	Pb ₃ (AsO ₄) ₂	4×10^{-36}	Mg ₃ (PO ₄) ₂	1×10^{-25}	AgIO ₃	3.0×10^{-9}	Zn ₃ (PO ₄) ₂	9.0×10^{-33}
BaSO ₃	8×10^{-7}	Co(OH) ₂	1.6×10^{-15}	Pb(N ₃) ₂	2.5×10^{-9}	MnCO ₃	1.8×10^{-11}	AgI	8.5×10^{-17}	ZnS*	2×10^{-25}
BaS ₂ O ₃	1.6×10^{-6}	Co(OH) ₃	1.6×10^{-44}	PbBr ₂	4.0×10^{-5}	Mn(OH) ₂	1.9×10^{-13}	AgNO ₂	6.0×10^{-4}		
BiOCl	1.8×10^{-31}	CoS*	4×10^{-21}	PbCO ₃	7.4×10^{-14}	MnS*	3×10^{-14}	Ag ₂ SO ₄	1.4×10^{-5}		
BiOOH	4×10^{-10}	CuCl	1.2×10^{-6}	PbCl ₂	1.6×10^{-5}	Hg ₂ Br ₂	5.6×10^{-23}	Ag ₂ S*	6×10^{-51}		
CdCO ₃	5.2×10^{-12}	CuCN	3.2×10^{-20}	PbCrO ₄	2.8×10^{-13}	Hg ₂ Cl ₂	1.3×10^{-18}	Ag ₂ SO ₃	1.5×10^{-14}		
Cd(OH) ₂	2.5×10^{-14}	CuI	1.1×10^{-12}	PbF ₂	2.7×10^{-8}	Hg ₂ I ₂	4.5×10^{-29}	AgSCN	1.0×10^{-2}		
CdC ₂ O ₄	1.5×10^{-8}	Cu ₃ (AsO ₄) ₂	7.6×10^{-36}	Pb(OH) ₂	1.2×10^{-15}	HgS*	2×10^{-53}	SrCO ₃	1.1×10^{-10}		
CdS*	8×10^{-28}	CuCO ₃	1.4×10^{-10}	PbI ₂	7.1×10^{-9}	NiCO ₃	6.6×10^{-9}	SrCrO ₄	2.2×10^{-5}		
CaCO ₃	2.8×10^{-9}	CuCrO ₄	3.6×10^{-6}	PbSO ₄	1.6×10^{-8}	Ni(OH) ₂	2.0×10^{-15}	SrF ₂	2.5×10^{-9}		
CaCrO ₄	7.1×10^{-4}	Cu[Fe(CN) ₆] ₃	1.3×10^{-16}	PbS*	3×10^{-28}	NiS*	3×10^{-19}	SrSO ₄	3.2×10^{-7}		
CaF ₂	5.3×10^{-9}	Cu(OH) ₂	2.2×10^{-20}	Li ₂ CO ₃	2.5×10^{-2}	ScF ₃	4.2×10^{-18}	TlBr	3.4×10^{-6}		
CaHPO ₄	1×10^{-7}	CuS*	6×10^{-37}	LiF	3.8×10^{-3}	Sc(OH) ₃	8.0×10^{-31}	TlCl	1.7×10^{-4}		
Ca(OH) ₂	5.5×10^{-6}	FeCO ₃	3.2×10^{-11}	Li ₃ PO ₄	3.2×10^{-9}	AgC ₂ H ₃ O ₂	2.0×10^{-3}	TlI	6.5×10^{-8}		

*: equilibrium for sulfides is $MS(s) + H_2O(l) \rightleftharpoons M^{2+}(aq) + HS^-(aq) + OH^-(aq)$ so K_{sp} has units $\text{mol}^3 \text{dm}^{-9}$.

13.4.3. Raoult's Law and Henry's Law for Ideal Liquid-Vapour Equilibria

Raoult's Law: in an ideal solution, vapour pressure decreases linearly with solute concentration:

$$p_S = x_S^{(L)} p_S^\ominus \quad (x_S: \text{mole fraction of solvent, } p_S^\ominus: \text{vapour pressure of pure solvent})$$



$$\text{For an ideal binary solution, } x = \frac{p - p_A^\ominus}{p_B^\ominus - p_A^\ominus}.$$

Most solutions are non-ideal, especially at higher concentrations.
 Positive deviation: p is higher than predicted; cohesion > adhesion.
 Negative deviation: p is lower than predicted; adhesion > cohesion.

Pressure curves with minima/maxima produce azeotropes.

$$\text{Entropy of mixing: } \Delta S_{mix}^\ominus = -nRT(x_1 \ln x_1 + x_2 \ln x_2).$$

Henry's Law: the solubility of a gas is directly proportional to its partial pressure:

$$b_S^{(L)} = K_H p_S \quad (b: \text{molality of dissolved gas, } p: \text{partial pressure of gas, } K_H: \text{Henry's law constant})$$

K_H is the solubility constant (equilibrium constant) for the equilibrium $A(g) \rightleftharpoons A(aq)$.

The Henry's law constant varies with temperature according to $K_H = K_H^\ominus \exp \left[\alpha \left(\frac{1}{T} - \frac{1}{T^\ominus} \right) \right]$
 where α is the constant value of $\frac{d \ln K_H}{d \left(\frac{1}{T} \right)}$ and (T^\ominus, K_H^\ominus) is a standard measurement.

Values of K_H^\ominus and α are given in the table for some commonly soluble gases in a water solvent, with the standard measurement at $T^\ominus = 298 \text{ K}$.

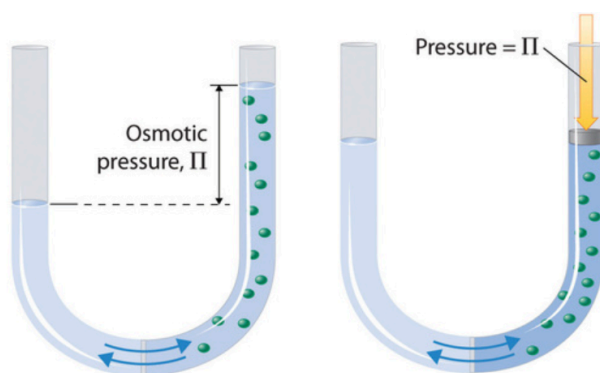
Gas	K_H^\ominus (mol kg ⁻¹ bar ⁻¹)	α (K)	Gas	K_H^\ominus (mol kg ⁻¹ bar ⁻¹)	α (K)
H ₂	0.00078	640	CO	0.0009	1600
He	0.00038	92	NO ₂	0.012	2500
N ₂	0.0006	1300	SO ₂	1.2	3100
O ₂	0.0013	1700	NH ₃	56	4200
Cl ₂	0.095	2100	PH ₃	0.0081	2000
Ar	0.00014	1500	CH ₄	0.0013	1900
CO ₂	0.034	2400	C ₂ H ₆	0.0019	2300

13.4.4. Osmotic Pressure

At the interface of two solutions with a **difference** in concentration c in a common solvent which can flow freely (semi-permeable membrane: ions cannot flow), solvent will flow into the more concentrated solution by osmosis, resulting in a net pressure gradient.

Van 't Hoff factor, i = moles of aqueous particles per mole of solute (ideal).

- Osmotic pressure: $\Pi = icRT$
For multiple species, the total concentration is used, so that ic is the moles of ions per unit volume.
- Force required for volume balance: $F = \Pi A$
- Moles of solute: $n = FL/(2iRT)$ ($c = n/V$, $V = AL/2$)
- Work done to compress by distance x : $W = \int_0^x F(x) dx = -nRT \ln\left(\frac{L}{2} - x\right)$



L : length of water in U-tube.

(minimum work: neglects enthalpy of mixing, neglects gravity, assumes slow compression (quasi-static), neglects hydrodynamic (drag) loss for pushing solvent through membrane, fouling of membrane).

Osmotic pressure is also generated at interfaces with ionic substances, with much higher magnitudes than with dissolved solutes. Poly-ionic nanoparticles with high surface areas are used to generate very high osmotic pressures in e.g. water desalination. The water molecules near the interface are associated (reduced activity) and expel solutes from the bound region (diffusioosmosis).

13.4.5. Boiling Point Elevation and Freezing Point Depression

Addition of a solute to a solvent results in an increase to the boiling point and a decrease to the freezing point of the system, proportional to the molality of the solute:

$$\Delta T_b = i K_b M \quad \text{and} \quad \Delta T_f = -i K_f M$$

(T_b : boiling point, T_f : freezing point, K_b : ebullioscopic constant, K_f : cryoscopic constant, M : molality, i : van 't Hoff factor)

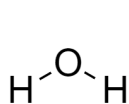
The van 't Hoff factor i is the number of moles of fully solvated particles formed per mole of dissolved solute. Incomplete dissociation (or re-association in solution) results in this being less than the number of constituent solute ions or particles.

Solvent	$T_b / ^\circ\text{C}$	$T_f / ^\circ\text{C}$	$K_b / ^\circ\text{C kg mol}^{-1}$	$K_f / ^\circ\text{C kg mol}^{-1}$
water	100	0	0.512	1.86
ethanol	78.4	-114.6	1.22	1.99
acetic acid	118	17	3.07	3.90
acetone	56	-95	1.71	0.850
ethylene glycol	197.5	-13.0	2.26	3.11
DMSO	191.9	18.52	3.22	3.85
pyridine	115.2	-41.63	2.83	4.26
phenol	181.8	40.89	3.55	6.84
aniline	184	-6	3.82	5.87
nitrobenzene	211	6	5.20	7.00
carbon tetrachloride	76.5	-22.99	5.03	30.0
chloroform	62.1	-63.5	3.63	4.70
benzene	80.1	5.49	2.53	5.12
cyclohexane	80.7	6.59	2.92	20.8
carbon disulfide	46.2	-111.5	2.34	3.83
diethyl ether	34.5	-116.2	2.02	1.79
camphor	208.0	179.8	5.95	40
naphthalene	218	80	5.80	6.94

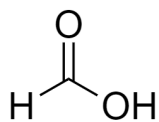
K_b and K_f can be considered the gradients of the liquidus and solidus lines on the phase diagram of the solvent-solute system, as linear approximations for dilute solutions.

13.4.5. Some Common Solvents

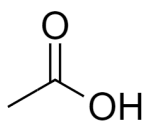
Polar Protic



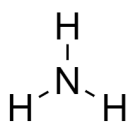
water



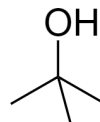
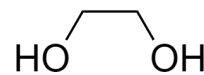
formic acid



acetic acid



ammonia

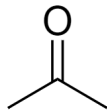
*tert*-butanol

ethylene glycol

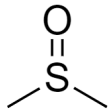
Polar Aprotic



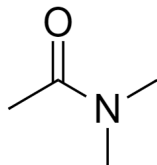
THF



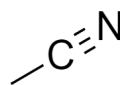
acetone



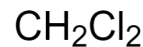
DMSO



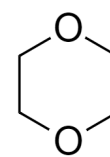
DMF



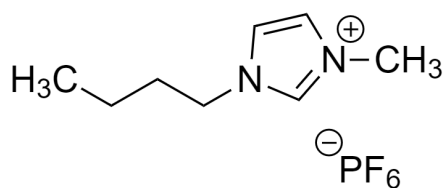
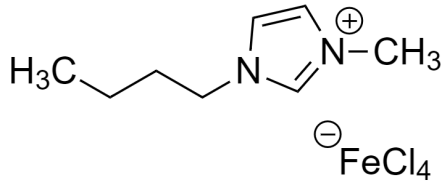
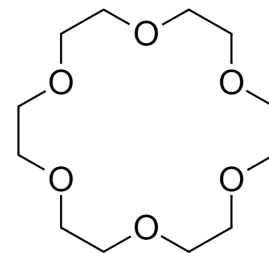
acetonitrile



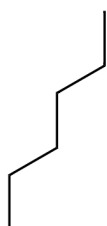
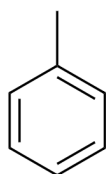
DCM



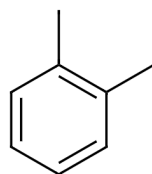
1,4-dioxane

BMIM-PF₆
(IL: ionic liquid)BMIM-FeCl₄
(MIL: magnetic ionic liquid)18-Crown-6
(Crown ether)

Nonpolar

*n*-hexane

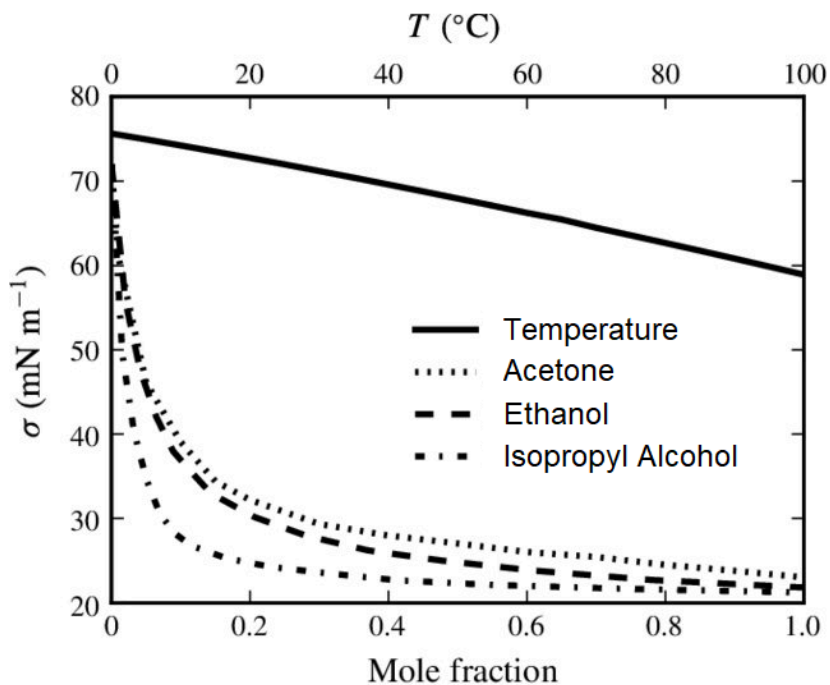
toluene

*o*-xylene

camphor

13.4.6. Surface Tensions of Some Liquid Mixtures

The surface tension σ of water-acetone, water-ethanol and water-isopropyl alcohol binary systems are shown, as well as the variation of σ for pure water with temperature.



13.4.7. Partition Coefficients for Common Solvents

For a binary system of two immiscible phases (one organic, one aqueous) with one solute:

Partition coefficient:
$$K_{ow} = P = \frac{[solute]_{organic}}{[solute]_{aqueous}} \quad \text{“Log P”} = \log_{10} K_{ow}$$

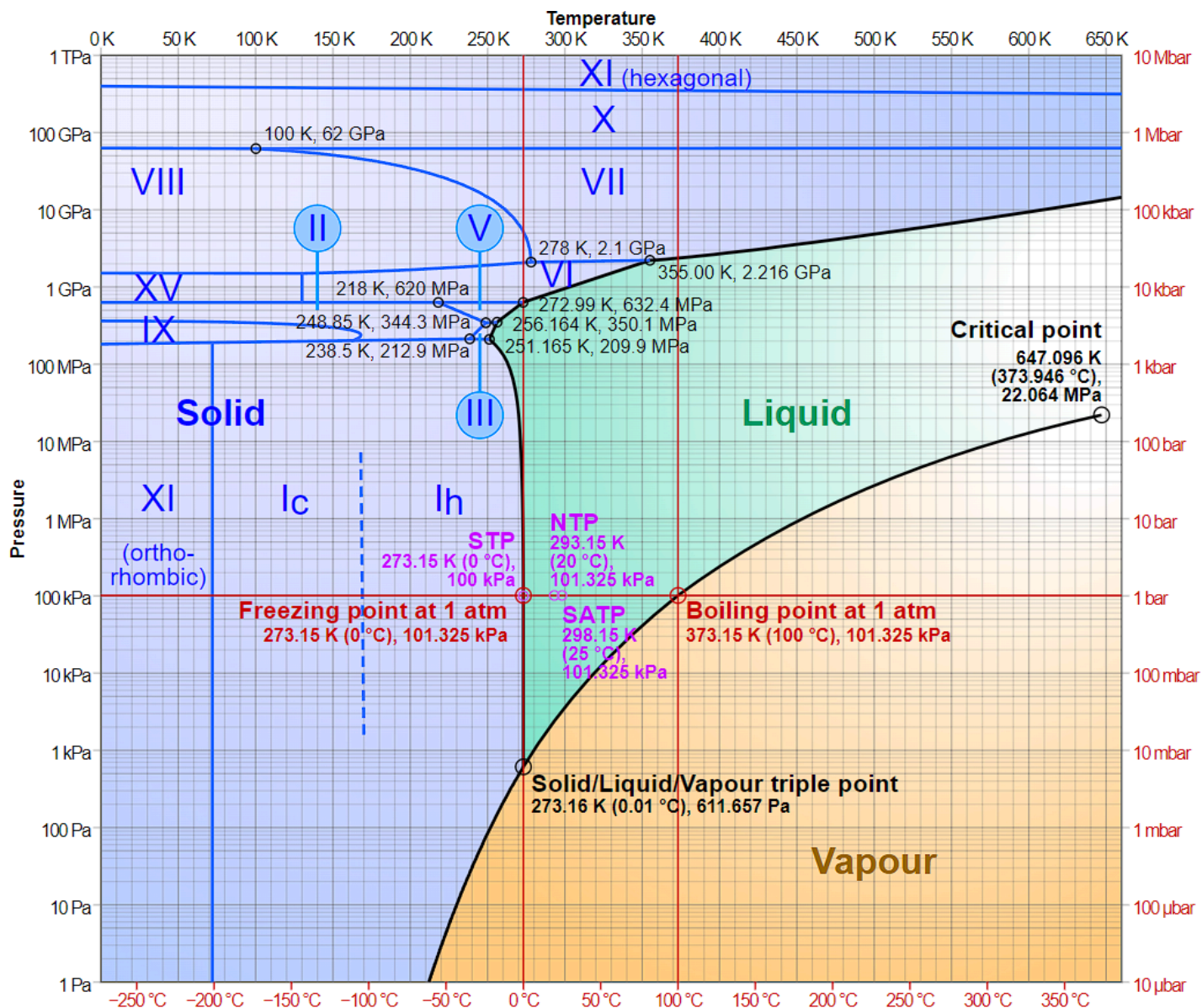
The organic phase is usually taken as octan-1-ol unless otherwise specified.

Fully miscible (hydrophilic, lipophobic)		Partially miscible		Immiscible (lipophilic, hydrophobic)	
Solute	Log P	Solute	Log P	Solute	Log P
dimethylsulfoxide	-1.3	propanol	0.28	diethyl ether	2.9
dioxane	-1.1	ethyl acetate	0.68	tetrachloromethane	3.0
<i>N,N</i> -dimethylformamide	-1.0	butanol	0.80	pentane	3.0
methanol	-0.76	diethyl ether	0.85	cyclohexane	3.2
acetonitrile	-0.33	butyl acetate	1.7	hexane	3.5
ethanol	-0.24	dipropyl ether	1.9	diphenyl ether	4.2
acetone	-0.23	chloroform	2.0	octane	4.5
		benzene	2.0	dodecanol	5.0
		toluene	2.5	hexyl ether	5.1
				dodecane	6.6
				dioctyl phthalate	9.6

13.4.8. Equilibrium Phase Diagrams of Solvents and Solid Solution Mixtures

For phase diagrams of metal alloys, see Section 6.7.13-14.

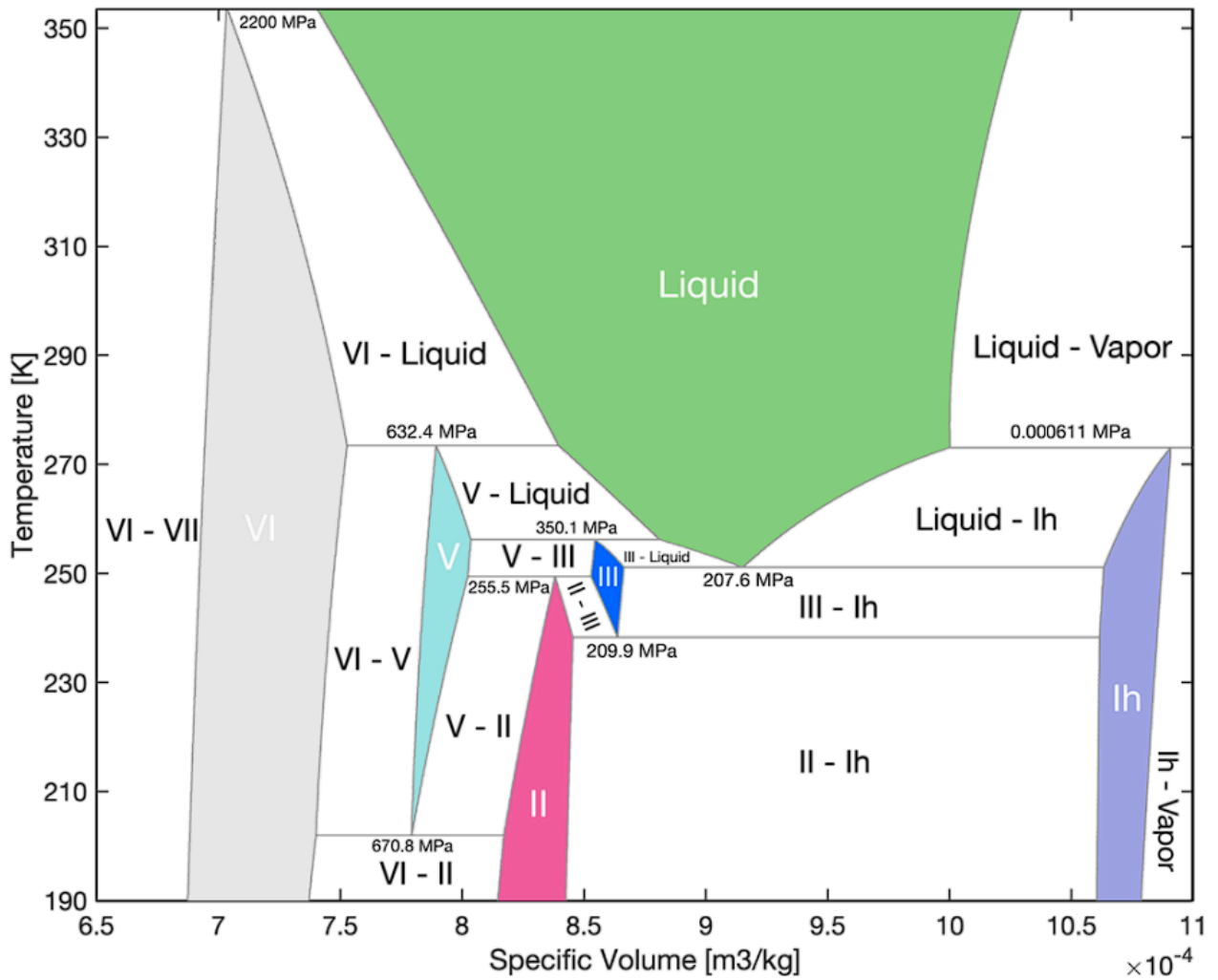
p - T , **Water (H₂O)**: state specified by pressure p and temperature T



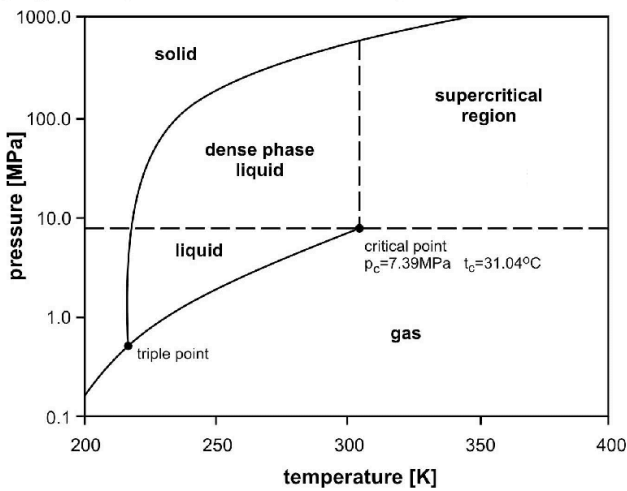
Notes:

- The phases ice I_h , ice I_c , ice II, ice III, etc are polymorphs of ice.
- At pressures below the triple point, sublimation/deposition is the only phase change.
- At temperatures and pressures above the critical point, water becomes supercritical.
- At pressures above 1 TPa, water enters a 'metallic' phase ($C2/m$).

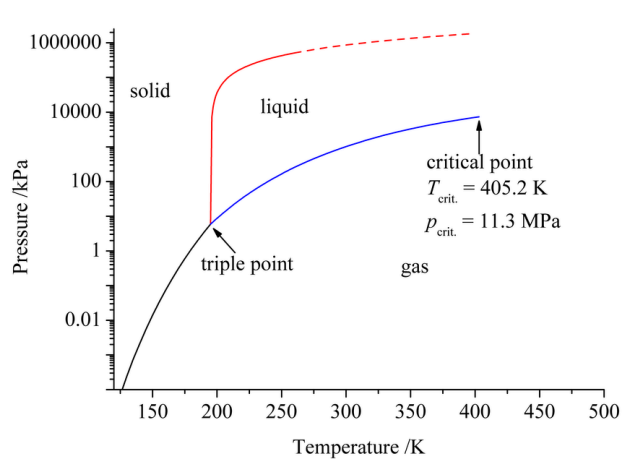
T - v , Water (H_2O): state specified by temperature T and specific volume v



p - T , Carbon Dioxide (CO_2)

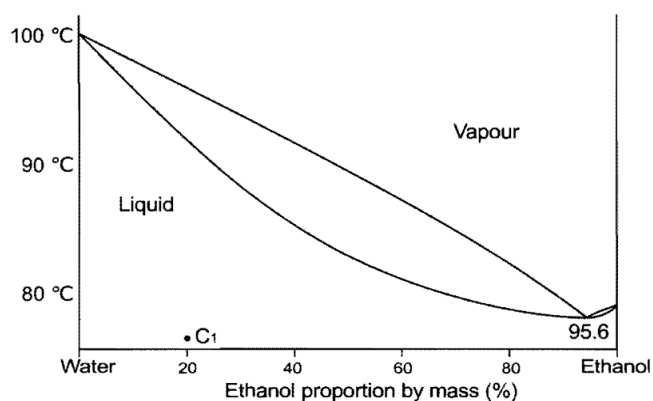


p - T , Ammonia (NH_3)

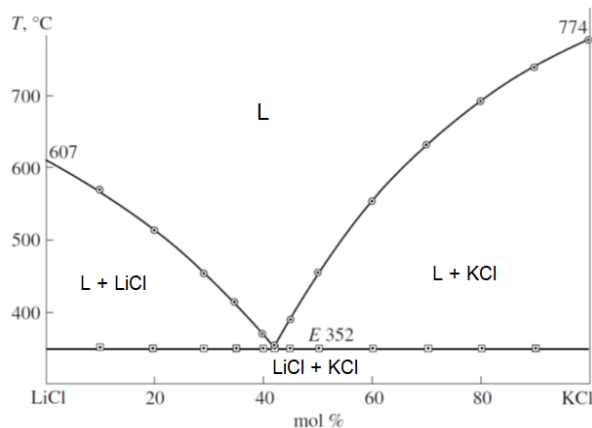


T-x Binary Phase Diagrams: The phase diagrams for some selected equilibria of solid, liquid and vapour phases recorded at a pressure of 1 bar are shown. Some azeotropes and eutectics (E) are indicated. L = liquid, V = vapour.

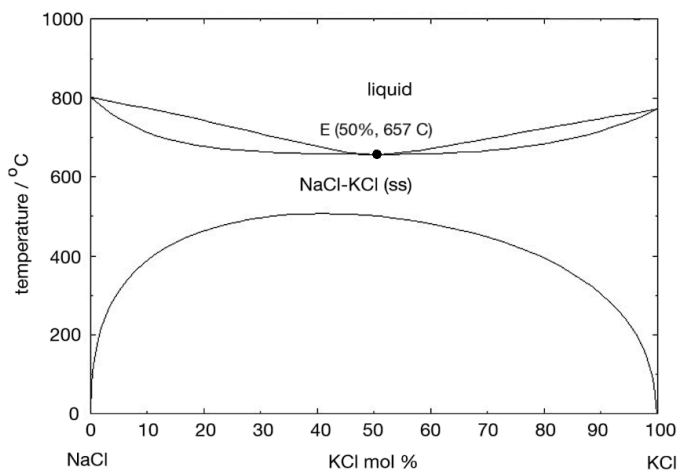
Water-Ethanol (L, V)



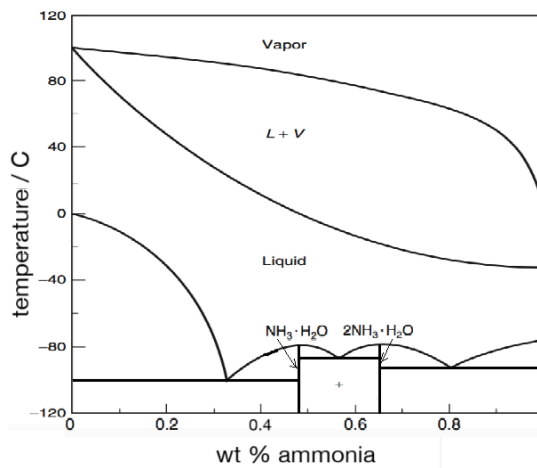
LiCl-KCl (S, L)



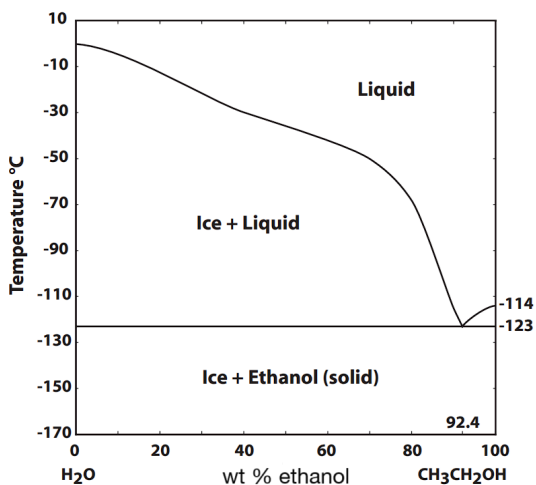
NaCl-KCl (S, L)



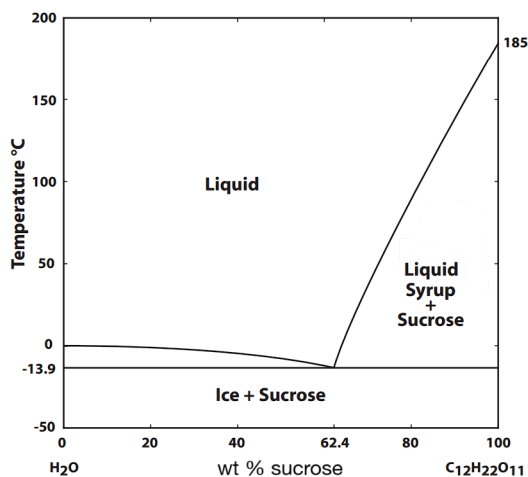
Water-Ammonia (S, L, V)



Water-Ethanol (S, L)



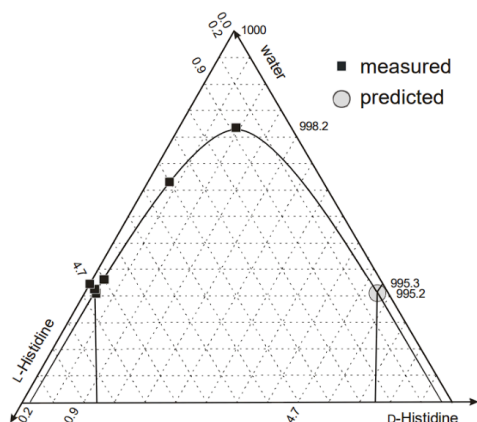
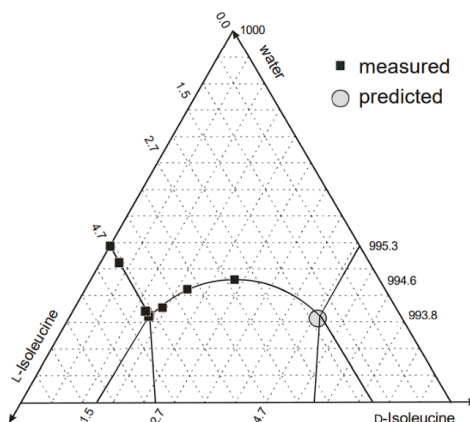
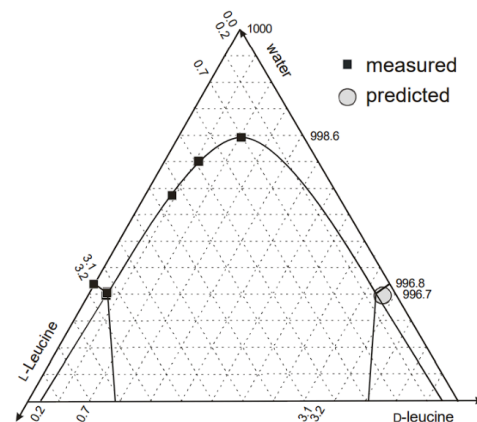
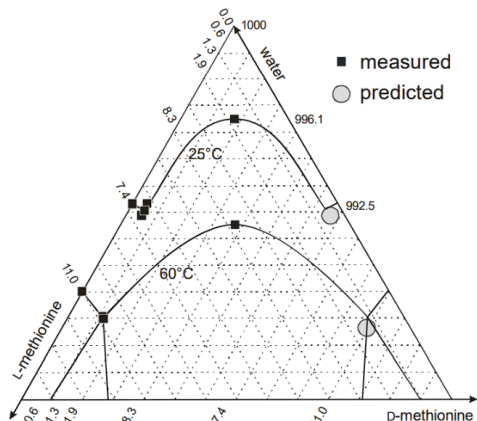
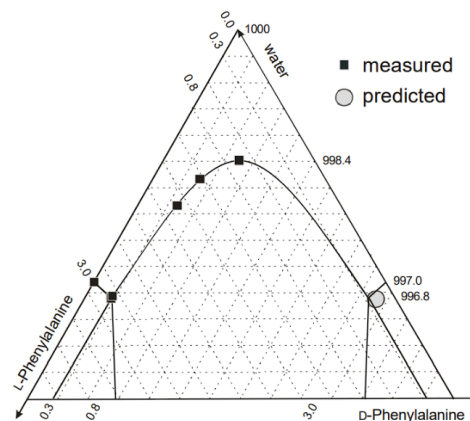
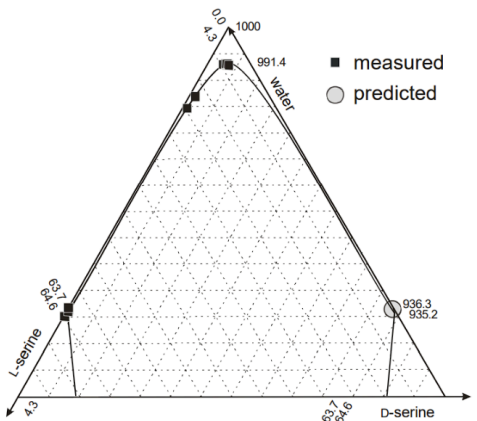
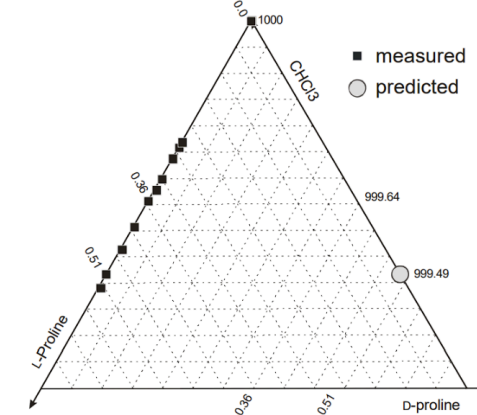
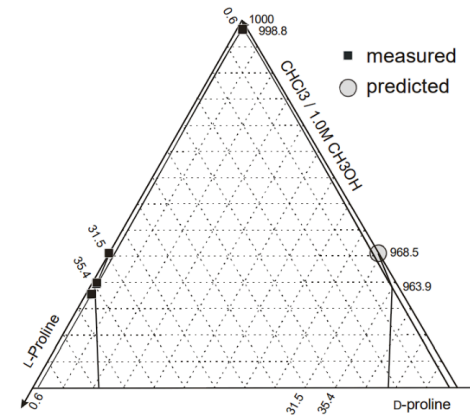
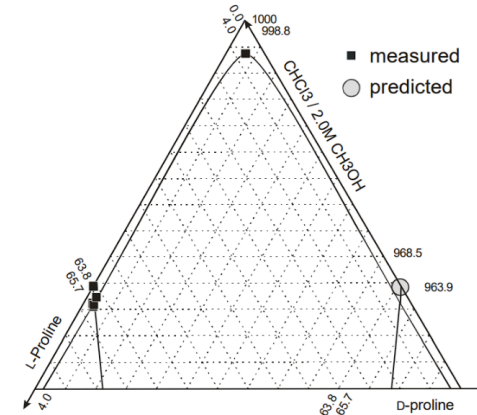
Water-Sucrose (S, L)



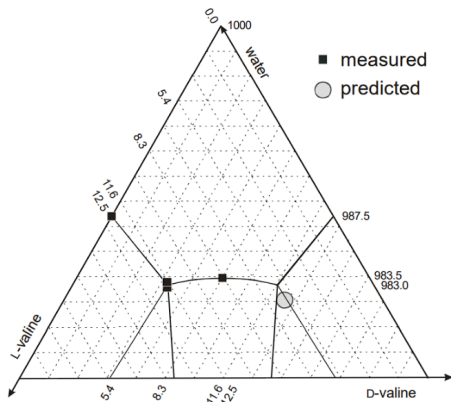
Enantioselective Crystallisation of Amino Acids and Catalysts (Ternary Phase Diagrams)

Compositions are given as 1000 × mole fraction. All data at 25 °C. The predicted eutectic composition is only shown on the minor enantiomer side of the phase diagram for clarity.

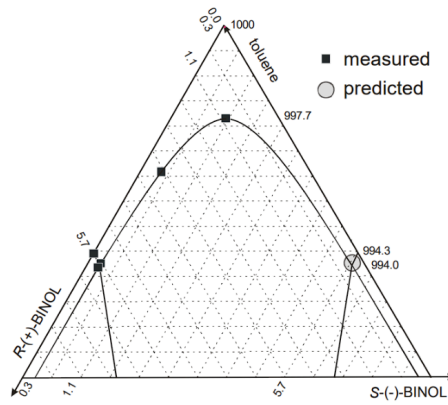
For amino acid biochemical data, see Section 16.5.10. For the catalyst structures, see Section 14.1.4.

L-His - D-His - H₂OL-Ile - D-Ile - H₂OL-Leu - D-Leu - H₂OL-Met - D-Met - H₂OL-Phe - D-Phe - H₂OL-Ser - D-Ser - H₂OL-Pro - D-Pro - CHCl₃L-Pro - D-Pro - CHCl₃/1M MeOHL-Pro - D-Pro - CHCl₃/2M MeOH

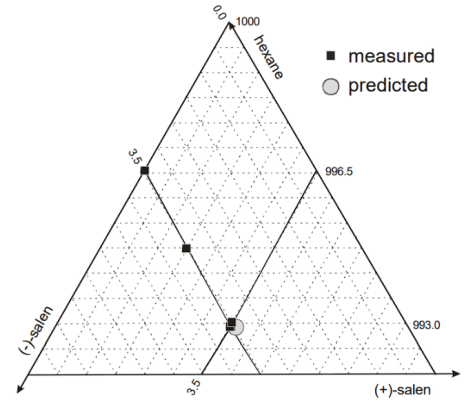
L-Val - D-Val - H₂O



R-BINOL - S-BINOL - toluene

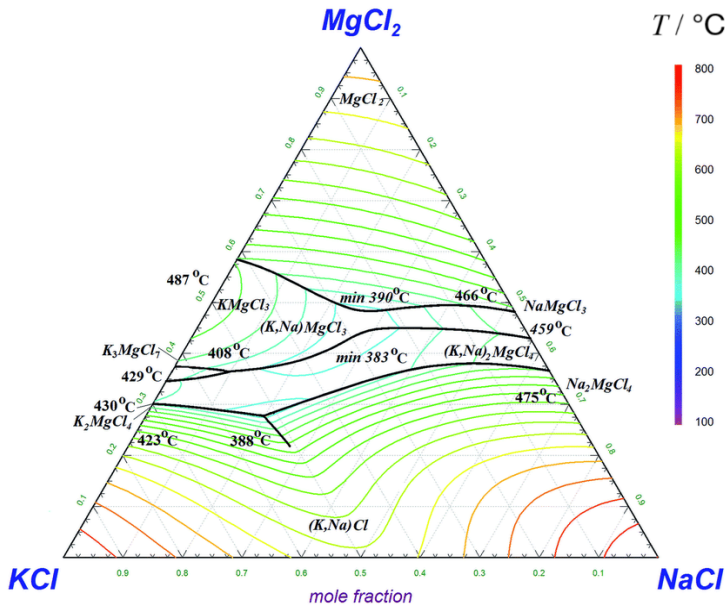


(-)-salen - (+)-salen - hexane

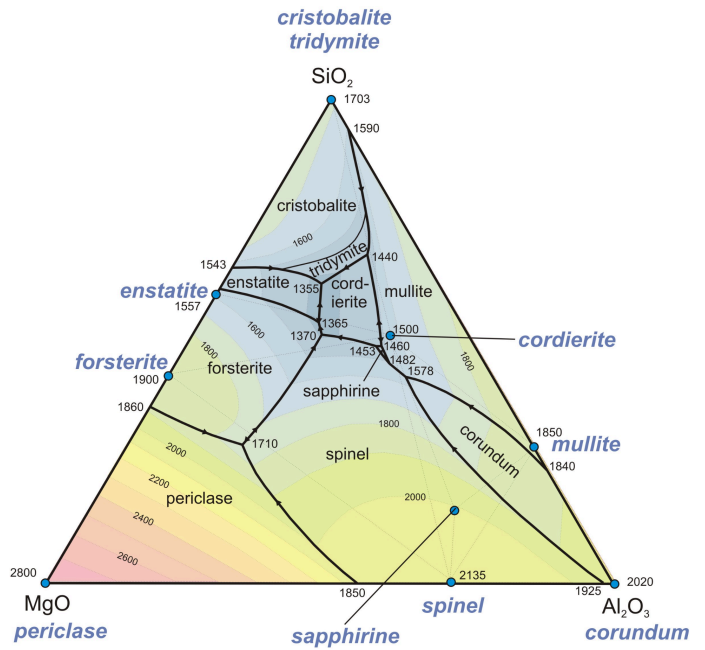


Temperature Dependence of Mineral Solid Solution Stability

MgCl₂ - KCl - NaCl



SiO₂ - MgO - Al₂O₃



13.5. Electrochemistry

13.5.1. Measurements of Electric Charge Flow

For an electrolyte with concentration c (consisting of n^+ moles of cations and n^- moles of anions per mole of dissolved electrolyte) with potential difference V between electrodes of effective area A , separated by distance L , with current flow I ,

- Resistance [Ω] and Resistivity [$\Omega \text{ m}$], $R = \frac{V}{I}$, $\rho = \frac{RA}{L}$ (cell constant: $\frac{L}{A}$)
- Conductance [S] and Conductivity [S m^{-1}] $G = \frac{1}{R} = \frac{I}{V}$, $\kappa = \frac{1}{\rho} = \frac{GL}{A} = \frac{L}{RA}$
- Molar conductivity [$\text{S cm}^2 \text{ mol}^{-1}$], $\Lambda_m = \frac{10^3 \times \kappa [\text{S cm}^{-1}]}{c [\text{mol dm}^{-3}]} = \frac{10^3 \times \frac{L}{A} [\text{cm}^{-1}]}{R [\Omega] \times c [\text{mol dm}^{-3}]}$
- Equivalent conductivity [$\text{S cm}^2 \text{ eq}^{-1}$], $\Lambda_{eq} = \frac{\Lambda_m}{n^+ + n^-}$

Kohlrausch's Law for Strong and Weak Electrolyte Conductivity

- At infinite dilution (as $c \rightarrow 0$), the molar conductivity of a **strong** electrolyte tends to a finite limiting conductivity, $\lim_{c \rightarrow 0} \Lambda_m = \Lambda_m^0$, while for **weak** electrolytes, Λ_m goes to a large but finite value.
- Kohlrausch's Law (independent ion migration): $\Lambda_m^0 = n^+ \lambda_+^0 + n^- \lambda_-^0$
- Ionic strength: $I = \frac{1}{2} \sum_{i=1}^n c_i z_i^2$ (c_i : concentration of ion i , z_i : charge on ion i)
- Debye-Hückel-Onsager equation (for **strong** electrolytes at dilute concentrations):

$$\Lambda_m = \Lambda_m^0 - (A + B\Lambda_m^0)\sqrt{c}, \quad \text{where } A = \frac{82.4}{(\epsilon_r T)^{1/2} \eta} \text{ and } B = \frac{8.2 \times 10^5}{(\epsilon_r T)^{3/2}}$$

- Temperature dependence: $\lambda^0(T) = \lambda_{298K}^0 (1 + \alpha \Delta T)$ where $\alpha \approx 0.02 \text{ K}^{-1}$ (0.0139 K^{-1} for H^+)
- Equivalent conductivity: $\Lambda_{eq} = \Lambda_m / |z|$ (z : ion charge, in units of e)
- Limiting conductivity (for **weak** electrolytes): $\Lambda_m^0(AB) := \Lambda_m^0(AX) + \Lambda_m^0(BY) - \Lambda_m^0(XY)$
- Degree of dissociation, $\alpha = \frac{\Lambda_m}{\Lambda_m^0}$; Dissociation constant, $K = \frac{c \alpha^2}{1 - \alpha} = \frac{c (\Lambda_m)^2}{\Lambda_m^0 (\Lambda_m^0 - \Lambda_m)}$.
- Diffusion coefficient: $D [\text{cm}^2 \text{ s}^{-1}] = \frac{RT \lambda^0}{|z| F^2}$ (Nernst-Einstein correlation).

13.5.2. Microscopic View of Electrode-Solution Interactions

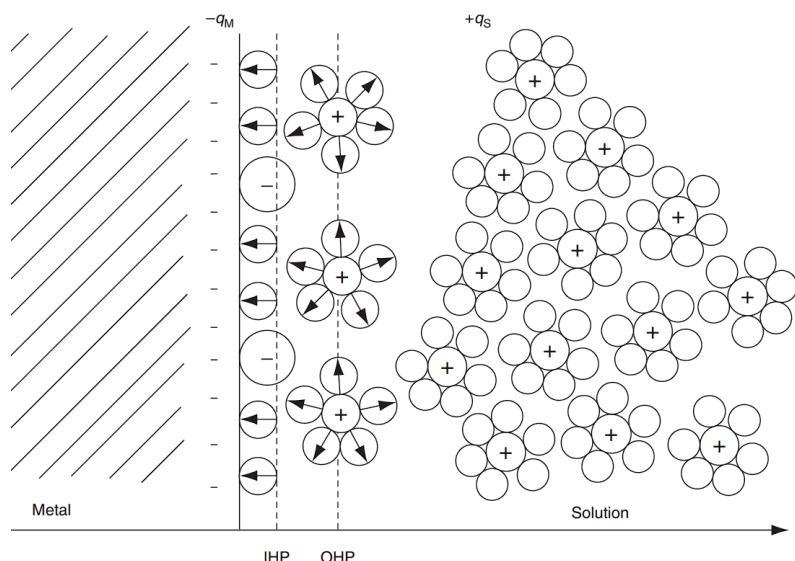
Anode: electrode in which conventional current leaves, associated with **oxidation**.

The anode is positively charged in an electrolytic cell and negatively charged in a galvanic cell.

Cathode: electrode in which conventional current enters, associated with **reduction**.

The cathode is negatively charged in an electrolytic cell and positively charged in a galvanic cell.

Electrical Double Layer (EDL, Helmholtz Layer) Formation at Electrode Interfaces



Within the inner Helmholtz plane (IHP), adsorbed ions and solvent molecules are in contact with the electrode surface. The outer Helmholtz plane (OHP) represents the furthest point at which solution counterions are interacting with the electrode; in the bulk solution, they are fully solvated and diffuse under the EMF.

Molecular Orbital Interactions

For band theory, see Section 8.6.1. For MO theory, see Section 13.1.11.

At an **inert (capacitive, polarisable), conducting** electrode (e.g. platinum or graphite):

- at **negative** potential ($-V$), the conduction band is partially filled, **raising** the Fermi level
- at **positive** potential ($+V$), the valence band is partially depleted, **lowering** the Fermi level

Interactions with nearby molecules in the solution can then occur:

- when the Fermi level is at or **above** the LUMO energy of a solution species, electron density can be accepted by the solution species from the electrode conduction band (**reduction**)
- when the Fermi level is at or **below** the HOMO energy of a solution species, electron density can be donated by the solution species into the electrode valence band (**oxidation**)

At a **reactive (Faradaic, non-polarisable), conducting** electrode (e.g. Cu, Zn, Ag, Au, Hg), the species may be the corresponding ion in solution (e.g. Ag^+ ions reacting with electrons in an Ag electrode at negative potential), leading to growth or depletion of the electrode metal.

13.5.3. Thermodynamics and Kinetics of Electrochemical Cells

Electrochemical reactions interconvert electrical and chemical energy of redox reactions.

- Anode half-reaction (oxidation): $a A \rightarrow c C + n e^-$
- Cathode half-reaction (reduction): $b B + n e^- \rightarrow d D$
- Overall reaction: $a A + b B \rightarrow c C + d D$ (n electrons transferred)
- Standard electrode potential: E^\ominus at standard conditions ($c = 1 \text{ mol dm}^{-3}$, $T = 298 \text{ K}$, $p = 1 \text{ bar}$). For a table of E^\ominus values (relative to SHE), see Section 13.5.22.
- **Cell potential:** $E_{\text{cell}} = E_{\text{cathode}} - E_{\text{anode}}$ (both taken as reduction potentials. Units: volts)
- **Ideal cell potential, non-standard conditions:** $E_{\text{cell}} = E^\ominus - \frac{RT}{nF} \ln \xi$ (**Nernst equation**)
(E^\ominus : standard electrode potential, $R = 8.314 \text{ J mol}^{-1} \text{ K}^{-1}$: ideal gas constant, T : temperature, $F = 96486 \text{ C mol}^{-1}$: Faraday's constant (charge of mole of electrons), $\xi = (\{C\}^c \{D\}^d) / (\{A\}^a \{B\}^b)$: reaction quotient)
- **Equilibrium constant:** $\ln K = \frac{nFE^\ominus}{RT}$ (equilibrium attained when $E = 0$, $\xi = K$)
- **Gibbs energy change (maximum reversible work):** $\Delta_r G^\ominus = -nF E^\ominus$ and $\Delta_r G = -nF E$
($\Delta G \neq 0$: cells are inherently non-equilibrium processes due to external work)
- **Current drawn:** $I(t) = nF r(t)$ (r [mol s^{-1}]: rate of reaction)
- Charge transferred: $\Delta Q = \int_0^{\Delta t} I(t) dt = I_{\text{avg}} \Delta t = i_{\text{avg}} A \Delta t$ (Δt : time duration)
- **Current due to kinetic overpotential η ,** for a unimolecular E mechanism electrode process:
 $O + n e^- \rightleftharpoons R$ (**Butler-Volmer equation**)

$$i = i_0 \left(\underbrace{e^{\frac{\alpha n F}{RT} \eta}}_{\text{anodic}} - \underbrace{e^{-\frac{(1-\alpha) n F}{RT} \eta}}_{\text{cathodic}} \right) \xrightarrow[\alpha = \frac{1}{2}]{\text{reversible}} i = 2i_0 \sinh \left(\frac{nF}{2RT} \eta \right) \xrightarrow[\text{about } \eta=0]{\text{linearised}} i = \left(\frac{RT}{i_0 n F} \right)^{-1} \eta$$

(i : current density [A cm^{-2}], i_0 : reversible current (at $\eta = 0 \text{ V}$ so $E = E_{\text{Nernst}}$),
 $\alpha = \frac{-1}{F} \frac{\partial(\Delta G_{ox}^\ddagger)}{\partial \phi}$: (anodic) charge transfer coefficient (fraction of current, equal to 0.5 if reversible),
 $\Delta G_{ox}^\ddagger = RT \ln \alpha$: Gibbs free activation energy of (anodic) reaction, $A_{TS} = \frac{2.303 RT}{\alpha n F}$: (anodic) Tafel slope (of η vs $\log_{10} i$ graph, equal to **reciprocal** of limiting slope of $\log_{10} \eta$ vs i graph), equal to 118 mV per decade for ($n = 1$, $T = 298 \text{ K}$, $\alpha = 0.5$))
- Approximation at high overpotentials: $\eta = \pm A_{TS} \log_{10} \frac{i}{i_0}$ (Tafel equation)

Note: n may be different in the anodic and cathodic branches if they have different mechanisms.

In addition to kinetic and Ohmic losses, there may also be concentration polarisation (back-diffusion due to concentration gradients during operation) and bubble overpotential (gas formation at the electrode decreases effective area) contributions to the overpotential. Typical ranges for electrolysis of water are $E_{\text{cell}} = 1.5 \text{ V}$, $E_{\text{Nernst}} = 1.29 \text{ V}$, $\eta = 10 \text{ mV}$, $IR = 300 \text{ mV}$.

Electrolytic cell: external electrical energy is supplied ($W < 0$) to an otherwise non-spontaneous chemical reaction to render it spontaneous. Typical application: chloralkali process.

For practical electrolytic cells, see Section 8.5.15.

- Non-ideal cell potential: $E_{\text{cell}} [\text{V}] = -E^{\ominus} + \frac{RT}{nF} \ln \xi + \eta_a + \eta_c + IR_{\Omega}$
(η : electrode kinetic overpotential for anode and cathode, I : current, R_{Ω} : electrolyte resistance)
- Loss of available power due to irreversibilities: $r\sigma [\text{W}] = rnF(\eta_a + \eta_c + iR_{\Omega})$
- Electrical power input: $P_{\text{in}} [\text{W}] = I E_{\text{cell}} = r(\Delta_r G + \sigma)$ (minimum input power: $P_{\text{in}} \geq r \Delta_r G$)
- Chemical energy output: $rQ_{\text{sys}} [\text{W}] = r\Delta_r H = r(\Delta_r G + T \Delta_r S)$; if $\sigma = -T \Delta_r S$ then cell is isothermal
- Coefficient of performance: $\eta = \frac{\text{chemical power output}}{\text{electrical power input}} = \frac{r \times \Delta_r H}{P_{\text{in}}}$ (maximum CoP: $\eta \leq \frac{\Delta_r H}{\Delta_r G}$)

Galvanic cell: energy from a spontaneous chemical reaction is converted to electrical energy ($W > 0$). Typical application: batteries and fuel cells.

For practical galvanic cells, see Section 8.5.8.

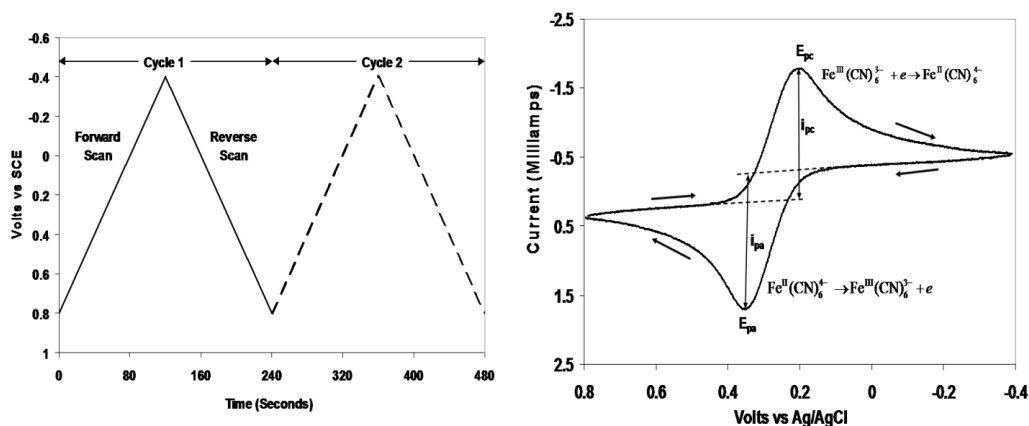
- Non-ideal cell potential: $E_{\text{cell}} [\text{V}] = E^{\ominus} - \frac{RT}{nF} \ln \xi - \eta_a - \eta_c - iR_{\Omega}$
(η : electrode kinetic overpotential for anode and cathode, I : current, R_{Ω} : electrolyte resistance)
- Loss of available power due to irreversibilities: $r\sigma [\text{W}] = rnF(\eta_a + \eta_c + iR_{\Omega})$
- Electrical power output: $P_{\text{out}} [\text{W}] = I E_{\text{cell}} = r(\Delta_r G - \sigma)$ (maximum output power: $P_{\text{out}} \leq r \Delta_r G$)
- Chemical energy input: $rQ_{\text{sys}} [\text{W}] = r\Delta_r H = r(\Delta_r G + T \Delta_r S)$; if $\sigma = -T \Delta_r S$ then cell is isothermal
- Efficiency: $\eta = \frac{\text{electrical power output}}{\text{chemical power input}} = \frac{P_{\text{out}}}{r \times \Delta_r H}$ (maximum efficiency: $\eta \leq \frac{\Delta_r G}{\Delta_r H} < 1$)

13.5.4. Charge Transfer Phenomena in Water

- **Solvation of ions:** aqueous cations are surrounded by a coordination sphere (primary solvation shell) of water molecules e.g. $\text{Na}^+ \rightarrow [\text{Na}(\text{H}_2\text{O})_6]^+$. Coordination numbers vary from 4 for Li^+ and Be^{2+} to 6 for most transition metals to 8-9 or higher for lanthanides / actinides. Additional water molecules (12 or more) associate with the metal ion through a secondary solvation shell by hydrogen bonding to coordinated water molecules.
- **Solvation of hydronium:** hydronium ions (H_3O^+) are solvated in water to form various associated species, including the Eigen cation H_9O_4^+ (hydronium with three hydrogen bonds to three water molecules) and the Zundel cation H_5O_2^+ (a proton forms a symmetric hydrogen bond to two water molecules).
- **Exclusion zone:** at the interface between water and hydrophilic solid (e.g. Nafion) or metal (e.g. electrodes), water molecules have reduced activity. Hydrophobic molecules, including microparticles, are expelled from this coherent region (diffusiophoresis, Section 13.4.4). Under intense IR radiation to ionise the coherent state, a current and p.d. is generated in pure water (oxyhydroelectric effect).
- **Grotthuss proton-hopping mechanism:** hypothesised transfer of protons between water molecules through hydrogen bonds in a linear fashion, at a much higher rate than by diffusion in bulk solution. At low temperatures, quantum tunnelling of protons contributes to this effect.
- **Pines mechanism:** recent research indicates a well-supported alternative to the Grotthuss mechanism, where groups of three water molecules (H_7O_3^+) shuttle a proton between them, with new water molecules ahead joining the group to continue the conduction.
- **Special pair dance:** hydronium ions alternate between Eigen and Zundel states. Since the exchange can occur in any direction, this mechanism transfers protons at an overall rate even faster than the Grotthuss mechanism.

13.5.5. Cyclic Voltammetry (CV)

A slow periodic (shifted triangular wave) voltage is applied to a working electrode in a galvanic cell setup. The current through the counter electrode is measured. The working electrode is typically a glassy carbon electrode (GCE).



For reversible electrode reactions,

- Peak current: $i_p = 0.4463 \times (nF)^{3/2} Ac \left(\frac{D\dot{v}}{RT} \right)^{1/2}$ (Randles-Sevcik equation)
- Peak voltages: $E^\ominus = \frac{1}{2} (E_{pa} + E_{pc})$ and $E_{pa} - E_{pc} = \frac{0.059 [V]}{n}$

Reaction mechanisms (E: redox step, C: chemical step)

- E mechanism: $O + n e^- \rightleftharpoons R$: has $i_{pa} = i_{pc}$ (if reversible; diffusion controlled)
- EC mechanism: $O + n e^- + A \rightleftharpoons R + A \rightarrow Z$: has $i_{pc} > i_{pa}$. If $Z = O$ (catalytic regeneration) then acts as a simple E mechanism instead.
- CE mechanism: $Z \rightarrow O + n e^- \rightleftharpoons R$: has $i_{pa} > i_{pc}$. As scan rate decreases, ratio approaches 1.
- Adsorption process: $i_p = \frac{n^2 F^2 \Gamma A \dot{v}}{4RT}$; charge consumed = $Q = \int i dv = nFA\Gamma$.

(\dot{v} : voltage sweep rate [$V s^{-1}$], D : diffusion coefficient [$cm^2 s^{-1}$], A : working electrode surface area [cm^2], c : bulk concentration [$mol cm^{-3} = mM$], Γ : surface coverage fraction)

For irreversible reactions (charge transfer coefficient $\alpha \neq 0.5$):

- Peaks for a redox couple are more widely separated.
- Voltage: $E_p = E^\ominus - \frac{RT}{\alpha nF} \left(0.78 - \ln \frac{k^\ominus}{\sqrt{D}} + \ln \left(\frac{\alpha nF}{RT} \right)^{1/2} \right)$
- Current: $i_p = 2.99 \times 10^5 [C mol^{-1} V^{-1/2}] \times \alpha^{1/2} n^{3/2} Ac D^{1/2} \dot{v}$

13.5.6. Chronoamperometry

A step change in potential (external overpotential) is applied to a working electrode using a potentiostat. The resulting current through the working electrode is measured over time.

Diffusion-controlled Faradaic current: $i_d = nFAc\left(\frac{D}{\pi t}\right)^{1/2}$ (Cottrell equation)

(c : ion concentration in bulk solution, t : time since step applied, D : diffusion coefficient of ion in solution, $i_d(t)$: time-dependent step response in current)

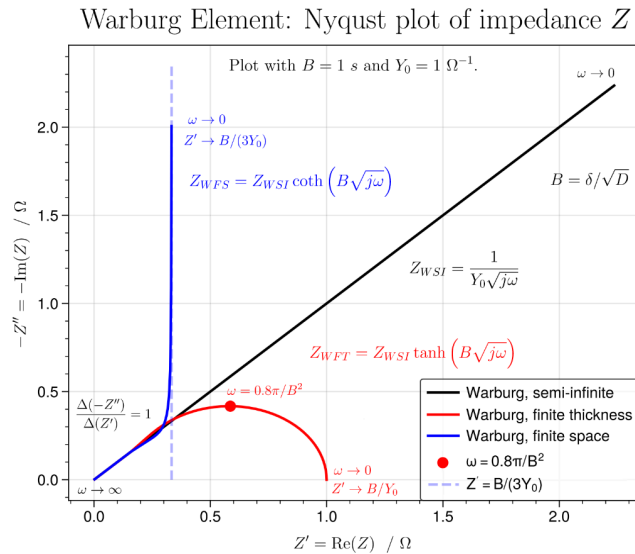
When the step is applied, ions in the immediate vicinity of the electrode are reacted and generate a high initial current. This current dissipates over time as the products form a diffusion layer, which ions from the bulk solution must traverse through before they can react at the electrode. The current decays to the equilibrium value.

The time-integrated current response over a period after the step yields the total charge transferred. A variation is to measure the charge transferred directly (chronocoulometry), which reduces the noise further by implicit integration (amplifier with capacitor)

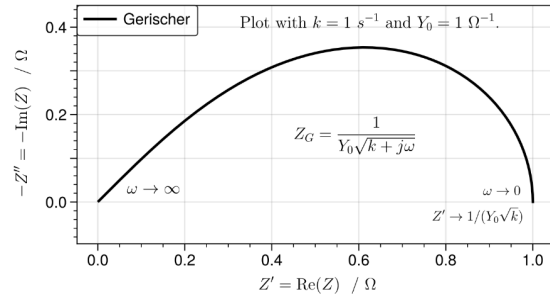
13.5.7. Electrical Impedance Spectroscopy (EIS)

The AC impedance of an electrode can be measured with electrical impedance spectroscopy (EIS). (Z : impedance, $Z' = \text{Re}(Z)$: resistance, $Z'' = \text{Im}(Z)$: reactance such that $Z = Z' + jZ''$)

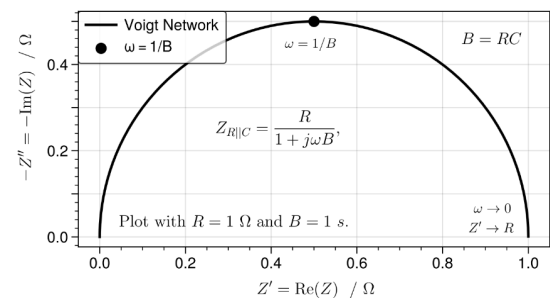
Nyquist Plots of Common Nonlinear Circuit Elements (Warburg, Gerischer, Voigt):



Gerischer Element: Nyquist Plot of Impedance Z



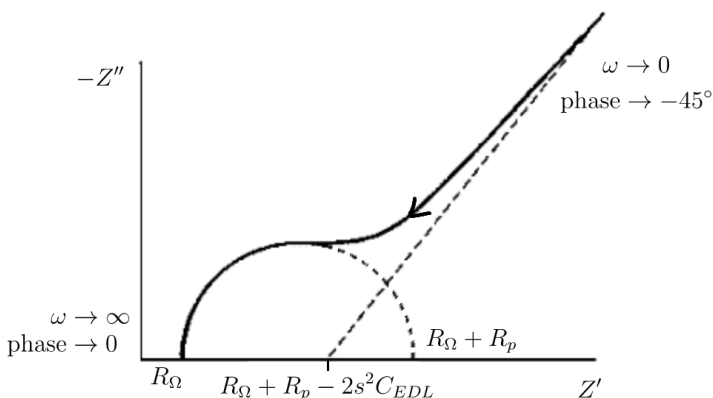
Voigt Network: Nyquist Plot of Impedance Z



(Y_0 : reference admittance ($1/Z$) at $\omega = 1 \text{ rad s}^{-1}$, B : time constant, k : rate constant for C step)

The constant-phase element (CPE) is also common, representing an imperfect double-layer capacitance: $Z_{CPE} = 1 / [(j\omega)^n C_{EDL}]$. Nyquist plot: straight line with $\theta = -\frac{\pi}{2}n$ ($n \leq 1$).

Randles cell: models a full single electrode: $Z_R = R_\Omega + [Z_{CPE} || (R_p + Z_{WSI})]$



(R_Ω : Ohmic resistance (electrolyte), Z_{CPE} : CPE representing electrical double layer, R_p : polarisation (charge transfer) resistance, Z_{WSI} : Warburg impedance (semi-infinite), s : Warburg constant, such that $Y_0 = (\sqrt{2} \text{ s})^{-1}$,

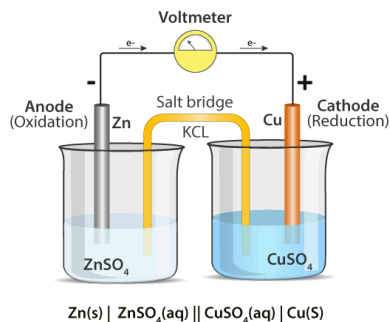
$$\text{also given by } s = \frac{RT}{\sqrt{2}n_e^2 F^2 A} \left(\frac{1}{\sqrt{D_{ox}} C_{ox}^*} + \frac{1}{\sqrt{D_{red}} C_{red}^*} \right)$$

(Nyquist plot shows $n = 1$ in the CPE; D : diffusion coefficient, c^* : surface concentration, n_e : moles of electrons)

13.5.8. Primary Galvanic Cells

Galvanic (voltaic) cell: a system which converts chemical energy to electrical energy.

Primary cell: a cell using irreversible reactions, so cannot be reused once fully discharged.



The half-reaction with the larger reduction potential E^{\ominus}_{red} will proceed as **reduction** (the **cathodic** reaction). The other half-reaction is an **oxidation** (the **anodic** reaction). From the salt bridge, anions flow to the anode solution, and cations flow to the cathode solution to maintain electroneutrality.

Left: Daniell cell, Zn | Zn²⁺ || Cu²⁺ | Cu, with KCl salt bridge.

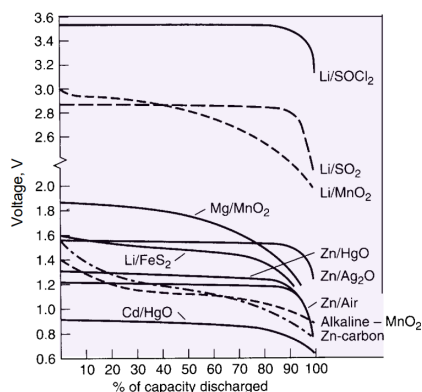
Reference Half-Cells (Standards and Secondary Standards):

(E^{\ominus} relative to SHE)

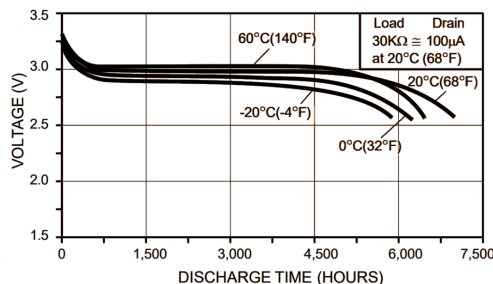
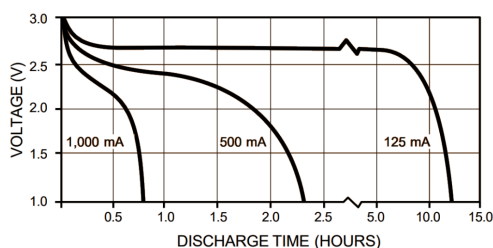
- Standard Hydrogen Electrode (SHE): H^+ (aq, 1 M) | H_2 (g, 1 bar) | Pt $E^{\ominus} \equiv 0.000$ V
- Silver Chloride Electrode: Ag (s) | AgCl (s) | KCl (aq, 3 M) $E^{\ominus} = 0.235$ V
- Saturated Calomel Electrode (SCE): Cl^- (aq, 4 M) | Hg_2Cl_2 (s) | Hg (l) | Pt $E^{\ominus} = 0.241$ V

Common Primary Cells: cell notation A | B || C | D implies A → B (anode, -ve) and C → D (cathode, +ve)

Cell	Anodic reaction (-ve)	Cathodic reaction (+ve)	E^{\ominus}	Notes and common applications
Daniell cell	$\text{Zn (s)} \rightarrow \text{Zn}^{2+} \text{ (aq)} + 2 \text{ e}^-$	$\text{Cu}^{2+} \text{ (aq)} + 2 \text{ e}^- \rightarrow \text{Cu (s)}$	1.10 V	The first battery invented (the Voltaic pile).
zinc-carbon cell (Leclanché type)	$\text{Zn (s)} \rightarrow \text{Zn}^{2+} \text{ (aq)} + 2 \text{ e}^-$	$2 \text{ MnO}_2 \text{ (s)} + 2 \text{ NH}_4^+ \text{ (aq)} + 2 \text{ e}^- \rightarrow \text{Mn}_2\text{O}_3 \text{ (s)} + 2 \text{ NH}_3 \text{ (aq)} + \text{H}_2\text{O (l)}$ (also formed: MnOOH , Mn_3O_4)	1.43 V	Common, low-cost primary battery; available in a variety of sizes. Used for e.g. flashlights, portable radios, toys, novelties, instruments...
alkaline dry cell	$\text{Zn (s)} + 2 \text{ OH}^- \text{ (aq)} \rightarrow \text{ZnO (s)} + \text{H}_2\text{O (l)} + 2 \text{ e}^-$ (intermediate: $\text{Zn(OH)}_2 \text{ (aq)}$)	$2 \text{ MnO}_2 \text{ (s)} + \text{H}_2\text{O (l)} + 2 \text{ e}^- \rightarrow \text{Mn}_2\text{O}_3 \text{ (s)} + 2 \text{ OH}^- \text{ (aq)}$	1.43 V	Most popular general-purpose premium battery (Duracell AA / AAA); good low-temperature and high-rate performance; moderate cost.
soluble lithium cell	$\text{Li (s)} \rightarrow \text{Li}^+ \text{ (aq)} + \text{e}^-$	$2 \text{ SOCl}_2 \text{ (l)} + 4 \text{ e}^- \rightarrow \text{S (s)} + \text{SO}_2 \text{ (l)} + 4 \text{ Cl}^- \text{ (aq)}$	3.65 V	High energy density; long shelf life; good performance over wide temperature range.
lithium-manganese button cell	$\text{Li (s)} \rightarrow \text{Li}^+ \text{ (aq)} + \text{e}^-$	$\text{MnO}_2 \text{ (s)} + x \text{ Li}^+ \text{ (aq)} + \text{e}^- \rightarrow \text{Li}_x\text{MnO}_2 \text{ (s)}$	3.3 V	High energy density; good rate capability and low-temperature performance; long shelf life; competitive cost.



Characteristic discharge curves for Li/MnO₂ cell for various I and T



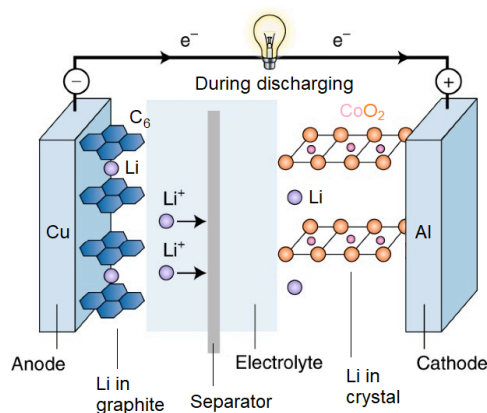
13.5.9. Secondary Galvanic Cells

Secondary cell: a cell using reversible reactions, so can be recharged after use and used again.

Cell	Anodic reaction (-) (forward is discharging)	Cathodic reaction (+) (forward is discharging)	Typical battery specifications	Notes and common applications
lead acid battery	$\text{PbO}_2 (\text{s}) + 4 \text{H}^+ (\text{aq}) + 2 \text{e}^- \rightleftharpoons \text{Pb}^{2+} (\text{aq}) + 2 \text{H}_2\text{O} (\text{l})$	$\text{Pb} (\text{s}) \rightleftharpoons \text{Pb}^{2+} (\text{aq}) + 2 \text{e}^-$	$E^\ominus = 2.1 \text{ V}$ $E_{\text{grav}} = 40 \text{ Wh kg}^{-1}$ $E_{\text{vol}} = 85 \text{ Wh L}^{-1}$ $P = 180 \text{ W kg}^{-1}$	<p>Dissolution-precipitation mechanism. Sulfuric acid at $0 < \text{pH} < 1$ is used, forming PbSO_4. The Pb is hardened by alloying with ~5% Sb, and shaped into a grid.</p> <p>Modifications include the SLI (Starting, Lighting, Ignition: cells stacked in series as planar grids), VRLA/SLA (valve regulated lead acid: less electrolyte), carbon-enhanced battery (a hybrid supercapacitor with one C cathode and twin PbO_2 anode).</p>
nickel-cadmium battery	$\text{Cd} + 2 \text{OH}^- \rightleftharpoons \text{Cd}(\text{OH})_2 + 2 \text{e}^-$	$\text{NiOOH} + \text{H}_2\text{O} + \text{e}^- \rightleftharpoons \text{Ni}(\text{OH})_2 + \text{OH}^-$	$E^\ominus = 1.2 \text{ V}$ $E_{\text{grav}} = 50 \text{ Wh kg}^{-1}$ $E_{\text{vol}} = 100 \text{ Wh L}^{-1}$ $P = 150 \text{ W kg}^{-1}$	<p>Long cycle life and fast recharging. However, has a memory effect (voltage depression) in some cases, due to physical changes in uncycled regions of the cathode.</p>
Ni-MH battery (metal hydride)	$\text{MH} + \text{OH}^- \rightleftharpoons \text{M} + \text{H}_2\text{O} + \text{e}^-$ <p>(M = alloy storing hydrogen)</p>	$\text{NiOOH} + \text{H}_2\text{O} + \text{e}^- \rightleftharpoons \text{Ni}(\text{OH})_2 + \text{OH}^-$	$E^\ominus = 1.2 \text{ V}$ $E_{\text{grav}} = 100 \text{ Wh kg}^{-1}$ $E_{\text{vol}} = 200 \text{ Wh L}^{-1}$ $P = 600 \text{ W kg}^{-1}$	<p>Oxygen recombination prevents gas build-up: Charged cathode: $4 \text{OH}^- \rightarrow 2 \text{H}_2\text{O} + \text{O}_2 + 4 \text{e}^-$ Charged anode: $4 \text{MH} + \text{O}_2 \rightarrow 4 \text{M} + 2 \text{H}_2\text{O}$</p>
Li-ion polymer battery (LiPo)	$\text{Li} \rightleftharpoons \text{Li}^+ + \text{e}^-$ <p>(Li is intercalated in graphite as LiC_6, between graphenes)</p>	$x \text{Li}^+ + \text{Li}_{1-x}\text{CoO}_2 + x \text{e}^- \rightleftharpoons \text{Li}^+[\text{CoO}_2]^-$ <p>(lithium-doped crystal substrate)</p>	$E^\ominus = 3.7 \text{ V}$ $E_{\text{grav}} = 200 \text{ Wh kg}^{-1}$ $E_{\text{vol}} = 500 \text{ Wh L}^{-1}$ $P = 300 \text{ W kg}^{-1}$	<p>Rechargeable ion battery, used in electric vehicles. Li^+ ions are exchanged between being intercalated in an anode (high energy state) and in a cathode (low energy state) to produce a voltage.</p> <p>See Section 13.5.10 for more info.</p>

13.5.10. Design of Rechargeable Ion Batteries

Principle of Operation: exchange of small cations from one intercalator to another of different energies to provide the cell EMF



Lithium-ion Cell: Anode intercalation prevents dendritic growth of solid lithium, which can puncture the electrolyte and cause the short-circuiting and breakdown of the cell. The electrolyte is a lithium salt e.g. LiPF_6 , which permits rapid diffusion of Li^+ . The separator is a nanoporous polymer structure e.g. PP, PE, which blocks electron diffusion while permitting Li^+ . When charging for the first time after the cell's construction, Li^+ ions are solvated by the electrolyte and react with the graphite to form a solid-electrolyte interface passivation layer (SEI layer), consuming about 5% of the lithium in the process. This prevents electrons contacting the electrolyte which would result in its degradation, and permits cycling.

Performance Metrics for Rechargeable Batteries

- Total charge capacity [A h]: $1 \text{ A h} = 3600 \text{ C}$
- Battery output: specific power [W kg^{-1}], power density [W L^{-1}]. A trade-off with battery capacity.
- Battery capacity: gravimetric energy density [W h kg^{-1}], volumetric energy density [W h L^{-1}]
- Discharge current: C-rate [h^{-1}] = $\frac{\text{output current required to fully discharge battery in one hour [A]}}{\text{charge capacity [A h]}}$
- Cycle life: number of charge-discharge cycles to lose performance. Depends on the depth of discharge and the quantitative metric used to assess extent of loss of performance.
- Cost: lifetime cost [$\$/\text{kWh/cycle}$], total per-unit cost [$\$$], material cost [$\$/\text{kg}^{-1}$]
- Self-discharge: voltage drop over time in open-circuit conditions, settling at the float voltage
- Reliability and safety: up-time, breakdown rate, maintenance costs, risk, hazard severity

Important performance metrics for EVs and grid-scale energy storage applications are:

- Electric sedan cars: per-unit cost > volumetric capacity > cycle life.
- Electric heavy vehicles (freight lorries, ships and planes): gravimetric capacity > cycle life > cost.
- Transmission load/frequency balancing: lifetime cost > safety and reliability > cycle life.
- Residential storage and smart grid: safety and reliability > lifetime cost > cycle life.

Battery Chemistry and Practicalities of Materials Selection

Many of the materials used in these batteries are critical materials (e.g. lithium, cobalt, manganese). Alternative battery chemistries are needed to alleviate strains on resources as batteries are crucial in sustainable energy technologies in the future. This is an active area of research, but technology readiness and maturity remains a hurdle.

The mining and refining of critical materials is subject to availability due to geopolitical and supply chain influences. As with most raw materials, mining companies have high leverage as they can sell their produce to refiners as commodities on the spot market, which is volatile. Battery companies with higher bargaining power may be able to negotiate fixed-price contracts to alleviate this uncertainty.

Variations in battery chemistry currently under research with potential applications include:

- High nickel, low cobalt cathode materials (e.g. $\text{LiNi}_{0.6}\text{Co}_{0.05}\text{Mn}_{0.35}\text{O}_2$), to reduce reliance on critical materials.
- Lithium iron phosphate (LFP, LiFePO_4) eliminates cobalt completely, as pursued by Tesla for use in EVs.
- Sodium ion cells, replacing Li^+ with Na^+ (eliminates Li). Less flammable but lower energy performance.
- Zinc ion cells, including the $\text{Na}_{0.12}\text{Zn}_{0.25}\text{V}_2\text{O}_5 \cdot 2.5 \text{H}_2\text{O}$ (NVZO) cathode. The NVZO battery uses water-based electrolyte to exploit the special pair dance mechanism (Section 13.5.4) giving exceptional kinetics and no flammability hazard. Challenges include hydrogen formation from electrolysis of water (requiring low operating voltage), and dendrite formation in the zinc anode.
- Solid state batteries (SSBs) use a solid phase electrolyte, allowing the use of metal anodes (lithium without graphite) as dendrite formation is no longer problematic for the cell.

Cathodes can be classed as layered (e.g. LiCoO_2), spinel (e.g. LiMn_2O_4), polyanionic (e.g. $\text{Li}_x\text{Fe}_2(\text{XO}_4)_3$, $\text{X} = \text{S} / \text{Mo} / \text{W}$) or olivine (e.g. LiFePO_4). Ion migration through the cathode lattice is dependent on the octahedral site stabilisation energy of a metal cation in interstitial voids, $\text{OSSE} = \text{CFSE}_{\text{octahedral}} - \text{CFSE}_{\text{tetrahedral}}$ (Section 15.5.8, crystal field theory).

Battery Engineering in Electric Vehicles (EVs)

EV technology is already widespread and growing in the automotive industry, for cars (e.g. Tesla Model Y, Hyundai Ioniq 6, Nissan Leaf) and many trains. EV adoption is less common for heavy-duty applications (trucks, planes, ships) due to the high power requirements.

Ion batteries are typically manufactured in a cylindrical geometry, in which thin-film intercalator and cathode materials are deposited onto metal electrode foils, placed in close contact with the electrolyte/separator between them and rolled up to save space. Current collectors are placed at the metal foils, and output current is used to power a brushless DC motor (for hybrid plug-in EVs) or induction motor (for high-performance pure EVs). Motors produce usable torque output across a wider band of speeds than internal combustion engines.

In an EV, ion cells are connected in series to increase the voltage, and these are stacked in parallel to increase the current, to form a single battery module. Several modules are further connected in series to form a battery pack, with typical ratings on the order of ~ 25 V and ~ 250 A (~ 6 kW, 200 Ah). The high cell density leads to heat production during operation, which can reduce the performance of the battery, and can be a fire hazard in defective assemblies.

A battery management system (BMS) is a digital system used to monitor the state of charge (SoC), temperature and voltage levels. Liquid-cooling (water with glycol for sub-freezing temperatures) is used to dissipate heat from the batteries, with the BMS setting the coolant flow rate using a control system to maintain optimal battery temperature. In some EVs (e.g. Tesla), BMS can also use cell balancing (voltage protection) to ensure all cells discharge at the same rate, preventing anomalous charging and discharging due to over/undervoltage.

13.5.11. Fuel Cell Batteries

Fuel cells: not rechargeable (primary), but never used up as long as reactants are supplied.

Cell	Anodic reaction (-) (forward is discharging)	Cathodic reaction (+) (forward is discharging)	E^\ominus	Notes and common applications
alkaline hydrogen fuel cell (AFC)	$\text{H}_2 + 2 \text{OH}^- \rightarrow 2 \text{H}_2\text{O} + 2 \text{e}^-$	$\text{O}_2 + 2 \text{H}_2\text{O} + 4 \text{e}^- \rightarrow 4 \text{OH}^-$	1.23 V	Maximum efficiency is ~70%. A recent development is the solid state alkaline fuel cell (SAFC) which prevents KOH being poisoned by CO_2 into K_2CO_3 .
proton exchange membrane (PEMFC)	$\text{H}_2 \rightarrow 2 \text{H}^+ + 2 \text{e}^-$	$\text{O}_2 + 4 \text{H}^+ + 4 \text{e}^- \rightarrow 2 \text{H}_2\text{O}$	1.23 V	The polyelectrolyte (ionomer) membrane conducts protons but blocks the gas fuels.
solid oxide fuel cell (SOFC)	$\text{H}_2 \rightarrow 2 \text{H}^+ + 2 \text{e}^-$; $2 \text{H}^+ + \text{O}^{2-} \rightarrow \text{H}_2\text{O}$	$\text{O}_2 + 4 \text{e}^- \rightarrow 2 \text{O}^{2-}$	1.23 V	High temperatures (600 - 1000 °C), no catalyst required. Oxide ions (O^{2-}) diffuse across the solid yttria-stabilised zirconia (YSZ) electrolyte. Requires fuel desulfurisation to avoid poisoning. They can be integrated in a gasification power plant for burning biomass/coal.
glucose biofuel cell (GBFC)	glucose ($\text{C}_6\text{H}_{12}\text{O}_6$) + 2OH^- \rightarrow gluconolactone ($\text{C}_6\text{H}_{10}\text{O}_6$) + $2 \text{H}_2\text{O} + 2 \text{e}^-$ (glucose oxidase enzyme catalysed)	$\text{O}_2 + 4 \text{H}^+ + 4 \text{e}^- \rightarrow 2 \text{H}_2\text{O}$ (laccase enzyme catalysed)	1.34 V	The enzymes require cofactors and very specific operating conditions to function. They are currently not as efficient as hydrogen fuel cells but are more sustainable. For more info, see Section 17.4.10.

13.5.12. Molten Salt Batteries and Liquid Metal Batteries

High-operating temperature batteries can be used to generate electricity from industrial waste heat, where chemical reactions are often much more efficient.

Molten salt batteries are the galvanic equivalent of molten salt electrolysis. The separator is a β -alumina solid electrolyte (BASE, sodium polyaluminate) which is a fast ion conductor. They typically use temperatures around $T = 300$ °C.

Established example: sodium-sulfur battery: $2 \text{Na} + 4 \text{S} \rightarrow \text{Na}_2\text{S}_4$. ($E = 2.0$ V)

Modern example: sodium-nickel chloride battery (NaNiCl_2 , ZEBRA battery).

Liquid metal batteries use molten metal electrodes, at very high temperatures ($T = 700$ °C).

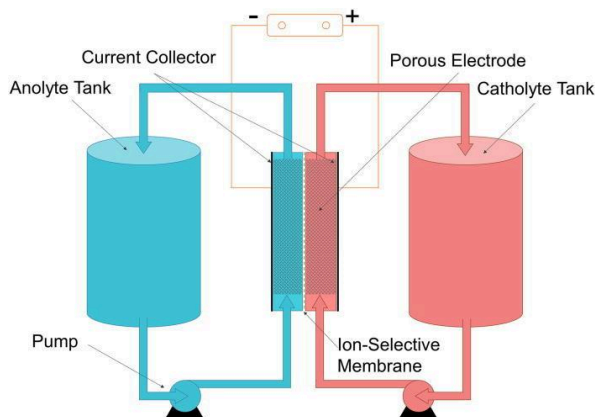
Example: a Mg (l) anode, Sb (l) cathode.

Anode: $\text{Mg}(\text{l}) \rightarrow \text{Mg}^{2+}(\text{l}) + 2 \text{e}^-$; Cathode: $\text{Mg}^{2+}(\text{l}) + 2 \text{e}^- \rightarrow \text{Mg}^{2+}(\text{in Sb})$

Mg^{2+} ions diffuse between the electrodes from the pure to the alloy state. Very high current densities are possible. At full charge, the cathode is pure Sb (l).

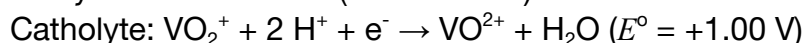
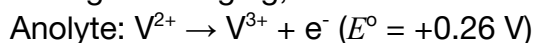
13.5.13. Redox Flow Batteries (RFBs, Redox Cells)

Redox flow batteries use continuous circulation of reactant solutions (anolyte/negolyte and catholyte/posolyte), like a rechargeable fuel cell. RFBs have been projected as useful for large grid-scale energy storage.



Vanadium Ion RFB (1.5 M VSO₄ in 2 M H₂SO₄: near pH 0)

During discharging,



Electrodes: porous carbon electrocatalysts
e.g. graphene, CNTs, WO₃-MWCNTs.

Separator: Nafion ionomer membrane (H⁺ exchange)
VO₂⁺ and VO²⁺ may be represented as V⁵⁺ and V⁴⁺.

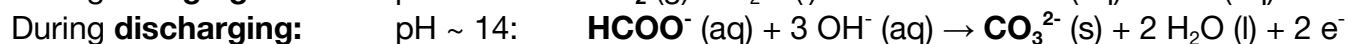
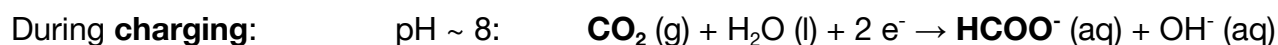
The volumetric flow rate sets the current and power output (up to a limit set by reaction kinetics). The volume of the supply tanks set the energy capacity, up to potentially very large sizes.

RFBs are typically constructed in stacks, with the tank feeding the electrolyte in series (high voltage) or in parallel (high current). Cell balancing by controlling the flow rate is necessary for safe and efficient operation, and state of charge (SoC) monitoring is done using an open-circuit test system to monitor open circuit voltage at the inlet and outlet of the electrolyte. Using a hybrid membrane of tungsten trioxide (WO₃) nanoparticles on graphene with teflon-reinforced Nafion, leakage of cations into the membrane is prevented.

Zinc-Bromine RFB: Zn/Zn²⁺ anolyte and Br₂/Br⁻ catholyte. During charging, zinc metal plates the anode and liquid bromine formation at the cathode. The bromine is corrosive and must be either stored in an organic complexed phase (e.g. *N*-methyl-*N*-ethylmorpholinium bromide, MEMBr), or using a porous monolithic carbon cryogel electrode to alleviate the high partial pressure of bromine. The catholyte flow contains additives to avoid zinc dendrite formation and facilitate uniform deposition.

Carbon Dioxide RFB: carbon negative generation of electricity

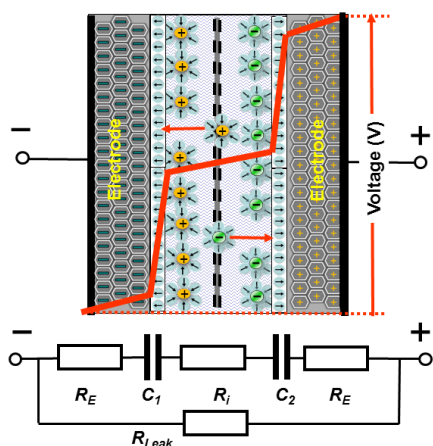
The anolyte reaction is run at different pH during charging/discharging to exploit the variable solubility of CO₂, cogenerating electricity and storing CO₂ as carbonate. The catholyte is Br₂/Br⁻.



The bifunctional anode electrocatalyst can be PdSn on LaCoO₃ perovskite. The high-pH conditions require NaOH which must be sourced sustainably (e.g. renewable chloro-alkali process: electrolysis of brine, at seawater desalination plants).

13.5.14. Supercapacitors

A capacitor consists of two high-surface-area inert electrodes separated by an ion-conducting electrolyte. There is a maximum allowable voltage between the electrodes in order to prevent 1) electrolysis and 2) breakdown from occurring, so the electrolyte behaves as a dielectric insulator (as in a regular capacitor) rather than an electrically-conductive medium.



Ions in the electrolyte are attracted to the electrodes, once they have been charged to some degree. The ions form an electrical double layer capacitance (EDLC), allowing the input charge to be stored in the electrodes.

Common electrolytes include salt water, salts in solid polymer matrices, quaternary ammonium salts in organic solvent, or ionic liquids.

Current leakage (self-discharge) can occur over long periods of time, in which charge is gradually depleted due to the finite resistance of the medium.

Energy density [J kg^{-1} or kWh kg^{-1}] depends on the geometry of the device, since the capacitance is dependent on shape and construction.

Power density [W kg^{-1}] depends on the impedance of the load it is connected to.

Supercapacitors are useful for energy storage, with high power density [W kg^{-1}] due to rapid charge exchange, but low energy density [$\text{kWh kg}^{-1} \sim \text{J kg}^{-1}$].

13.5.15. Electrolysis and Electrolytic Cells

Electrolysis with Inert Electrodes: ions in liquid or solution discharge at electrodes

Inert electrodes (e.g. graphite, platinum, carbon nanotubes) are conductive and polarisable. They develop static surface charges (like a capacitor) when an external DC EMF is applied. These charges are used as electron sources and sinks to facilitate redox reactions with the electrolyte, which results in a continuous current flow as the reactions proceed.

For the electrolysis of **molten** (pure anhydrous) ionic salts X^+Y^- (l),

- the **cation** X^+ is **reduced** to its elemental form at the **cathode** (-ve electrode)
- the **anion** Y^- is **oxidised** to its elemental form at the **anode** (+ve electrode)

For the electrolysis of **aqueous** ionic salts X^+Y^- (aq), neglecting overpotential effects:

- If $E^\ominus(X) < E^\ominus(H_2O)$ then **water is reduced** to H_2 and OH^- (X less reactive than H_2)
- If $E^\ominus(O_2) < E^\ominus(Y)$ then **water is oxidised** to O_2 and H^+ (typically: oxyanions)
- Otherwise, the same rules apply as in the electrolysis of molten X^+Y^- (l).

The reduction potentials of oxygen and water are $E^\ominus(H_2O) = -0.83$ V and $E^\ominus(O_2) = +1.23$ V.

Simple metal reactivity series: $K > Na > Li > Ca > Mg > Al > C > Zn > Fe > H_2 > Cu > Ag > Au > Pt$
(for aqueous electrolysis: **metal more reactive than H_2 : produces H_2 (g) at the cathode; otherwise produces the metal**)

Quantitative electrolysis: $I = nrF$ (I : current [A], r : reaction rate [$mol\ s^{-1}$], $F = 96500$ C mol^{-1})

Examples:

Electrolyte	Anode product	Cathode product
NaCl (l)	$2 Cl^- (l) \rightarrow Cl_2 (g) + 2 e^-$	$Na^+ (l) + e^- \rightarrow Na (s)$
NaCl (aq) or HCl (aq)	$2 Cl^- (l) \rightarrow Cl_2 (g) + 2 e^-$	$2 H_2O (l) + 2 e^- \rightarrow H_2 (g) + 2 OH^- (aq)$
CuBr ₂ (aq)	$2 Br^- (l) \rightarrow Br_2 (g) + 2 e^-$	$Cu^{2+} (aq) + 2 e^- \rightarrow Cu (s)$
H ₂ SO ₄ (aq)	$4 OH^- (aq) \rightarrow O_2 (g) + 2 H_2O (l) + 4 e^-$	$2 H^+ (aq) + 2 e^- \rightarrow H_2 (g)$

Electrolysis with Reactive Electrodes: ions compete with electrode to react

Examples:

Anode	Cathode	Electrolyte	Anode product	Cathode product
Cu	Cu	CuSO ₄ (aq)	$Cu \rightarrow Cu^{2+} + 2 e^-$	$Cu^{2+} + 2 e^- \rightarrow Cu$
Ag	any metal	AgNO ₃ (aq)	$Ag \rightarrow Ag^+ + e^-$	$Ag^+ + e^- \rightarrow Ag$

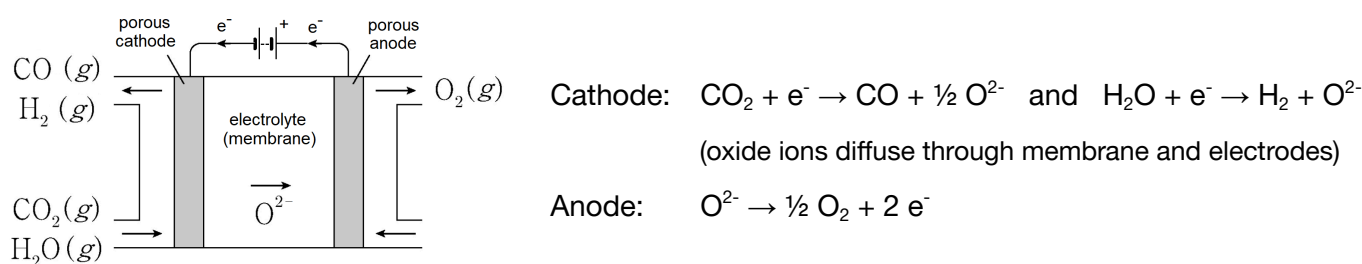
The silver nitrate with silver anode is used for electroplating, as the cathode is covered in silver.

13.5.16. Solid Oxide Electrolysis Cells (SOECs)

SOECs use a solid electrolyte instead of water. They allow for high current density, high efficiency and good stability. A common use is in high-temperature steam electrolysis (HTE), which performs the water-splitting reaction on steam at efficiencies of ~80%, higher than at room temperature.

To minimise energy input, the heat source to provide the temperature can come from the output of a suitably integrated system, such as the steam tube of a combined-cycle gas turbine (heat recovery, Section 7.2.13), cogeneration (CHP), or the water circuit of an LWR nuclear power plant.

Another application is the high-temperature co-electrolysis with carbon dioxide for its removal:



The CO_2 can be sourced from carbon capture schemes, while the $\text{H}_2 + \text{CO}$ product is syngas and can be converted to methane (synfuel) via Fischer-Tropsch synthesis (Section 14.2.1). In order to minimise net carbon emissions, the electrical power input as well as the heat source for the high temperature must be supplied from sustainable sources.

The electrodes are made of porous oxide composites. Common anode materials are nickel-YSZ (yttria stabilised zirconia, $\text{Ni-Y}_2\text{O}_3\text{-ZrO}_2$), or perovskites. A common cathode material is LSM (lanthanum strontium manganite, $\text{La}_{1-x}\text{Sr}_x\text{MnO}_3$). The high temperatures (~700 °C) can lead to degradation of the mechanical properties of these materials.

Solid oxide fuel cells (SOFCs) use similar materials for the reverse process, as a fuel cell.

Reversible solid oxide cells (rSOCs) use bifunctional electrolytes to allow fuel cell and electrolysis processes to take place in the same device, and are versatile load balancing components to achieve high energy efficiency in power plants.

13.5.17. Limiting Molar Ionic Conductivities Table

Cations: (values of λ^0 are given in $\text{S cm}^2 \text{ mol}^{-1}$, measured at 298 K (25 °C))

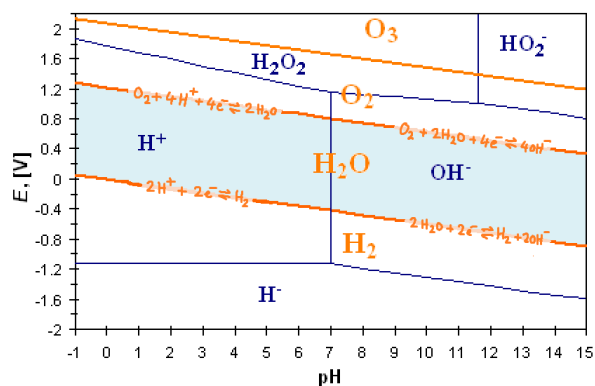
Ion (1+)	λ^0	Ion (1+)	λ^0	Ion (2+)	λ^0
H ⁺ (as H ₃ O ⁺)	349.6	(CH ₃) ₃ NH ⁺	47.2	Zn ²⁺	108.6
Li ⁺	38.7	(CH ₃) ₄ N ⁺	44.9	Pb ²⁺	142.0
Na ⁺	50.08	C ₅ H ₁₂ N ⁺	37.2	UO ₂ ²⁺	64
K ⁺	73.50	Ion (2+)	λ^0	Ion (3+)	λ^0
Rb ⁺	77.8	Be ²⁺	90	Al ³⁺	183
Cs ⁺	77.2	Mg ²⁺	106.0	Fe ³⁺	204
Ag ⁺	61.9	Ca ²⁺	119.0	La ³⁺	209.1
NH ₄ ⁺	73.5	Sr ²⁺	118.9	Ce ³⁺	209.4
CH ₃ CH ₂ NH ₃ ⁺	47.2	Ba ²⁺	127.2		
(CH ₃ CH ₂) ₂ NH ₂ ⁺	42.0	Mn ²⁺	106.2		
(CH ₃ CH ₂) ₃ NH ⁺	34.3	Fe ²⁺	108.0		
(CH ₃ CH ₂) ₄ N ⁺	32.6	Co ²⁺	105.6		
(CH ₃ CH ₂ CH ₂ CH ₂) ₄ N ⁺	19.5	Ni ²⁺	107.0		
(CH ₃) ₂ NH ₂ ⁺	51.8	Cu ²⁺	107.2		

Anions: (values of λ^0 are given in $\text{S cm}^2 \text{ mol}^{-1}$, measured at 298 K (25 °C))

Ion (1-)	λ^0	Ion (1-)	λ^0	Ion (2-)	λ^0
OH ⁻	199.1	IO ₄ ⁻	54.5	CO ₃ ²⁻	138.6
F ⁻	55.4	HCO ₃ ⁻	44.5	HPO ₄ ²⁻	66
Cl ⁻	76.35	H ₂ PO ₄ ⁻	57	SO ₄ ²⁻	160.0
Br ⁻	78.1	HSO ₄ ⁻	50	C ₂ O ₄ ²⁻	148.2
I ⁻	76.8	HC ₂ O ₄ ⁻	40.2	Ion (3-)	λ^0
NO ₂ ⁻	71.8	HCOO ⁻	54.6	PO ₄ ³⁻	207
NO ₃ ⁻	71.46	CH ₃ COO ⁻	40.9	Fe(CN) ₆ ³⁻	302.7
ClO ₃ ⁻	64.6	C ₆ H ₅ COO ⁻	32.4	Ion (4-)	λ^0
ClO ₄ ⁻	67.3			Fe(CN) ₆ ⁴⁻	442.0

The values of λ for H⁺ (aq) and OH⁻ (aq) are higher due to ion-hopping mechanisms (Section 13.5.4), in which solvent water molecule clusters exchange protons and hydroxyl groups.

13.5.18. Pourbaix Diagrams (Electrochemical Phase Diagrams)



Pourbaix diagram of water: all E against SHE

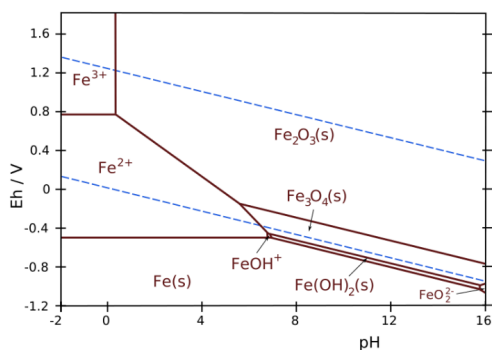
Thermodynamically stable products shown in orange. Corresponding redox agents shown in blue.

Above the upper limit for H_2O , oxygen gas is formed. Below the lower limit for H_2O , hydrogen gas is formed.

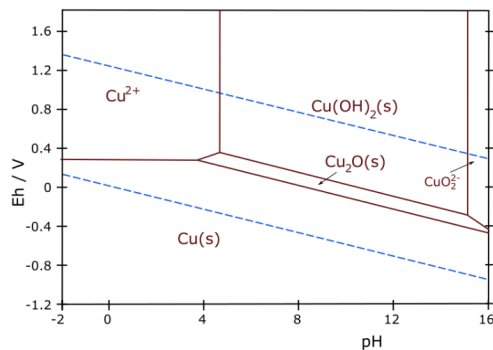
H_2O limit bounds: $0 < E + 0.0592 \text{ pH} < 1.229$.

Pourbaix diagrams for metals: upper (oxidation) and lower (reduction) H_2O limits in dotted lines.

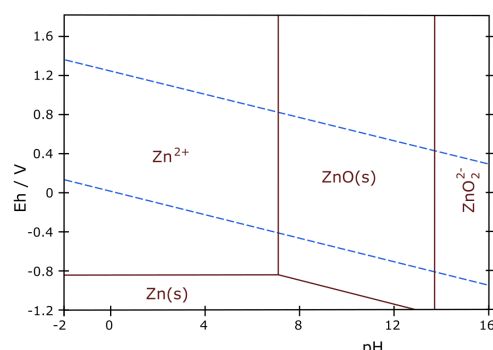
If the thermodynamically stable species is solid, then a film of this species plates the metal and renders it immune to further corrosion (i.e. the metal is passivated, Section 13.5.20). If the stable species is aqueous, the metal dissolves to form this ion, and the metal is corroded. Kinetics (solubility) may result in a thermodynamically stable oxide still failing to prevent corrosion.



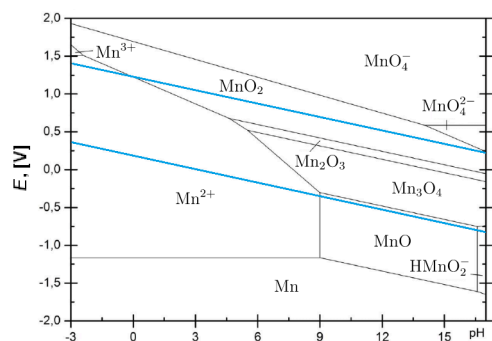
Iron (Fe)



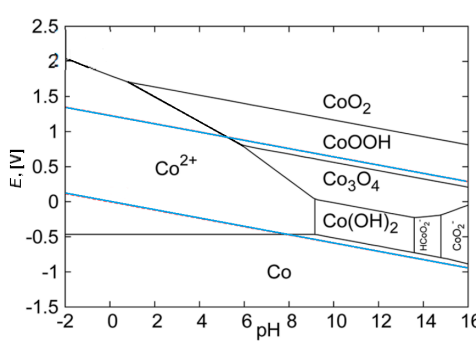
Copper (Cu)



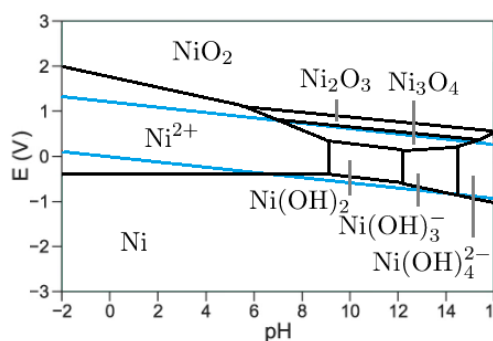
Zinc (Zn)



Manganese (Mn)



Cobalt (Co)



Nickel (Ni)

13.5.19. Standard Electrode Potentials (Reduction Potentials, E^\ominus , Relative to SHE)Sorted from highest to lowest E^\ominus :

$\text{H}_4\text{XeO}_6 + 2\text{H}^+ + 2\text{e}^- \rightarrow \text{XeO}_3 + 3\text{H}_2\text{O}$	+3.0	$\text{Hg}_2\text{SO}_4 + 2\text{e}^- \rightarrow 2\text{Hg} + \text{SO}_4^{2-}$	+0.62
$\text{F}_2 + 2\text{e}^- \rightarrow 2\text{F}^-$	+2.87	$\text{MnO}_4^{2-} + 2\text{H}_2\text{O} + 2\text{e}^- \rightarrow \text{MnO}_2 + 4\text{OH}^-$	+0.60
$\text{O}_3 + 2\text{H}^+ + 2\text{e}^- \rightarrow \text{O}_2 + \text{H}_2\text{O}$	+2.07	$\text{MnO}_4^- + \text{e}^- \rightarrow \text{MnO}_4^{2-}$	+0.56
$\text{S}_2\text{O}_8^{2-} + 2\text{e}^- \rightarrow 2\text{SO}_4^{2-}$	+2.05	$\text{I}_2 + 2\text{e}^- \rightarrow 2\text{I}^-$	+0.54
$\text{Ag}^+ + \text{e}^- \rightarrow \text{Ag}$	+1.98	$\text{Cu}^+ + \text{e}^- \rightarrow \text{Cu}$	+0.52
$\text{Co}^{3+} + \text{e}^- \rightarrow \text{Co}^{2+}$	+1.81	$\text{I}_3^- + 2\text{e}^- \rightarrow 3\text{I}^-$	+0.53
$\text{H}_2\text{O}_2 + 2\text{H}^+ + 2\text{e}^- \rightarrow 2\text{H}_2\text{O}$	+1.78	$\text{NiOOH} + \text{H}_2\text{O} + \text{e}^- \rightarrow \text{Ni}(\text{OH})_2 + \text{OH}^-$	+0.49
$\text{Au}^+ + \text{e}^- \rightarrow \text{Au}$	+1.69	$\text{Ag}_2\text{CrO}_4 + 2\text{e}^- \rightarrow 2\text{Ag} + \text{CrO}_4^{2-}$	+0.45
$\text{Pb}^{4+} + 2\text{e}^- \rightarrow \text{Pb}^{2+}$	+1.67	$\text{O}_2 + 2\text{H}_2\text{O} + 4\text{e}^- \rightarrow 4\text{OH}^-$	+0.40
$2\text{HClO} + 2\text{H}^+ + 2\text{e}^- \rightarrow \text{Cl}_2 + 2\text{H}_2\text{O}$	+1.63	$\text{ClO}_4^- + \text{H}_2\text{O} + 2\text{e}^- \rightarrow \text{ClO}_3^- + 2\text{OH}^-$	+0.36
$\text{Ce}^{4+} + \text{e}^- \rightarrow \text{Ce}^{3+}$	+1.61	$[\text{Fe}(\text{CN})_6]^{3+} + \text{e}^- \rightarrow [\text{Fe}(\text{CN})_6]^{4-}$	+0.36
$2\text{HBrO} + 2\text{H}^+ + 2\text{e}^- \rightarrow \text{Br}_2 + 2\text{H}_2\text{O}$	+1.60	$\text{Cu}^{2+} + 2\text{e}^- \rightarrow \text{Cu}$	+0.34
$\text{MnO}_4^- + 8\text{H}^+ + 5\text{e}^- \rightarrow \text{Mn}^{2+} + 4\text{H}_2\text{O}$	+1.51	$\text{Hg}_2\text{Cl}_2 + 2\text{e}^- \rightarrow 2\text{Hg} + 2\text{Cl}^-$	+0.27
$\text{Mn}^{3+} + \text{e}^- \rightarrow \text{Mn}^{2+}$	+1.51	$\text{AgCl} + \text{e}^- \rightarrow \text{Ag} + \text{Cl}^-$	+0.22
$\text{Au}^{3+} + 3\text{e}^- \rightarrow \text{Au}$	+1.40	$\text{Bi} + 3\text{e}^- \rightarrow \text{Bi}$	+0.20
$\text{Cl}_2 + 2\text{e}^- \rightarrow 2\text{Cl}^-$	+1.36	$\text{Cu}^{2+} + \text{e}^- \rightarrow \text{Cu}^+$	+0.16
$\text{Cr}_2\text{O}_7^{2-} + 14\text{H}^+ + 6\text{e}^- \rightarrow 2\text{Cr}^{3+} + 7\text{H}_2\text{O}$	+1.33	$\text{Sn}^{4+} + 2\text{e}^- \rightarrow \text{Sn}^{2+}$	+0.15
$\text{O}_3 + \text{H}_2\text{O} + 2\text{e}^- \rightarrow \text{O}_2 + 2\text{OH}^-$	+1.24	$\text{AgBr} + \text{e}^- \rightarrow \text{Ag} + \text{Br}^-$	+0.07
$\text{O}_2 + 4\text{H}^+ + 4\text{e}^- \rightarrow 2\text{H}_2\text{O}$	+1.23	$\text{Ti}^{4+} + \text{e}^- \rightarrow \text{Ti}^{3+}$	0.00
$\text{ClO}_4^- + 2\text{H}^+ + 2\text{e}^- \rightarrow \text{ClO}_3^- + \text{H}_2\text{O}$	+1.23	$2\text{H}^+ + 2\text{e}^- \rightarrow \text{H}_2$	0, by definition
$\text{MnO}_2 + 4\text{H}^+ + 2\text{e}^- \rightarrow \text{Mn}^{2+} + 2\text{H}_2\text{O}$	+1.23	$\text{Fe}^{3+} + 3\text{e}^- \rightarrow \text{Fe}$	-0.04
$\text{Br}_2 + 2\text{e}^- \rightarrow 2\text{Br}^-$	+1.09	$\text{O}_2 + \text{H}_2\text{O} + 2\text{e}^- \rightarrow \text{HO}_2^- + \text{OH}^-$	-0.08
$\text{Pu}^{4+} + \text{e}^- \rightarrow \text{Pu}^{3+}$	+0.97	$\text{Pb}^{2+} + 2\text{e}^- \rightarrow \text{Pb}$	-0.13
$\text{NO}_3^- + 4\text{H}^+ + 3\text{e}^- \rightarrow \text{NO} + 2\text{H}_2\text{O}$	+0.96	$\text{In}^+ + \text{e}^- \rightarrow \text{In}$	-0.14
$2\text{Hg}_2^{2+} + 2\text{e}^- \rightarrow \text{Hg}_2^{2+}$	+0.92	$\text{Sn}^{2+} + 2\text{e}^- \rightarrow \text{Sn}$	-0.14
$\text{ClO}^- + \text{H}_2\text{O} + 2\text{e}^- \rightarrow \text{Cl}^- + 2\text{OH}^-$	+0.89	$\text{AgI} + \text{e}^- \rightarrow \text{Ag} + \text{I}^-$	-0.15
$\text{Hg}_2^{2+} + 2\text{e}^- \rightarrow \text{Hg}$	+0.86	$\text{Ni}^{2+} + 2\text{e}^- \rightarrow \text{Ni}$	-0.23
$\text{NO}_3^- + 2\text{H}^+ + \text{e}^- \rightarrow \text{NO}_2 + \text{H}_2\text{O}$	+0.80	$\text{Co}^{2+} + 2\text{e}^- \rightarrow \text{Co}$	-0.28
$\text{Ag}^+ + \text{e}^- \rightarrow \text{Ag}$	+0.80	$\text{In}^{3+} + 3\text{e}^- \rightarrow \text{In}$	-0.34
$\text{Hg}_2^{2+} + 2\text{e}^- \rightarrow 2\text{Hg}$	+0.79	$\text{Ti}^+ + \text{e}^- \rightarrow \text{Ti}$	-0.34
$\text{Fe}^{3+} + \text{e}^- \rightarrow \text{Fe}^{2+}$	+0.77	$\text{PbSO}_4 + 2\text{e}^- \rightarrow \text{Pb} + \text{SO}_4^{2-}$	-0.36
$\text{BrO}^- + \text{H}_2\text{O} + 2\text{e}^- \rightarrow \text{Br}^- + 2\text{OH}^-$	+0.76	$\text{V}^{2+} + 2\text{e}^- \rightarrow \text{V}$	-1.19
$\text{Ti}^{3+} + \text{e}^- \rightarrow \text{Ti}^{2+}$	-0.37	$\text{Ti}^{2+} + 2\text{e}^- \rightarrow \text{Ti}$	-1.63
$\text{Cd}^{2+} + 2\text{e}^- \rightarrow \text{Cd}$	-0.40	$\text{Al}^{3+} + 3\text{e}^- \rightarrow \text{Al}$	-1.66
$\text{In}^{2+} + \text{e}^- \rightarrow \text{In}^+$	-0.40	$\text{U}^{3+} + 3\text{e}^- \rightarrow \text{U}$	-1.79
$\text{Cr}^{3+} + \text{e}^- \rightarrow \text{Cr}^{2+}$	-0.41	$\text{Sc}^{3+} + 3\text{e}^- \rightarrow \text{Sc}$	-2.09
$\text{Fe}^{2+} + 2\text{e}^- \rightarrow \text{Fe}$	-0.44	$\text{Mg}^{2+} + 2\text{e}^- \rightarrow \text{Mg}$	-2.36
$\text{In}^{3+} + 2\text{e}^- \rightarrow \text{In}^+$	-0.44	$\text{Ce}^{3+} + 3\text{e}^- \rightarrow \text{Ce}$	-2.48
$\text{S} + 2\text{e}^- \rightarrow \text{S}^{2-}$	-0.48	$\text{La}^{3+} + 3\text{e}^- \rightarrow \text{La}$	-2.52
$\text{In}^{3+} + \text{e}^- \rightarrow \text{In}^{2+}$	-0.49	$\text{Na}^+ + \text{e}^- \rightarrow \text{Na}$	-2.71
$\text{U}^{4+} + \text{e}^- \rightarrow \text{U}^{3+}$	-0.61	$\text{Ca}^{2+} + 2\text{e}^- \rightarrow \text{Ca}$	-2.87
$\text{Cr}^{3+} + 3\text{e}^- \rightarrow \text{Cr}$	-0.74	$\text{Sr}^{2+} + 2\text{e}^- \rightarrow \text{Sr}$	-2.89
$\text{Zn}^{2+} + 2\text{e}^- \rightarrow \text{Zn}$	-0.76	$\text{Ba}^{2+} + 2\text{e}^- \rightarrow \text{Ba}$	-2.91
$\text{Cd}(\text{OH})_2 + 2\text{e}^- \rightarrow \text{Cd} + 2\text{OH}^-$	-0.81	$\text{Ra}^{2+} + 2\text{e}^- \rightarrow \text{Ra}$	-2.92
$2\text{H}_2\text{O} + 2\text{e}^- \rightarrow \text{H}_2 + 2\text{OH}^-$	-0.83	$\text{Cs}^+ + \text{e}^- \rightarrow \text{Cs}$	-2.92
$\text{Cr}^{2+} + 2\text{e}^- \rightarrow \text{Cr}$	-0.91	$\text{Rb}^+ + \text{e}^- \rightarrow \text{Rb}$	-2.93
$\text{Mn}^{2+} + 2\text{e}^- \rightarrow \text{Mn}$	-1.18	$\text{K}^+ + \text{e}^- \rightarrow \text{K}$	-2.93
		$\text{Li}^+ + \text{e}^- \rightarrow \text{Li}$	-3.05

Sorted from A-Z:

$\text{Ag}^+ + \text{e}^- \rightarrow \text{Ag}$	+0.80	$\text{Ca}^{2+} + 2\text{e}^- \rightarrow \text{Ca}$	-2.87
$\text{Ag}^{2+} + \text{e}^- \rightarrow \text{Ag}^+$	+1.98	$\text{Cd}(\text{OH})_2 + 2\text{e}^- \rightarrow \text{Cd} + 2\text{OH}^-$	-0.81
$\text{AgBr} + \text{e}^- \rightarrow \text{Ag} + \text{Br}^-$	+0.0713	$\text{Cd}^{2+} + 2\text{e}^- \rightarrow \text{Cd}$	-0.40
$\text{AgCl} + \text{e}^- \rightarrow \text{Ag} + \text{Cl}^-$	+0.22	$\text{Ce}^{3+} + 3\text{e}^- \rightarrow \text{Ce}$	-2.48
$\text{Ag}_2\text{CrO}_4 + 2\text{e}^- \rightarrow 2\text{Ag} + \text{CrO}_4^{2-}$	+0.45	$\text{Ce}^{4+} + \text{e}^- \rightarrow \text{Ce}^{3+}$	+1.61
$\text{AgF} + \text{e}^- \rightarrow \text{Ag} + \text{F}^-$	+0.78	$\text{Cl}_2 + 2\text{e}^- \rightarrow 2\text{Cl}^-$	+1.36
$\text{AgI} + \text{e}^- \rightarrow \text{Ag} + \text{I}^-$	-0.15	$\text{ClO}^- + \text{H}_2\text{O} + 2\text{e}^- \rightarrow \text{Cl}^- + 2\text{OH}^-$	+0.89
$\text{Al}^{3+} + 3\text{e}^- \rightarrow \text{Al}$	-1.66	$\text{ClO}_4^- + 2\text{H}^+ + 2\text{e}^- \rightarrow \text{ClO}_3^- + \text{H}_2\text{O}$	+1.23
$\text{Au}^+ + \text{e}^- \rightarrow \text{Au}$	+1.69	$\text{ClO}_4^- + \text{H}_2\text{O} + 2\text{e}^- \rightarrow \text{ClO}_3^- + 2\text{OH}^-$	+0.36
$\text{Au}^{3+} + 3\text{e}^- \rightarrow \text{Au}$	+1.40	$\text{Co}^{2+} + 2\text{e}^- \rightarrow \text{Co}$	-0.28
$\text{Ba}^{2+} + 2\text{e}^- \rightarrow \text{Ba}$	+2.91	$\text{Co}^{3+} + \text{e}^- \rightarrow \text{Co}^{2+}$	+1.81
$\text{Be}^{2+} + 2\text{e}^- \rightarrow \text{Be}$	-1.85	$\text{Cr}^{2+} + 2\text{e}^- \rightarrow \text{Cr}$	-0.91
$\text{Bi}^{3+} + 3\text{e}^- \rightarrow \text{Bi}$	+0.20	$\text{Cr}_2\text{O}_7^{2-} + 14\text{H}^+ + 6\text{e}^- \rightarrow 2\text{Cr}^{3+} + 7\text{H}_2\text{O}$	+1.33
$\text{Br}_2 + 2\text{e}^- \rightarrow 2\text{Br}^-$	+1.09	$\text{Cr}^{3+} + 3\text{e}^- \rightarrow \text{Cr}$	-0.74
$\text{BrO}^- + \text{H}_2\text{O} + 2\text{e}^- \rightarrow \text{Br}^- + 2\text{OH}^-$	+0.76	$\text{Cr}^{3+} + \text{e}^- \rightarrow \text{Cr}^{2+}$	-0.41
$\text{Cs}^+ + \text{e}^- \rightarrow \text{Cs}$	-2.92	$\text{MnO}_4^- + 2\text{H}_2\text{O} + 2\text{e}^- \rightarrow \text{MnO}_2 + 4\text{OH}^-$	+0.60
$\text{Cu}^+ + \text{e}^- \rightarrow \text{Cu}$	+0.52	$\text{Na}^+ + \text{e}^- \rightarrow \text{Na}$	-2.71
$\text{Cu}^{2+} + 2\text{e}^- \rightarrow \text{Cu}$	+0.34	$\text{Ni}^{2+} + 2\text{e}^- \rightarrow \text{Ni}$	-0.23
$\text{Cu}^{2+} + \text{e}^- \rightarrow \text{Cu}^+$	+0.16	$\text{NiOOH} + \text{H}_2\text{O} + \text{e}^- \rightarrow \text{Ni}(\text{OH})_2 + \text{OH}^-$	+0.49
$\text{F}_2 + 2\text{e}^- \rightarrow 2\text{F}^-$	+2.87	$\text{NO}_3^- + 2\text{H}^+ + \text{e}^- \rightarrow \text{NO}_2 + \text{H}_2\text{O}$	-0.80
$\text{Fe}^{2+} + 2\text{e}^- \rightarrow \text{Fe}$	-0.44	$\text{NO}_3^- + 4\text{H}^+ + 3\text{e}^- \rightarrow \text{NO} + 2\text{H}_2\text{O}$	+0.96
$\text{Fe}^{3+} + 3\text{e}^- \rightarrow \text{Fe}$	-0.04	$\text{NO}_3^- + \text{H}_2\text{O} + 2\text{e}^- \rightarrow \text{NO}_2^- + 2\text{OH}^-$	+0.10
$\text{Fe}^{3+} + \text{e}^- \rightarrow \text{Fe}^{2+}$	+0.77	$\text{O}_2 + 2\text{H}_2\text{O} + 4\text{e}^- \rightarrow 4\text{OH}^-$	+0.40
$[\text{Fe}(\text{CN})_6]^{3+} + \text{e}^- \rightarrow [\text{Fe}(\text{CN})_6]^{4-}$	+0.36	$\text{O}_2 + 4\text{H}^+ + 4\text{e}^- \rightarrow 2\text{H}_2\text{O}$	+1.23
$2\text{H}^+ + 2\text{e}^- \rightarrow \text{H}_2$	0, by definition	$\text{O}_2 + \text{e}^- \rightarrow \text{O}_2^-$	-0.56
$2\text{H}_2\text{O} + 2\text{e}^- \rightarrow \text{H}_2 + 2\text{OH}^-$	-0.83	$\text{O}_2 + \text{H}_2\text{O} + 2\text{e}^- \rightarrow \text{HO}_2^- + \text{OH}^-$	-0.08
$2\text{HBrO} + 2\text{H}^+ + 2\text{e}^- \rightarrow \text{Br}_2 + 2\text{H}_2\text{O}$	+1.60	$\text{O}_3 + 2\text{H}^+ + 2\text{e}^- \rightarrow \text{O}_2 + \text{H}_2\text{O}$	+2.07
$2\text{HClO} + 2\text{H}^+ + 2\text{e}^- \rightarrow \text{Cl}_2 + 2\text{H}_2\text{O}$	+1.63	$\text{O}_3 + \text{H}_2\text{O} + 2\text{e}^- \rightarrow \text{O}_2 + 2\text{OH}^-$	+1.24
$\text{H}_2\text{O}_2 + 2\text{H}^+ + 2\text{e}^- \rightarrow 2\text{H}_2\text{O}$	+1.78	$\text{Pb}^{2+} + 2\text{e}^- \rightarrow \text{Pb}$	-0.13
$\text{H}_4\text{XeO}_6 + 2\text{H}^+ + 2\text{e}^- \rightarrow \text{XeO}_3 + 3\text{H}_2\text{O}$	+3.0	$\text{Pb}^{4+} + 2\text{e}^- \rightarrow \text{Pb}^{2+}$	+1.67
$\text{Hg}_2^{2+} + 2\text{e}^- \rightarrow 2\text{Hg}$	+0.79	$\text{PbSO}_4 + 2\text{e}^- \rightarrow \text{Pb} + \text{SO}_4^{2-}$	-0.36
$\text{Hg}_2\text{Cl}_2 + 2\text{e}^- \rightarrow 2\text{Hg} + 2\text{Cl}^-$	+0.27	$\text{Pt}^{2+} + 2\text{e}^- \rightarrow \text{Pt}$	+1.20
$\text{Hg}_2^{2+} + 2\text{e}^- \rightarrow \text{Hg}$	+0.86	$\text{Pu}^{4+} + \text{e}^- \rightarrow \text{Pu}^{3+}$	+0.97
$2\text{Hg}_2^{2+} + 2\text{e}^- \rightarrow \text{Hg}_2^{2+}$	+0.92	$\text{Ra}^{2+} + 2\text{e}^- \rightarrow \text{Ra}$	-2.92
$\text{Hg}_2\text{SO}_4 + 2\text{e}^- \rightarrow 2\text{Hg} + \text{SO}_4^{2-}$	+0.62	$\text{Rb}^+ + \text{e}^- \rightarrow \text{Rb}$	-2.93
$\text{I}_2 + 2\text{e}^- \rightarrow 2\text{I}^-$	+0.54	$\text{S} + 2\text{e}^- \rightarrow \text{S}^{2-}$	-0.48
$\text{I}_3^- + 2\text{e}^- \rightarrow 3\text{I}^-$	+0.53	$\text{S}_2\text{O}_8^{2-} + 2\text{e}^- \rightarrow 2\text{SO}_4^{2-}$	+2.05
$\text{In}^+ + \text{e}^- \rightarrow \text{In}$	-0.14	$\text{Sc}^{3+} + 3\text{e}^- \rightarrow \text{Sc}$	-2.09
$\text{In}^{2+} + \text{e}^- \rightarrow \text{In}^+$	-0.40	$\text{Sn}^{2+} + 2\text{e}^- \rightarrow \text{Sn}$	-0.14
$\text{In}^{3+} + 2\text{e}^- \rightarrow \text{In}^+$	-0.49	$\text{Sn}^{4+} + 2\text{e}^- \rightarrow \text{Sn}^{2+}$	+0.15
$\text{K}^+ + \text{e}^- \rightarrow \text{K}$	-2.93	$\text{Sr}^{2+} + 2\text{e}^- \rightarrow \text{Sr}$	-2.89
$\text{La}^{3+} + 3\text{e}^- \rightarrow \text{La}$	-2.52	$\text{Ti}^{2+} + 2\text{e}^- \rightarrow \text{Ti}$	-1.63
$\text{Li} + \text{e}^- \rightarrow \text{Li}$	-3.05	$\text{Ti}^{3+} + \text{e}^- \rightarrow \text{Ti}^{2+}$	-0.37
$\text{Mg}^{2+} + 2\text{e}^- \rightarrow \text{Mg}$	-2.36	$\text{Ti}^{4+} + \text{e}^- \rightarrow \text{Ti}^{3+}$	0.00
$\text{Mn}^{2+} + 2\text{e}^- \rightarrow \text{Mn}$	-1.18	$\text{Ti}^+ + \text{e}^- \rightarrow \text{Ti}$	-0.34
$\text{Mn}^{3+} + \text{e}^- \rightarrow \text{Mn}^{2+}$	+1.51	$\text{U}^{3+} + 3\text{e}^- \rightarrow \text{U}$	-1.79
$\text{MnO}_2 + 4\text{H}^+ + 2\text{e}^- \rightarrow \text{Mn}^{2+} + 2\text{H}_2\text{O}$	+1.23	$\text{U}^{4+} + \text{e}^- \rightarrow \text{U}^{3+}$	-0.61
$\text{MnO}_4^- + 8\text{H}^+ + 5\text{e}^- \rightarrow \text{Mn}^{2+} + 4\text{H}_2\text{O}$	+1.51	$\text{V}^{2+} + 2\text{e}^- \rightarrow \text{V}$	-1.19
$\text{MnO}_4^- + \text{e}^- \rightarrow \text{MnO}_4^{2-}$	+0.56	$\text{V}^{3+} + \text{e}^- \rightarrow \text{V}^{2+}$	-0.26
		$\text{Zn}^{2+} + 2\text{e}^- \rightarrow \text{Zn}$	-0.76

13.6. Acid-Base Chemistry

13.6.1. Acids and Bases

Theory of acids and bases:

	Acid	Base
Lewis Theory	lone pair acceptor	lone pair donor
Brønsted-Lowry Theory	proton donor	proton acceptor

For a general Brønsted-Lowry acid-base equilibrium $HA + B \rightleftharpoons A^- + BH^+$,

- A^- is the **conjugate base** of HA
- BH^+ is the **conjugate acid** of B
- HA is **reduced** to A^-
- B is **oxidised** to BH^+

If HA and B are the same molecule then this is a self-ionisation reaction and the compound is said to be **amphoteric** (can be behave as an acid or base; simultaneous oxidation and reduction).

Measures of acidity and basicity in aqueous solutions are:

- $pH = -\log_{10} [H^+]$ (aqueous 'protons' are solvated as hydronium ions, H_3O^+ (aq))
- $pOH = -\log_{10} [OH^-]$
- $pH + pOH = pK_w$ of water = 14 (for water at 25 °C)

Redox chemistry:

- Oxidation is gain of oxygen / loss of electrons / loss of hydrogen / gain of oxidation state
- Reduction is loss of oxygen / gain of electrons / gain of hydrogen / loss of oxidation state

Strong and weak acids and bases:

- Strong acids and strong bases dissociate completely into ions in aqueous solution.
- Weak acids and weak bases dissociate partially into ions in aqueous solution.

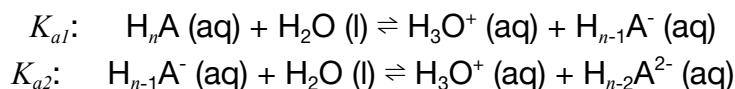
The main strong acids are HCl, HNO₃, H₂SO₄, HBr, HI, HClO₄, HClO₃.

The main strong bases are LiOH, NaOH, KOH, RbOH, CsOH, Mg(OH)₂*, Ca(OH)₂*, Sr(OH)₂, Ba(OH)₂.

* These substances are usually still considered strong bases despite being sparingly soluble in water. Up to the solubility limit, the compounds dissociate completely into ions (strong electrolyte), whereas a weak base (e.g. Fe(OH)₃) would primarily form molecular clusters (in this case, the complex [Fe(OH)₃(H₂O)₃]), preventing complete dissociation into free OH⁻ ions while remaining dissolved.

13.6.2. Dissociation Constants of Weak Acids

The dissociation constants K_a are defined as equilibrium constants for the reaction



...

$$\text{so that } K_{a1}[\text{H}_n\text{A}] = \frac{[\text{H}^+][\text{H}_{n-1}\text{A}^-]}{[\text{H}_n\text{A}]}, \quad K_{a2}[\text{HA}] = K_{a1}[\text{H}_{n-1}\text{A}^-] = \frac{[\text{H}^+][\text{H}_{n-2}\text{A}^{2-}]}{[\text{H}_{n-1}\text{A}^-]}, \dots$$

Values for weak acids (measured at 25 °C unless specified otherwise) are given below.

Name	Formula	K_{a1}	K_{a2}	K_{a3}
Acetic acid	CH ₃ COOH	1.75×10^{-5}	-	-
Arsenic acid	H ₃ AsO ₄	5.5×10^{-3}	1.7×10^{-7}	5.1×10^{-12}
Benzoic acid	C ₆ H ₅ COOH	6.25×10^{-5}	-	-
Boric acid	H ₃ BO ₃	$5.4 \times 10^{-10*}$	$>1 \times 10^{-14*}$	-
Bromoacetic acid	CH ₂ BrCOOH	1.3×10^{-3}	-	-
Carbonic acid	H ₂ CO ₃	4.5×10^{-7}	4.7×10^{-11}	-
Chloroacetic acid	CH ₂ ClCOOH	1.3×10^{-3}	-	-
Chlorous acid	HClO ₂	1.1×10^{-2}	-	-
Chromic acid	H ₂ CrO ₄	1.8×10^{-1}	3.2×10^{-7}	-
Citric acid	C ₆ H ₈ O ₇	7.4×10^{-4}	1.7×10^{-5}	4.0×10^{-7}
Cyanic acid	HCNO	3.5×10^{-4}	-	-
Dichloroacetic acid	CHCl ₂ COOH	4.5×10^{-2}	-	-
Fluoroacetic acid	CH ₂ FCOOH	2.6×10^{-3}	-	-
Formic acid	HCOOH	1.8×10^{-4}	-	-
Hydrazoic acid	HN ₃	2.5×10^{-5}	-	-
Hydrocyanic acid	HCN	6.2×10^{-10}	-	-
Hydrofluoric acid	HF	6.7×10^{-4}	-	-
Hydrogen selenide	H ₂ Se	1.3×10^{-4}	1.0×10^{-11}	-
Hydrogen sulfide	H ₂ S	8.9×10^{-8}	1×10^{-19}	-
Hydrogen telluride	H ₂ Te	$2.5 \times 10^{-3}\ddagger$	1×10^{-11}	-

Dissociation constants of weak acids, continued

Name	Formula	K_{a1}	K_{a2}	K_{a3}
Hypobromous acid	HBrO	2.8×10^{-9}	-	-
Hypochlorous acid	HClO	4.0×10^{-8}	-	-
Hypoiodous acid	HIO	3.2×10^{-11}	-	-
Iodic acid	HIO ₃	1.7×10^{-1}	-	-
Iodoacetic acid	CH ₂ I ₂ COOH	6.6×10^{-4}	-	-
Nitrous acid	HNO ₂	5.6×10^{-4}	-	-
Oxalic acid (ethanedioic acid)	HOOC ₂ COOH	5.6×10^{-2}	1.5×10^{-4}	-
Periodic acid	HIO ₄	2.3×10^{-2}	-	-
Phenol	C ₆ H ₅ OH	1.0×10^{-10}	-	-
Phosphoric acid	H ₃ PO ₄	6.9×10^{-3}	6.2×10^{-8}	4.8×10^{-13}
Phosphorous acid	H ₃ PO ₃	$5.0 \times 10^{-2*}$	$2.0 \times 10^{-7*}$	-
Resorcinol (benzene-1,2-diol)	C ₆ H ₄ (OH) ₂	4.8×10^{-10}	7.9×10^{-12}	-
Selenic acid	H ₂ SeO ₄	(strong)	2.0×10^{-2}	-
Selenious acid	H ₂ SeO ₃	2.4×10^{-3}	4.8×10^{-9}	-
Sulfuric acid	H ₂ SO ₄	(strong)	1.0×10^{-2}	-
Sulfurous acid	H ₂ SO ₃	1.4×10^{-2}	6.3×10^{-8}	-
<i>meso</i> -Tartaric acid (2,3-dihydroxybutanedioic acid)	C ₄ H ₆ O ₆	6.0×10^{-4}	1.4×10^{-5}	-
L(+)-Tartaric acid	C ₄ H ₆ O ₆	1.3×10^{-3}	4.0×10^{-5}	-
Telluric acid	H ₂ TeO ₄	$2.1 \times 10^{-8}‡$	$1.0 \times 10^{-11}‡$	-
Tellurous acid	H ₂ TeO ₃	5.4×10^{-7}	3.7×10^{-9}	-
Trichloroacetic acid	CCl ₃ COOH	2.2×10^{-1}	-	-
Trifluoroacetic acid	CF ₃ COOH	3.0×10^{-1}	-	-

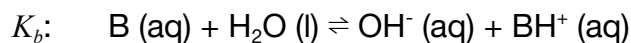
Table notes:

* values are measured at 20 °C. ‡ values are measured at 18 °C.

pKa: $pK_a = -\log_{10} K_a$ so that acids approach 'strong' as $pK_a \rightarrow -\infty$.

13.6.3. Dissociation Constants of Weak Bases

The dissociation constants K_b are defined as equilibrium constants for the reaction



$$\text{so that } K_b[B] = \frac{[\text{OH}^-][\text{BH}^+]}{[B]}$$

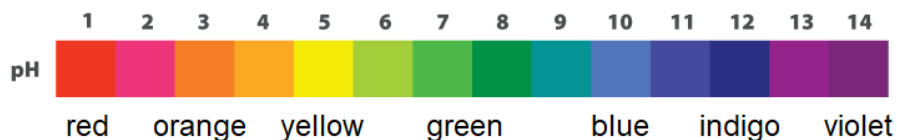
Values for weak bases (measured at 25 °C) are given below.

Name	Formula	K_b
Ammonia	NH_3	1.8×10^{-5}
Aniline	$\text{C}_6\text{H}_5\text{NH}_2$	7.4×10^{-10}
<i>n</i> -Butylamine	$\text{C}_4\text{H}_9\text{NH}_2$	4.0×10^{-4}
<i>sec</i> -Butylamine	$(\text{CH}_3)_2\text{CHCH}_2\text{NH}_2$	3.6×10^{-4}
<i>tert</i> -Butylamine	$(\text{CH}_3)_3\text{CNH}_2$	4.8×10^{-4}
Dimethylamine	$(\text{CH}_3)_2\text{NH}$	5.4×10^{-4}
Ethylamine	$\text{C}_2\text{H}_5\text{NH}_2$	4.5×10^{-4}
Hydrazine	N_2H_4	1.3×10^{-6}
Hydroxylamine	NH_2OH	8.7×10^{-9}
Methylamine	CH_3NH_2	4.6×10^{-4}
Propylamine	$\text{C}_3\text{H}_7\text{NH}_2$	3.5×10^{-4}
Pyridine	$\text{C}_5\text{H}_5\text{N}$	1.7×10^{-9}
Trimethylamine	$(\text{CH}_3)_3\text{N}$	6.3×10^{-5}

$$\text{p}K_b: \quad \text{p}K_b = -\log_{10} K_b$$

13.6.4. Colour Ranges of Indicators

Universal Indicator (Full Range)



Binary Indicators

Indicator	pH Range	Colour in Low pH	Colour in High pH
Thymol Blue	1.2 - 2.8	red	yellow
2,4-Dinitrophenol (2,4-DNP)	2.4 - 4.0	colourless	yellow
Methyl yellow	2.9 - 4.0	red	yellow
Methyl orange	3.1 - 4.4	red	orange
Bromophenol blue	3.0 - 4.6	yellow	indigo
α -Naphthyl red	3.7 - 5.0	red	yellow
Methyl red	4.4 - 6.2	red	yellow
<i>p</i> -Nitrophenol	5.0 - 7.0	colourless	yellow
Phenol red	6.4 - 8.0	yellow	red
α -Naphtholphthalein	7.3 - 8.7	pink	green
Thymol blue	8.0 - 9.6	yellow	blue
Phenolphthalein	8.0 - 10.0	colourless	red
Thymolphthalein	9.4 - 10.6	colourless	blue
Nile blue	10.1 - 11.1	blue	red
Trinitrobenzoic acid	12.0 - 13.4	colourless	orange-red

Indicators for Complexometric Titrations

Concentrations of metal cations (e.g. Ca^{2+}) can be determined using complexometric titrations, in which a chelating solution (e.g. EDTA) removes metal cations from solution. An indicator which changes colour in the presence of these cations can be used to indicate the endpoint, such as:

Indicator	Commonly used cations	Colour without cations	Colour with cations
Eriochrome Black T	Ca^{2+} , Mg^{2+}	blue	red
Calconcarboxylic acid	Ca^{2+} , Mg^{2+}	blue	red
Fast Sulphon Black F	Cu^{2+}	green	purple

13.6.5. Titration Curves

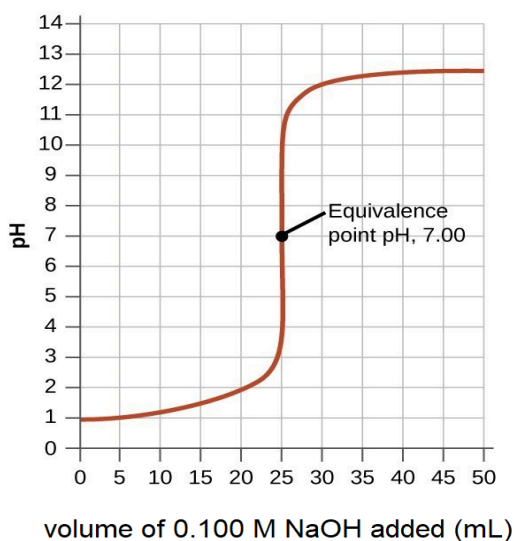
To set up a titration, put the standard solution (titrant, of known concentration) in the burette and the unknown solution (analyte) in the conical flask.

At the equivalence point, moles of acid = moles of base $\rightarrow c_{acid}V_{acid} = c_{base}V_{base}$.

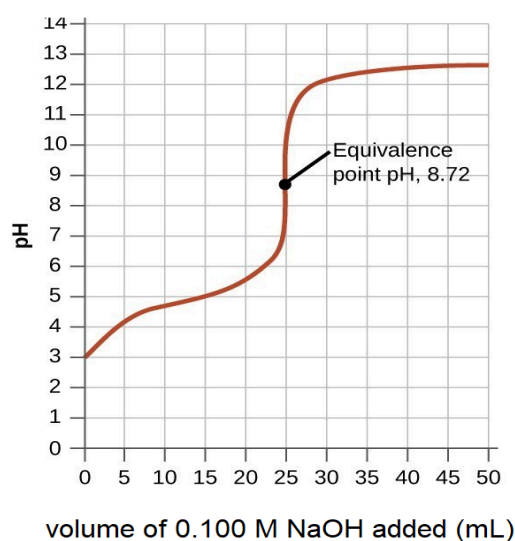
At the half-equivalence point ($V = \frac{V_{acid,eq}}{2}$) for a weak acid titration, $[HA] = [A^-] \rightarrow pH = pK_a$.

Titration curves with single equilibria:

Titration of HCl with NaOH
(strong acid + strong base)

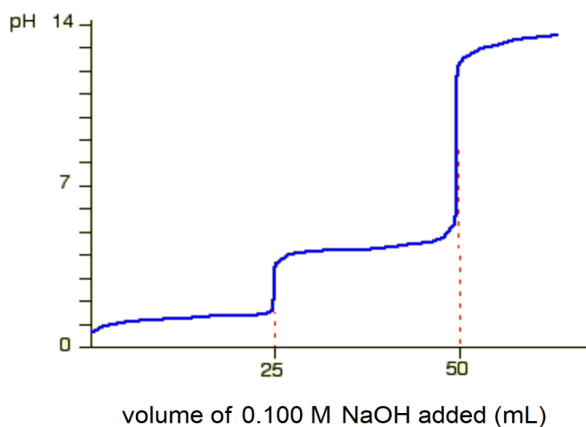


Titration of CH_3COOH with NaOH
(weak acid + strong base)

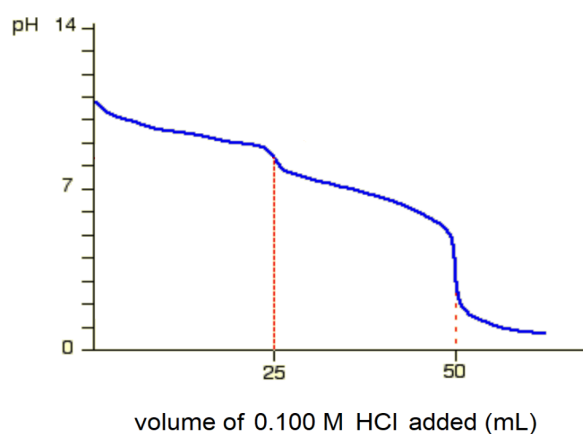


Titrations with multiple equilibria:

Titration of $C_2H_4O_2$ with NaOH
(weak acid + strong base)



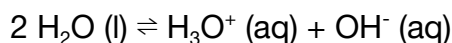
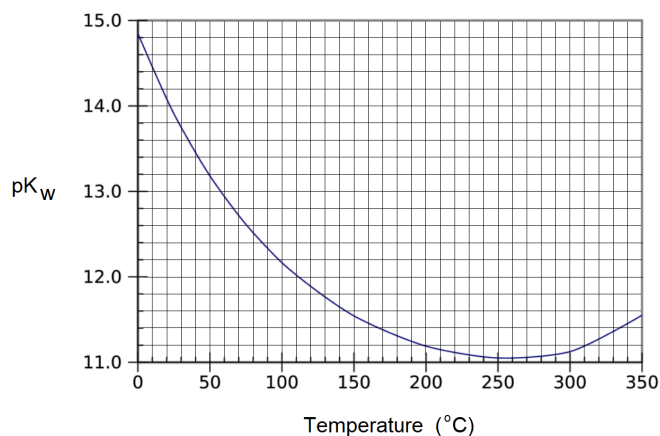
Titration of Na_2CO_3 with HCl
(strong acid + weak base)



13.6.6. Buffers and the Henderson-Hasselbalch Equations

Autoionisation Product of Water

Water is amphoteric: it partially self-ionises into protons and hydroxide ions:



The equilibrium constant (ionic product), $K_w = [\text{H}_3\text{O}^+][\text{OH}^-]$, varies with temperature:

$$pK_w = -\log_{10} K_w \quad \quad \quad pH + pOH = pK_w$$

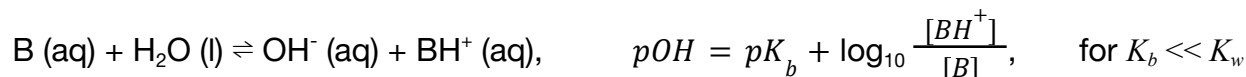
In pure water, $[\text{H}^+] = [\text{H}_3\text{O}^+] = [\text{OH}^-]$, so $K_w = [\text{H}^+]^2$.

At 25 °C, $pK_w = 14$, $K_w = 1 \times 10^{-14} \text{ mol}^2 \text{ dm}^{-6}$.

Weak Acid Buffer: when a weak acid HA is mixed with a salt of its conjugate base A⁻, the equilibrium shifts to maintain the value of K_a for the weak acid:



Weak Base Buffer: when a weak base B is mixed with a salt of its conjugate acid BH⁺, the equilibrium shifts to maintain the value of K_b for the weak base.



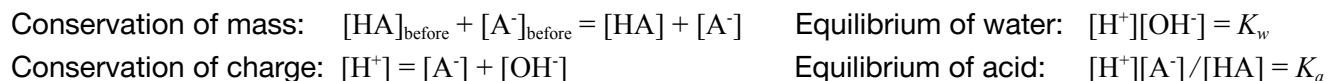
(These are the Henderson-Hasselbalch equations, and can be derived with an 'ICE' table.)

Degree of Dissociation / Ionisation: $\alpha = \frac{[\text{ion}]}{[\text{neutral, initial}]}$ so that $\frac{[\text{neutral}]}{[\text{neutral, initial}]} = 1 - \alpha$.

Percentage Ionisation: $\frac{[\text{ion}]}{[\text{neutral}]} = \frac{\alpha}{1 - \alpha}$ so $\% \text{ ionised} = \alpha = \left(1 + \left(\frac{[\text{ion}]}{[\text{neutral}]} \right)^{-1} \right)^{-1} \times 100\%$.

Calculations with Very Weak Acids or Very Weak Bases

If $pK_a \approx pK_w$, then the autoionisation of water will contribute a significant proportion of the protons to the final pH of the solution, and the above analysis (which typically assumes negligible change of water) is invalid. Therefore, both the equilibrium of the water and of the solute must be considered:



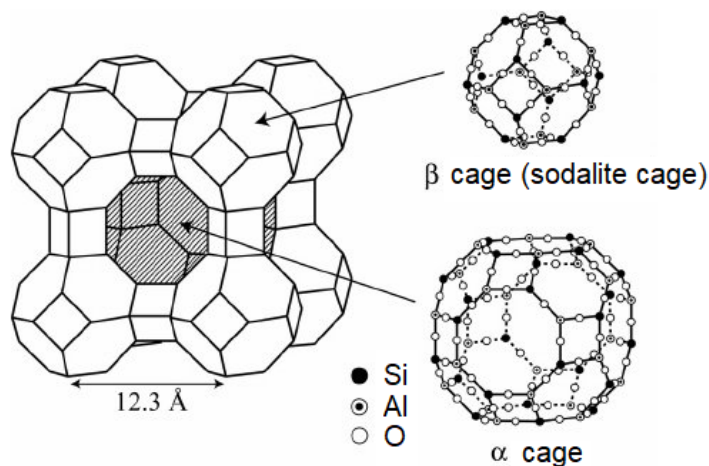
The resulting equations are nonlinear (cubic in $[\text{H}^+]$) and require numerical methods to solve.

C14. SURFACE AND PARTICLE CHEMISTRY

14.1. Catalysis

14.1.2. Structures and Applications of Some Inorganic Catalysts

Zeolites



Aluminosilicate Zeolite A

Typical applications of ZSM-5 (pentasil zeolite; zeolite sieve of molecular porosity 5):

- Isomerisation of *meta*-xylene to *para*-xylene.
- Vapour-phase alkylation of benzene with ethene into ethylbenzene.
- Dehydration of alcohols into alkanes.
- Hydrated zeolites are used as ion exchangers in the softening of hard water.

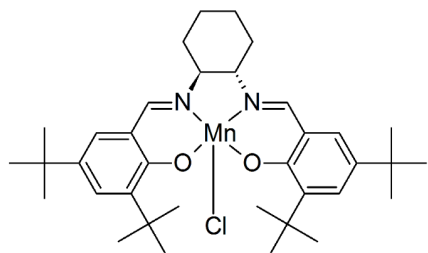
Alkali Metal Catalysts

- Soda lime (NaOH + CaO): for decarboxylation
- Ziegler-Natta Catalyst ($\text{TiCl}_4 + \text{Al}(\text{CH}_2\text{CH}_3)_3$): for addition polymerisation of ethene

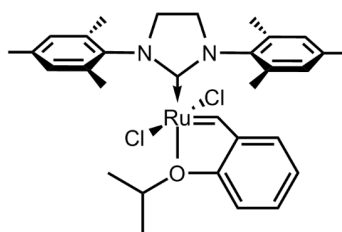
Transition Metal Catalysts

- Raney Nickel (Ra-Ni): for reducing C-S bonds to C-H bonds, or hydrogenation
- Lindlar Catalyst (Pd-BaSO_4 , quinoline): for partial hydrogenation of alkynes
- Palladium on charcoal (Pd-C): for hydrogenation of alkenes
- Sodium-ammonia electride salt ($\text{Na} + \text{NH}_3(l)$; $[\text{Na}(\text{NH}_3)_6]^+e^-$): for the Birch reduction

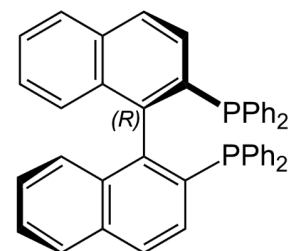
14.1.3. Structures and Applications of Some Organometallic Catalysts



Jacobsen's Salen Catalyst
(*S, S*) active

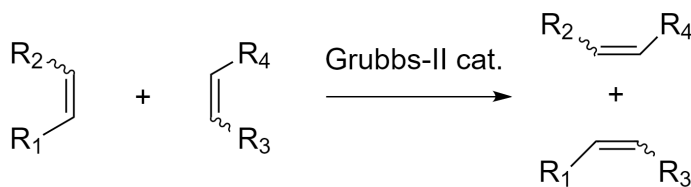


Grubbs II Catalyst



BINAP
(BINOL derivative)

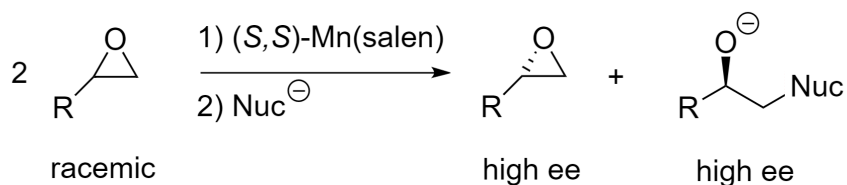
Typical application of the Grubbs II catalyst: alkene metathesis.



The Ru=CH-Ph group undergoes [2+2] cyclisation with an alkene bond, and is replaced in its future catalytic cycles.

In a ring-closing metathesis (RCM), an intramolecular reaction occurs between two alkene bonds separated by any number of carbons to form a ring.

Typical application of the Jacobsen catalyst: enantiomeric resolution of terminal epoxides.



In the Jacobsen HKR (hydrolytic kinetic resolution), the nucleophile is water, forming the vicinal diol as the second product.

14.1.4. Kinetics of Heterogeneous Catalysis

Heterogeneous catalysis requires adsorption at some point in the mechanism. The adsorption step can be written as $A + S \rightleftharpoons AS$ where A is a reactant, S is an adsorption site on the catalyst and AS is the adsorbed complex. The various types of mechanism are:

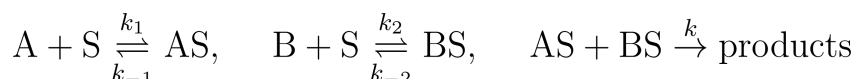
Simple Decomposition: $A + S \xrightleftharpoons[k_{-1}]{k_1} AS \xrightarrow{k_2} \text{products}$

The rate of product formation follows the Michaelis-Menten equation, most suitable for enzyme-substrate type reactions (see also Section 16.5.11):

$$r = \frac{k_1 k_2 [A][S]}{k_1 [A] + k_{-1} + k_2}; \quad \text{if } [S] \text{ is large, } r = r_{max} \frac{[A]}{[A] + K_m} \quad \text{where} \quad K_m = \frac{[A][S]}{[AS]} = \frac{k_{-1} + k_2}{k_1}.$$

- Adsorption equilibrium constant: $K = k_1/k_{-1}$.
- Surface coverage: $\theta = \frac{r}{k_2 [S]} = \frac{[AS]}{[S]}$
- If the rate-limiting step is adsorption, the equation is $r \approx k_1 [A][S]$ (second order)
- If the rate-limiting step is reaction, then $\theta \approx \frac{K [A]}{1 + K [A]} \rightarrow r \approx \frac{K k_2 [A][S]}{1 + K [A]}$ (Langmuir isotherm)

Bimolecular Langmuir-Hinshelwood Mechanism:



Two molecules A and B adsorb on neighbouring sites and react in their adsorbed state.

$$r = k [S]^2 \frac{K_1 K_2 [A][B]}{(1 + K_1 [A] + K_2 [B])^2}$$

where the equilibrium constants are $K_1 = k_1/k_{-1}$ and $K_2 = k_2/k_{-2}$.

Example: hydrogenation of ethene on metal catalysts.

Bimolecular Eley-Rideal Mechanism:



Only one reactant molecule A adsorbs, which then reacts directly with free molecules of B.

$$r = k [S][B] \frac{K [A]}{1 + K [A]}$$

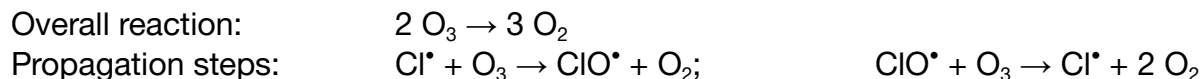
where the equilibrium constant is $K = k_1/k_{-1}$.

14.1.5. Photocatalytic Decomposition Reactions

High-energy radiation ($h\nu$) induces homolysis (homolytic fission) of weak chemical bonds, forming reactive free radicals.

Decomposition of Ozone

CFCs form radicals due to UV radiation in the stratosphere: $R-Cl + h\nu \rightarrow R^\bullet + Cl^\bullet$



Decomposition of Peroxides

The O-O bond is weak and gradually decomposes: $HO-OH + h\nu \rightarrow HO^\bullet + ^\bullet OH$

14.1.6. Autocatalysis

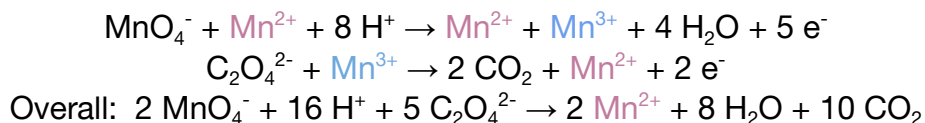
Autocatalysis: a reaction in which the product(s) act(s) as a catalyst for the reaction. The autocatalyst produces more of itself as the reaction proceeds. For $A + B \rightleftharpoons 2 B$, rates are

$$-\frac{d[A]}{dt} = \frac{d[B]}{dt} = k_+[A][B] - k_-[B]^2 \Rightarrow [B](t) = \frac{[A]_0 + [B]_0}{\left(\frac{[A]_0}{[B]_0} - \frac{k_-}{k_+}\right) e^{-k_+([A]_0 + [B]_0)t} + 1 + \frac{k_-}{k_+}}$$

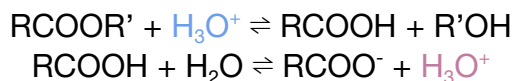
Autocatalytic set: a set of reactions in which the products of each reaction act as a catalyst for one or more other reactions in the set.

Examples of autocatalysis:

- Redox reaction of MnO_4^- (aq) with $C_2O_4^{2-}$ (aq) in acid, autocatalysed by Mn^{2+} (aq) product



- Hydrolysis of esters, autocatalysed by the carboxylic acid product



- Reduction of copper metal with nitric acid, autocatalysed by adsorbed NO (g) product
- Photopolymerisation, autocatalysed by the high-refractive index polymer regions
- Soai reaction of pyrimidine-5-carbaldehyde with diisopropylzinc, autocatalysed by the chiral product (asymmetric autocatalysis: amplifies the ee of the product).

14.2. Separation Processes and Chemical Engineering

14.2.1. Fossil Fuels

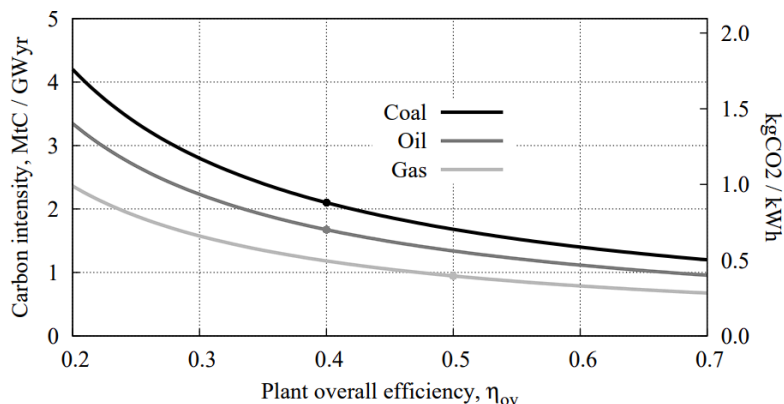
Fossil fuels are non-renewable energy sources found underground. There are three types:

Coal is formed from ancient dead plants on the ground, compacted and heated over millions of years to form **peat**, **lignite**, **bituminous coal** and **anthracite** (increasing time and carbon content). It is primarily found in the Carboniferous layer of the geologic column. It contains large heterocyclic organic molecules with some nitrogen and sulfur content. Distillation of coal without air forms coke (near pure carbon, porous), by removing tar (brown liquid of HCs).

Oil (crude oil, petroleum) is formed from ancient dead plants on the ocean floor, buried under layers of sediment. It is extracted using drilling or hydraulic fracturing (fracking). It is a highly variable liquid mixture of hydrocarbons (HCs) and polycyclic aromatic hydrocarbons (PAHs).

Gas (natural gas) is released during the decay process of ancient dead plants, trapped in underground reservoirs. It is extracted using drilling/fracking and is usually stored as liquefied natural gas (LNG). It is primarily composed of methane (CH_4) with some CO_2 , N_2 and H_2S .

Burning of fossil fuels is responsible for the majority of global anthropogenic greenhouse gas emissions and directly contributes to global warming. For this reason, fossil fuels are being phased out across the world in favour of cleaner energy sources, although economic competition of new technologies can be challenging, as fossil fuel economies are mature, optimised and often subsidised.



Carbon and CO_2 emissions for:

- Coal-fired ($\eta \sim 40\%$)
- Oil-fired ($\eta \sim 40\%$)
- Gas-fired (CCGT: $\eta \sim 50-60\%$)

Emissions follows

coal > oil > natural gas

14.2.2. Feedstock Processing

Fractionation (Fractional Distillation): physical separation of crude oil into components by molecular weight (boiling point). The fractions are bitumen (bottom: $>C_{70}$, $>400\text{ }^\circ\text{C}$), fuel oil (C_{21-70} , $\sim 370\text{ }^\circ\text{C}$), diesel oil (C_{15-20} , $\sim 300\text{ }^\circ\text{C}$), kerosene/paraffin (C_{10-14} , $\sim 200\text{ }^\circ\text{C}$), gasoline/petrol (C_{5-9} , $\sim 70\text{ }^\circ\text{C}$), and natural gas (top: C_{1-4} , $\sim 20\text{ }^\circ\text{C}$).

Cracking: higher alkanes are broken down into smaller alkanes using one of:

Thermal cracking: free radical recombination at $700\text{ }^\circ\text{C}$ and 70 atm. Forms many alkenes.

Catalytic cracking: splitting at $500\text{ }^\circ\text{C}$ with zeolite catalyst. Forms branched and aromatics.

Steam cracking: rapid high pressure steam flow at $850\text{ }^\circ\text{C}$. Forms many alkenes.

Flue Gas Desulfurisation (FGD): sulfur impurities (SO_2) in burned fuels can be removed (scrubbed) from smoke stacks using a CaO/CaCO_3 slurry, forming solid CaSO_4 (plaster of Paris). Wet scrubbers can also remove soluble gases (HCl , NH_3). This has helped prevent acid rain.

Catalytic Converter: the catalytic converter in cars consists of a Pt/Pd/Rh metal painted onto a ceramic honeycomb support. Exhaust toxins (NO_x , CO , C_xH_y) are converted to less harmful products (N_2 , CO_2 , $\text{H}_2\text{O} + \text{CO}_2$, respectively). Sulfur oxides can poison the catalyst over time. Nitrogen oxides react with a urea solution, $\text{CO}(\text{NH}_2)_2$ (diesel exhaust fluid e.g. AdBlue)

Gasification: uses coal / biomass / hydrocarbons to form syngas ($\text{H}_2 + \text{CO}$) by pyrolysis.

Biogasification: uses organic waste to form biogas ($\text{CH}_4 + \text{CO}_2$) by pyrolysis.

14.2.3. Petrochemical Reactions and Transformations

Addition Polymerisation: conversion of small alkene monomers to polymers (often plastics).

Conditions: radical initiator, high pressure. Common products: polyethylene (PE), polypropylene (PP), polyvinyl chloride (PVC), polystyrene (PS).

Condensation Polymerisation: conversion of difunctional monomers to polymers.

Conditions depend on the chemistry. Common products: nylon, polyesters, polyurethanes.

Vulcanisation of Natural Rubber: cross-linking of natural rubber (polyisoprene) by heating with elemental sulfur, forming polysulfide bridges between chains, improving its elastomeric properties.

Fermentation: conversion of glucose to ethanol using yeast and/or enzymes.

Isomerisation: conversion of straight-chained alkanes to branched alkanes.

Conditions: $\text{AlCl}_3 + \text{HCl}$ catalyst, 200 °C, 35 atm.

Alkylation: addition of hydrocarbons (often alkenes) to produce higher alkanes.

Conditions: HF catalyst (or more recently: BMIM- PF_6 ionic liquid catalyst).

Common applications: 2-methylpropene + 2-methylpropane \rightarrow 2,2,4-trimethylpentane (petrol).

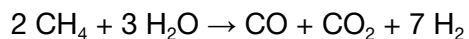
Aromatisation (Reforming): dehydrogenation of aliphatic hydrocarbons to give aromatics.

Conditions: 500 °C, Pt catalyst. Common application: *n*-heptane \rightarrow toluene + 3 H_2 .

Hydrogenation: addition of H_2 to alkenes to give the alkane. Uses Raney Ni catalyst.

Controlled Oxidation: catalytic oxidation of organic molecules at moderate temperatures can lead to formation of other useful chemicals instead of combustion e.g. toluene \rightarrow benzyl hydroperoxide / benzaldehyde, methane \rightarrow methanol, depending on conditions and catalysts.

Steam-Methane Reforming (SMR): forms syngas from methane:



Water Gas Shift Reaction (WGSR): purifies syngas to hydrogen: $\text{CO} + \text{H}_2\text{O} \rightleftharpoons \text{CO}_2 + \text{H}_2$

Boudouard reaction: a relevant equilibrium occurring in many processes: $2 \text{CO} \rightleftharpoons \text{CO}_2 + \text{C}$

Sabatier Process: forms methane: $\text{CO}_2 + 4 \text{H}_2 \rightarrow \text{CH}_4 + 2 \text{H}_2\text{O}$.

Conditions: 350 °C, 3 MPa, Ni/Ru cat.

Fischer-Tropsch Synthesis (FT): uses syngas ($\text{H}_2 + \text{CO}$) to form higher alkanes (often liquids i.e. as part of a coal liquefaction process after gasification). Conditions: 200 °C, 1 MPa.

Wacker Process: uses ethylene to form acetaldehyde (ethanal): $\text{CH}_2\text{CH}_2 + \frac{1}{2} \text{O}_2 \rightarrow \text{CH}_3\text{CHO}$
Conditions: PdCl_2 and CuCl_2 catalysts.

Hydroformylation (Oxo Process): uses syngas and alkenes to form aldehydes.
Conditions: $\text{CO} + \text{H}_2$, 100 °C, 50 atm, Rh/Co-based catalyst.

Haber Process: uses hydrogen and nitrogen to form ammonia: $\text{N}_2 + 3 \text{H}_2 \rightleftharpoons 2 \text{NH}_3$
Conditions: 450 °C, 200 atm, Fe catalyst.

Cumene Process: uses benzene and propene to form phenol and propanone:

1) $\text{C}_6\text{H}_6 + \text{C}_3\text{H}_6 \rightarrow \text{C}_6\text{H}_5\text{iPr}$; 2) $\text{C}_6\text{H}_5\text{iPr} + \text{O}_2 \rightarrow \text{C}_6\text{H}_5\text{OH} + \text{CH}_3\text{COCH}_3$.

Conditions: 250° C, 30 atm, phosphoric acid, oxidation in air.

14.2.4. Separation and Purification Techniques

Packed Bed / Adsorbent Column: batchwise filling of a packed column of adsorbent beads, purifying the liquid over time as impurities become stuck to the column. The purified liquid falls out at the bottom for collection, and can be sent to the top again for multiple passes of purification.

Gravity Separation: a variety of methods where denser matter falls to the bottom of a mixture, such as by shaking, vibrating or sedimentation.

Centrifugation: high-speed rotation of a mixture, with separation to the edges occurring due to different densities.

Cake Filtration: cyclical fluid flow through a porous adsorbent, which removes particulate matter from the stream, growing the 'cake filter' in the process.

Solvent Extraction: addition of a specific solvent to solubilise the desired target, leaving the remainder in its own phase, so that the solvent phase can be extracted easily.

Chromatography: a variety of methods are possible. Allows for separation by exploiting differential adsorption to a stationary phase and a solvent (mobile phase), as well as characterisation and identification based on residence times.

Magnetic Separation: uses magnets to remove magnetic impurities e.g. metals from a slurry.

Pressure-Swing Adsorption: used to extract a specific component of a gas mixture. High pressure and an adsorbent is used to fix the desired gas, leaving the rest free to be removed. When the pressure is released, the desired gas desorbs and can be extracted.

Cryogenic Distillation: liquefaction of a gas mixture followed by fractional distillation to extract the different gases as they boil separately.

Membrane Separation / Gas Permeation: uses semi-permeable membranes to separate gases by particle size and permeability.

Cyclones: impure gas carrying particulate matter flows down a spiral rapidly and is sucked back up in the middle, leaving the particles on the bottom edge of the cyclone. The outlet air is purified.

14.2.5. Hydrogen as Fuel

An alternative to burning natural gas as fuel is to use hydrogen (H_2). Depending on the implementation, this can be far more sustainable than using fossil fuels and may be on par with renewables.

Hydrogen Fuel Cells for Hydrogen-Powered Vehicles

Hydrogen is used as an input to fuel cells (see Section 13.5.11). Currently, fuel cells are somewhat inefficient (~50%) and are one of the key bottlenecks in a hydrogen economy. The primary application is fuel cell vehicles (FCVs), a type of electric vehicle (EV), although there are competing approaches for this and related sectors e.g. electric road systems (ERS), especially for heavy vehicles (public transport, long-haul road and rail freight).

Hydrogen Production: sustainability depends on how it was produced, which can vary significantly:

- **Green Hydrogen:** electrolysis of water using renewable electricity from solar/wind
- **Pink Hydrogen:** electrolysis of water using renewable electricity from nuclear
- **Turquoise Hydrogen:** pyrolysis of natural gas using renewable electricity, releasing solid carbon
- **Blue Hydrogen:** methane reforming of natural gas and carbon capture and storage.
- **Grey Hydrogen:** methane reforming of natural gas (no CCS).
- **Black / Brown Hydrogen:** gasification of coal (black: bituminous, brown: lignite) with no CCS.

Green Hydrogen: Renewable electricity (green: solar/wind, pink: nuclear) powers an electrolysis system to split water into hydrogen and oxygen. The hydrogen is compressed and stored in tanks for transport. Since the hydrogen becomes water again when burned, this is a circular reaction and is effectively a form of energy storage (with inefficiencies) rather than an energy source.

Blue Hydrogen: Oil and gas (fossil fuels) are extracted from the Earth by drilling/fracking. The methane is converted to syngas using steam-methane reforming (SMR) or autothermal reforming (ATR), and then to purer H_2/CO_2 using the water-gas shift reaction (WGSR). The CO_2 side product is removed from the stream into a carbon capture and storage (CCS) facility, leaving pure H_2 . The hydrogen is, as before, compressed and bottled for transport.

14.2.6. General Continuously Stirred Tank Reactor (CSTR)

For a single non-steady, non-isothermal homogeneous CSTR with negligible shaft work:

- dependent variables: volume V , concentrations of species $c_A \dots$, temperature T
- controlled variables: volumetric flow rates Q_{in} and $Q_{out} = Q$, concentration in $c_{A,in}$
- independent variable: time t

Considering a control volume (CV) around the reactor contents:

Mass balance on a species A (each term has units of kg s^{-1} or mol s^{-1} depending on choice):

$$\underbrace{\frac{d}{dt}(Vc_A)}_{\substack{\text{net change in} \\ \text{moles of A} \\ \text{in CV}}} = \underbrace{Q_{in}c_{A,in}}_{\text{mole flux in}} - \underbrace{Qc_A}_{\text{mole flux out}} + \underbrace{\nu_A k V c_A^n}_{\text{rate of reaction}}$$

Energy balance (each term has units of $\text{J s}^{-1} = \text{W}$): assuming enthalpy $h = c_p T$:

$$\underbrace{\frac{d}{dt}(\rho V c_p T)}_{\substack{\text{net change in} \\ \text{energy in CV}}} = \underbrace{\rho_{in} Q_{in} \left(c_{p,in} T_{in} + \frac{1}{2} v_{in}^2 + g z_{in} \right)}_{\text{enthalpy flux in}} - \underbrace{\rho Q \left(c_p T + \frac{1}{2} v_{out}^2 + g z_{out} \right)}_{\text{enthalpy flow out}} + \underbrace{\nu_A k V (\Delta H) c_A^n}_{\substack{\text{heat generated} \\ \text{by reaction}}} + \underbrace{\dot{Q} - \dot{W}}_{\substack{\text{external heat} \\ \text{and work} \\ \text{transferred} \\ \text{into CV}}}$$

(ν_A : stoichiometric coefficient, k : reaction rate constant, n : order of reaction wrt A, ρ : density of flow, c_p : specific heat capacity of flow, T : temperature, v : flow speed, g : acceleration due to gravity, z : elevation, ΔH : specific enthalpy change for the reaction, \dot{Q} : heat transferred into CV (e.g. steam tube heater, coolant flow, conduction through vessel walls), \dot{W} : work done by CV (e.g. hydrodynamic impeller shaft work))

These equations are often simplified e.g. LHS = 0 (steady state), fluid properties are constant and independent of temperature, neglect kinetic/gravitational contributions to enthalpy flux, assume temperature-independent rate constant.

14.2.7. Two-Dimensional Cylindrical Plug Flow Reactor (PFR)

For a cylindrical, laminar flow, diffusive, non-isothermal homogeneous PFR with no gravitational effects, sedimentation or mixing,

- dependent variables: concentrations of species $c_A \dots$, temperature T
- controlled variables: axial velocity profile $u(r)$
- independent variables: axial position x , radial position r , time t .

Considering an annular control volume at position (x, r) with axial thickness dx and radial thickness dr :

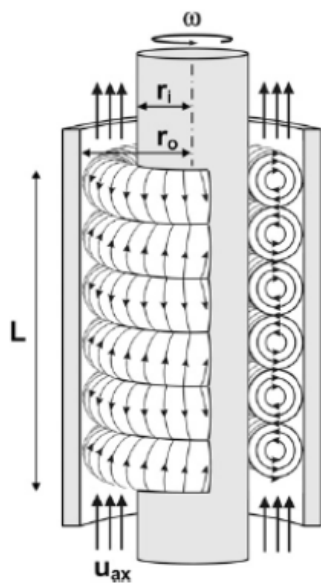
Mass balance on a reactant species A (each term has units concentration per time)

$$\underbrace{\frac{\partial c_A}{\partial t}}_{\text{net concentration change}} = \underbrace{-u \frac{\partial c_A}{\partial x}}_{\text{axial convective flux}} + \underbrace{\nu_A k c_A^n}_{\text{rate of reaction}} + \underbrace{D \left(\frac{\partial^2 c_A}{\partial r^2} + \frac{1}{r} \frac{\partial c_A}{\partial r} + \frac{\partial^2 c_A}{\partial x^2} \right)}_{D \nabla^2 c_A: \text{diffusive flux}}$$

Energy balance (each term has units temperature per unit time)

$$\underbrace{\frac{\partial T}{\partial t}}_{\text{temperature change}} = \underbrace{-u \frac{\partial T}{\partial x}}_{\text{axial convective flux}} + \underbrace{\frac{\nu_A k \Delta H}{\rho c_p} c_A^n}_{\text{rate of reaction}} + \underbrace{\frac{\lambda}{\rho c_p} \left(\frac{\partial^2 T}{\partial r^2} + \frac{1}{r} \frac{\partial T}{\partial r} + \frac{\partial^2 T}{\partial x^2} \right)}_{\alpha \nabla^2 T: \text{diffusive flux}}$$

14.2.8. Taylor-Couette Reactor (TCR)



The Taylor number is the cylindrical Reynolds number,

$$Ta = \frac{\rho^2 \omega^2 r_i (r_o - r_i)^3}{\mu^2}$$

For $Ta > Ta_c$, axisymmetric vortices form, where

$$Ta_c = 41.3 \times \frac{(1 + \Lambda)^2}{2\Lambda\sqrt{(1 - \Lambda)(3 + \Lambda)}}; \quad \Lambda = \frac{r_i}{r_o}$$

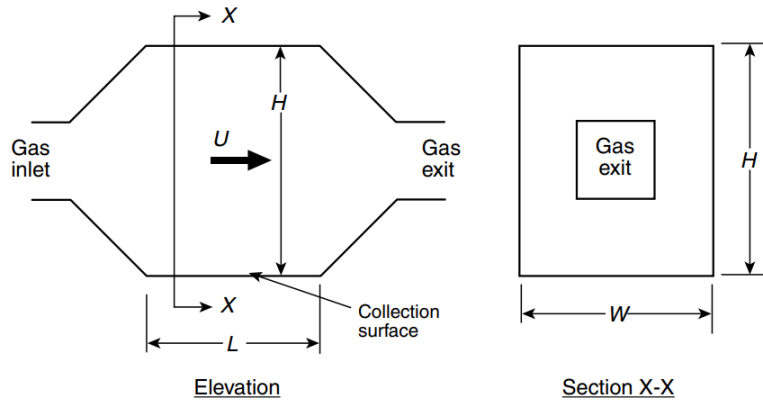
The Péclet number, $Pe = \frac{u_{ax} L}{D}$ describes the ratio of advection to diffusion.

When $Pe \rightarrow 0$, the TCR approaches a CSTR.

When $Pe \rightarrow \infty$, the TCR approaches a PFR.

14.2.9. Settling Chamber for Gravity Separation

For a gas flow of speed U (defined such that the flow rate is $Q = HW \times U$ in the below geometry) and density ρ_f containing particles of diameter x and density ρ_p to be removed:



If Stokes' law applies to the particle flow regime ($Re_p < 0.3$):

Terminal velocity:

$$U_T = \frac{x^2 g (\rho_p - \rho_f)}{18\mu}$$

Collection efficiency:

$$\eta = \frac{U_T L}{HU}$$

14.2.10. Fluid Flow Through a Packed Bed

For a packed column of height L , area A , fluid density ρ_f and particle density ρ_p and (mean surface-volume) particle diameter x :

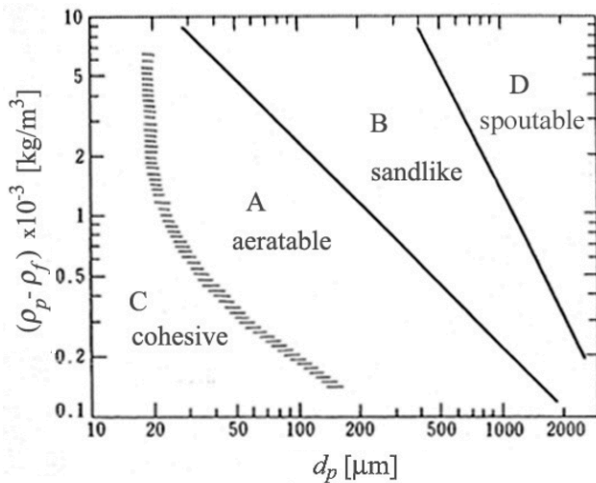
- Porosity (voidage ratio) $\varepsilon = \frac{V_{void}}{V_{total}} = 1 - \frac{M_p}{\rho_p AL}$
- Superficial velocity (through the packed region): $U_i = \frac{U}{\varepsilon}$
- Pressure drop in laminar flow: $\frac{-\Delta p}{L} = 180 \frac{\mu U}{x^2} \frac{(1-\varepsilon)^2}{\varepsilon^3}$ (Carman-Kozeny equation)
- Pressure drop in turbulent flow: $\frac{-\Delta p}{L} = 150 \frac{\mu U}{x^2} \frac{(1-\varepsilon)^2}{\varepsilon^3} + 1.75 \frac{\rho_f U^2}{x} \frac{1-\varepsilon}{\varepsilon^3}$ (Ergun equation)
- Pressure drop in a fluidised bed: $-\Delta p = (1 - \varepsilon)(\rho_p - \rho_f)gL$
- Modified Reynolds number: $Re^* = \frac{xU \rho_f}{\mu (1-\varepsilon)} = \frac{Re_x}{1-\varepsilon}$
- Modified friction factor: $f^* = \frac{-\Delta p}{L} \frac{x}{\rho_f U^2} \frac{\varepsilon^3}{1-\varepsilon} = 1.75 + \frac{150}{Re^*}$

14.2.11. Cake Filtration

- For an incompressible cake, cake resistance $r_c = \frac{-\Delta p}{\mu UL} = \frac{150}{x^2} \frac{(1 - \epsilon)^2}{\epsilon^3}$.
- Volume of cake formed per unit volume of passing filtrate: $\phi = \frac{LA}{V}$
- Instantaneous filtrate volumetric flow rate (no medium resistance): $\frac{dV}{dt} = \frac{A^2(-\Delta p)}{r_c \mu \phi V}$.
- If Δp is constant then $\frac{dV}{dt}$ is inversely proportional to V and $t = \frac{r_c \mu \phi}{2A^2(-\Delta p)} V^2$.
- If $\frac{dV}{dt}$ is constant then Δp is proportional to V .

14.2.12. Geldart Groupings of Powders and Minimum Bubbling Velocity

Fluidisation behaviour can be predicted by classification based on density relative to the fluidisation medium and size.



	Group C	Group A	Group B	Group D
Most obvious characteristic	Cohesive, difficult to fluidize	Ideal for fluidization. Exhibits range of non-bubbling fluidization	Starts bubbling at U_{mf}	Coarse solids
Typical solids	Flour, cement	Cracking catalyst	Building sand	Gravel, coffee beans
Property				
Bed expansion	Low because of channelling	High	Moderate	Low
De-aeration rate	Initially fast, then exponential	Slow, linear	Fast	Fast
Bubble properties	No bubbles—only channels	Bubbles split and coalesce. Maximum bubble size	No limit to size	No limit to size
Solids mixing	Very low	High	Moderate	Low
Gas backmixing	Very low	High	Moderate	Low
Spouting	No	No	Only in shallow beds	Yes, even in deep beds

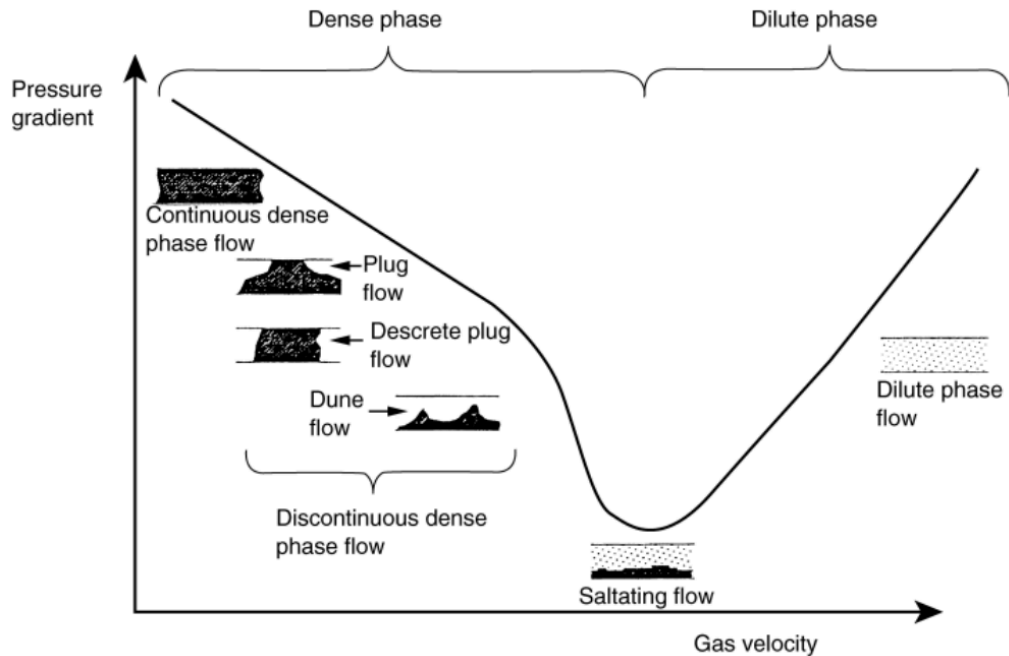
Correlation for minimum bubbling velocity: $U_{mb} = 2.07 e^{0.716 F} \frac{x_p \rho_g^{0.06}}{\mu^{0.347}}$

where F is the fraction of powder less than 45 μm in size.

Group A: $U_{mb} > U_{mf}$, Group B, D: $U_{mb} = U_{mf}$.

14.2.13. Phases of Pneumatic Transport

When a solid phase is dispersed in a flowing gas phase, the mode of transport and pressure drop depends on the gas velocity.

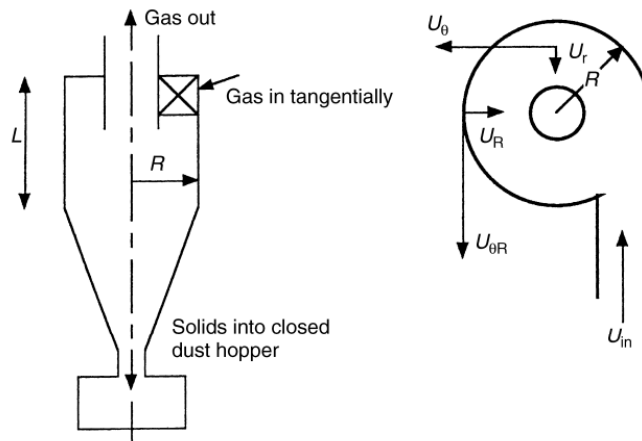


The overall pressure drop consists of inertial, frictional and static head effects:

$$\Delta p = \underbrace{\frac{1}{2}\epsilon\rho_f U_f^2}_{\text{fluid acceleration}} + \underbrace{\frac{1}{2}(1-\epsilon)\rho_p U_p^2}_{\text{particle acceleration}} + \underbrace{\bar{F}_{fw}L}_{\text{fluid-wall friction}} + \underbrace{\bar{F}_{pw}L}_{\text{particle-wall friction}} + \underbrace{\rho_f L \epsilon g \sin \theta}_{\text{fluid head}} + \underbrace{\rho_p L (1-\epsilon) g \sin \theta}_{\text{particle head}}$$

(U_f : gas velocity, ρ_f : gas density, U_p : particle velocity, ρ_p : particle density, ϵ : porosity, L : length of tube, F_{fw} : gas-wall friction per unit volume, F_{pw} : particle-wall friction per unit volume, g : gravitational acceleration, θ : angle of inclination of tube to horizontal)

14.2.14. Gas Cyclone Separators



Pressure drop between gas inlet and gas outlet (Euler number):

$$Eu = \frac{\Delta p}{\frac{1}{2}\rho_f U^2}$$

Azimuthal velocity distribution:

$$U_\theta(r) \times r^{1/2} = \text{constant}$$

Critical particle diameter for separation:

$$x_{50}^2 \approx \frac{18\mu}{\rho_p - \rho_f} \frac{U_R}{U_{\theta R}^2} R$$

Performance of geometrically similar cyclones (Stokes number):

$$Stk_{50} = \frac{x_{50}^2 \rho_p U}{36 \mu R}$$

Grade efficiency:

$$\eta = \frac{(x/x_{50})^2}{1 + (x/x_{50})^2}$$

Euler-Stokes correlation:

$$Eu = \sqrt{\frac{12}{Stk_{50}}}$$

14.2.15. Particle Size Reduction in Ball Milling

Breakage energy per unit mass of feed: $\frac{dE}{dx} = -\frac{k}{x^n}$

Kick's law: $n = 1$ (by mass), Rittinger's law: $n = 2$ (by surface area), Bond's law: $n = 1.5$ (by $\sqrt{\frac{S}{V}}$)

Product size distribution: $\frac{dm_i}{dt} = \sum_{j=1}^{i-1} (b(i,j)S_j m_j) - S_i m_i$

(m_i : mass fraction of particles in size interval i ,

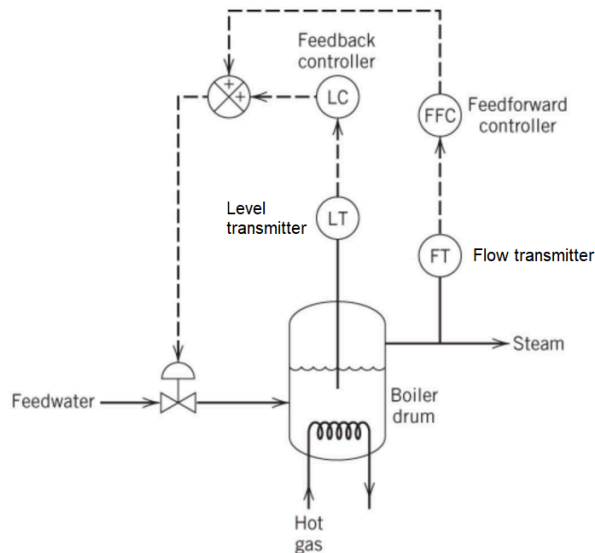
$b(i,j)$: fraction of breakage product from size interval j which falls into size interval i ,

S_j : probability of a particle of size j being broken in unit time.)

14.2.16. Process and Instrumentation Diagram (P&ID) Abbreviations

	Locally mounted instrument		Flow alarm		Unit shut down
	Board mounted instrument		Flow element		Position/unit switch closed
	Pressure controller		Flow indicator		Shut down valve relay
	Pressure indicator		Flow recorder		Shut down valve
	Pressure recording		Flow recording controller		Position/limit indicator open
	Pressure indicating controller		Temperature alarm		Temperature relay
	Pressure recording controller		Temperature indicator		Spectacle blind open
	Pressure safety valve		Temperature recorder		Spectacle blind closed
	Relief valve		Temperature recording controller		Orifice flanges
	Level alarm		Temperature well		Piping speciality item
	Level alarm high		Gate valve		Instrument air line
	Level alarm low		Globe valve		Instrument electrical
	Level controller		Check valve		Instrument capillary tubing
	Level glass		Control valve		Pipe
	Level indicator		Plug valve		Transmitter
	Level indicating controller		Ball valve		Hand control valve
	Level recording controller		Butterfly valve		

Example: water boiler with feedforward and feedback control (see Section 9.4.10):



14.3. Colloids and Nanoparticle Chemistry

14.3.1. Classification of Colloidal Systems

Dispersed phase	Dispersion medium	Colloid type	Examples
Solid	Solid	Solid sol	ruby glass, alloys
Solid	Liquid	Sol	paint, starch, proteins, ink
Solid	Gas	Solid aerosol	smoke, volcanic dust
Liquid	Solid	Gel	cheese, butter, agar, gelatin
Liquid	Liquid	Emulsion / Liquid crystal	milk, mayonnaise, latex
Liquid	Gas	Liquid aerosol	fog, cloud, hair spray
Gas	Solid	Solid foam	aerogel, rubber, styrofoam, pumice
Gas	Liquid	Foam	foam, whipped cream, soda water
Gas	Gas	–	none at standard conditions

14.3.2. Preparation and Purification of Colloids

Lyophilic colloids form readily by simply mixing the two phases.

Lyophobic colloids require input work, and can be formed by:

- Oxidation: e.g. $2 \text{H}_2\text{S} (\text{aq}) + \text{O}_2 (\text{bubbled through}) \rightarrow 2 \text{H}_2\text{O} + 2 \text{S} (\text{colloidal})$
- Reduction: e.g. $2 \text{AuCl}_3 (\text{aq}) + 3 \text{SnCl}_2 \rightarrow 3 \text{SnCl}_4 + 2 \text{Au} (\text{gold sol; 'Purple of Cassius'})$
- Hydrolysis: e.g. $\text{FeCl}_3 (\text{aq}) + \text{H}_2\text{O} (\text{boiling}) \rightarrow 3 \text{HCl} + \text{Fe}(\text{OH})_3 (\text{colloidal})$
- Decomposition: e.g. $\text{As}_2\text{O}_3 + 3 \text{H}_2\text{S} \rightarrow 3 \text{H}_2 + \text{As}_2\text{S}_3 (\text{sol})$
- Mechanical dispersion: grind particles, form suspension, use colloidal mill (rapidly rotating disks shear the particles into microparticles)
- Electrical dispersion (Bredig's arc method): for sols of Pt, Ag, Au, Cu; a high-voltage electrical discharge is struck between metal electrodes in an ice bath, releasing metal microparticles. Add KOH as a stabiliser.
- Peptisation: addition of an electrolyte to a precipitate reforms the colloid.
- Supercritical antisolvent precipitation (SAS, Section 14.2.11) and electrohydrodynamic atomisation (EHDA, Section 14.2.10), are modern methods for colloid synthesis.

Colloids can be purified using electrodialysis, ultrafiltration and ultracentrifugation.

14.3.3. Micellisation of Surfactants

- Gibbs free energy change for micellization: $\Delta G = RT \ln c_{CMC}$
- Ionic surfactants typically have a 'Krafft temperature', T_K , where micellisation occurs for $T > T_K$.
- Nonionic surfactants typically have a 'cloud point', T_c , where micellisation occurs for $T < T_c$.
- Micelle aggregation number, N : number of surfactant molecules per micelle.
- Phillips criterion for the CMC: $\left[\frac{d^3\phi}{dc} \right]_{c=c_{CMC}} = 0$ (ϕ is a property in Section 14.4.4.)

The CMC for some common surfactants in aqueous solution (in mM) are shown below.

Surfactant	Type	$c_{CMC} / \text{mmol dm}^{-3}$
sodium lauryl sulfate (SLS)	anionic	9.95
sodium dodecyl sulfate (SDS)	anionic	8.099
sodium stearate (SS)	anionic	0.071
cetrimonium bromide (CTAB)	cationic	0.92
cetylpyridinium chloride (CPC)	cationic	1
lauryl betaine	zwitterionic	1.18
cocamidopropyl betaine	zwitterionic	0.974
penta(ethyleneglycol)-monododecyl ether (C12E5)	nonionic	0.065
poloxamer L35 (Pluronic L35, PEO ₁₁ PPO ₁₆ PEO ₁₁)	nonionic	5.3
poloxamer L121 (Pluronic L121, PEO ₅ PPO ₆₈ PEO ₅)	nonionic	0.001
polysorbate 80 (E433)	nonionic	0.012
nonylphenol ethoxylate-9 (NP-9)	nonionic	0.097
Triton X-100	nonionic	0.22

Surfactant micellisation is influenced by various factors:

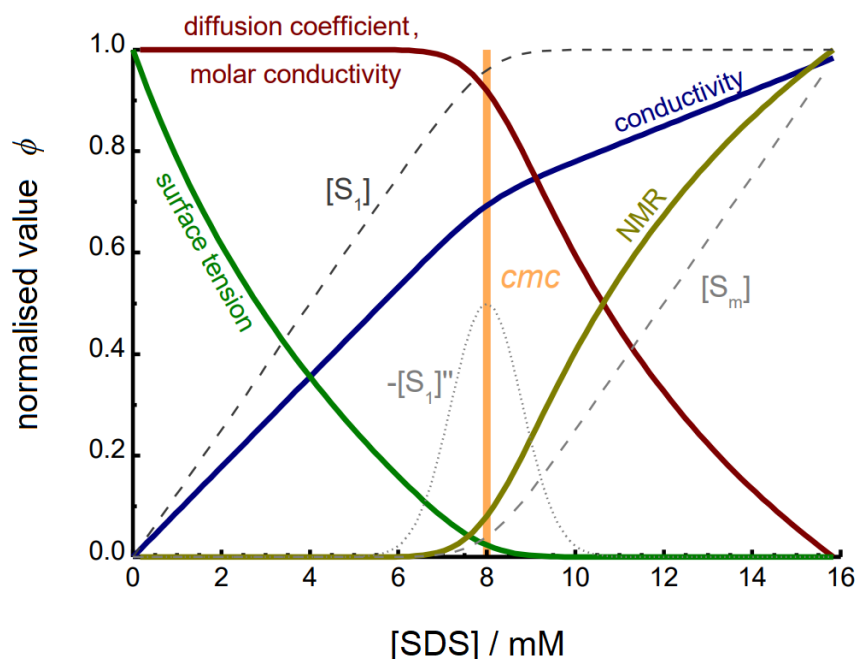
- Addition of salts containing kosmotropic anions decreases the CMC and forms larger micelles. Addition of salts containing chaotropic anions increases the CMC and forms smaller micelles. These effects are more significant in ionic surfactants than nonionic surfactants.
- Surfactant molecules with longer hydrophobic chains have smaller CMC.
- Increasing the temperature decreases the CMC.

14.3.4. Isothermal Physical Properties of Amphiphilic Colloids (Surfactant Solutions)

The graph shows normalised values of:

- electrical conductivity σ (normalised to $\sigma_\infty = 71.8 \text{ mS m}^{-1}$)
- molar conductivity Λ_m (normalised to $\Lambda_m^0 = 72 \text{ S cm}^2 \text{ mol}^{-1}$)
- self-diffusion coefficient D (normalised to $D_0 = 5.04 \times 10^{-10} \text{ m}^2 \text{ s}^{-1}$)
- surface tension γ (normalised to $\gamma_0 = 71.8 \text{ mN m}^{-1}$)
- NMR chemical shift δ (measured in D_2O) (normalised to $\delta_{16\text{mM}}^{(\text{H}^1)} = 0.97 \text{ ppm}$)
- monomer phase concentration $[\text{S}_1]$, (normalised to $[\text{S}_1]_\infty = 8 \text{ mM}$)
- micelle phase concentration $[\text{S}_m]$ (normalised to $[\text{S}_m]_\infty = 8 \text{ mM}$)

against the concentration of SDS (sodium dodecyl sulfate) in water (in mmol dm^{-3}) at 25°C .



Other properties include:

- In a lyophilic colloid (suspension in water), viscosity is higher and surface tension is lower than the bulk solvent.
- In associated colloids, deviations of colligative properties are smaller than in the bulk solvent due to lower Van 't Hoff factor (lower particle count).

14.3.5. DLVO Theory and the Electrical Double Layer of Colloidal Particles

For colloidal particles of diameter x separated by closest-distance D ,

- Van der Waals cohesive force: $V_{vdW}(D) = \frac{-Ax}{24D}$ $F_{vdW}(D) = \frac{-Ax}{24D^2}$
- Electrical double layer repulsive force: $V_{EDL}(D) = \pi\epsilon x \Psi_0^2 e^{-\kappa D}$ $F_{EDL}(D) = \pi\epsilon x \Psi_0^2 \kappa e^{-\kappa D}$
- Overall force: $F = F_{vdW} + F_{EDL} = \pi\epsilon x \Psi_0^2 \kappa e^{-\kappa D} - \frac{Ax}{24D^2}$.

(A : Hamaker constant, Ψ_0 : surface potential, κ : Debye screening parameter, ϵ : permittivity of medium. The zeta potential ζ approximates Ψ_0 .)

An excluded volume with additional radius approximately equal to the the Debye length $\lambda = \frac{1}{\kappa}$ is formed around the solid particle, representing the extent of the diffuse layer of the EDL.

- Debye constant variation with salt concentration: $\kappa [nm^{-1}] = 3.29 \sqrt{I}$, $\lambda [nm] = \frac{0.304 nm}{\sqrt{I}}$
(I [$mol\ dm^{-3}$]: ionic strength)
- Surface charge on colloidal particle: $\sigma [C\ m^{-2}] = \epsilon \zeta \kappa$ (Gouy-Chapman equation)

Nanobubbles in water (gaseous cavities) also acquire surface charge like colloidal particles.

14.3.6. Surface Electrostatic Data for Common Particulate Materials

Isoelectric Point (IEP) and Hamaker Constants for Interfaces

The isoelectric point (IEP) and Hamaker constant A for the force between particles of (Material 1) and (Material 3), through a medium of (Material 2), are given in the tables.

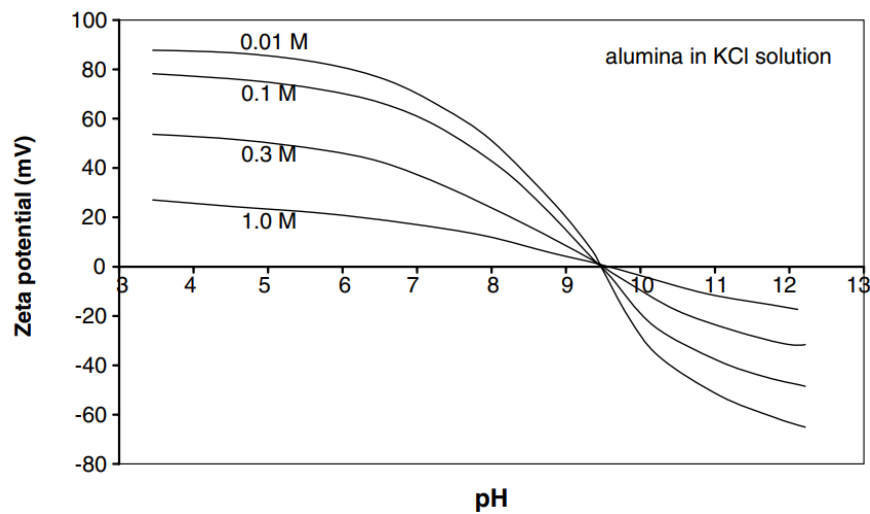
Material	pH of IEP
Silica	2–3
Alumina	8.5–9.5
Titania	5–7
Zirconia	7–8
Hematite	7–9
Calcite	8
Oil	3–4
Air	3–4

Material 1	Material 2	Material 3	Hamaker constant (approximate) (J)
Alumina	Air	Alumina	15×10^{-20}
Silica	Air	Silica	6.5×10^{-20}
Zirconia	Air	Zirconia	20×10^{-20}
Titania	Air	Titania	15×10^{-20}
Alumina	Water	Alumina	5.0×10^{-20}
Silica	Water	Silica	0.7×10^{-20}
Zirconia	Water	Zirconia	8.0×10^{-20}
Titania	Water	Titania	5.5×10^{-20}
Metals	Water	Metals	40×10^{-20}
Air	Water	Air	3.7×10^{-20}
Octane	Water	Octane	0.4×10^{-20}
Water	Octane	Water	0.4×10^{-20}
Silica	Water	Air	-0.9×10^{-20}

(silica: SiO_2 , alumina: Al_2O_3 , titania: TiO_2 , zirconia: ZrO_2 , hematite: Fe_2O_3 , calcite: CaCO_3 , oil: liquid hydrocarbons, air: air microbubbles.)

Zeta Potential for Alumina Particles in Strong Electrolyte

Zeta potential ζ of alumina particles as a function of pH and salt concentration. (Data from Johnson et al., 2000)



14.3.8. Non-Newtonian Fluid Viscosity

Newtonian fluid: μ is independent of shear rate and time. For non-Newtonian fluids:

Shear rate dependence:

- Shear-thinning (pseudoplastic): μ decreases with shear rate
e.g. molten polymers, ketchup, whipped cream, blood, paint, nail polish.
- Shear-thickening (dilatant): μ increases with shear rate
e.g. cornstarch suspensions in water.

Time dependence:

- Thixotropic: μ decreases with time (under a constant shear rate)
e.g. ketchup, toothpaste, shaving cream.
- Rheopectic: μ increases with time (under a constant shear rate)
e.g. printer inks, synovial fluid, gypsum paste.

Most gels, colloids and biofluids are thixotropic while rheopexy is rarer. They may be shear-thinning or thickening.

14.3.9. Flory-Huggins Solution Theory of Polymeric Colloids

Brownian Motion of Colloidal Particles

Mean Free Path:
$$\bar{L} = \frac{1}{\sqrt{2}n_v \pi d^2} = \frac{RT}{N_A P} \frac{1}{\sqrt{2} \pi d^2} = \frac{\mu}{P} \sqrt{\frac{\pi k_B T}{2m}}$$

Mean Squared Displacement:
$$\overline{x^2} = 2Dt \text{ (in 1D); } \overline{x^2} = 4Dt \text{ (in 2D); } \overline{x^2} = 6Dt \text{ (in 3D)}$$

Diffusion coefficient:
$$D = \frac{kT}{3\pi\eta\mu} \text{ (Stokes-Einstein relation)}$$

($n_v = \frac{n}{N_A V}$: number of particles per unit volume, d : diameter of particles, μ : viscosity of medium, P : pressure, M_r : relative molecular mass of particle (per mole))

Forces between hard colloidal particles with a polymeric surface:

- Bridging flocculation: attractive, maximised when surface coverage is ~50%.
- Steric repulsion: repulsive, maximised when surface coverage is ~100%.

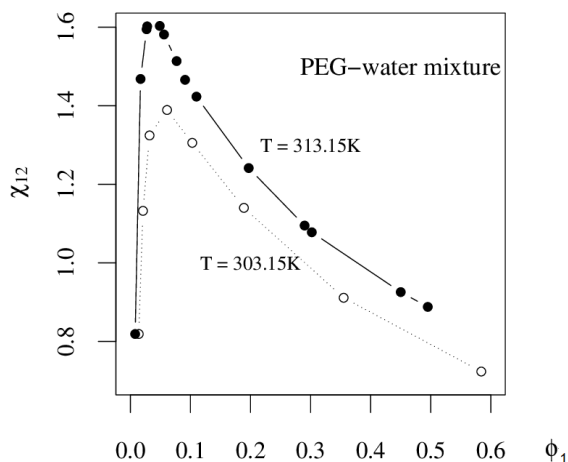
The Gibbs free energy of mixing between solvent (n_1 moles, volume fraction ϕ_1) and polymer (n_2 moles, volume fraction ϕ_2) is $\Delta G_m = RT[n_1 \ln \phi_1 + n_2 \ln \phi_2 + n_1 \phi_2 \chi_{12}]$

(T : temperature, R : gas constant, χ_{12} : polymer-solvent interaction parameter, $V_{m.s}$: actual volume of a polymer segment.)

Interaction parameter:
$$\chi_{12} = \frac{V_{seg}(\delta_a - \delta_b)^2}{RT} \text{ } (\delta: \text{Hildebrand solubility parameter})$$

Dimensionless free energy per unit volume:
$$f = \frac{\phi}{N} \ln \phi + (1 - \phi) \ln(1 - \phi) + \chi\phi(1 - \phi)$$

The value of χ_{12} for some polymer-solvent systems (varying with solvent fraction ϕ_1) are given below. PEG-water varies with solvent fraction and its variation is shown in the graph.



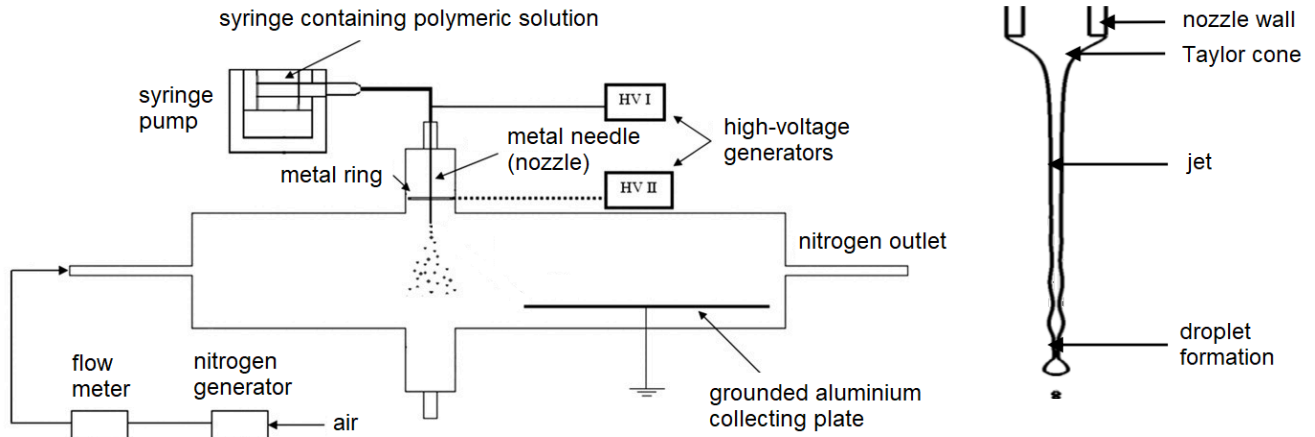
Polymer	Solvent	χ_{12}	Temp / °C
EVA	cyclohexane	0.490	30
EVA	THF	0.411	30
carbosilane dendrimer	benzene	0.85	35
PCL	ethyl acetate	1.466	25

14.3.10. Electro spraying and Electrohydrodynamic Atomisation (EHDA)

EHDA is a modern technique for synthesising loaded microparticles.

General flow diagram of EHDA:

Close-up of nozzle tip:

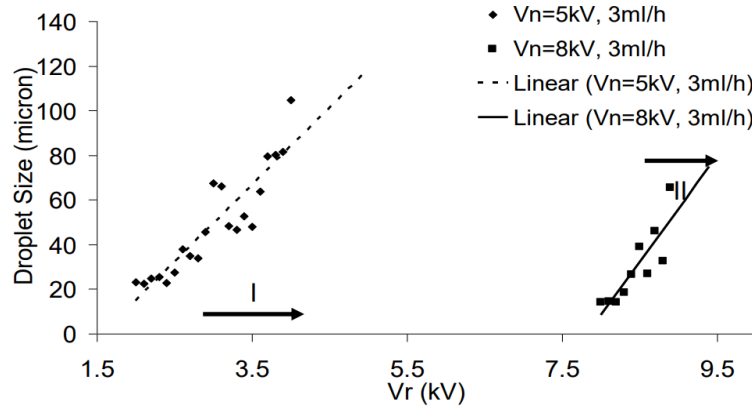


Droplet size variation with different ring electrical potential (V_r)

Nozzle potentials

I: $V_n = 5 \text{ kV}$

II: $V_n = 8 \text{ kV}$



The cone-jet model for the Taylor cone formed at the nozzle tip implies that

$$I \propto \sqrt{\gamma \kappa Q} \quad \text{and} \quad d \propto \left(\frac{\rho \epsilon_0 Q^4}{I^2} \right)^{1/6} \propto \sqrt{Q}$$

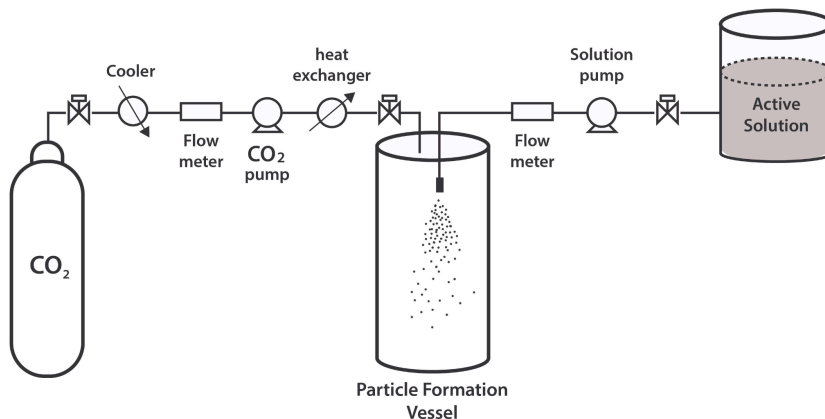
(d : droplet diameter, c : constant, Q : volumetric flow rate, ρ : liquid density, γ : liquid surface tension, κ : liquid electrical conductivity, I : current, ϵ_0 : vacuum permittivity.)

Modifications to EDHA include coaxial EDHA (CEDHA): two polymer flows in the nozzle, in coflow.

14.3.11. Supercritical Antisolvent Precipitation (SAS)

SAS is a modern technique for synthesising loaded nanoparticles.

General flow diagram of SAS (using scCO₂ as the antisolvent):



$$\text{Encapsulation Efficiency (EE)} = \frac{\text{amount of active compound in nanovesicle suspension}}{\text{total amount of active compound initially in solution}} (\times 100\%)$$

Important parameters affecting the particle size distribution, EE and particle morphology, are the sCO₂ pressure, temperature and flow rate, the physical and chemical properties of the active compound and the encapsulant, and the nozzle geometry.

Modifications to SAS include:

- SAS with enhanced mass transfer (SAS-EM): uses ultrasonication, typically decreasing particle size further, and can be used to control particle morphology.
- Atomised Rapid Injection for Solvent Extraction (ARISE): removes the capillary injector, allowing for higher throughput.

For the phase diagram of CO₂, see Section 14.4.7.

14.3.12. Applications of Nanoparticles and Nanostructures

Well-established nanotechnologies include:

- **Titanium dioxide and/or zinc oxide** (TiO_2 -NPs / ZnO -NPs): used in sunscreen to reflect and scatter UVA and UVB radiation.
- **Silver (Ag-NPs)**: used in textiles for their antimicrobial properties. When these textiles are washed however, Ag-NPs can be released into rivers which are toxic to fish.
- **Graphene**: used in thin-film electronics as an excellent conductor.
- **Graphene oxide**: graphene with -OH pairs, epoxide bridges and -COOH groups. Used in fast-switching electronics and photonics/optoelectronics.
- **Tungsten trioxide graphene composite**: used for energy storage, gas sensors and heterogeneous or photocatalysis.
- **Carbon nanotubes**: extremely high tensile strength along the fibre direction.
- **Buckyballs** (buckminsterfullerene, C_{60}): used as a model for drug delivery by encapsulation.
- **Quantum dots**: made of semiconductors e.g. C, Si, Ge, PbS, CdSe, CdTe, InAs, InP. Used in photonics, quantum information processing and medical diagnostics.

C15. INORGANIC AND ENVIRONMENTAL CHEMISTRY

15.1. Metallurgy

15.1.1. Common Names and Formulas of Ores and Minerals

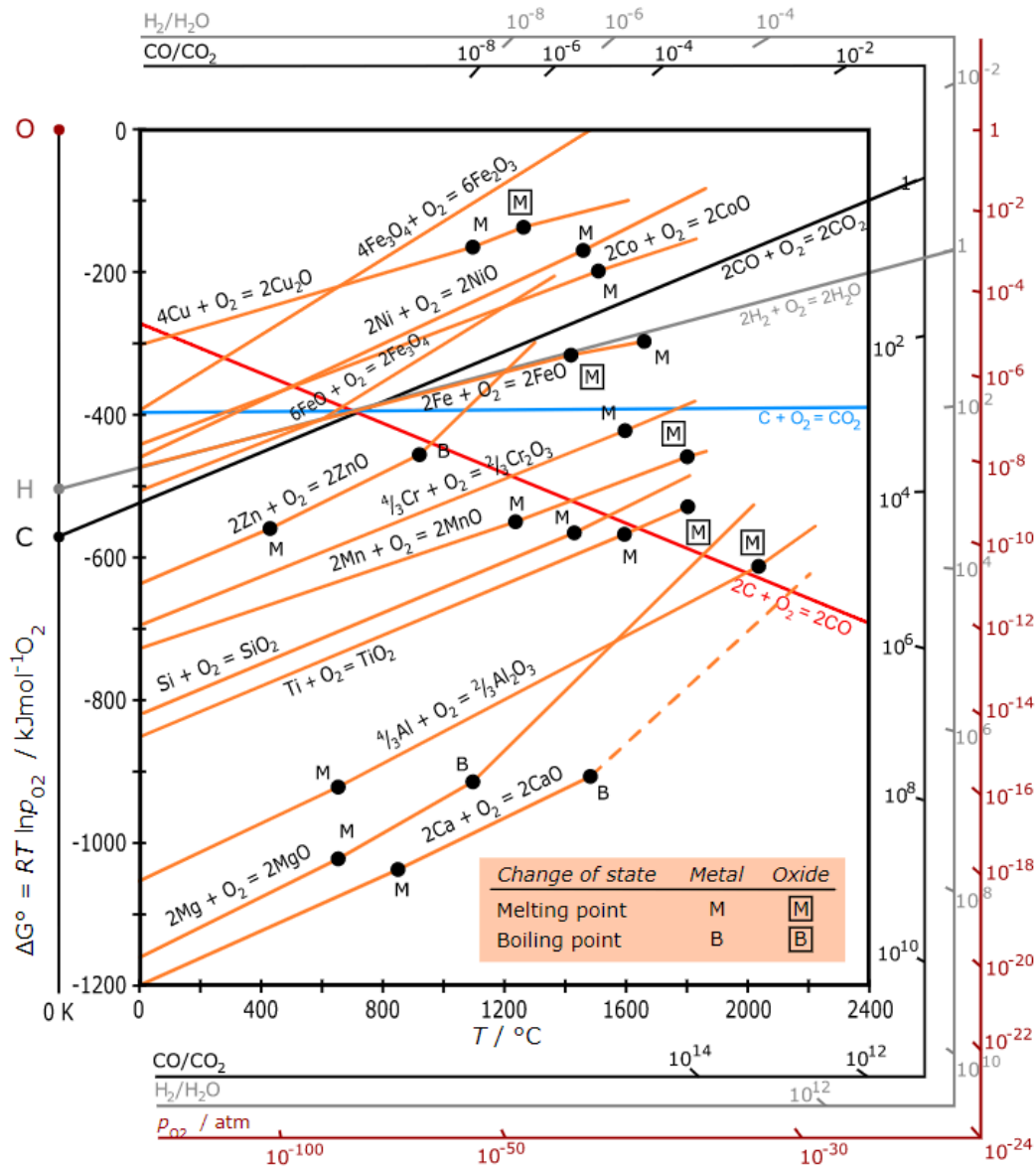
Metal	Ores	Composition	Metal	Ores	Composition
aluminium (Al)	bauxite	$\text{Al}_2\text{O}_3 \cdot 2 \text{H}_2\text{O}$	zinc (Zn)	sphalerite	ZnS
	diaspore	$\text{Al}_2\text{O}_3 \cdot \text{H}_2\text{O}$		calamine	ZnCO_3
	corundum (ruby: with Cr, sapphire: with Fe, Ti)	Al_2O_3		zincite	ZnO
iron (Fe)	haematite	Fe_2O_3	lead (Pb)	galena	PbS
	magnetite	Fe_3O_4		anglesite	PbSO_4
	siderite	FeCO_3		cerussite	PbCO_3
	iron pyrite	FeS_2	magnesium (Mg)	carnallite	$\text{K}_2\text{MgCl}_4 \cdot 6 \text{H}_2\text{O}$
	limonite	$\text{FeO}(\text{OH})$		magnesite	MgCO_3
copper (Cu)	chalcopyrite	CuFeS_2		dolomite	$\text{MgCO}_3 \cdot \text{CaCO}_3$
	copper glance	CuS_2		olivine	$\text{Mg}_2\text{SiO}_4 \cdot \text{Fe}_2\text{SiO}_4$
	cuprite	Cu_2O	epsom salt	$\text{MgSO}_4 \cdot 7 \text{H}_2\text{O}$	
	malachite	$\text{CuCO}_3 \cdot \text{Cu}(\text{OH})_2$	tin (Sn)	cassiterite	SnO_2
	azurite	$2 \text{CuCO}_3 \cdot \text{Cu}(\text{OH})_2$	silver (Ag)	argentite	Ag_2S
beryllium (Be)	beryl / emerald	$\text{Be}_3\text{Al}_2(\text{SiO}_3)_6$		pyrargyrite	Ag_3SbS_3
mercury (Hg)	cinnabar	HgS	cobalt (Co)	cobaltite	CoAsS
uranium (U)	pitchblende	$\text{UO}_2 + \text{U}_3\text{O}_8$	tungsten (W)	scheelite	CaWO_4
silicon* (Si)	quartz	SiO_2		wolframite	$(\text{Fe}, \text{Mn})\text{WO}_4$
cerium** (Ce)	monazite	$(\text{Ce}, \text{La}, \text{Nd}, \text{Th})\text{PO}_4$	chromium (Cr)	chromite	FeCr_2O_4

* silicon is a metalloid so quartz does not qualify as an ore. It is a common gangue mineral.

** monazite often contains a wide variety of lanthanides and actinides (rare-earths).

15.1.3. Ellingham Diagram for Oxidation Reactions

The lower the position of a metal's line in the Ellingham diagram, the greater is the stability of its oxide. If the curves for two metals at a given temperature are compared, the metal with the **lower** Gibbs free energy of oxidation on the diagram **will reduce the oxide with the higher** Gibbs free energy of formation e.g. carbon can reduce Cr_2O_3 to Cr above $1200\text{ }^\circ\text{C}$ by oxidation to CO.



(The dotted line for forming CaO (g) indicates hypothetical (experimentally unknown) values).

Contours of p_{O_2} , $\frac{p_{\text{H}_2}}{p_{\text{H}_2\text{O}}}$ and $\frac{p_{\text{CO}}}{p_{\text{CO}_2}}$ (partial pressures at equilibrium) are shown on the sides, which each point to the **O**, **H** and **C** points respectively on $T = 0\text{ K}$.

15.1.4. Metal Extraction Techniques

The typical processes for metal extraction from ores are:

1. **Pulverisation:** the ore is mechanically crushed and ground into a powder by e.g. ball milling, stamp milling.
2. **Dressing:** impurities in the ore are removed, concentrating the desired product.
3. **Extraction:** the crude metal is chemically extracted by converting the ore to a compound which is more suitable for reduction, often an oxide, then reduced to the metal.
4. **Refining:** the metal is purified using a technique specific to the desired application.

Methods of dressing (mineral processing) include hydraulic washing (gravity separation), electromagnetic separation, froth flotation processes and base leaching processes (hydrometallurgy).

Methods of pre-conversion of concentrated ores to their oxide (pyrometallurgy):

- Calcination (carbonate \rightarrow oxide + CO_2 , by thermolysis without oxygen)
- Roasting (sulfide + $\text{O}_2 \rightarrow$ oxide + SO_2 , by heating with oxygen); may include self-reduction e.g. Cu_2S , PbS due to reaction with its own oxide to form the metal.

Methods of reduction of the to the metal:

- Smelting: heating of the oxide with coal or coke (C) or aluminium powder (thermite) in a blast furnace, with addition of flux (acidic flux e.g. borax, SiO_2 to remove basic impurities, basic flux e.g. MgO , CaCO_3 to remove acidic impurities), which converts gangue to easily-removable slag.
- Metal displacement: e.g. sulfide + $\text{O}_2 \rightarrow$ sulfate, or sulfide + $\text{NaCN} \rightarrow$ metallic cyanide complex, which reacts with electropositive metals e.g. Cu to give the pure metal by a displacement reaction.
- Electrolysis: molten salt (electrometallurgy) or aqueous salt (electrowinning) electrolysis using a graphite anode and a metal cathode.

Methods of refining to a pure metal:

- Liquefaction: readily fusible metals can be melted at a temperature where the impurities remain solid.
- Distillation: volatile metals can be vaporised at a temperature where the impurities remain solid.
- Zone refining (fractional crystallisation): segregation of impurities from the liquid state forms ultrapure grains on recrystallisation. Used for pure semiconductors.
- Column chromatography: the mixture is put in a liquid or gaseous medium which is moved through an adsorbent, which adsorbs at different levels, and can be eluted once adsorption has finished.
- Vapour phase refining: the metal is converted to a volatile compound, then heated to decompose from the gas phase to the pure metal, which deposits.
- Electrorefining: aqueous or molten electrolysis using a solution of the metal as the electrolyte. The anode is the impure metal, depositing its insoluble inert impurities ('anode mud': often containing precious metals), while the cathode accumulates pure metal.

15.1.5. Industrial Metal Extraction Processes

Lithium

- **Ore processing:** spodumene ($\text{LiAl}(\text{SiO}_3)_2$) is mined from Li-rich pegmatite deposits, crushed and gravity separated. It is then roasted to convert it to lithium carbonate or lithium hydroxide, which may be used as chemicals or converted to metallic lithium by electrolytic refining.
- **Brine extraction:** brine deposits in salt flats or underground reservoirs are pumped to the surface and evaporated to concentrate the salts. Lithium is selectively precipitated from the solution using soda ash or sodium hydroxide (e.g. $2 \text{Li}^+ + \text{Na}_2\text{CO}_3 \rightarrow \text{Li}_2\text{CO}_3 + 2 \text{Na}^+$) to form Li_2CO_3 or LiOH , which is filtered, washed and dried.

Sodium, Potassium

- **Downs process** (1923): electrolysis of the molten sodium chloride using a graphite anode and iron cathode: e.g. $2 \text{NaCl} \rightarrow 2 \text{Na} + \text{Cl}_2$
- **Solvay process** (1863): produces soda ash (Na_2CO_3) from brine (NaCl) and limestone (CaCO_3) solutions, catalysed by ammonia in several chemical reactions.

Magnesium

- **Molten electrolysis:** anhydrous magnesium chloride is fused with NaCl and CaCl_2 to lower the melting point and electrolysed. The chloride can be made by either heating carnallite ($\text{MgCl}_2 \cdot 6 \text{H}_2\text{O}$) in catalytic HCl gas or smelting the oxide via $\text{MgO} + \text{C} + \text{Cl}_2 \rightarrow \text{MgCl}_2 + \text{CO}$.

Chromium, Vanadium, Niobium, Molybdenum

- **Goldschmidt aluminothermic process** (1895): smelting of the oxide using powdered aluminium (thermite): e.g. $3 \text{V}_2\text{O}_5 + 10 \text{Al} \rightarrow 5 \text{Al}_2\text{O}_3 + 6 \text{V}$

Aluminium

- **Bayer process** (1888): bauxite ore is roasted to oxidise ferric oxide impurities (FeO) to Fe_2O_3 . The roasted ore is then base-hydrolysed and the hydroxide is calcined:
 $\text{Al}_2\text{O}_3 + \text{NaOH} \rightarrow \text{NaAlO}_2 + \text{H}_2\text{O} \rightarrow \text{Al}(\text{OH})_3 (+ \text{NaOH}) \rightarrow \text{Al}_2\text{O}_3$.
- **Serpuk process** (1903): bauxite ore with silica impurities is smelted at 2000°C in air with coke to give the nitride, which is readily hydrolysed to give the hydroxide and ammonia, which is calcined: $\text{Al}_2\text{O}_3 + \text{N}_2 + \text{C} \rightarrow \text{AlN}$; $\text{AlN} + \text{H}_2\text{O} \rightarrow \text{Al}(\text{OH})_3 + \text{NH}_3$; $\text{Al}(\text{OH})_3 \rightarrow \text{Al}_2\text{O}_3$.
- **Hall-Héroult process** (1886): electrolysis of a fused matrix of Al_2O_3 and cryolite (Na_3AlF_6) or fluorspar (CaF_2), which are added to lower melting point and increase conductivity, using a graphite anode and steel cathode: $2 \text{Al}_2\text{O}_3 + 3 \text{C} \rightarrow 4 \text{Al} + 3 \text{CO}_2$.
- **Hoopes process** (1925): electrolytic refining of Al to very high purity (~99.98%).

Copper, Zinc

- **Froth floatation** (1905): copper pyrites (CuFeS_2) are crushed into the powdered ore and sieved into a water-pine oil mixture and roasted in air to give the sulfide ore (Cu_2S)
- **Bessemerisation** (1856): smelting with O_2 and SiO_2 converts FeS impurities to FeSiO_3 (slag). The Cu_2S self-reduces with CuO to give Cu (blister copper, ~99% pure) and SO_2 .
- **Electrolytic refining** to ~99.9% purity using Cu electrodes in acidic CuSO_4 electrolyte, with inert impurities such as Sb, Se, Te, Ag dropping out in the anode mud.
- **Phytomining** (1998): hyperaccumulator plants are grown to high biomass density in soil with copper ore (bioleaching), then dried and incinerated in air to produce copper-rich ash (phytoextraction). The copper ash is displaced by scrap iron in sulfuric acid.

Gold, Silver

- **MacArthur-Forrest cyanide process** (1887): the ore is leached with dilute NaCN in air to form $\text{Na}[\text{Au}(\text{CN})_2]$, and then displaced by scrap zinc powder to precipitate Au.
- **Ziervogel process** (1885): argentite (Ag_2S) is oxidised to silver sulfate at 85°C , which is reacted with scrap copper or iron metal to precipitate silver metal:

$$\text{Ag}_2\text{S} + 2 \text{O}_2 \rightarrow \text{AgSO}_4; \quad \text{AgSO}_4 + \text{Cu} \rightarrow \text{CuSO}_4 + \text{Ag}$$
- **Patio process** (1557): mercury and magistral (burnt pyrites - sulphates and oxides of copper and iron) are added to the powdered mineral containing saline. The mixture is kept for several days. An amalgam of silver (mercurial silver) is formed. On washing, drying and subsequent distillation, silver metal is obtained.
- **Parkes process** (1850): a liquid-liquid extraction of silver from lead to produce bullion. Zinc is added to the molten lead, in which silver is much more soluble. The $\text{Zn}(\text{Ag})$ phase separates and the zinc can be boiled away to leave pure silver.

Lead

- **Froth floatation process**: galena is concentrated as PbS .
- **Betts process** (1904): electrolytic refining in molten fluorosilicates ($\text{H}_2\text{SiF}_6 + \text{PbSiF}_6$). Uses a pure lead cathode and an impure lead anode. Pure lead plates the cathode.
- **Betterton-Kroll process** (1922): add Ca-Mg alloy to remove Bi and Sb impurities at 350°C . Skim off the dross (surface layer film) containing $\text{CaMgBi}_2 + \text{CaMgSb}_2$, passing it through a hydraulic press to recover molten lead in this layer leaving ~99.99% pure lead in the bulk.
- **Air reduction**: PbS is fused in a reverberatory furnace in air to give PbO and PbSO_4 , which self-reduce more PbS into crude lead metal. Carbon reduction: PbS is mixed with lime and heated in a sinterer to give PbO , then mixed with coke and smelted in a blast furnace to form crude lead metal.

Titanium, Zirconium

- **Kroll process** (1940): TiCl_4 or ZrCl_4 is reduced by liquid magnesium metal at $825\text{ }^\circ\text{C}$ to give MgCl_2 and porous spongy Ti or Zr, which is purified by leaching or vacuum distillation. The sponge is crushed, pressed and melted in a consumable carbon electrode vacuum arc furnace. The melted ingot solidifies under vacuum, and can be remelted to remove inclusions and ensure uniformity.

Uranium

- **Milling:** ore is extracted from underground shafts, transported to mills and crushed. The pulped ore is leached with acid/base/peroxide, where uranium oxides are converted to uranyl complexes (UO_2^{2+}) which form yellowcake (mainly U_3O_8).
- **In situ leaching:** if processing on-site, the leaching solution is injected through drill holes into the ore. The leachate is pumped to the surface and recovered.
- **Smelting:** yellowcake is smelted into purified UO_2 .
- **Enrichment:** uranium oxides are reacted with fluorine to form uranium hexafluoride gas (UF_6). The gas is spun in a centrifuge so that the fissile lighter isotope (^{235}U) accumulates in the centre at elevated concentration (low enriched uranium: $<20\%$ ^{235}U , highly enriched uranium: $>20\%$ ^{235}U , weapons-grade uranium: $>90\%$ ^{235}U).

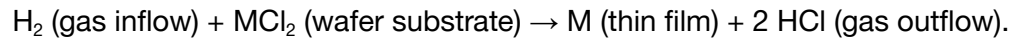
Iron and Steel

- Iron ores (magnetite, haematite and limonite) are concentrated by **gravity separation** followed by **electromagnetic separation**. The ore is then **calcined and roasted in air** to remove moisture and impurities as CO_2 , SO_2 and As_2O_3 , while oxidising FeO to Fe_2O_3 . This is then **smelted** in a blast furnace (with coke and limestone) to form sponge iron, then to pig iron (impure iron with C, Mn and Si). Pig iron can be remelted and cooled to form cast iron, with $\sim 5\%$ carbon.
- **Duplex process for steelmaking** (1930): molten pig iron is first treated in an acid-lined Bessemer converter to remove Si, Mn and a part of C. The molten pig iron is then transferred to a base-lined (calcined dolomite) open-hearth furnace to remove P and remaining C to the desired carbon content, with small amounts of alloy metals e.g. Mn, Cr, V, Co, Ni, Mo, W being added to improve mechanical, thermal and electrochemical properties.

15.1.6. Specialised Manufacturing Methods for Single Crystal Materials

These are materials consisting of a single macroscopic grain (i.e. all atoms are fully aligned across the bulk structure with no grain boundaries). Useful in the semiconductor industry (silicon), optoelectronics (graphene, sapphires, InP, CdTe), high-performance electrical conductors (copper, silver), and single crystal turbine blades (SX nickel superalloys). Methods include:

- Czochralski method: nucleation with a small crystal, slowly pulled up and out of the melt.
- Liquid phase electroepitaxy (LPEE): electrochemical deposition onto a substrate.
- Chemical vapour deposition (CVD): used for semiconductors and nanomaterials. Formation of thin films on a hot substrate by chemical reaction e.g.



- Investment casting: used for metals. A helical 'pigtail' is used to cull unwanted crystal growth orientations from a cooling melt.

15.2. Earth Science, Geochemistry and Physical Geography

15.2.1. Properties of the Earth's Atmosphere

Components of the Atmosphere:

The 'dry' atmosphere is (by moles): 78.08% N₂, 20.95% O₂, 0.93% Ar and ~0.04% CO₂ (as of 2022). Water vapour can also be present (up to 3%). Trace gases include Ne, He, CH₄, Kr, Xe, H₂, N₂O, CO, O₃, HCHO, NO_x, NH₃, SO₂, present at ppb levels, and sometimes variable due to environmental factors.

Troposphere (up to 6 - 18 km):

- All common weather occurs in the troposphere, including the three-cell circulation (Section 15.2.2).
- It extends highest over the tropics, and lowest over the poles.
- Hurricanes occupy the whole vertical extent, flattening out at the tropopause.
- The 'planetary boundary layer', where flow is influenced by landscape, extends to ~0.1-2 km.

Stratosphere (up to 50 km):

- The ozone layer is at ~15 - 40 km, which absorbs all high energy radiation (UVC and above).
- Temperature increases towards the stratopause.
- Some military aircraft fly in the stratosphere.
- The Armstrong limit, above which humans require a pressurised suit to survive, is at 19 km.

Mesosphere (up to 85 km):

- Temperature decreases towards the mesopause, cooling to around -143 °C.
- Meteors burn up in the mesosphere. Very bright meteors are called bolides.

Thermosphere (up to 690 km):

- High energy UV causes photoionisation to a plasma state (ionosphere), with temperatures reaching 2000 °C dependent on solar activity.

Exosphere (beyond 690 km and up to ~100,000 km):

- Highly rarefied gas gravitationally bound by Earth's gravity, consisting mainly of hydrogen.

15.2.2. Electromagnetism and Thermodynamics in Geophysics

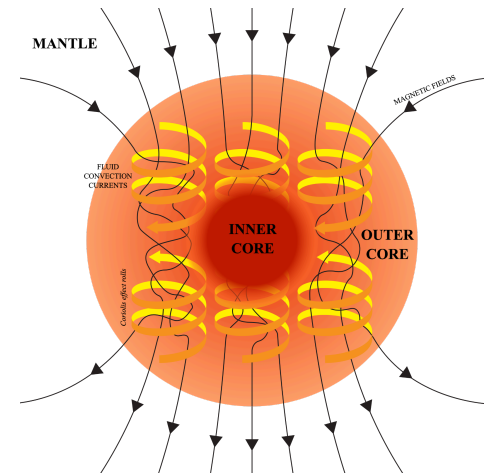
For the theories of electromagnetism, plasma physics and magnetohydrodynamics, see Section 8.5.

Dynamo Theory: a rotating, convecting, electrically-conducting fluid sustains a magnetic field.

The liquid iron-nickel outer core is conductive and is organised into vortices by the Coriolis force (Taylor columns). The initial weak magnetic field at Earth's formation was primordial, but is then amplified and sustained by magnetic induction and thermal convection in the outer core. Only ~1% of the field intensity extends out of the surface of the Earth.

Magnetic field evolution is described by the MHD induction equation: $\partial \mathbf{B} / \partial t = \eta \nabla^2 \mathbf{B} + \nabla \times (\mathbf{v} \times \mathbf{B})$.

To sustain a planetary dynamo, the magnetic Reynolds number must be $Re_m > 100$.



Electromagnetic Phenomena in the Earth's Atmosphere: ionosphere as an RF waveguide

- Auroras occur in geomagnetic storms (from coronal mass ejections), when incoming high-energy electrons accelerated by magnetic reconnection collide with plasma ions, emitting light by fluorescence.
- Radio waves from below are reflected and refracted by the plasma, enabling radio transmission. The natural frequency of standing radio waves due to reflection causes Schumann resonances at ~8 , which can be excited by RF emission from lightning strikes. Oscillations from strong radio waves can cause interference by cross-modulation (Luxembourg effect).
- Residual atmospheric gases are free from turbulence and stratify by molecular mass (turbosphere).
- The Karman line, an arbitrary line designating 'outer space', is at 100 km.
- The International Space Station (ISS) orbits at ~400 km.
- The anacoustic zone, where the atmosphere is rarified enough to prevent audible sound propagation, begins at 160 km (higher frequencies are attenuated first).
- The outer magnetosphere deflects solar wind up to ~60,000 km (magnetopause).

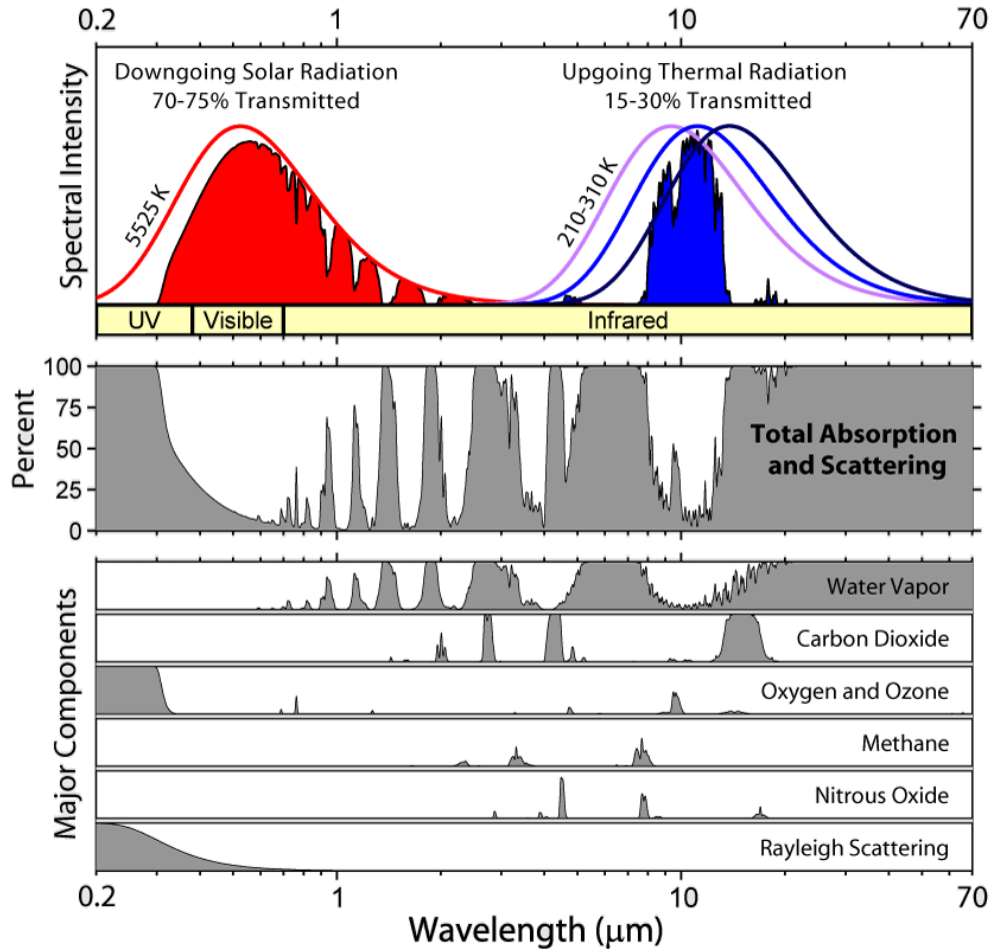
Thermodynamics of the Earth

The Earth as a whole is nearly a closed system. Sources of mass transfer in and out of the Earth include:

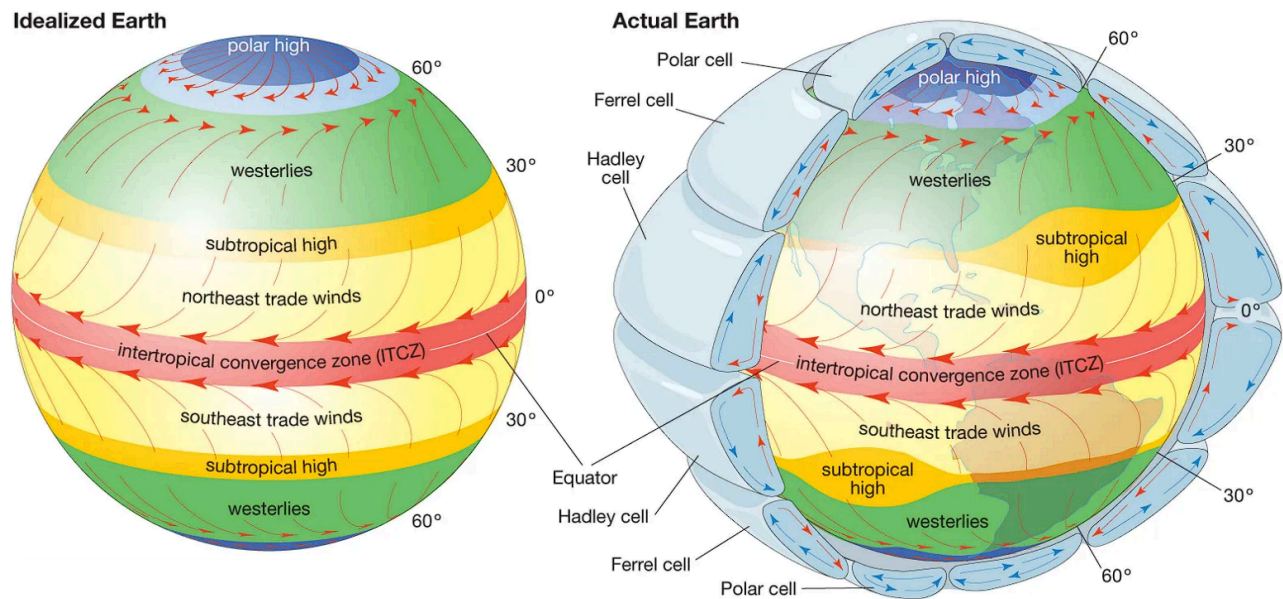
- Atmospheric escape of hydrogen and helium into space (-10^8 kg per year)
- In-falling of micrometeorites and cosmic dust ($+4.5 \times 10^7$ kg per year)
- Launch of spacecraft into space (-6.5×10^4 kg per year)
- Mass defect due to radioactivity (-1.6×10^4 kg per year)

Transmission Spectrum of the Atmosphere to Insolation and Radiant Heat

The Sun emits radiation (insolation) at a near-black body spectrum with $T = 5525\text{ K}$, of which ~75% (mainly wavelengths at UVB and longer) is transmitted to the ground. The Earth's own thermal emission spectrum emits IR radiation which is partially absorbed and reflected back to the surface by greenhouse gases in the atmosphere.



15.2.2. Three-Cell General Atmospheric Circulation Model



Surface winds circulate by natural convection within cells due to variation in temperature.

- **Hadley cells:** between 30° N/S (the Tropic of Cancer and Tropic of Capricorn, respectively). Carries the trade winds from the subtropical highs to the intertropical convergence zone (ITCZ, near-equator).
- **Ferrel cells:** between 30° N/S and 60° N/S. Carries the westerly jet streams from the subtropical highs to the subpolar lows in Rossby waves (high wind shear, large-scale undulations due to Coriolis forces).
- **Polar cells:** between 60° N/S and 90° N/S (the North pole and South pole respectively). Carries the polar easterlies from the poles to the subpolar lows.

15.2.3. Continents and Oceans on Earth



15.2.6. Natural Causes for Changes in Earth's Climate

The Earth's climate depends broadly on its temperature, which is influenced by the amount of solar insolation (radiant power) received from the Sun. Changes in orientation of the Earth relative to the Sun, as well as changes in the output of the Sun, produce natural climate variation.

Milankovitch cycles: changes in the orbit of the Earth over long periods of time. Equatorial regions are more affected by variation in eccentricity/precession. Polar regions are more affected by variation in obliquity.

- Eccentricity: Earth's elliptical orbit varies in eccentricity from 0.005 (low eccentricity → more climate stability) to 0.058 (high eccentricity → less climate stability) with period 100,000 years.
- Obliquity: Earth's axial tilt relative to the ecliptic varies from 22.1° (less tilt → less extreme seasons) to 24.5° (more tilt → more extreme seasons) with period 41,000 years.
- Precession: Earth's axis precesses about the ecliptic plane normal with period 25,700 years.

Solar cycles: changes in the magnetic activity and total radiant power of the Sun over time.

- Sunspots (regions of high coronal temperature and strong magnetic field, associated with more solar flares and coronal mass ejections (CMEs)) appear with fluctuating counts with period 11 years.
- The variation in solar irradiance over a sunspot cycle is small (~0.1%).
- Other (irregular) variations can have a stronger effect on the climate.

Seasons: depends on the part of the Earth facing direct sunlight

- June/Northern Solstice: the Sun is directly overhead on the Tropic of Capricorn (23.3° N).
- December/Southern Solstice: the Sun is directly overhead on the Tropic of Cancer (23.3° S).
- Equinoxes (Spring, Autumn): the Sun is directly overhead on the Equator (0° N).

Above the Arctic Circle (66.3° N), the Sun never sets around the June solstice, and never rises around the December solstice, and vice versa for below the Antarctic Circle (66.3° S).

Eclipses and Tides: depends on the relative locations of the Sun and the Moon.

The Moon is tidally locked with the Earth (same face points towards Earth). It orbits with inclination 5.14° to the ecliptic, with negligible axial tilt and eccentricity 0.05.

- Solar Eclipse: when the moon falls between the Sun and the Earth, obscuring the Sun.
- Lunar Eclipse: when the Earth falls between the Sun and the moon, obscuring the moon.
- High tide: when and where the Moon is directly overhead (neglecting phase lag)
- Low tide: occurs between the points facing and antipodal to the moon (neglecting phase lag)
- Spring tide: more extreme tides in which the Sun and the Moon are aligned (New Moon, Full Moon)
- Neap tide: less extreme tides in which the Sun and the Moon are perpendicular (1st/3rd quarter)

The El Niño Southern Oscillation (ENSO): the most significant global climate fluctuation

Changes to the temperature gradients in the equatorial Pacific Ocean can affect the nominally East-to-West trade winds, causing severe weather in tropical regions e.g. floods in Peru, droughts in India. The oscillations are irregular: the warming phase is called an 'El Niño year' and the cooling phase is called a 'La Niña year'.

15.2.7. Properties of the Earth's Crust

Elemental Composition of the Crust

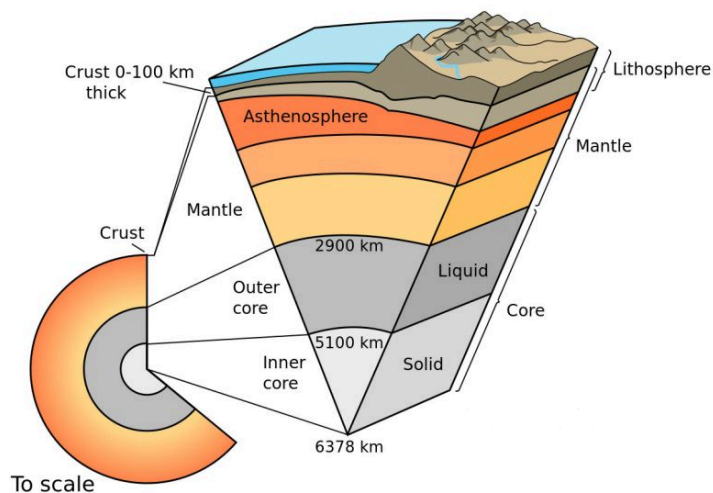
Component	wt. %
Oxygen, O	46.60%
Silicon, Si	27.72%
Aluminium, Al	8.13%
Iron, Fe	5.00%

Component	wt. %
Calcium, Ca	3.63%
Sodium, Na	2.83%
Potassium, K	2.59%
Magnesium, Mg	2.09%

The mantle is mainly peridotite (such as olivine, MgFeSiO_4)

The core is mainly iron (85.5%) as well as nickel.

Layers of the Earth



Oceanic crust: thin, high-density basalt

Continental crust: thick, low-density granite rocks

Mohorovičić discontinuity (Moho): separates the oceanic crust from the asthenosphere near an oceanic ridge.

Lithosphere: the crust and the uppermost solid mantle

Asthenosphere: the hot fluid mantle in which convection currents flow

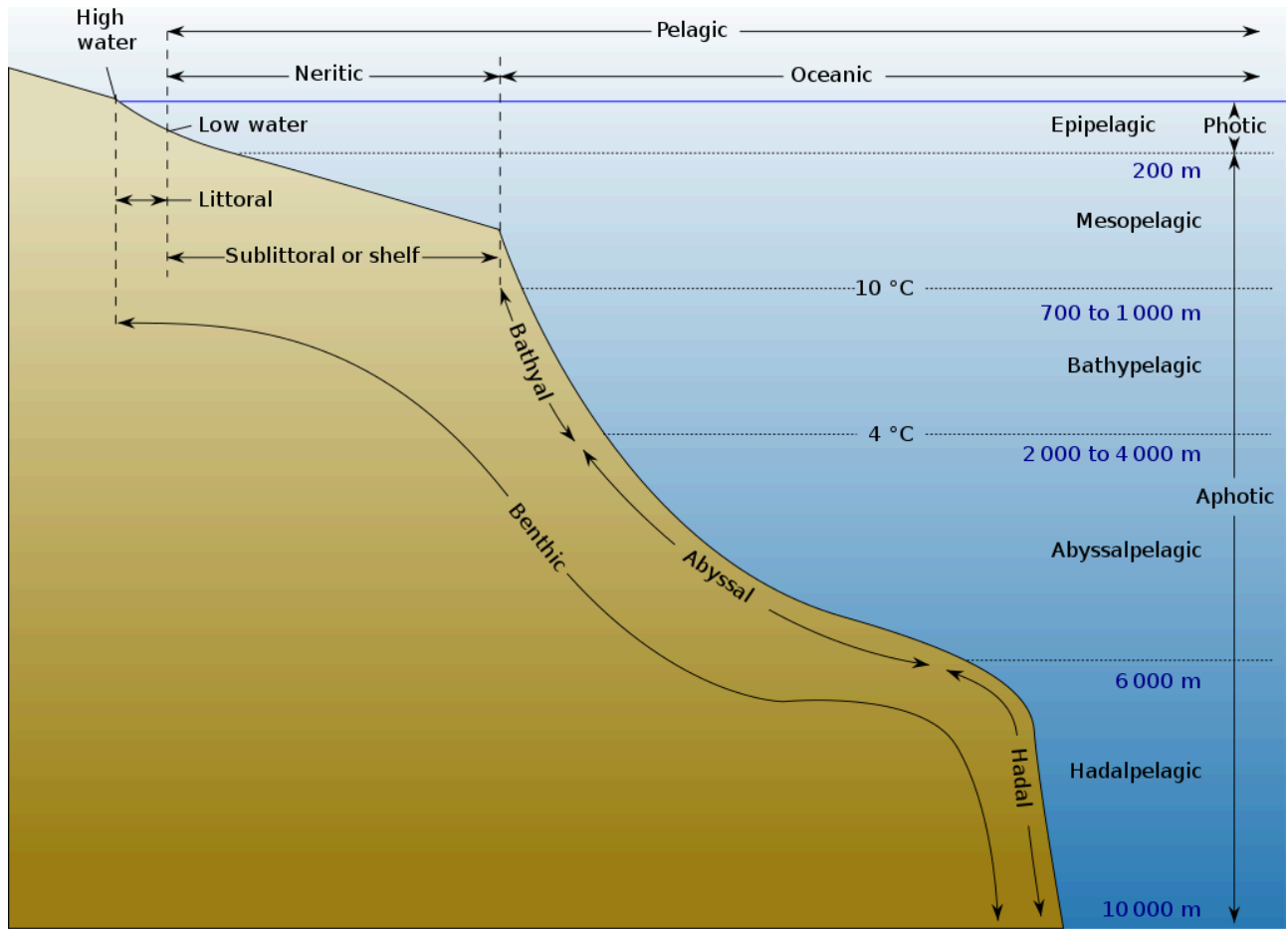
Mesosphere: the rigid lower mantle, made of ultramafic peridotites

D" layer: a heterogeneous layer between the lower mantle and outer core with a large temperature gradient.

Outer core: liquid iron and nickel at $T \sim 5500 \text{ }^\circ\text{C}$ and $p \sim 3 \times 10^8 \text{ atm} = 30 \text{ TPa}$.

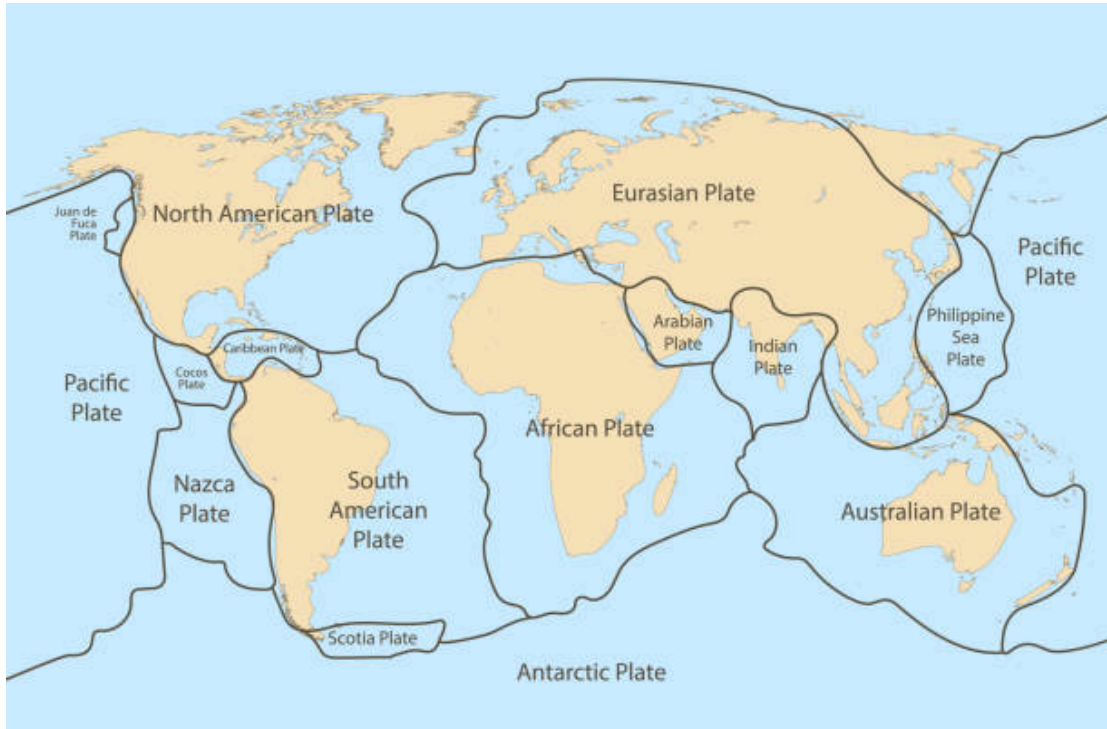
Inner core: solid iron and nickel, rotating faster than the outer core (superrotation). The motion of molten metal is equivalent to an electric current, which generates a circulating magnetic field (magnetohydrodynamics). This creates a dynamo effect by driving a current through the outer core, which is thought to create the Earth's magnetic field (the dynamo theory).

15.2.9. Layers of the Ocean and Oceanic Crust



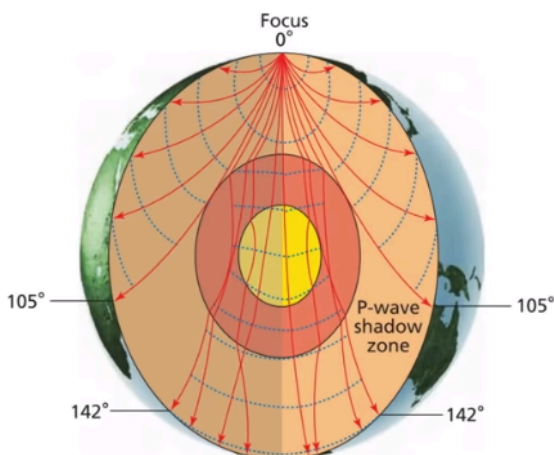
15.2.10. Current Boundary Locations of the Earth’s Tectonic Plates

Tectonic plates drift on the mantle over time, colliding and causing various geological activity (earthquakes, tsunamis, volcanoes, mountains) at and around their boundaries.

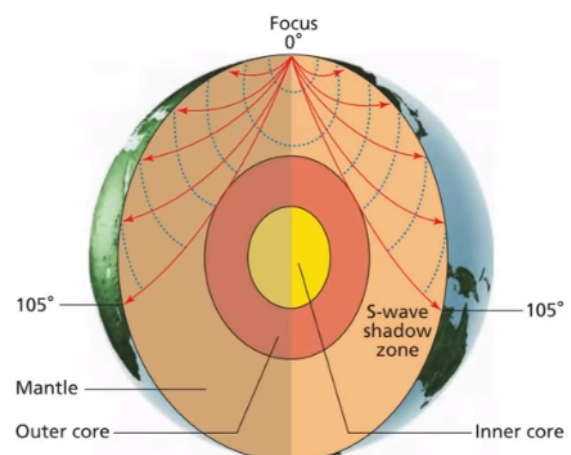


15.2.11. Trajectories of Primary (P) and Secondary (S) Waves Through Earth

During an earthquake, P-waves (faster, longitudinal) and S-waves (slower, transverse) propagate from the focus (hypocentre).



P-waves: refracted at phase boundaries.

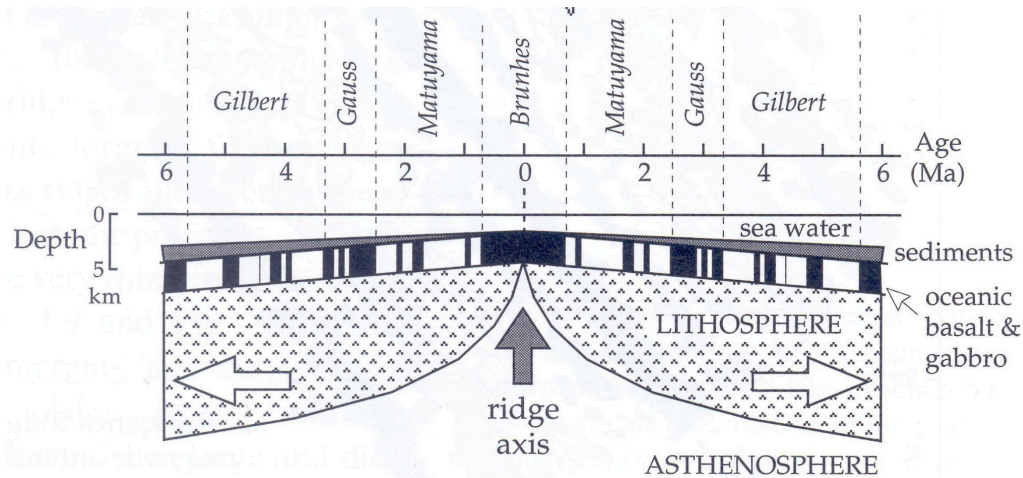


S-waves: absorbed (blocked) by liquid.

15.2.12. Evidence for Tectonic Theory: Vine-Matthews Hypothesis and The Wilson Cycle

Vine-Matthews Hypothesis: at a mid-oceanic ridge, the rate of seafloor spreading is linked to geomagnetic reversals due to magnetic striping. This is observed at the mid-Atlantic ridge.

The most recent chrons are named Brunhes, Matuyama, Gauss, Gilbert...



Wilson Cycle: volcanism on plates induced by stationary vertical 'hotspots' (mantle plumes) leads to the formation of chains of volcanoes (a seamount) as the plate moves, which are then gradually eroded.

15.2.13. Geological Classification of Rocks

Rocks within the Earth can be classified as:

- **Igneous** rock (e.g. granite, basalt, obsidian): formed from crystallisation of magma.
- **Sedimentary** rock (e.g. sandstone, limestone, shale): formed from lithification of sediment by compaction and cementing.
- **Metamorphic** rock (e.g. gneiss, schist, slate): formed by metamorphism of sedimentary or igneous rocks under high pressure and temperature.

15.2.14. Biomes and The Characteristics of Deserts and Rainforests

Biomes are described by the unique interdependence of climate, water (or permafrost in the case of tundra and polar regions), soils, plants, animals and the actions of people who live within them.

Desert environments:

- Causes of desertification: climate change, population growth, removal of fuel wood, overgrazing, over-cultivation and soil erosion.
- Strategies used to reduce the risk of desertification: water and soil management, tree planting and use of appropriate technology.

Rainforest environments:

- Causes of deforestation: subsistence and commercial farming, logging, road building, mineral extraction, energy development, settlement, population growth.
- Impacts of deforestation – economic development, soil erosion, contribution to climate change.

15.2.15. Protection of Natural Landscapes

Landscapes may be protected by:

- Hard engineering – (coastal) sea walls, rock armour, gabions and groynes; (rivers) dams and reservoirs, straightening, embankments, flood relief channels.
- Soft engineering – (coastal) beach nourishment and reprofiling, dune regeneration, coastal realignment (managed retreat); (rivers) flood warnings and preparation, flood plain zoning, planting trees and river restoration.

15.2.16. Transport Phenomena in Coastal, River, Glacial and Urban Environments**Coastal processes** and landforms:

- Weathering – mechanical, chemical.
- Mass movement – sliding, slumping and rock falls.
- Erosion – hydraulic power, abrasion and attrition. Forms landscapes such as headlands and bays, cliffs and wave cut platforms, caves, arches, stacks and stumps.
- Transportation – longshore drift.
- Deposition – forms landscapes such as beaches, sand dunes, spits and bars.

Fluvial processes and landforms:

- erosion – hydraulic action, abrasion, attrition, solution, vertical and lateral erosion. Forms landscapes such as V-shaped valleys, interlocking spurs, waterfalls, gorges, meanders and ox-bow lakes.
- transportation – traction (rolling), saltation (bouncing), suspension and solution.
- deposition – forms landscapes such as levées, flood plains and estuaries.

Glacial processes and landforms:

- freeze-thaw weathering
- erosion – abrasion and plucking. Forms landscapes such as corries, arêtes, pyramidal peaks, truncated spurs, glacial troughs, ribbon lakes and hanging valleys.
- movement and transportation – rotational slip and bulldozing.
- deposition – till and outwash. Forms landscapes such as erratics, drumlins, and types of moraine (lateral, ground, terminal, recessional, medial, supraglacial).

Urban environments typically do not permit water infiltration due to the low permeability of paving materials e.g. concrete / tarmac. Instead, surface runoff occurs. Freeze-thaw cycling may lead to erosive damage e.g. potholes. Sustainable drainage systems (SuDS) may be used to avoid excess runoff. For information on geotechnical engineering of water and drainage systems, see Section 6.5.3.

Changes to natural environments can have a significant impact on the local wildlife. Over longer periods of time, environmental changes can lead to speciation (evolution by diversification).

15.2.17. Natural Hazards

Natural hazards and extreme adverse weather events can cause extensive damage through mass transport in a variety of ways.

- **Volcanic eruptions:** upthrust of magma through a vent and surface flows of lava. Volcanic ash (tephra; particulate matter e.g. PM10) is also released into the atmosphere which can cause widespread pollution, acid rain and cooling due to albedo decrease. Especially explosive eruptions can cause pyroclastic flows (hot fast gas streams) and/or lahars (dense mudslides) down the volcano cone.

Volcanic activity often occurs near tectonic plate subduction zones, or above mantle hotspots.

Volcanoes can be classed as shield volcanoes (gentle slope, small crater) or composite cone volcanoes (steep slope, large crater (caldera), viscous lava).

- **Earthquakes:** rapid shaking or vibration (tremors) of land due to tectonic plates shearing on a fault line. If an earthquake occurs near the ocean floor, the impulse may trigger formation of large waves which accumulate and rush towards shores (tsunamis).
- **Landslides:** mass movement of land down a slope, such as lahars (mud down a volcano), avalanches (snow down a mountain).
- **Geysers:** a hot spring with a high-pressure reservoir. Violently discharges boiling water and steam from fissures in the surface of rocks. Usually found near volcanoes, with heat provided by magma. Geysers do not typically cause widespread damage, but can harm individuals local to them.
- **Tropical Storms:** high-speed circular winds forming over warm oceans which spin due to Coriolis forces and migrate due to the global wind currents (usually the trade winds). Named cyclones (South Pacific/Indian ocean), hurricanes (Atlantic/north-eastern Pacific ocean) or typhoons (north-western Pacific ocean). Summer (wet) monsoons are larger-scale seasonal wind patterns accompanied by persistent torrential rain.
- **Extreme weather:** e.g. drought (extended periods of dryness and low cloud cover, common in arid climates), flash floods (powerful water flows, often due to torrential rain on a large drainage basin), sandstorms (transport of sand in wind currents in deserts), blizzards (transport of precipitation (sleet), ice (hail) and snow in wind currents in cold climates). There has been a recent increase in adverse weather events, with the evidence pointing to global warming as the main driving factor, as more energy in the climate allows for more chaotic weather patterns.

15.2.18. Water Chemistry

Natural water sources contain a range of ions: Ca^{2+} , Mg^{2+} , Na^+ , K^+ , HCO_3^- , CO_3^{2-} , Cl^- , SO_4^{2-} , PO_4^{3-} , NO_3^- . These can be influenced by local geology, soil, hydrology and nearby human activity.

Concentration

Normality of an ion [milliequivalents, mEq] = $\frac{\text{concentration [mg / L]}}{\text{ion molecular mass [mol / g]}} \times \text{ion charge}$

Parts per million [ppm] = concentration [mg / L] (since density of water $\approx 10^6$ mg / L)

Alkalinity and Corrosivity: buffering capacity of water against acids

Water alkalinity is due to CO_3^{2-} , HCO_3^- and OH^- ions. Water acidity is due to dissolved CO_2 (carbonic acid equilibrium).

- “P alkalinity”: titrate using phenolphthalein.
- “M alkalinity”: titrate using methyl orange.
- “T alkalinity”: total alkalinity. Measured in ppm.

Carbonate scale (e.g. limescale, CaCO_3) can form on surfaces at high pH. Corrosion (weathering) can occur at low pH.

Langelier saturation index (LSI): the difference between the water pH and the pH at CaCO_3 saturation. $\text{LSI} > 0 \rightarrow$ scale-forming. $\text{LSI} < 0 \rightarrow$ corrosive. $\text{LSI} = 0 \rightarrow$ balanced.

Water Fluoridation and Chlorination: sanitation of bodies of water used by people.

Fluoride (F^-) is supplied to public drinking water sources as hexafluorosilicic acid (H_2SiF_6 , $[\text{F}^-] \sim 1$ ppm). It helps to combat tooth decay by forming fluorapatite ($\text{Ca}_{10}(\text{PO}_4)_6\text{F}_2$) in the enamel, which dissolves less readily than the naturally present hydroxyapatite ($\text{Ca}_{10}(\text{PO}_4)_6(\text{OH})_2$). This baseline intake of fluoride is helped by brushing teeth with fluoride toothpaste (contains NaF , $[\text{F}^-] \sim 1000$ ppm).

Chlorine (Cl_2) can be added to water as an antibacterial agent, typically in swimming pools. However, due to its equilibrium with hypochlorous acid (HClO), its effectiveness is strongly dependent on pH. It is typically supplied in solid form (calcium hypochlorite, $\text{Ca}(\text{ClO})_2$). Stabilisers such as cyanuric acid ($(\text{CONH})_3$) can be added, which also protects the chlorine from UV degradation by converting it to trichloroisocyanuric acid.

Water bromination is a more stable and less irritating alternative to chlorination.

15.3. Reactions of Inorganic Compounds

15.3.1. Reactions Involving Group 1 Metals

Reactions of pure Group 1 metals: (M = {Li, Na, K, Rb, Cs})

- $M(s) + H_2O(l) \rightarrow MOH(aq) + \frac{1}{2} H_2(g)$ hydroxide formation
- $M(s) + H_2(g) \rightarrow MH(s)$ hydride formation
- $M(s) + \frac{1}{2} S(s) \rightarrow \frac{1}{2} M_2S(s)$ sulfide formation
- $M(s) + \frac{1}{2} X_2 \rightarrow MX(s)$ halide: X = {F₂, Cl₂, Br₂, I₂}
- $M(s) + NH_3(g) \rightarrow MNH_2(s) + \frac{1}{2} H_2(g)$ amide formation
- $M(s) + 2 NH_3(l) \rightarrow [M(NH_3)]^+ + e^-(NH_3)$ solubility in liquid ammonia

Formation of oxides, peroxides and superoxides:

- $Li(s) + \frac{1}{4} O_2(g) \rightarrow \frac{1}{2} Li_2O(s)$ lithium oxide
- $Na(s) + \frac{1}{2} O_2(g) \rightarrow \frac{1}{2} Na_2O_2(s)$ sodium peroxide
- $K(s) + O_2(g) \rightarrow KO_2(s)$ also {Rb, Cs} superoxide

Reactions of Group 1 metal hydroxides, monoxides, peroxides and superoxides:

- $MOH(aq) + NH_4Cl(s) \rightarrow NH_3(g) + MCl(aq) + H_2O(l)$
- $M_2O(s) + H_2O(l) \rightarrow MOH(aq)$
- $M_2O_2(s) + 2 H_2O(l) \rightarrow 2 MOH(aq) + H_2O_2(l)$
- $M_2O_2(aq) + 2 CO_2(g) \rightarrow M_2CO_3(aq) + O_2(g)$

Acid-base reactions of metal hydroxides, oxides and carbonates:

- $MOH(aq) + H^+(aq) \rightarrow M^+(aq) + H_2O(l)$
- $MOH(aq) + \frac{1}{2} CO_2(g) \rightarrow \frac{1}{2} M_2CO_3(s) + \frac{1}{2} H_2O(l)$ carbonate formation
- $M_2O_2(s) + H_2SO_4(aq) \rightarrow M_2SO_4(aq) + H_2O_2(l)$ at ~ 0 °C
- $M_2CO_3(aq) + HNO_3(aq) \rightarrow 2 MNO_3(aq) + CO_2(g) + H_2O(l)$

Thermal decomposition of metal oxyanions:

- $M_2CO_3(s) \rightarrow M_2O(s) + CO_2(g)$
- $MHCO_3(s) \rightarrow M_2CO_3(s) + H_2O(g) + CO_2(g)$
- $LiNO_3(s) \rightarrow \frac{1}{2} Li_2O(s) + NO_2(g) + \frac{1}{4} O_2(g)$
- $NaNO_3(s) \rightarrow NaNO_2(s) + \frac{1}{2} O_2(g)$ other nitrates are stable
- $Li_2SO_4(s) \rightarrow Li_2O(s) + SO_2(g) + \frac{1}{2} O_2(g)$ other sulfates are stable
- $MClO(s) \rightarrow MCl(s) + \frac{1}{2} O_2(g)$
- $LiClO_3(s) \rightarrow LiCl(s) + \frac{3}{2} O_2(g)$ all other chlorites are stable

15.3.2. Reactions of Group 2 Metals

Reactions of pure Group 2 metals: (M = {Be, Mg, Ca, Sr, Ba})

- $M(s) + 2 H_2O(l) \rightarrow M(OH)_2(aq) + H_2(g)$ except Mg (forms oxide)
- $M(s) + \frac{1}{2} X_2 \rightarrow MX(s)$ halide: X = {F₂, Cl₂, Br₂, I₂}
- $M(s) + 2 NH_3(g) \rightarrow M(NH_2)_2(s) + H_2(g)$ amide formation
- $M(s) + 2 NH_3(l) \rightarrow [M(NH_3)]^+ + e^-(NH_3)$ solubility in liquid ammonia

Formation of oxides and peroxides:

- $Be(s) + \frac{1}{2} O_2(g) \rightarrow BeO(s)$ {Be, Mg, Ca} oxide
- $Sr(s) + O_2(g) \rightarrow SrO_2(s)$ {Sr, Ba} peroxide
- $Mg(s) + H_2O(l) \rightarrow MgO(s) + H_2O(l)$

Reactions of Group 2 metal oxides, hydroxides and sulfates:

- $MO(s) + H_2O(l) \rightarrow M(OH)_2$ {Be, Mg}(OH)₂ are insoluble
- $M(OH)_2 + \frac{1}{2} NH_4Cl(aq) \rightarrow MCl_2(aq) + 2 NH_4OH(aq)$
- $MSO_4(aq) + NaOH(aq) \rightarrow M(OH)_2 + Na_2SO_4(aq)$ {Sr, Ba}SO₄ are insoluble

Acid-base reactions of metal hydroxides, oxides and carbonates:

- $M(OH)_2(aq) + 2 H^+(aq) \rightarrow M^{2+}(aq) + 2 H_2O(l)$
- $MO(aq) + CO_2(g) \rightarrow MCO_3(aq)$ using SiO₂ gives MSiO₃ (silicate)
- $M_2CO_3(aq) + HNO_3(aq) \rightarrow 2 MNO_3(aq) + CO_2(g) + H_2O(l)$

Thermal decomposition of carbonates:

- $MCO_3(s) \rightarrow MO(s) + CO_2(g)$ stability increases going down the group

15.3.3. Reactions Involving Boron

Formation of boron:

- $\text{Na}_2\text{B}_4\text{O}_7$ (borax) + 2 HCl + 5 H₂O → 4 H₃BO₃ (orthoboric acid) + 2 NaCl;
2 H₃BO₃ → B₂O₃ (boric oxide) + 3 H₂O;
B₂O₃ + 3 Mg → 2 B + 3 MgO
- KBF₄ (potassium tetrafluoroborate) + 3 K → 4 KF + B

Reactions of boron:

- 4 B + 3 O₂ → 2 B₂O₃
- 2 B + N₂ → 2 BN (boron nitride)
- 2 B + 2 NaOH + 2 H₂O → 2 NaBO₂ (sodium metaborate) + 3 H₂
- 2 B + 3 H₂SO₄ → 2 H₃BO₃ (orthoboric acid) + 3 SO₂
- 2 B + 3 H₂S → B₂S₃ (boron sulfide) + 3 H₂

Formation and reactions of B₂H₆ (diborane):

(contains 3c-2e bonds)

- 2 BF₃ + 6 LiH → B₂H₆ + 6 LiF
- Mg₃B₂ (magnesium boride) + 6 HCl (aq) → 3 MgCl₂ + B₂H₆
- B₂H₆ + 3 H₂O → H₃BO₃ + 3 H₂
- B₂H₆ + 3 O₂ → B₂O₃ + 3 H₂O
- 3 B₂H₆ + 6 NH₃ → 2 B₃N₃H₆ (borazine / borazole) + 12 H₂ (isoelectronic to benzene)
- B₂H₆ + 2 NaH → 2 NaBH₄ (sodium borohydride)

Reactions of boron compounds:

- 2 B₂O₃ + 7 C → B₄C (boron carbide) + 6 CO (electric arc furnace)
- B₂O₃ + 2 NH₃ → 2 BN (boron nitride) + 3 H₂O (forms amorphous BN)
- BN + Li₃N → Li₃BN₂ (lithium nitridoborate)
- 2 BCl₃ + 2 Hg → Hg₂Cl₂ + B₂Cl₄
- 6 NaBH₄ + 3 (NH₄)₂SO₄ → 2 B₃N₃H₆ + 3 Na₂SO₄ + 18 H₂ (intermediate: B₃N₃H₃Cl₃)

Reactions of orthoboric acid and borax:

- 2 H₃BO₃ → B₂O₃ + 3 H₂O (thermal decomposition)
- H₃BO₃ + H₂O ⇌ B(OH)₄⁻ + H⁺
- Na₂B₄O₇ + H₂SO₄ + 5 H₂O → Na₂SO₄ + 4 H₃BO₃
- Na₂B₄O₇ → NaBO₂ + B₂O₃

15.3.4. Reactions Involving Carbon

For combustion reactions, see Section 15.3.6.

Industrial reactions of carbon compounds: (syngas: CO + H₂ mixture)

- $\text{CO}_2 + 2 \text{H}_2 \rightarrow \text{C (graphite)} + 2 \text{H}_2\text{O}$ (Bosch reaction; Fe catalyst, 600 °C)
- $\text{CO} + \text{H}_2\text{O} \rightleftharpoons \text{CO}_2 + \text{H}_2$ (Water-gas shift reaction (WGSR))
- $\text{CH}_4 + \text{H}_2\text{O} \rightleftharpoons \text{CO} + 3 \text{H}_2$ (Steam-methane reforming (SMR))
- $n \text{CO} + (2n + 1) \text{H}_2 \rightarrow \text{C}_n\text{H}_{2n+2} + n \text{H}_2\text{O}$ (Fischer-Tropsch synthesis (FTS))
- $\text{CH}_4 + \text{CO}_2 \rightarrow 2 \text{CO} + 2 \text{H}_2$ (dry reforming)

Hydration of inorganic carbides forms organic gases:

- $\text{CaC}_2 + 2 \text{H}_2\text{O} \rightarrow \text{C}_2\text{H}_2 \text{ (acetylene)} + \text{Ca(OH)}_2$ (also Mg₂C)
- $\text{BeC}_2 + 4 \text{H}_2\text{O} \rightarrow \text{CH}_4 \text{ (methane)} + 2 \text{Be(OH)}_2$ (very slow)
- $\text{SiC} + 2 \text{H}_2\text{O} \rightarrow \text{CH}_4 + \text{SiO}_2$
- $\text{Al}_4\text{C}_3 + 12 \text{H}_2\text{O} \rightarrow 3 \text{CH}_4 + 4 \text{Al(OH)}_3$
- $\text{Mg}_2\text{C}_3 \text{ (magnesium allylenide)} + 4 \text{H}_2\text{O} \rightarrow \text{C}_3\text{H}_4 \text{ (propyne)} + \text{Mg(OH)}_2$

Other reactions of metal carbides:

- $\text{CaC}_2 + \text{N}_2 \rightarrow \text{CaNCN (calcium cyanamide; nitrolime)} + \text{C}$ (Frank-Caro process)
- $\text{BaC}_2 + \text{N}_2 \rightarrow \text{Ba(CN)}_2 \text{ (barium cyanide)}$

15.3.5. Reactions Involving Nitrogen

Formation of nitrogen:

- $\text{NH}_4\text{Cl (aq)} + \text{NaNO}_2 \text{ (aq)} \rightarrow \text{N}_2 + \text{H}_2\text{O} + \text{NaCl}$
- $(\text{NH}_4)_2\text{Cr}_2\text{O}_7$ (ammonium dichromate) $\rightarrow \text{N}_2 + 4 \text{H}_2\text{O} + \text{Cr}_2\text{O}_3$ (thermal decomp.)
- $4 \text{NH}_3 + 6 \text{NO} \rightarrow 5 \text{N}_2 + 6 \text{H}_2\text{O}$
- $\text{Ba(N}_3)_2$ (barium azide) $\rightarrow \text{Ba} + 3 \text{N}_2$
- NH_2NH_2 (hydrazine) + $2 \text{H}_2\text{O}_2$ (hydrogen peroxide) $\rightarrow \text{N}_2 + 4 \text{H}_2\text{O}$

Formation of nitrogen oxides:

- $4 \text{NH}_3 + 5 \text{O}_2 \rightarrow 4 \text{NO}$ (nitric oxide) + $6 \text{H}_2\text{O}$
- $2 \text{NO} + \text{O}_2 \rightarrow 2 \text{NO}_2$ (nitrogen dioxide)
- $2 \text{NO}_2 \rightleftharpoons \text{N}_2\text{O}_4$ (dinitrogen tetroxide) (dimerisation)
- $3 \text{NO}_2 + \text{H}_2\text{O} \rightarrow 2 \text{HNO}_3 + \text{NO}$ (Ostwald process, V_2O_5 cat.)
- $2 \text{NaNO}_2 + 2 \text{FeSO}_4 + 3 \text{H}_2\text{SO}_4 \rightarrow \text{Fe}_2(\text{SO}_4)_3 + 2 \text{NaHSO}_4 + 2 \text{H}_2\text{O} + 2 \text{NO}$
- $\text{NH}_4\text{NO}_3 \rightarrow \text{N}_2\text{O}$ (nitrous oxide) + $2 \text{H}_2\text{O}$
- $\text{NO} + \text{NO}_2 \rightarrow \text{N}_2\text{O}_3$

Reactions of nitric acid:

- $\text{HNO}_3 + 2 \text{H}_2\text{SO}_4 \rightarrow \text{NO}_2^+$ (nitronium ion) + $\text{H}_3\text{O}^+ + 2 \text{HSO}_4^-$
- $8 \text{HNO}_3 + 3 \text{Cu} \rightarrow 3 \text{Cu}(\text{NO}_3)_2 + 2 \text{NO} + 4 \text{H}_2\text{O}$
- $\text{HNO}_3 + 3 \text{HCl} \rightarrow \text{NOCl} + \text{Cl}_2 + 2 \text{H}_2\text{O}$ (aqua regia formation)
- $\text{Au (s)} + \text{HNO}_3 + 4 \text{HCl} \rightarrow \text{HAuCl}_4$ (chloroauric acid) + $\text{NO} + \text{H}_2\text{O}$

Formation and reactions of ammonia and ammonium compounds:

- $\text{N}_2 + 3 \text{H}_2 \rightarrow 2 \text{NH}_3$ (Haber-Bosch process)
- $\text{NH}_4\text{Cl} + \text{NaOH} \rightarrow \text{NH}_3 + \text{NaCl} + \text{H}_2\text{O}$
- $8 \text{NH}_3 + 3 \text{Cl}_2 \rightarrow 6 \text{NH}_4\text{Cl} + \text{N}_2$ (excess Cl_2 forms NCl_3 and HCl instead)
- $\text{NH}_3 \text{ (aq)} + \text{NaClO} \rightarrow \text{NH}_2\text{Cl}$ (chloramine) + $\text{NaCl} + \text{H}_2\text{O}$ (also forms NHCl_2 , NCl_3)

Formation and reaction of metal nitrides, azides and amides:

- $3 \text{Mg} + \text{N}_2 \rightarrow \text{Mg}_3\text{N}_2$ (magnesium nitride)
- $\text{Mg}_3\text{N}_2 + 6 \text{H}_2\text{O} \rightarrow 3 \text{Mg(OH)}_2 + 2 \text{NH}_3$
- $2 \text{Na} + 2 \text{NH}_3 \text{ (l)} \rightarrow 2 \text{NaNH}_2$ (sodium amide) + H_2
- $2 \text{NaNH}_2 + \text{N}_2\text{O} \rightarrow \text{NaN}_3$ (sodium azide) + $\text{NaOH} + \text{NH}_3$
- $\text{NaNO}_3 + 3 \text{NaNH}_2 \rightarrow \text{NaN}_3 + 3 \text{NaOH} + \text{NH}_3$
- $\text{NaN}_3 + \text{HCl} \rightarrow \text{HN}_3$ (hydrazoic acid) + NaCl
- $2 \text{NaN}_3 + 2 \text{HNO}_2$ (nitrous acid) $\rightarrow 3 \text{N}_2 + 2 \text{NO} + 2 \text{NaOH}$

15.3.6. Reactions Involving Oxygen

General hydrocarbon combustion reactions:

- $C_xH_y + \left(x + \frac{y}{4}\right)O_2 \rightarrow x CO_2 + \frac{y}{2} H_2O$ (complete)
- $C_xH_y + \left(x + \frac{y}{4} - a - \frac{b}{2}\right)O_2 \rightarrow a C + b CO + (x - a - b) CO_2 + \frac{y}{2} H_2O$ (incomplete)
(undetermined coefficients satisfy $a \geq 0, b \geq 0, 0 \leq a + b \leq x$)

Aliphatic hydrocarbon C_xH_y has $x + 1 - \frac{y}{2}$ (C=C) bonds, $\frac{y}{2} - 2$ (C-C) bonds and y (C-H) bonds.

The maximum enthalpy of combustion is achieved for complete combustion ($a = b = 0$).

Reactions of oxygen:

- $H_2 + O_2 \rightarrow H_2O$ (combustion of hydrogen forms water)
- $2 SbF_5 (l) + 2 O_2 (g) + F_2 (g) \rightarrow 2 [O_2]^+[SbF_6]^-$ (oxidation by strong Lewis acid)

15.3.7. Reactions Involving Aluminium

Reactions of aluminium:

- $4 Al + 3 O_2 \rightarrow 2 Al_2O_3$ (nanoscopic oxide surface layer impermeable to O_2)
- $2 Al + 3 Cl_2 \rightarrow 2 AlCl_3$ (forms Al_2Cl_6 dimers only in the liquid/vapour state)
- $2 Al + 3 Br_2 \rightarrow Al_2Br_6$ (dimer is stable at lower temperatures)
- $2 Al + 3 H_2SO_4 \rightarrow Al_2(SO_4)_3 + 3 H_2$
- $2 Al + 2 NaOH + 6 H_2O \rightarrow 2 NaAl(OH)_4$ (sodium aluminate hydrate) + $3 H_2$
- $Al + Fe_2O_3 \rightarrow Al_2O_3 + Fe$ (thermite reaction)

Reactions of aluminium oxides:

- $Al_2O_3 + 6 HCl \rightarrow 2 AlCl_3 + 3 H_2O$
- $Al_2O_3 + 6 NaOH \rightarrow 2 NaAlO_2$ (sodium aluminate) + H_2O

15.3.7. Reactions Involving Silicon

Formation of silicon:

- $\text{SiO}_2 + 2 \text{C} \rightarrow \text{Si} + 2 \text{CO}$
- $\text{SiC} + \text{SiO}_2 \rightarrow \text{Si (s)} + \text{SiO (g)} + \text{CO (g)}$ (ultrapure silicon for semiconductors)
- $\text{SiO}_2 + 2 \text{Mg} \rightarrow \text{MgO} + \text{Si}$

Reactions of silicon:

- $\text{Si} + \text{O}_2 \rightarrow \text{SiO}_2$
- $\text{Si} + 2 \text{F}_2 \rightarrow \text{SiF}_4 \text{ (g)}$
- $\text{Si} + 2 \text{Cl}_2 \rightarrow \text{SiCl}_4 \text{ (l)}$
- $\text{Si} + 2 \text{Mg} \rightarrow \text{Mg}_2\text{Si}$ (magnesium silicide) (n-type semiconductor)

Reactions of silicon compounds:

- $\text{SiCl}_4 + 2 \text{H}_2\text{O} \rightarrow \text{SiO}_2 + 4 \text{HCl}$
- $\text{SiO}_2 + 6 \text{HF} \rightarrow \text{H}_2\text{SiF}_6$ (hexafluorosilicic acid) (used in water fluoridation)
- $4 \text{SiH}_4 \text{ (silane) (g)} + 3 \text{O}_2 \rightarrow 2 \text{Si}_2\text{O}_3 + 6 \text{H}_2\text{O}$

Reactions of metal silicides:

- $\text{Mg}_2\text{Si} + 4 \text{HCl (aq)} \rightarrow 2 \text{MgCl}_2 \text{ (aq)} + \text{SiH}_4 \text{ (g)}$ (thermally decomposes to $\text{Si} + 2 \text{H}_2$)

15.3.8. Reactions Involving Phosphorus

Formation of phosphorus (white phosphorus):

- $2 \text{Ca}_3(\text{PO}_4)_2 + 10 \text{C} + 6 \text{SiO}_2 \rightarrow 6 \text{CaSiO}_3 + 10 \text{CO} + \text{P}_4$ (white phosphorus)

Allotrope formation of phosphorus:

- white P (tetrahedral P_4 molecules) \rightarrow red P (polymeric P_4 units) (heating in CO_2)
- red P \rightarrow α -black P (amorphous) (heating in insulated tube)
- white P \rightarrow β -black P (graphite-like P_6 units) (heat at high pressure)

Reactions of phosphorus:

- $\text{P}_4 + 5 \text{O}_2 \rightarrow \text{P}_4\text{O}_{10}$ (yellow phosphorus: oxide impurities)
- $\text{P}_4 + 10 \text{Cl}_2 \rightarrow 4 \text{PCl}_5$ (s) (excess, otherwise forms PCl_3)
- $\text{P}_4 + 3 \text{NaOH} + 3 \text{H}_2\text{O} \rightarrow \text{PH}_3$ (phosphine) + $3 \text{NaH}_2\text{PO}_2$
- $\text{P}_4 + 20 \text{HNO}_3 \rightarrow 4 \text{H}_3\text{PO}_4 + 20 \text{NO}_2 + 4 \text{H}_2\text{O}$
- $\text{P} + 5 \text{HNO}_3 \rightarrow \text{H}_3\text{PO}_4 + 5 \text{NO}_2 + \text{H}_2\text{O}$

Formation of metal phosphides:

- P (white) + $3 \text{Na} \rightarrow \text{Na}_3\text{P}$
- P_4 (white) + $3 \text{CuSO}_4 + 6 \text{H}_2\text{O} \rightarrow \text{Cu}_3\text{P}_2 + 2 \text{H}_3\text{PO}_3 + 3 \text{H}_2\text{SO}_4$
- $\text{Ca}_3(\text{PO}_4)_2 + 8 \text{C} \rightarrow \text{Ca}_3\text{P}_2 + 8 \text{CO}$ (carbothermal reduction)

Reactions of metal phosphides:

- $\text{Na}_3\text{P} + 3 \text{H}_2\text{O} \rightarrow 3 \text{NaOH} + \text{PH}_3$ (also Li_3P)
- $\text{Cu}_3\text{P}_2 + 5 \text{CuSO}_4 + 8 \text{H}_2\text{O} \rightarrow 8 \text{Cu} + 5 \text{H}_2\text{SO}_4 + 2 \text{H}_3\text{PO}_4$

Reactions of phosphorus oxides:

- $\text{P}_4\text{O}_6 + 6 \text{H}_2\text{O} \rightarrow 4 \text{H}_3\text{PO}_3$ (phosphonic acid)
- $\text{P}_4\text{O}_{10} + 6 \text{H}_2\text{O} \rightarrow 4 \text{H}_3\text{PO}_4$ (phosphoric acid)
- $\text{P}_4\text{O}_{10} + 4 \text{HNO}_3 \rightarrow 2 \text{N}_2\text{O}_5 + 4 \text{HPO}_3$

Acid-base reactions of phosphorus oxides:

- H_3PO_3 (phosphorous acid) + $\text{NaOH} \rightarrow \text{NaH}_2\text{PO}_3$ (Na dihydrogen phosphite) + H_2O
- $\text{P}_4\text{O}_6 + 8 \text{NaOH} \rightarrow 4 \text{Na}_2\text{HPO}_3$ (Na hydrogen phosphite) + H_2O

15.3.9. Reactions Involving Sulfur

Reactions of sulfur:

- $S + O_2 \rightarrow SO_2$
- $2 S + Cl_2 \rightarrow S_2Cl_2$ (disulfur dichloride)
- $S + Na_2SO_3$ (sodium sulfite) $\rightarrow Na_2S_2O_3$ (sodium thiosulfate) (boil in absence of air)

Reactions of sulfur oxides:

- $SO_2 + CaO \rightarrow CaSO_3$
- $SO_3 + CaO \rightarrow CaSO_4$
- $SO_2 + H_2O \rightleftharpoons H_2SO_3$ (sulfurous acid)
- $SO_3 + H_2O \rightarrow H_2SO_4$
- $Na_2S_2O_3 + HCl \rightarrow 2 NaCl + SO_2 + S + H_2O$
- $2 SO_2 + O_2 \rightleftharpoons 2 SO_3$ (Contact process, step 1)
- $SO_3 + H_2SO_4 \rightarrow H_2S_2O_7$ (oleum) (Contact process, step 2, V_2O_5 cat., 450 °C)

Reactions of sulfuric acids:

- $H_2SO_4 + 2 Br^- + 2 H^+ \rightarrow Br_2 + SO_2 + 2 H_2O$ (H_2SO_4 is an oxidising agent)
- $H_2SO_4 + 8 I^- + 8 H^+ \rightarrow 4 I_2 + H_2S + 4 H_2O$ (I^- is a stronger reducing agent than Br^-)
- $2 H_2SO_4 + HNO_3 \rightarrow NO_2^+$ (nitronium ion) + H_3O^+ + $2 HSO_4^-$
- $H_2SO_4 + 2 NH_3 \rightarrow (NH_4)_2SO_4$
- $H_2SO_4 + H_2O_2 \rightarrow H_2SO_5$ (persulfuric acid) + H_2O (piranha solution formation)
- $2 H_2SO_4 + C \rightarrow CO_2 + 2 H_2O + 2 SO_2$ (carbon from e.g. dehydration of sucrose)
- $H_2S_2O_7 + H_2O \rightarrow 2 H_2SO_4$ (Contact process, step 3)

Acid-base reactions:

- $SO_2 + 2 NaOH \rightarrow Na_2SO_3$ (sodium sulfite) + H_2O
- $Na_2SO_3 + H_2O + SO_2 \rightarrow 2 NaHSO_3$ (sodium bisulfite)

15.3.10. Reactions Involving Chlorine

Formation of chlorine:

- $2 \text{NaCl} + 3 \text{H}_2\text{SO}_4 + \text{MnO}_2 \rightarrow \text{Cl}_2 + \text{MnSO}_4 + 2 \text{NaHSO}_4 + 2 \text{H}_2\text{O}$ (also Br_2, I_2)
- $4 \text{HCl} + \text{O}_2 \rightarrow 2 \text{Cl}_2 + 2 \text{H}_2\text{O}$ (Deacon's process)

Reactions of chlorine:

- $\text{Cl}_2 + \text{H}_2 \rightarrow 2 \text{HCl}$
- $3 \text{Cl}_2 + 2 \text{Fe} \rightarrow 2 \text{FeCl}_3$ (also F_2, Br_2 : using I_2 forms FeI_2)
- $\text{Cl}_2 + \text{Be} \rightarrow \text{BeCl}_2$ (BeCl_2 forms polymeric chains in the solid state)
- $\text{Cl}_2 + \text{H}_2\text{O} \rightleftharpoons \text{HCl} + \text{HClO}$ (hypochlorous acid)
- $2 \text{Cl}_2 + 2 \text{H}_2\text{O} \rightarrow 4 \text{HCl} + \text{O}_2$ (HClO undergoes photolysis in sunlight)
- $\text{Cl}_2 + 2 \text{NaOH} \rightarrow \text{NaClO}$ (sodium hypochlorite) + $\text{NaCl} + \text{H}_2\text{O}$ (cold, dilute NaOH)
- $3 \text{Cl}_2 + 6 \text{NaOH} \rightarrow \text{NaClO}_3$ (sodium chlorate) + $5 \text{NaCl} + 3 \text{H}_2\text{O}$ (hot, concentrated NaOH)

Reactions of chlorine oxides:

- Cl_2O_7 (dichlorine heptoxide) + $\text{H}_2\text{O} \rightarrow \text{HClO}_4$ (perchloric acid)
- Cl_2O (chlorine monoxide) + $\text{H}_2\text{O} \rightleftharpoons 2 \text{HClO}$

Acid-base reactions:

- $\text{HClO}_4 + \text{NaOH} \rightarrow \text{NaClO}_4$ (sodium perchlorate) + H_2O
- $\text{NaClO} + \text{HCl} \rightarrow \text{Cl}_2 + \text{H}_2\text{O} + \text{NaCl}$
- $\text{Cl}_2\text{O}_7 + 2 \text{NaOH} \rightarrow 2 \text{NaClO}_4 + \text{H}_2\text{O}$

Reactions of chlorates:

- $\text{NaClO} + \text{C}_3\text{H}_6\text{O}$ (propanone) $\rightarrow \text{CHCl}_3$ (chloroform) + CH_3COONa (haloform rxn)
- $\text{NaClO} + \text{H}_2\text{O}_2 \rightarrow \text{NaCl} + \text{H}_2\text{O} + \text{O}_2^*$ (reactive singlet oxygen, $\text{O}_2 (^1\Delta_g)$ is produced)

15.3.11. Reactions Involving Noble Gases

Noble gases are inert to most reactions, but under harsh and/or specialised conditions can react to form binary compounds and complexes.

Helium and neon do not form any stable chemical compounds under any laboratory conditions. Argon, krypton, xenon and radon can react in some extreme cases.

Reactions Involving Argon:

- $\text{Ar} + \text{HF} \rightarrow \text{HArF}$ (argon fluorohydride) (stable below $-246\text{ }^\circ\text{C}$)

Reactions Involving Krypton:

- $\text{Kr} + \text{F}_2 \rightarrow \text{KrF}_2$ (UV light, stable below $-78\text{ }^\circ\text{C}$)
- $3 \text{KrF}_2 + \text{Xe} \rightarrow \text{XeF}_6 + 3 \text{Kr}$

Reactions Involving Xenon:

- $\text{Xe} + \text{F}_2 \rightarrow \text{XeF}_2$ (s) (UV light)
- $\text{XeF}_2 + 2 \text{F}_2 \rightarrow \text{XeF}_6$ (120 $^\circ\text{C}$ with NiF_2 cat.)
- $\text{XeF}_6 \rightarrow \text{XeF}_4 + \text{F}_2$ (pyrolysis, NaF cat.)
- $\text{XeF}_6 + 3 \text{H}_2\text{O} \rightarrow \text{XeO}_3 + 6 \text{HF}$ (hydrolysis)
- $2 \text{XeO}_3 + 2 \text{Ba}(\text{OH})_2 \rightarrow \text{Xe} + \text{Ba}_2\text{XeO}_6$ (barium perxenate) + $\text{O}_2 + 2 \text{H}_2\text{O}$

Reactions Involving Radon:

- $\text{Rn} + \text{F}_2 \rightarrow \text{RnF}_2$ (stable below $250\text{ }^\circ\text{C}$)
- $2 \text{Rn} + 3 \text{O}_2 \rightarrow 2 \text{RnO}_3$ (above $500\text{ }^\circ\text{C}$)
- $\text{Rn} + 2 [\text{O}_2]^+[\text{SbF}_6]^- \rightarrow [\text{RnF}]^+[\text{Sb}_2\text{F}_{11}]^- + 2 \text{O}_2$ (room temperature)

For chemical reactions, radon can be generated from the decay of thorium-228 or radium-224. The radon compounds then decay into lead-208.

15.4. Periodicity Trends

15.4.1. Trends in Physical Properties of the Elements

Property	→ Trend along period(s)	↓ Trend down group(s)
Atomic radius	decreases	increases
Electronegativity, ionisation energy and electron affinity	increases	decreases
Effective nuclear charge	increases	
Halide covalent character	increases	decreases
Group 2 hydroxide and nitrate solubility in water		increases
Group 2 sulfate and carbonate solubility in water		decreases
Group 7 ion (halides) solubility in water and ammonia		decreases
Group 1 and 2 hydroxide, carbonate, sulfate and nitrate thermal stability		increases
Group 7 boiling point		increases
Oxidising power	increases	decreases
Anion reducing power	decreases	increases
Metal oxide, hydroxide and hydride basicity	decreases	increases
Transition metal melting point	decreases	
Metal electrical conductivity	increases	increases

15.4.2. Inert Pair Effect and the Lanthanide Contraction

Poor shielding (by inner d and f shells) and relativistic stabilisation (contraction of s orbitals) makes **outer 5s and 6s electrons less likely to participate in bonding**. This results in large cations being stable in lower oxidation state than expected e.g. In^+ , Tl^+ , Sn^{2+} , Pb^{2+} , Sb^{3+} , Bi^{3+} , Te^{4+} , Po^{4+} , I^{5+} : in these ions, the $5s^2$ and $6s^2$ pairs are inert. As a result, 6s electrons are drawn closer to the nucleus, decreasing the atomic radius of the lanthanides and post-lanthanide elements (including the actinides and transactinides).

These ions may mimic smaller ions, such as Na^+ or Ca^{2+} in biological organisms, while disrupting their usual functions, causing heavy metal poisoning.

The very low melting point of mercury ($[\text{Xe}] 4f^{14} 5d^{10} 6s^2$) is fundamentally due to the contracted 6s orbital and the inert pair effect. The $6s^2$ electrons in Hg are localised and do not contribute significantly to the metal's conduction band, significantly weakening the metallic bonds such that Hg is a liquid at room temperature.

15.4.3. Electron Deficient and Hypervalent Molecules (Octet Rule Exceptions)

Electron-deficient molecules contain atoms with less than 8 valence electrons.

Hypervalent molecules contain atoms with more than 8 valence electrons.

Examples of electron-deficient species: BF_3 , BeH_2 , AlCl_3 , B_2H_6 , carbenes ($\text{R}-\text{C}:-\text{R}'$)

Examples of hypervalent species ('expanded octets'): PCl_5 , SF_6 , ClF_3 , ClO_2^- , I_3^- , XeF_4

Electron deficient species often contain 3c-2e bonds.

Hypervalent species often contain 3c-4e bonds.

15.5. Coordination and Organometallic Chemistry

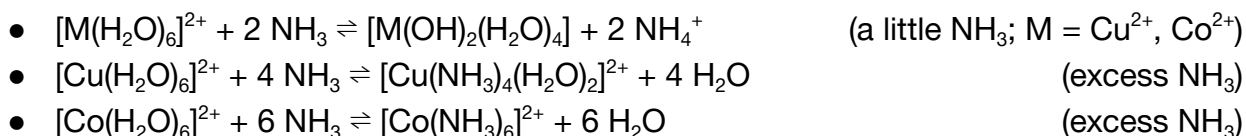
15.5.1. Reactions of Aqueous Ions (Metal Aquo Complexes)

Metal ions M^{n+} are coordinated to water molecules in aqueous solution (primary solvation).

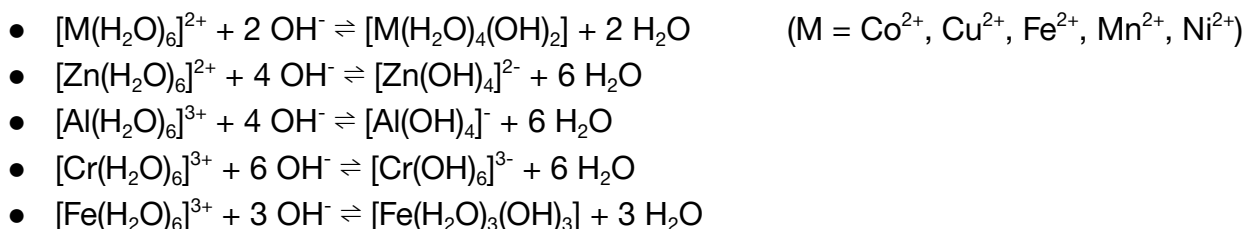
Reactions with HCl:



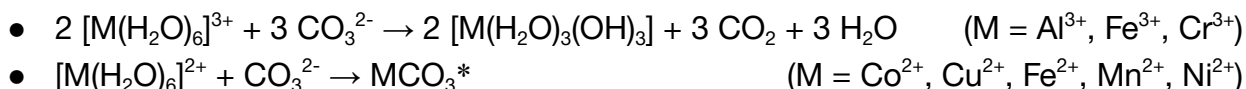
Reactions with NH_3 :



Reactions with NaOH:



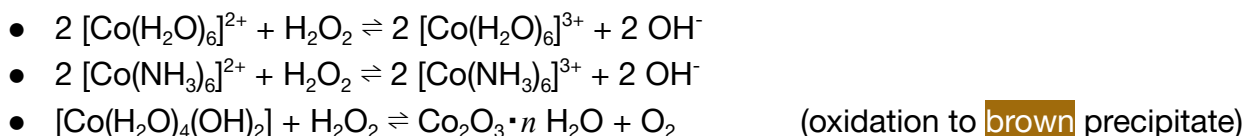
Reactions with Na_2CO_3 :



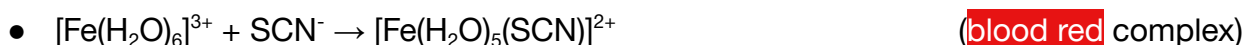
* the "basic carbonate" is of the form $x MCO_3 \cdot y M(OH)_2 \cdot z H_2O$.

The M^{3+} aqueous ions are more acidic than the M^{2+} ions due to its higher polarising power (Section 15.5.10).

Reactions with H_2O_2 :



Other reactions:



15.5.2. Colours of Common Aqueous Metal Complexes

The colours of some compounds differ to the colours given in Section 15.4.5. This is due to alterations of the central metal ion HOMO-LUMO gap due to the presence of e.g. hydration spheres, strong-field ligands (Section 15.5.8.), etc.

$[\text{Cr}(\text{H}_2\text{O})_6]^{3+}$ violet-blue-grey	$[\text{Fe}(\text{H}_2\text{O})_6]^{2+}$ pale green	$[\text{Co}(\text{H}_2\text{O})_6]^{2+}$ pink	$[\text{Ni}(\text{H}_2\text{O})_6]^{2+}$ green	$[\text{Cu}(\text{H}_2\text{O})_6]^{2+}$ light blue	$[\text{CuCl}_4]^{2-}$ yellow-green
$[\text{Cr}(\text{OH})_6]^{3-}$ green	$[\text{Cr}(\text{NH}_3)_6]^{3+}$ purple	$[\text{Cu}(\text{NH}_3)_4(\text{H}_2\text{O})_2]^{2+}$ very dark blue	$[\text{CoCl}_4]^{2-}$ deep blue	$[\text{Co}(\text{NH}_3)_6]^{2+}$ dirty yellow	$[\text{Fe}(\text{H}_2\text{O})_6]^{3+}$ pale yellow
		$[\text{Cr}(\text{H}_2\text{O})_5\text{SO}_4]^+$ green	$[\text{Fe}(\text{H}_2\text{O})_5\text{SCN}]^{2+}$ deep red		

15.5.3. Naming of Mononuclear Complex Salts

The cation is named before the anion. The metal oxidation state is given in Roman numerals. The ligands are given before the metal ion, in alphabetical order (**not** including prefixes).

Rename:

- Anion ligands: 'ide' → 'o' (exception: Cl⁻ is chlorido); 'ite' → 'ito'; 'ate' → 'ato'
- Positive groups: 'ine' / 'ia' → 'ium'
- Multiple groups if ligand already includes: 'di' → 'bis'; 'tri' → 'tris'; 'tetra' → 'tetrakis'
- Complex anion: '(metal)ium/um' → '(metal)ate', (with exceptions below)

For complex anions, non-trivial names are:

lead → plumbate; gold → aurate; tin → stannate; silver → argentate; iron → ferrate;
aluminium → aluminate; manganese → manganate; copper → cuprate; nickel → nickelate;
antimony → antimonate; arsenic → arsenate; bismuth → bismuthate; tungsten → tungstate;
tantalum → tantalate; mercury → mercurate.

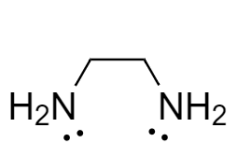
Common ligand names: Cl⁻ = chlorido; NH₃ = ammine; OH⁻ = hydroxy; H₂O = aqua.

Examples:

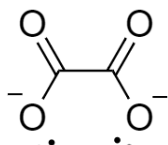
- $[\text{CoSO}_4(\text{NH}_3)_4]\text{NO}_3$ is sulfatotetraamminecobalt(III) nitrate
- $(\text{NH}_2\text{NH}_3)[\text{NiCl}_3(\text{OH})]$ is hydrazinium hydroxytrichloridonickelate(II)
- $[\text{Cr}(\text{en})_3][\text{V}(\text{H}_2\text{O})(\text{CN})_5]_2$ is trikis(ethylenediamine)chromium(IV) di(aquapentacyanovanadate(III))

15.5.4. Abbreviations for Common Large Ligands

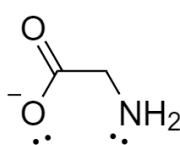
In the structures below, only the lone pairs which form dative bonds are shown.



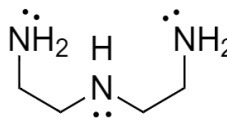
en
(ethylenediamine)



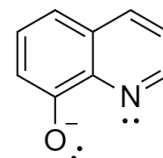
ox
(oxalato)



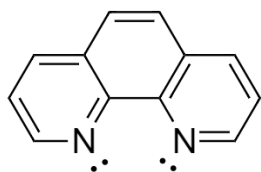
gly
(glycinato)



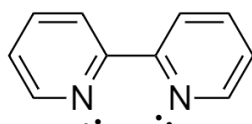
dien
(diethylenetriamine)



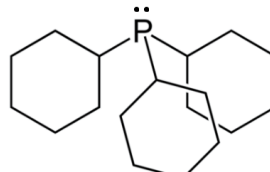
oxine
(8-hydroxyquinolato)



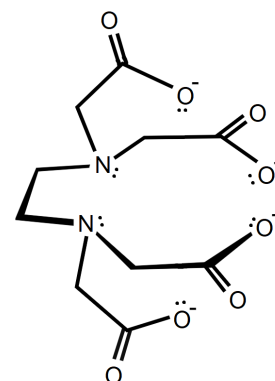
phen
(1,10-phenanthroline)



bipy
(2,2'-bipyridine)



$\text{P}(\text{Cy})_3$
(tricyclohexylphosphine)



EDTA
(ethylenediaminetetraacetic acid)

15.5.5. Bonding in Coordination Complexes

Ligands form coordinate (dative) covalent bonds to metal ion centres.

Polydentate Ligands:

- **Denticity** (κ): number of sites of electron density used for covalent bonding
- Ligands may be monodentate (κ^1), bidentate (κ^2), tridentate (κ^3), hexadentate (κ^6) etc.
- **Bite angle**: the L-M-L bond angle on a bidentate ligand L-R-L.
- **Chelate effect**: ligand substitution to higher denticity is entropically favourable.
- Examples of polydentate ligands are given in Section 15.5.4 (e.g. ethylenediamine, κ^2).

Multiple Bonding Ligands:

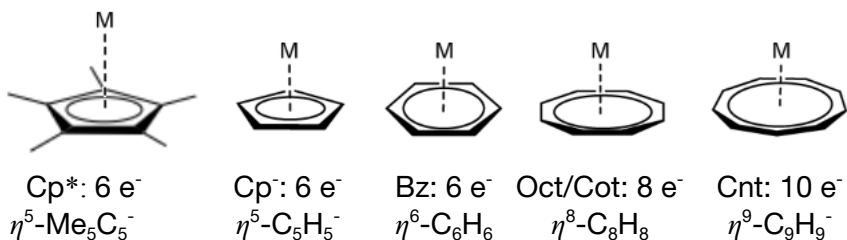
- Ligands with multiple lone pairs can form multiple dative bonds e.g. M=O (oxide), M=S (sulfide), M≡N (nitride), M=NR (imide)
- **Backbonding**: ligands with empty π^* LUMOs can accept $d-\pi^*$ backbonding, stabilising the complex e.g. M-NO⁺ (nitrosyl), M-CO (carbonyl).
- **Alkylidenes** (CR₂): forms M=C double bonds. **Fischer (singlet)** carbenes have σ (sp^2-d) dative bonding and π ($d-p$) backbonding. **Schrock (triplet)** carbenes have double σ bonding.
- **Alkylidynes** (CR): forms M≡C triple bonds. **Fischer (doublet)** carbynes have σ ($sp-d$) dative bonding, σ ($p-d$) covalent bonding and σ ($d-p$) dative bonding. **Schrock (quartet)** carbynes have triple σ bonding.

Bridging Ligands:

- Bridging ligands are named with the symbol μ to indicate the bridges in polynuclear complexes.
- sp^3 -hybridised oxide (O²⁻), sulfide (S²⁻) or halide (Cl⁻, Br⁻) ions can act as bridging ligands.
- Hydride (H⁻) can act as a 3c-2e bridge, donating 1 e⁻ in each bond.
- Peroxide (O₂²⁻) can act as either a bidentate ligand (3 membered ring) or a bridging ligand.

Polyhapto Ligands:

- **Hapticity** (η): number of delocalised electrons in a ligand that coordinates to the metal centre
- In **metal-alkene complexes** (e.g. Zeise's salt, [PtCl₃(η^2 -C₂H₄)]), the π HOMO of the alkene donates electrons into the empty metal d orbital. $d-\pi^*$ backbonding can also occur, indicated by drawing the complex as a 3 membered ring (the Dewar-Chatt-Duncanson model).
- **Aromatic polyhapto ligands** and their hapticity and electron counts (also: Cp' = MeCp, Cp'' = Me₂Cp)

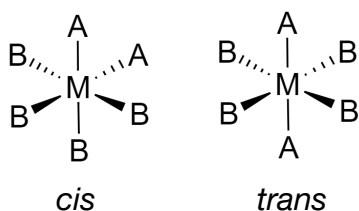


- The hapticity η of many ligands may vary. **Alkynes** may be either η^4 or η^2 . **Allylic** carbanions (e.g. C₃H₅⁻) may be η^3 or η^1 . Aromatic polyhapto ligands can shift coordination numbers by a slippage or folding mechanism, e.g. Cp⁻ may slip from η^5 to η^3 .
- **Sandwich complex**: two polyhapto ligands. May be homoleptic (same η) or heteroleptic (different η).

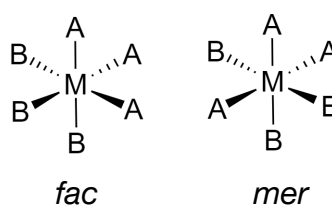
15.5.6. Stereoisomerism of Heteroleptic Complexes

Geometric Isomerism: complexes are *cis* when similar ligands are adjacent (90° bond angle) and *trans* when similar ligands are opposite (180° bond angle).

Octahedral complex of form MA_2B_4 :

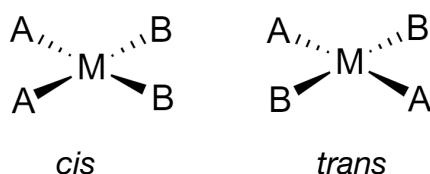


Octahedral complex of form MA_3B_3 :

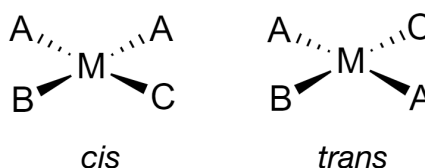


Octahedral complexes of form $M(ABCDEF)$ in general have 15 isomers.

Square planar complex of form MA_2B_2 :

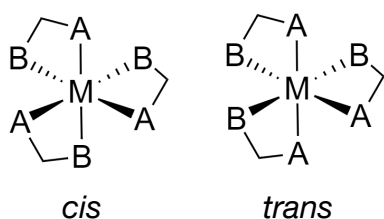


Square planar complex of form MA_2BC :

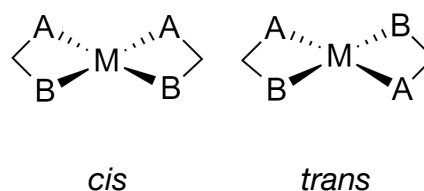


Square planar complexes of form $M(ABCD)$ in general have 3 isomers.

Octahedral, bidentate ligands:



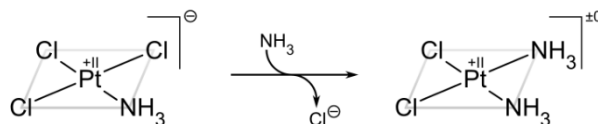
Square planar, bidentate ligands:



Kinetic Trans Effect: existing ligands are *trans*-directing to incoming substituent ligands

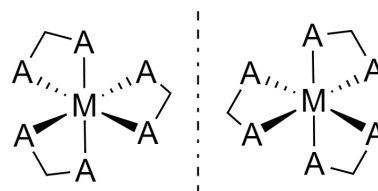
(Weak, directs *cis*) F^- , H_2O , OH^- < NH_3 < py < Cl^- < Br^- < I^- , SCN^- , NO_2^- , $SC(NH_2)_2$, Ph^- < SO_3^{2-} < PR_3 , AsR_3 , SR_2 , CH_3^- < H^- , NO , CO , CN^- , C_2H_4 (Strong, directs *trans*)

For example, $[PtCl_3NH_3]^- + NH_3 \rightarrow cis-[PtCl_2(NH_3)_2]$ (cisplatin) since $Cl^- > NH_3$ directs the incoming NH_3 *trans* to a Cl^- (overall *cis* square planar).



Optical Isomerism in Homoleptic Complexes

E.g. for three identical symmetric bidentate ligands:



15.5.7. Valence Bond Theory for Correlating Spin State with Hybridisation

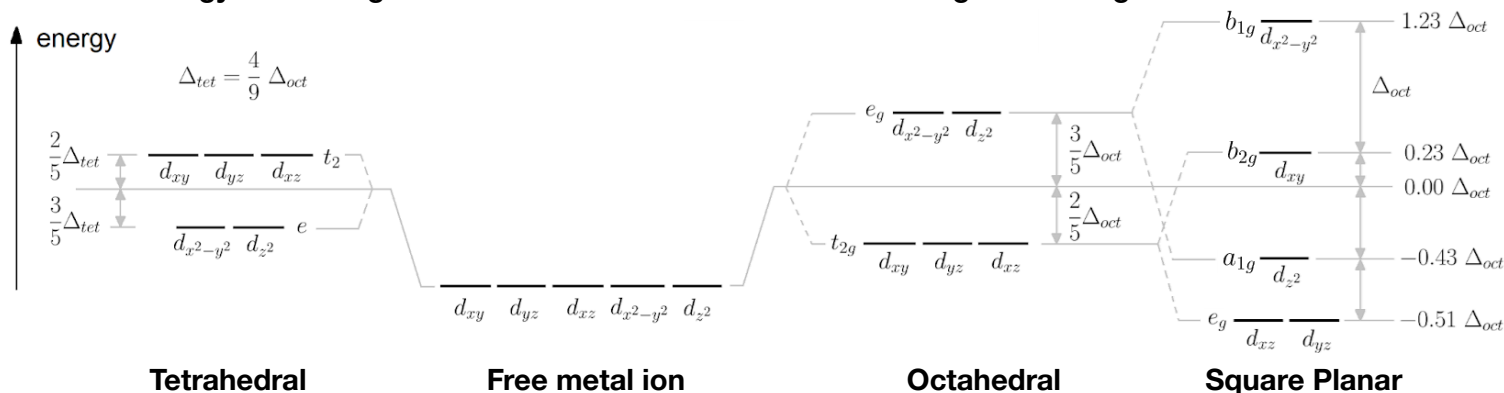
Hybridised VBT is a basic (often insufficient) model for bonding in complexes.

- A high-spin complex uses sp^3d^2 hybridisation with its outer (4d) orbital.
- A low-spin complex uses sp^2d^3 hybridisation with its inner (3d) orbital.

15.5.8. Crystal Field Theory (CFT)

CFT is an ionic bonding model in which ligands split the d orbital of a transition metal ion into non-degenerate sets of orbitals, occupied by the metal ion's valence electrons. Ligands may be strong field (low spin, e^- are filled by Aufbau/Hund rules) or weak field (high spin, orbitals are filled unpaired-first) (the spectrochemical series, Section 15.5.9).

Energy Level Diagrams for Metal Ions in a Field of Point Negative Charges:



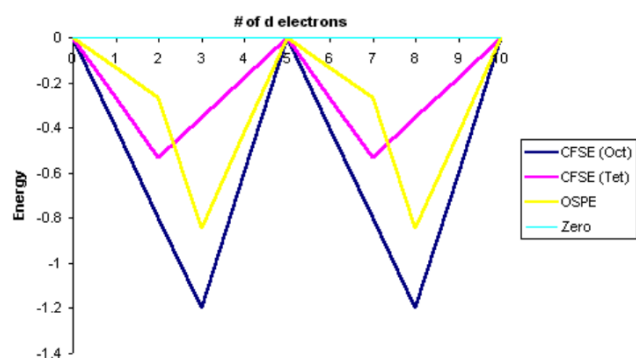
For other geometries, the splitting patterns are, in ascending energy order:

Square Pyramidal ($\{d_{xz}, d_{yz}\}, d_{xy}, d_{z^2}, d_{x^2-y^2}\}$); Trigonal/Pentagonal Bipyramidal ($\{d_{xz}, d_{yz}\}, \{d_{xy}, d_{x^2-y^2}\}, d_{z^2}$); Square Antiprismatic ($d_{z^2}, \{d_{xy}, d_{x^2-y^2}\}, \{d_{xz}, d_{yz}\}$).

The energy levels are related (for oct and tet) by ($P > 0$: pairing energy for mutual repulsion)

$$E_{\text{ligand}} = \underbrace{n_{t_{2g}} \left(-\frac{2}{5} \Delta \right) + n_{e_g} \left(\frac{3}{5} \Delta \right)}_{\text{energy relative to barycentre}} + \underbrace{\left(n_{\text{pairs}}^{t_{2g}} + n_{\text{pairs}}^{e_g} \right) P}_{\text{pairing energy}} \quad E_{\text{isotropic}} = \underbrace{n_{\text{pairs}}^d P}_{\text{pairing energy in degenerate d orbital}}$$

- Crystal field stabilisation energy, $CFSE = E_{\text{ligand}} - E_{\text{isotropic}}$
- Octahedral site preference energy, $OSPE = CFSE_{(\text{oct})} - CFSE_{(\text{tet})}$



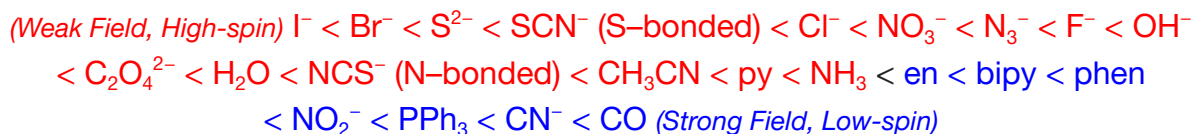
CFSE and OSPE for high-spin complexes (shown left) depend only on the number of d electrons, in units of Δ_{oct} .

- d^3 and d^8 strongly favour octahedral.

Low-spin complexes depend on P .

15.5.9. Spectrochemical Series and Spin States

In order of ligand strength i.e. increasing values of Δ :



15.5.10. Magnetic Moment due to Electron Configuration

The total magnetic moment of a compound (atom, ion, molecule or complex) is due to the contribution of unpaired electrons (possessing spin) and electrons in orbitals with non-zero angular momentum.

Quantisation of magnetic moment (Bohr magneton): $\mu_B = \frac{e\hbar}{2m_e} = 9.274 \times 10^{-24} \text{ A m}^2$

Spin-only magnetic moment: $\mu_s = g\sqrt{S(S+1)}\mu_B = \sqrt{n(n+2)}\mu_B$ ($g = 2.0023$: e^- g-factor)

Orbital magnetic moment: $\mu_l = \sqrt{L(L+1)}\mu_B$ (z-component has $\mu_l^{(z)} = m_l\mu_B$)

Total magnetic moment: $\mu = \mu_s + \mu_l$

(n : number of unpaired electrons, S : sum of the spin quantum numbers and L : sum of all angular momentum quantum numbers of all electrons (d , e_g , t_{2g} etc all have $l = 2$).

For low-spin complexes, $\mu_s = 0$ since all electrons are paired in the t_{2g} orbital.

The contribution to the magnetic moment from the nuclear spin is negligible in size compared to the electrons, although the interactions have significance in e.g. NMR. The nuclear contribution is responsible for the slight diamagnetism of e.g. hydrogen.

If both spin and orbital contributions to μ are present, the resulting magnetic fields interact (spin-orbit coupling, fine structure splitting, Zeeman effect). Interaction with the nuclear magnetic moment produces further slight interactions (hyperfine structure splitting).

Bulk Magnetisation: may occur spontaneously in ferromagnets (domain regions)

Theoretical bulk saturation magnetisation, $M_{\max} [\text{A m}^{-1}] = \frac{n_{\text{atoms/cell}}}{V_{\text{cell}}} \times \mu = \frac{\rho N_A \mu}{M_r}$.

Theoretical bulk saturation magnetic flux density, $B_{\max} [\text{T}] = \mu_0 M_{\max}$

(n_a : number of atoms or complexes per unit cell, V_{cell} : volume of unit cell, μ : magnetic moment, $\mu_0 = 4\pi \times 10^{-7} \text{ T m}^2 \text{ A}^{-1}$: permeability of vacuum, ρ : mass density, $N_A = 6.022 \times 10^{23} \text{ mol}^{-1}$: Avogadro's number, M_r : molar mass (in kg mol^{-1}). For unit cell counts, see Section 13.2.1.)

15.5.11. Electron Counting of Complexes

To determine the total number of electrons a central metal ion's valence shell:

1. Calculate the oxidation state of the metal ion, its electron configuration and valence electrons.
2. Calculate the number of electrons donated by each ligand to the metal; add together.

18 electron rule: neglecting valence *f* orbitals, a complex is usually most stable with 18 e⁻ valence electrons. Some tetravalent complexes may also be stable with 16 e⁻, in which case:

- Tetrahedral (16 e⁻, high spin d⁸ complexes): [CuCl₄]²⁻, [CoCl₄]²⁻, [Zn(CO)₄]²⁻
- Square planar (16 e⁻, low spin d⁸ complexes): [NiCl₂(NH₃)₂], [PtCl₄]²⁻, [PtCl₃(η²-C₂H₄)]⁻

Example: [W(PMe₃)₃Cl₂(η⁵-Cp)]⁺. The ligands have charges Cl⁻ and Cp⁻, so the metal centre is W⁴⁺. Normally, tungsten has configuration [Xe] 6s² 4f¹⁴ 5d⁴ so W⁴⁺ is [Xe] 4f¹⁴ 5d². The ligands PMe₃ (2 e⁻), Cl⁻ (2 e⁻) and η⁵-Cp⁻ (6 e⁻) provide 16 valence electrons. The total number of non-*f*-orbital valence electrons on the metal centre is then 2 + 16 = 18 e⁻ (stable for an octahedral complex).

The number of electrons donated by the various ligands are (using the ionic counting convention)

Ligand	# e ⁻	Ligand	# e ⁻	Ligand	# e ⁻
H ⁻ (hydro)	2	NR ²⁻ (imido), PR ²⁻	4 or 6	NO ⁺ (nitrosyl)	2
X ⁻ (halido)	2	N ³⁻ (nitride), P ³⁻	6	NO ₂ ⁻ (nitrito)	2
OH ⁻ (hydroxo), RO ⁻ (alkoxo)	2	CO (carbonyl)	2	CNR (isociano)	2
H ₂ O (aqua)	2	CR ₃ ⁻ (carbanion)	2	η ³ -C ₃ H ₅ ⁻ (allyl)	4
O ²⁻ (oxido), S ²⁻ (sulfo)	4 or 6	CR ₂ (alkylidene)*	2	η ⁵ -C ₅ H ₅ ⁻ (Cp)	6
O ₂ ²⁻ (peroxo)	4	CR ⁻ (alkylidyne)*	4	η ³ -C ₅ H ₅ ⁻ (Cp)	4
NR ₃ (ammine), PR ₃	2	C ₂ R ₄ (alkene)	2	η ⁶ -C ₆ H ₆ (Bz)	6
NR ₂ ⁻ (amido), PR ₂ ⁻	2 or 4	C ₂ R ₂ (alkyne)	2 or 4	η ¹ -C ₆ H ₅ ⁻	2

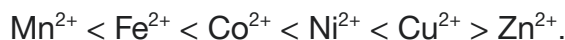
Electron counting conventions: in the above table, the ionic convention is used.

- **Ionic convention:** number of e⁻ donated = hapticity + negative formal charge
- **Covalent / neutral convention:** formal charges omitted; number of e⁻ donated = hapticity
- The convention affects the oxidation state of the metal ion, but if used consistently, does not affect the overall electron count.
- *In the ionic scheme, alkylidenes may be Fischer-type carbenes (singlet: CR₂, 2 e⁻) or Schrock-type carbenes (triplet: CR₂²⁻, 4 e⁻). In the covalent scheme, they are always CR₂, 2 e⁻. Similarly, alkylidynes may be CR³⁻, 6 e⁻ or CR⁻, 4 e⁻.

15.5.12. Irving-William Series of Divalent Complex Stability

The complexes of divalent cations (M^{2+}) of late 3d transition metals show increasing stability with decreasing atomic radius due to higher charge density.

The first stepwise stability constants ($\log K_1$) follows the trend

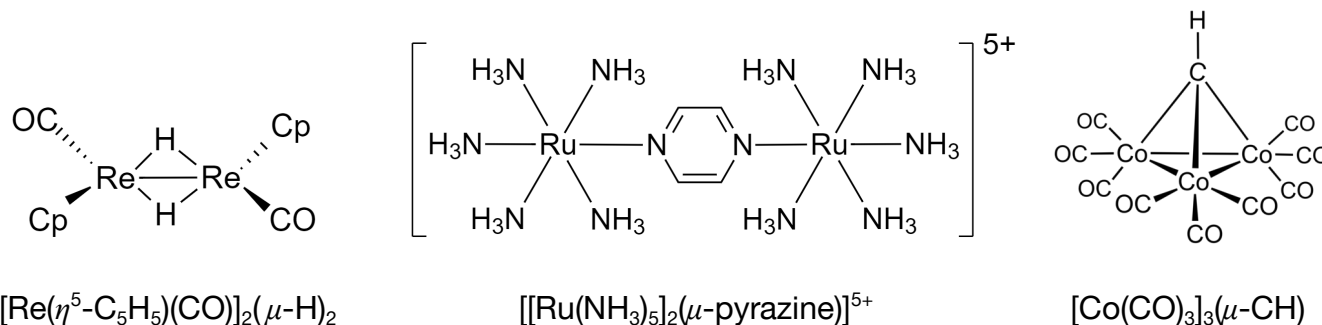


The maximal stability of Cu^{2+} is not predicted by CFT, and is due to formation of Jahn-Teller distorted octahedral complexes (Section 15.5.15).

15.5.13. Polynuclear Complexes

Ligands may donate their lone pair(s) to multiple metal centres. These are known as bridging ligands. Each metal ion is most stable at its full electron count, and there may be metal-metal bonds present.

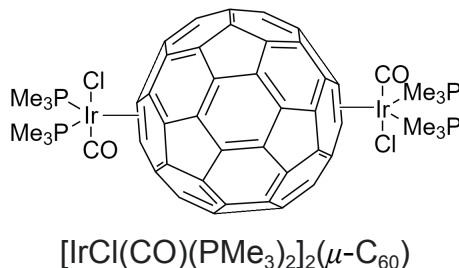
Formulas of polynuclear complexes are written with μ to indicate the bridging ligand:



Hydride ligands donate $1 e^-$ into each metal-hydride bond, for its normal total of $2 e^-$.

Halide ligands may donate multiple lone pairs.

Buckminsterfullerene (C_{60}) can act as a π ligand:

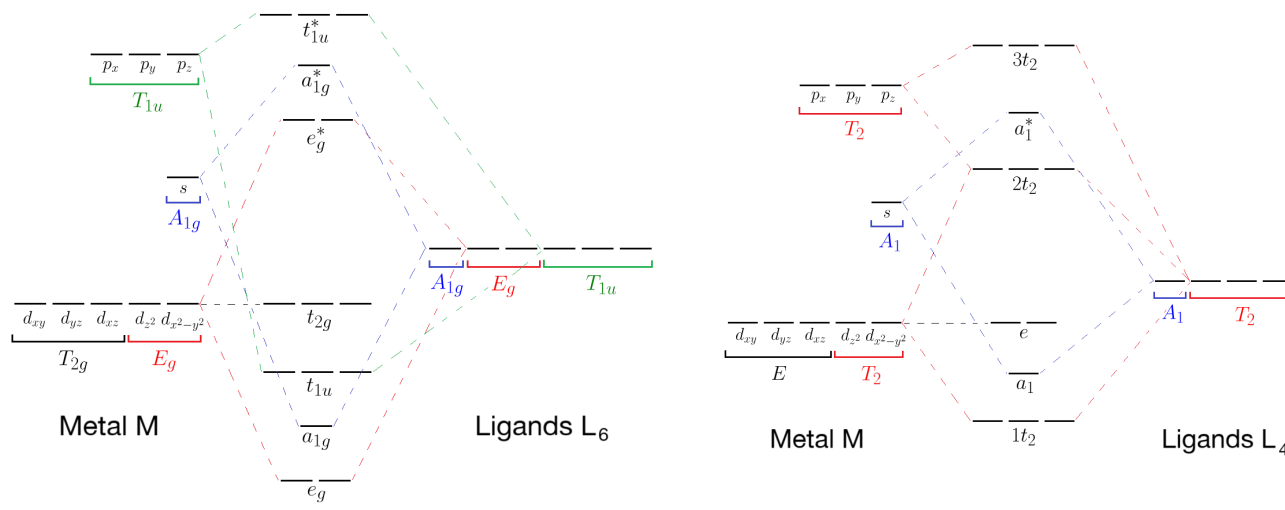


Some solid state complexes can form polymer-like chains e.g. BeCl_2 .

15.5.14. Ligand Field Theory

Ligand Field Theory (LFT) applies MO theory to CFT, allowing it to be used for metal complexes which are not perfectly ionic e.g. organometallic complexes.

The frontier (valence) orbitals of a period n metal ion are $\{(n-1)d, ns, np\}$. These split into orbitals given by their irreducible representations under the point group of the molecular geometry.



Octahedral (O_h): ML_6

$$\Delta_{oct} = \text{energy of } e_g^* - \text{energy of } t_{2g}$$

Tetrahedral (T_d): ML_4

$$\Delta_{tet} = \text{energy of } 2t_2 - \text{energy of } e$$

If π back-bonding occurs, e and $2t_2$ can drop in energy.

Ligand contributions can be determined with projection operators (Section 13.2.10).

Total electron pairing energy: $\Pi_{total} = \Pi_c + \Pi_e$

Π_c is the Coulombic repulsion term due to two electrons present in the same sub-orbital.

Π_e is the stabilising exchange energy of electrons in degenerate orbitals with the same spin.

For $n e^-$ in a degenerate set of n orbitals with same spin, there are ${}^n C_2 = \frac{n(n-1)}{2}$ multiples of Π_e .

π -acceptor ligands (CO, NO, CN^- , pyridine) have empty π^* orbitals that accept electrons from metal T_{2g} d -orbitals. This backbonding effect strengthens the metal-ligand bond but weakens ligand multiple bonds. In the spectrochemical series (Section 15.5.9), π -donors are towards the small Δ_o end while π -acceptors are towards the large Δ_o end. σ -only ligands are intermediate.

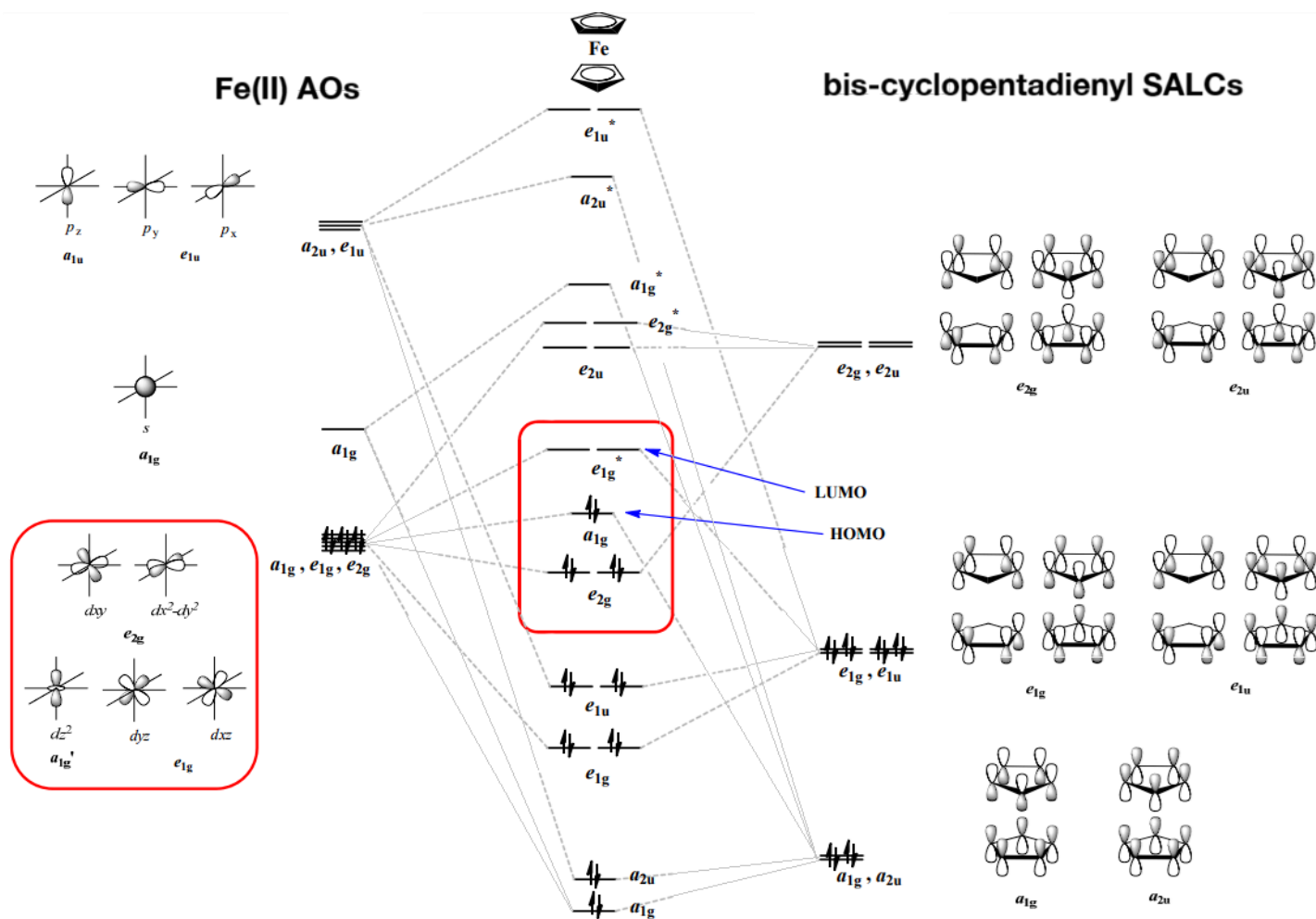
4d and 5d metals are usually low spin due to stronger σ bonds and also due to decreased electron repulsion in their larger d orbitals.

Example: molecular orbitals of ferrocene $[\text{Fe}(\eta^5\text{-C}_5\text{H}_5)_2]$ using SALCs

The frontier orbitals of the cyclopentadienyl anion Cp^- (C_5H_5^-) are 5 sets of delocalised p orbitals totalling 6 electrons. Each ring is in the D_{5h} point group. The staggered conformation of bis-cyclopentadienyl has 10 sets of p orbitals with 12 electrons in the D_{5d} point group. The reducible representation is $\Gamma = \{E: 10, 5\sigma_d: 2\}$. The irreducible representation in D_{5d} is $\Gamma = A_{1g} \oplus E_{1g} \oplus E_{2g} \oplus A_{2u} \oplus E_{1u} \oplus E_{2u}$.

The bonding $\text{Fe}^{2+} = [\text{Ar}] 3d^6$ atomic orbitals transform in D_{5d} as

$$\left\{ A_{1g}: (s, d_{z^2}), E_{1g}: (d_{yz}, d_{xz}), E_{2g}: (d_{x^2-y^2}, d_{xy}), A_{2u}: (p_z), E_{1u}: (p_x, p_y) \right\}$$



15.5.15. Jahn-Teller Effect

Nonlinear molecules may distort their geometry to remove the degeneracy (equality of energy) of unequally occupied orbitals. This lowers the energy of the complex as a whole.

- e_g orbitals split into d_{z^2} and $d_{x^2-y^2}$ orbitals.
- t_{2g} orbitals split into d_{xz} , d_{yz} and d_{xy} orbitals.

Asymmetry in e_g causes a strong Jahn-Teller effect (e.g. low-spin d^7 or d^9 , high-spin d^4), while asymmetry in t_{2g} causes a weak Jahn-Teller effect.

- If $d_{x^2-y^2} > d_{z^2}$ (i.e. d_{z^2} is **occupied**) then there is tetragonal **elongation** along the z -axis.
- If $d_{x^2-y^2} < d_{z^2}$ (i.e. d_{z^2} is **vacant**) then there is tetragonal **compression** along the z -axis.

Jahn-Teller theory cannot predict the direction, only its presence and strength.

Jahn-Teller distortion is a permanent effect, occurring in the aqueous and pure (solid/liquid/gas) states.

15.5.16. Polarisability of Ligands

Transition metal centres (M) act as Lewis acids. Ligands (L) act as Lewis bases. The formation of the transition metal complex (ML) is considered an acid-base reaction.

Hard-Soft Acid Base Theory (HSAB theory)

	thermodynamics	ionic radius	charge	charge density	polarisability	MO energy
Hard acid	$\Delta_f G_{M^{n+}}^\ominus < 0$	small	high +ve	high	low	high LUMO
Soft acid	$\Delta_f G_{M^{n+}}^\ominus > 0$	large	high -ve	low	high	low LUMO
Hard base	$\alpha_{ML}^* < 0$	small	high -ve	high	low	high HOMO
Soft base	$\alpha_{ML}^* > 0$	large	low -ve	low	high	low HOMO

For a given base (ligand), $RT \ln K_{ML} = \alpha_{ML}^* \Delta_f G_{M^{n+}}^\ominus - \beta_{ML}^* r_{M^{n+}} + \gamma_{ML}^* \Delta_{hyd} G_{M^{n+}}^\ominus - \delta_{ML}^*$, where (α_{ML}^* , β_{ML}^* , γ_{ML}^* , δ_{ML}^*) are constants fit across a range of metal ions M^{n+} . Hard acid-hard base (more ionic) and soft acid-soft base (more covalent) interactions are more favourable - the interaction energy term $\alpha_{ML}^* \Delta_f G_{M^{n+}}^\ominus > 0$, as species which are more 'polarisable' have **less** 'polarising power'.

(K_{ML} : stability constant of ML, $\Delta_f G_{M^{n+}}^\ominus$: Gibbs free energy of formation for M^{n+} , $\Delta_{hyd} G_{M^{n+}}^\ominus$: Gibbs free energy of hydration for M^{n+} (solvation energy), $r_{M^{n+}}$: effective ionic radius of M^{n+})

Classification of Metals and Ligands:

<p>Hard Bases F^-, Cl^-, H_2O, OH^-, O^{2-}, ROH, RO^-, R_2O, CH_3COO^-, NO_3^-, ClO_4^-, CO_3^{2-}, SO_4^{2-}, PO_4^{3-}, IO_3^-, NH_3, RNH_2, N_2H_4, Glu, ADP, ATP, AMP-5'</p>	<p>Intermediate Bases Br^-, NO_2^-, N_3^-, N_2, SO_3^{2-}, $C_6H_5NH_2$, C_5H_5N, His, Asp</p>	<p>Soft Bases H^-, I^-, H_2S, SH^-, S^{2-}, RSH, RS^-, R_2S, SCN^-, CN^-, RNC, CO, $S_2O_3^{2-}$, R_3P, $(RO)_3P$, R_3As, C_2H_4, C_6H_6, en, $EDTA^{4-}$, Cys, Gly</p>
<p>Hard Acids HX, $*H^+$, Li^+, Na^+, K^+, Rb^+, Cs^+, $*Be^{2+}$, Mg^{2+}, Ca^{2+}, Sr^{2+}, Ba^{2+}, BF_3, BCl_3, $B(OR)_3$, Al^{3+}, Ga^{3+}, $Al(CH_3)_3$, $AlCl_3$, Ti^{3+}, V^{3+}, Cr^{3+}, Mn^{2+}, Fe^{3+}, Co^{3+}, Eu^{2+}, U^{3+}, Np^{3+}</p>	<p>Intermediate Acids $B(CH_3)_3$, NH_4^+, Fe^{2+}, Co^{2+}, Ni^{2+}, Zn^{2+}, Rh^{3+}, Cd^{2+}, Ir^{3+}, Os^{2+}, Sn^{2+}, Pb^{2+}, Tl^+</p>	<p>Soft Acids BH_3, $Tl(CH_3)_3$, Bi^{3+}, Cu^+, Ag^+, Au^+, Cu^{2+}, Hg_2^{2+}, Hg^{2+}, CH_3Hg^+, Pd^{2+}, Pt^{2+}, Pt^{4+}, Au^{3+}, Ru^{3+}, Br_2, I_2, all π acceptors</p>

15.5.17. Organometallic Reactions

M-L bond strength increases down the group ($5d > 4d > 3d$).

Ligand Substitution: $ML_x + n L' \rightarrow ML_{x-n}L'_n + n L$

Associative (S_NAc -like): $ML_x + L' \rightarrow ML_xL' \rightarrow ML_{x-1}L' + L$. Preferred by $16 e^-$ uncrowded complexes.

Dissociative (S_N1 -like): $ML_x \rightarrow ML_{x-1} + L$, $ML_{x-1} + L' \rightarrow ML_{x-1}L'$. Preferred by $18 e^-$ crowded complexes.

Interchange (S_N2 -like): $ML_x + L' \rightarrow ML_{x-1}L' + L$. Preferred by $18 e^-$ complexes.

Reductive activation (R): $ML_x + e^- \rightarrow ML_x^-$. Preferred when the LUMO is nonbonding / antibonding.

Oxidative activation (O): $ML_x \rightarrow ML_x^+ + e^-$. Preferred when the HOMO is nonbonding / antibonding.

The regioselectivity of substitution is subject to the trans effect (Section 15.5.6).

Oxidative Addition and Reductive Elimination: $M^{(n)} + A-B \rightleftharpoons A-M^{(n+2)}-B$

Preferred with metals with stable oxidation states separated by $2 e^-$. Common substrates:

H-H, Si-H, B-B, B-H, Sn-H, Sn-Sn, N-H, O-H, S-H, C-X, C-H (in e.g. CH_4 , C_6H_6).

Concerted oxidative addition: The σ_{A-B} bond donates electron density into the empty M d_{z^2} orbital, and may also accept backbonding from M d orbitals into the σ_{A-B}^* bond. The result is *cis* addition of A and B into the complex, pushing one ligand into an alternate position.

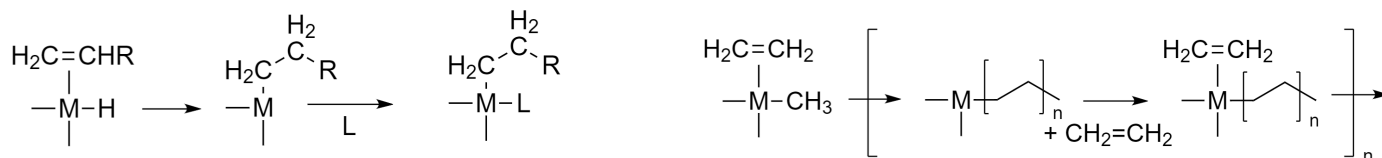
Stepwise oxidative addition: electrophilic addition-like mechanism.

Reductive elimination: the reverse of oxidative addition. The leaving bonds M-A and M-B must be *cis* to each other. A common pattern is reduction followed by oxidation with a different substrate (effectively a redox substitution).

Migratory Insertion: $L_n-\overset{X}{\underset{|}{M}}-Y \rightleftharpoons L_n-M-X-Y \longrightarrow L_n-\overset{L'}{\underset{|}{M}}-X-Y$

Ligand insertion is reversible. There is no change in the oxidation state of M. To interchange, X and Y must be *cis* to each other. The ligands must contain π bonds (e.g. CO).

Hydrometalation (reverse β -hydride elimination): Carbometalation (Ziegler-Natta addition polymerisation):



Ligand Attack

Metathesis

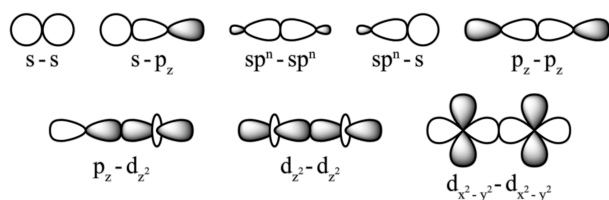
C16. ORGANIC AND BIOCHEMISTRY

16.1. Bonding and Forces in Organic Molecules

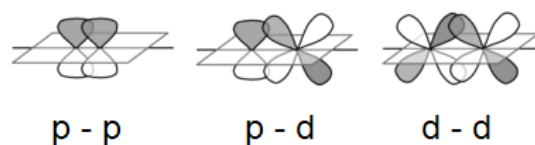
16.1.1. Sigma and Pi Bonding Between Atomic and Hybridised Orbitals

Bonding occurs when orbital wavefunctions superpose in-phase (represented as same shade).

Sigma (σ) bonds:



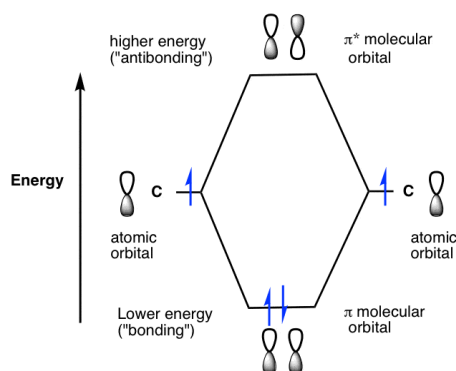
Pi (π) bonds:



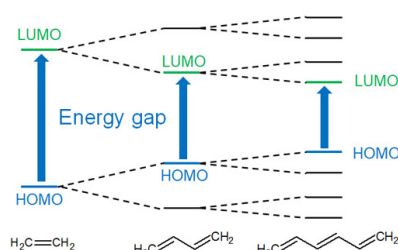
16.1.2. Carbon-Carbon Pi Bonding and Resonance

A pi bonding orbital (π) has neighbouring p-orbitals in phase, while a pi antibonding orbital (π^*) has neighbouring p-orbitals in antiphase.

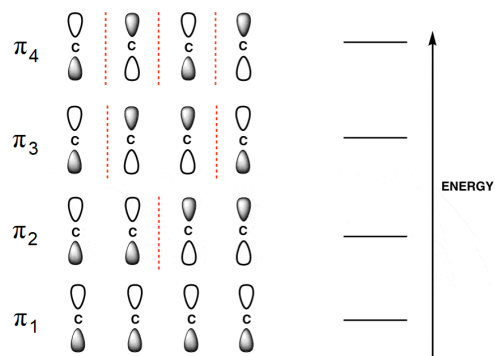
Two neighbouring p-orbitals in antiphase will have a nodal plane between them. There are no transverse nodes at the lowest level, above which they are distributed symmetrically in the system. The HOMO-LUMO gap decreases with the extent of conjugation.



MO diagram for a $C=C$ π bond



MOs of conjugated alkenes



Nodal planes for buta-1,3-diene

Huckel's rule for aromatic conjugation: $(4n + 2) e^-$ for aromaticity, $4n e^-$ for antiaromaticity.

16.1.3. Mechanisms of Bond-Mediated Electron Density Redistribution

- **Inductive effect (I):** electron density is pushed/pulled through sigma bonds, due to electronegativity differences. This is a permanent effect.
- **Mesomeric effect (M):** electron density is delocalised through pi bonds, due to electronic **resonance**. This is a permanent effect, in which the molecular orbitals are a quantum superposition of contributing classical resonance structures.
- **Electromeric effect (E):** electron density is pushed/pulled through pi bonds, due to the presence of an nearby electrophile or nucleophile. This is a temporary effect.

16.1.4. Tautomerism

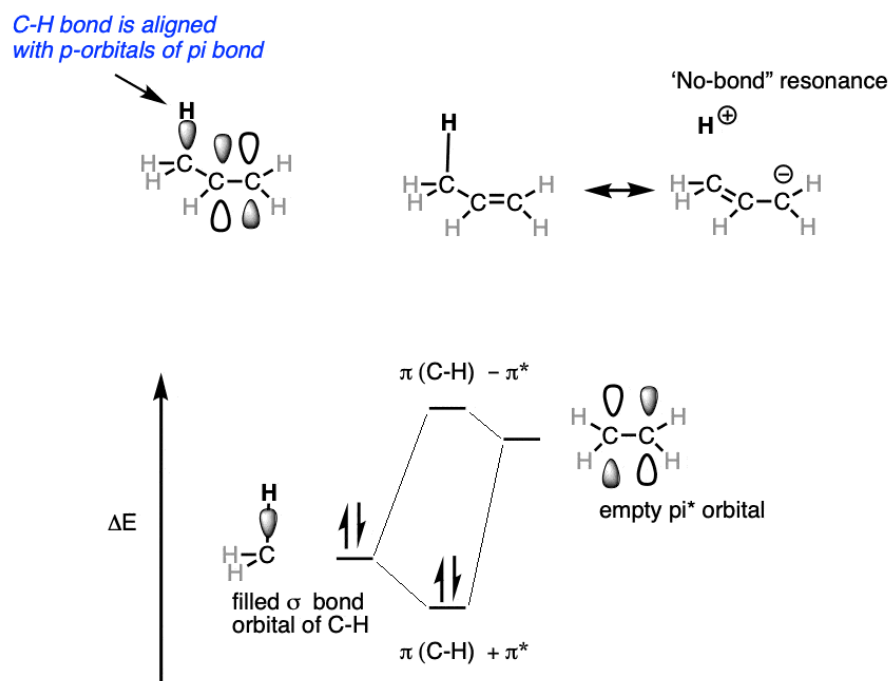
Tautomerism occurs in molecules with rapidly interconverting states, through intermolecular reactions with the solvent, typically proton transfers to and from water molecules.

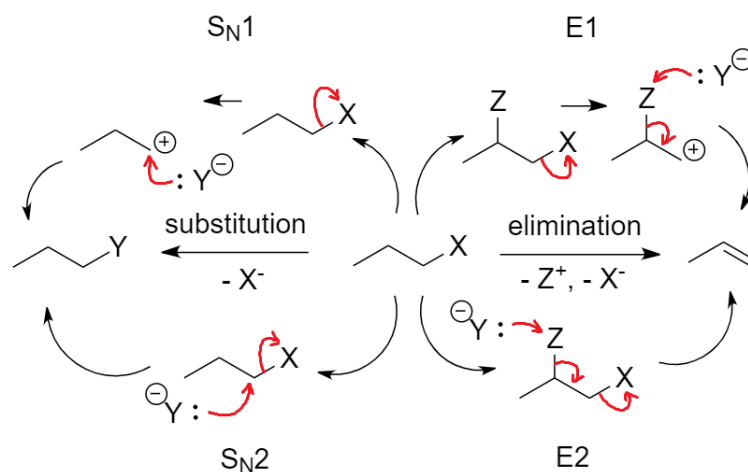
- **Keto-enol tautomerism:** $\text{RCOCH}_2\text{R}'$ (**ketone**) \rightleftharpoons RC(OH)=CH-R (enol). The keto form predominates in most cases, but the enol form is stabilised when conjugating C=C bonds are present in R e.g. phenols, or in 1,3-diketones.
- **Amide-imidic acid tautomerism:** RCONHR' (**amide**) \rightleftharpoons $\text{RC(OH)NR}'$ (imidic acid). The amide form predominates in water or oxygen, while the imidic acid form predominates in ammonia or methane. In cyclic amides (lactams), the corresponding imidic acid is a lactim, important for tautomerism in DNA and RNA nucleobases.
- **Enamine-imine tautomerism:** $\text{R}_2\text{C(NH}_2\text{)CR}'$ (enamine) \rightleftharpoons $\text{R}_2\text{C(NH)CHR}'$ (imine). The imine is stabilised in acid, the enamine is stabilised in base. Imine (Schiff base) formation is important in many biochemical pathways.

Others include oxime-nitroso, amino acid-ammonium carboxylate (zwitterion formation), ketene-ynol, tetrazole-azide, nitro-nitronic acid and phosphite-phosphonic acid tautomerism.

16.1.4. σ - π^* Hyperconjugation (No-Bond Resonance)

For a C-H σ -bond to be eligible for hyperconjugation, the α C must be sp^3 hybridised. The C-H σ -bonds can then be conjugated with an adjacent C=C π -bond by interaction with an empty π^* antibonding orbital. A resonance structure is formed, weakening the C-H bonds.



16.1.5. Nucleophilic Substitution (S_N) and Elimination (E)

(X: leaving group, Y: nucleophile (S_N) or base (E), Z: acidic group (often a proton).)

Note that if Y is added in a polar solvent, a molecule of solvent may take the role of Y.

Conditions for favouring mechanisms:

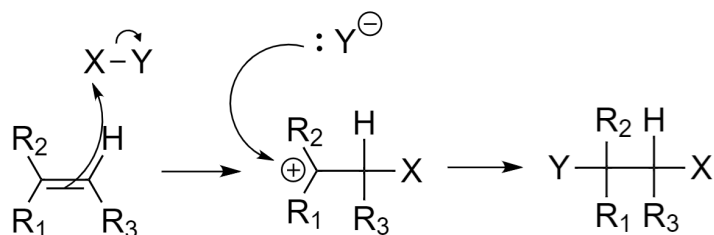
- Substrate R: Steric hindrance on the substrate RX promotes S_N1 . Sterically open substrates promote S_N2 and E2.
- Reactant Y: Strong bases / charged nucleophiles (e.g. NaOH, Cl^-) promote S_N2 and E2. Weak bases / neutral nucleophiles (e.g. EtOH, NH_3), as well as strong acids (e.g. H_2SO_4), promote S_N1 and E1.
- Solvent: Polar protic solvents (e.g. H_2O , EtOH) promote E2 and inhibit S_N2 by solvating Y with hydrogen bonding. Polar aprotic solvents (e.g. DMSO, acetone) promote S_N2 and inhibit E2 by replacing Y as a less effective base.
- Temperature: High temperatures promote E1. Low temperatures promote S_N1 .

Note that:

- A strong base in an alcohol solvent will favour E over S_N (alkoxide is strong & bulky base)
- S_N1 , E1 are unimolecular, with 1st-order rate kinetics: $r = k [Y]$
- S_N2 , E2 are bimolecular (concerted; concurrent), with 2nd-order rate kinetics: $r = k [Y][RX]$
- S_N reactions involve an inversion of stereochemistry.
- S_N1 and E1 allow for proton transfers (1,2-hydride shifts) if an adjacent carbocation is more stable, and 1,2-methyl shifts if a neighbouring carbon is 4° (forming a 3° carbocation).

16.1.6. Electrophilic Addition

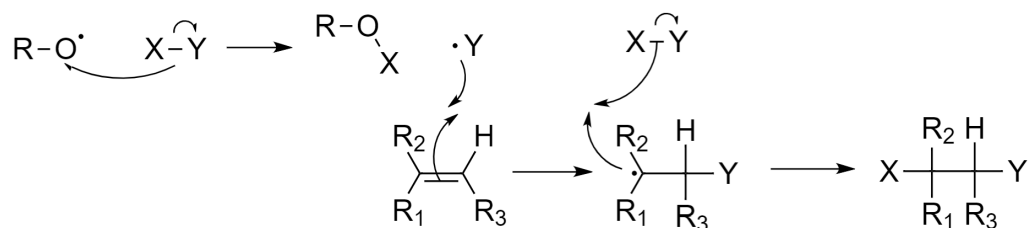
Markovnikov addition: the carbocation resides on the highest-order carbon.



(X-Y: electrophile, X: more electropositive, Y: more electronegative)

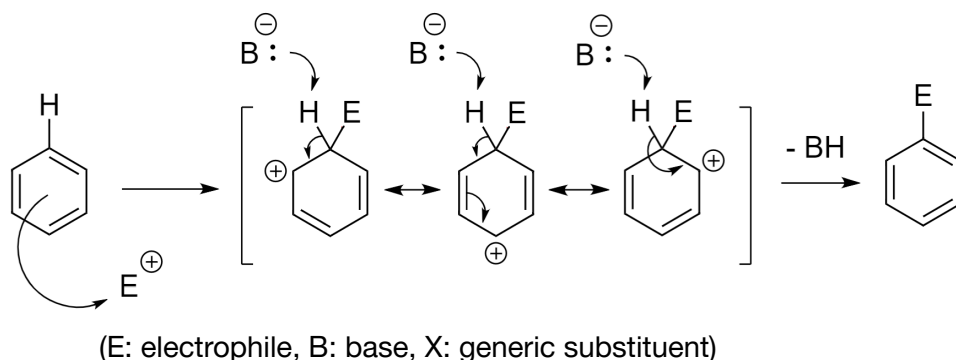
Anti-Markovnikov addition: the radical lies on the highest-order carbon.

In the presence of free radicals generated by e.g. R-O-O-R peroxide decomposition,

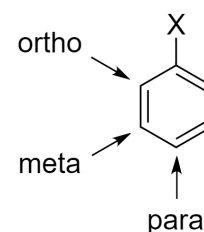


Rearrangements may occur to stabilise the transition state. In order of migratory aptitude,

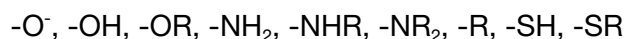
hydride shift > methyl shift > alkyl shift

16.1.7. Electrophilic Aromatic Substitution (EAS, S_NAr)

Substituents on an aromatic system influence the stability of the intermediate carbocation formed when an electrophile attacks. The stability of the carbocation is increased by resonance, hyperconjugation and positive inductive effects, in decreasing order of significance. A more stable carbocation indicates a higher regioselectivity towards substitution at the cationic position.

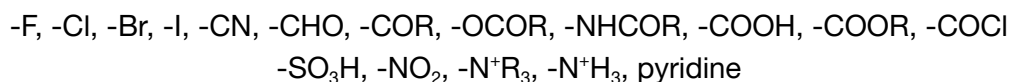


- **Electron-Releasing Groups (ERGs)** exhibit **positive** mesomeric and inductive effects (+M, +I). They decrease acidic strength. When present in an aromatic system, they favour substitution at the **ortho and para** positions, and are typically **activating** groups, increasing the rate of electrophilic substitution, **except** the halogens, which are deactivating. Examples of ERGs are:



Alkyl groups exhibit +I effects, with magnitude $3^\circ > 2^\circ > 1^\circ > -CH_3 > -H$, and increasing with the number of carbon atoms in the group e.g. *tert*-butyl \gg methyl.

- **Electron-Withdrawing Groups (EWGs)** exhibit **negative** mesomeric and inductive effects (-M, -I). They increase acidic strength. When present in an aromatic system, they favour substitution at the **meta** positions, and are typically **deactivating** groups, decreasing the rate of electrophilic substitution. Examples of EWGs are:

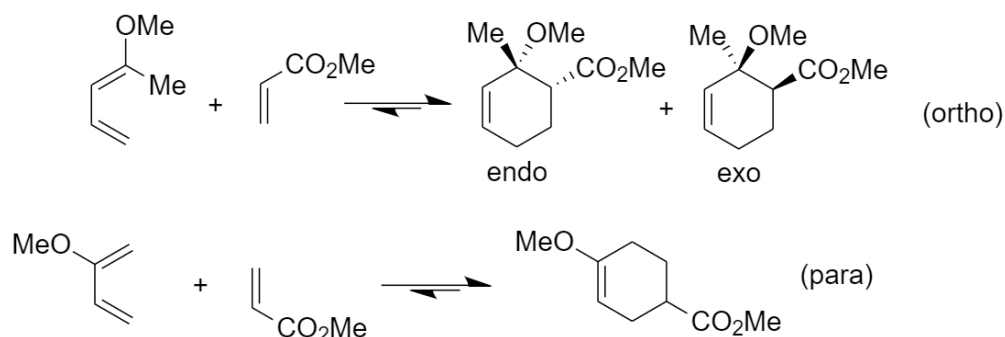


If multiple aromatic systems are present in a molecule, substitution will favour the one which is more activating, with the other being treated as a substituent e.g. 2-phenylpyridine can be mononitrated at the *meta* position on the benzene ring.

16.1.8. Pericyclic Reactions and Rearrangements

In a pericyclic reaction, π electrons move to form σ bonds in concerted fashion.

Diels-Alder Reaction: when an *s-cis*-diene reacts with a dienophile, two diastereomers form due to the different orientations in which the molecules may react:



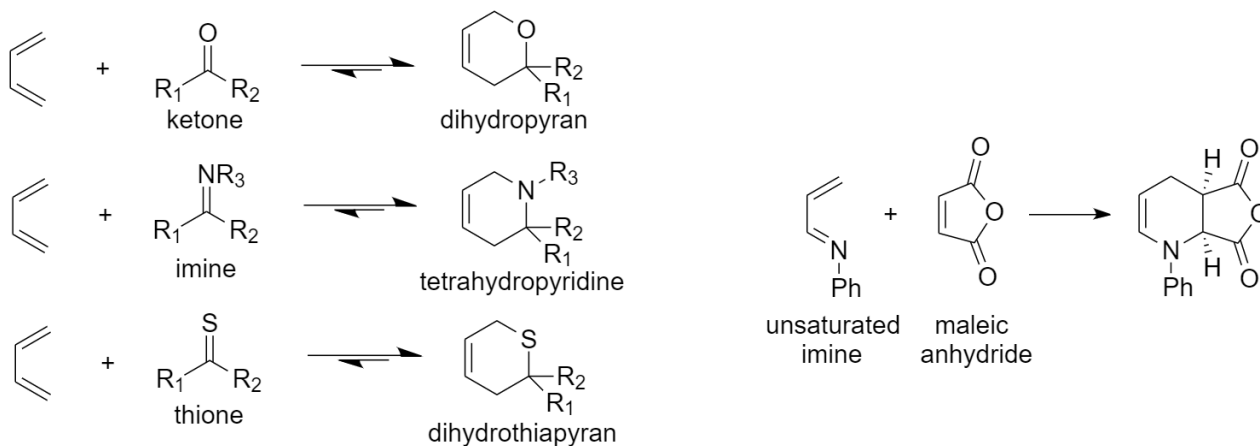
The enantiomers of each form will also be produced if they are not *meso* compounds.

- The *endo* form is the kinetically favoured product.
- The *exo* form is the thermodynamically favoured product.

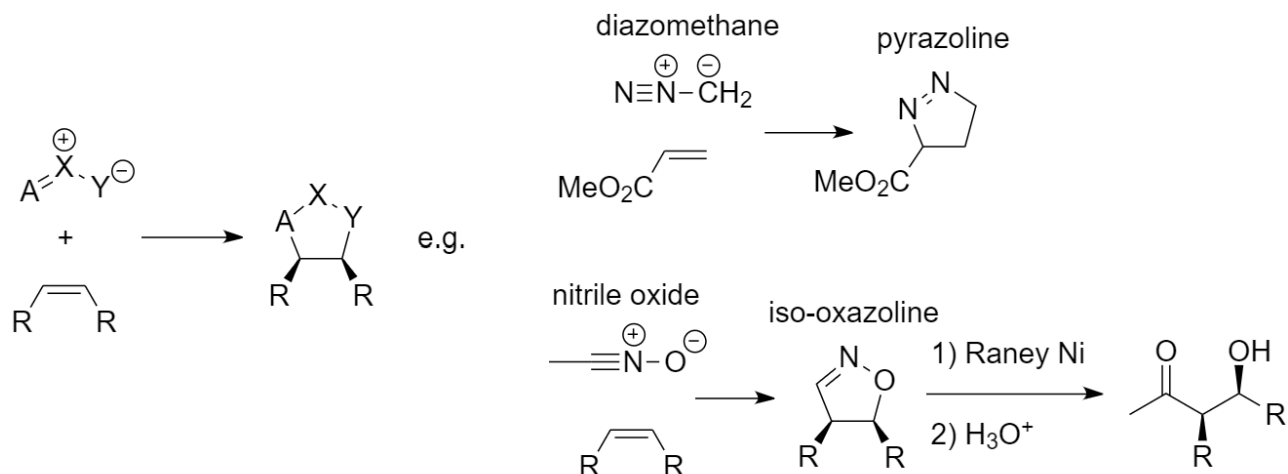
Rate increases with EWGs on dienophile and ERGs on the diene.

The two forms exist due to the fact that the diene can 'descend' onto the dienophile with the C group oriented in the same (*exo*) or opposite (*endo*) direction as the B group.

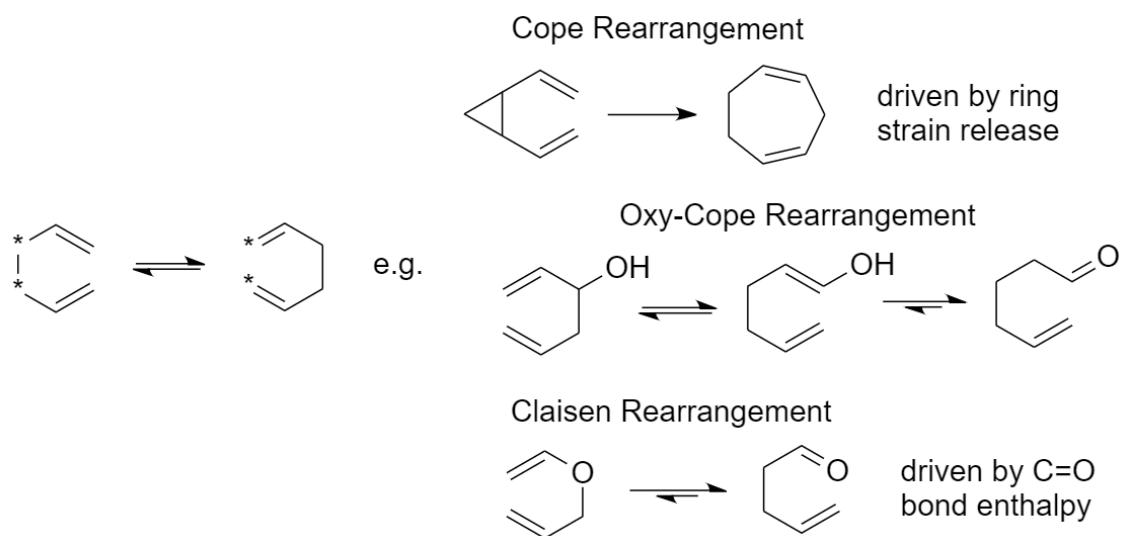
Heteroatomic Diels-Alder Reaction: atoms on the diene or dienophile can be replaced with e.g. O, N, S, as long as the dienophile remains electron-withdrawing and the diene remains electron-releasing, to form e.g. dihydropyran, tetrahydropyridines, dihydrothiapyran.



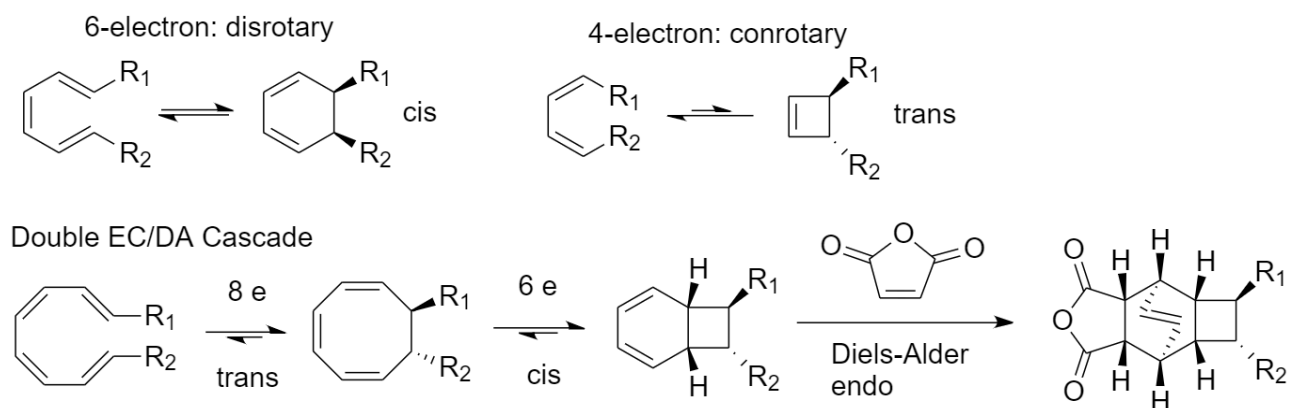
1,3-Dipolar Cycloadditions: unsaturated ylides react with alkenes to form a 5-membered ring in similar concerted [4+2] cycloaddition.



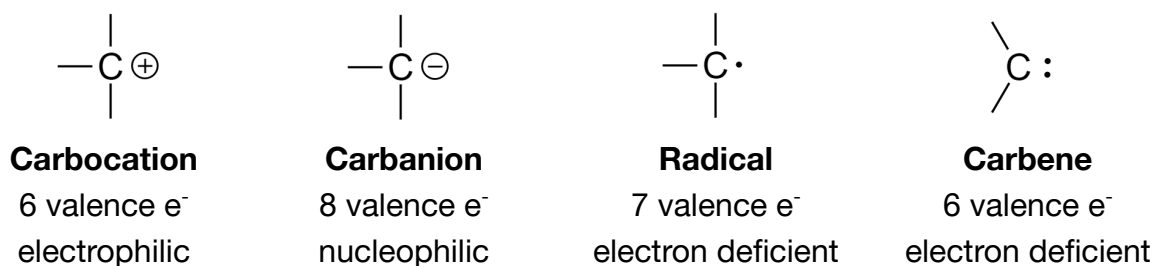
Sigmatropic Shifts: a [3+3] shift to form γ - δ unsaturated compounds.



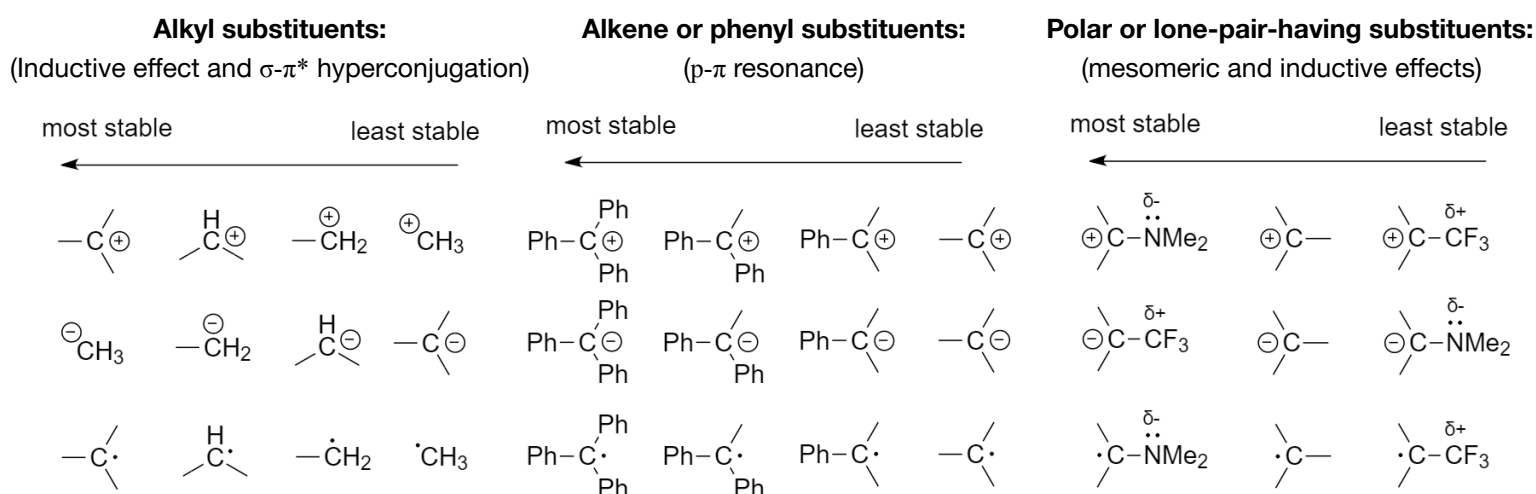
Electrocyclisation: formation of a σ bond to close a ring.



16.1.9. Types of Carbon Species (Carbocations, Carbanions, Radicals, Carbenes)



Carbocations, Carbanions and Radicals vary in stability depending on substituents:



Carbenes: reactive sp² hybridised carbons.

- **Triplet carbene:** diradical. One unpaired e⁻ in an sp² orbital and one unpaired e⁻ in a p orbital.
- **Singlet carbene:** paired electrons in an sp² orbital, empty p orbital.

Most chemical reactions which form carbenes (e.g. RCN₂ → RC:, CHCl₃ + NaOH → :CCl₂) result in the singlet state unless light is used to excite the electrons (photochemistry).

Addition of singlet carbenes onto π bonds is concerted with simultaneous sp² → π^* donation and π → p acceptance to form a cyclopropane ring. Stereochemistry is preserved.

Addition of triplet carbenes does not preserve stereochemistry since the process is stepwise. After the first bond formation, the remaining unpaired electron must change spin to form, which takes time (phosphorescence / spin-orbit coupling) so bonds may rotate.

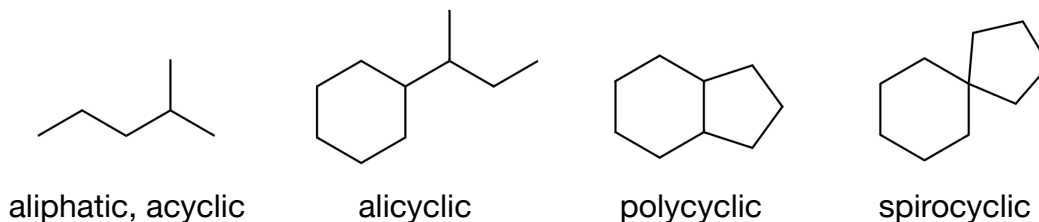
16.1.10. Woodward-Hoffmann Rules and Frontier Molecular Orbital Theory

16.1.11. Felkin-Ahn Model of Asymmetric Induction

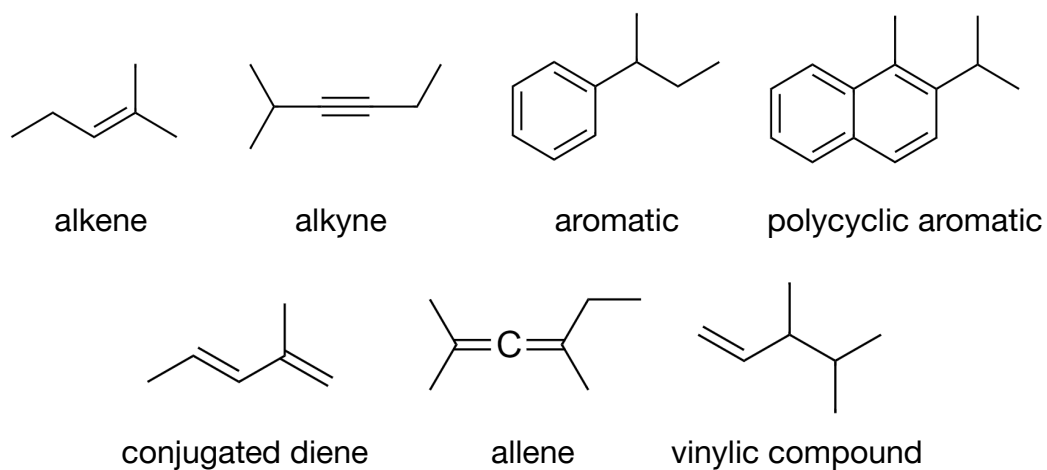
16.2. Structure of Organic Molecules

16.2.1. Classification of Hydrocarbons

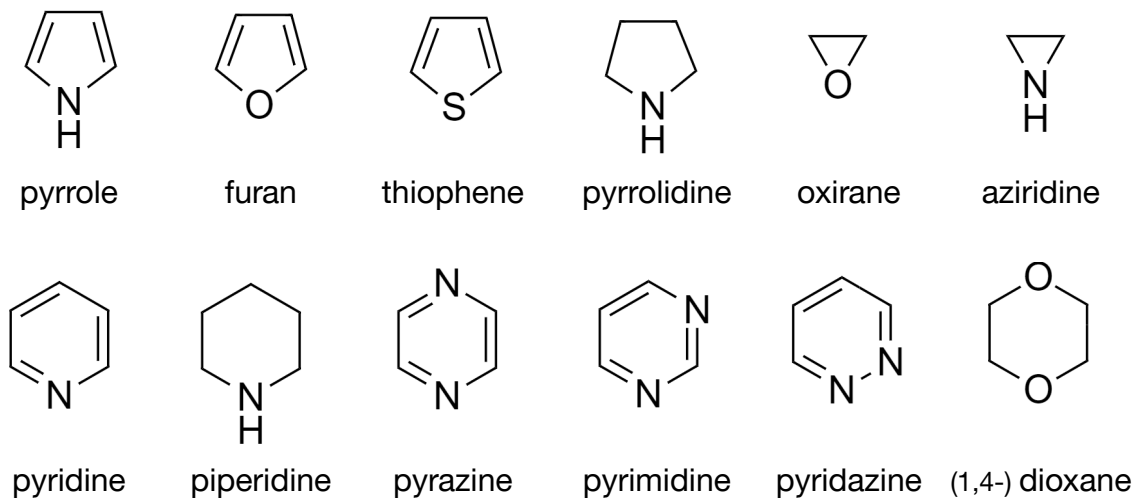
Saturated



Unsaturated

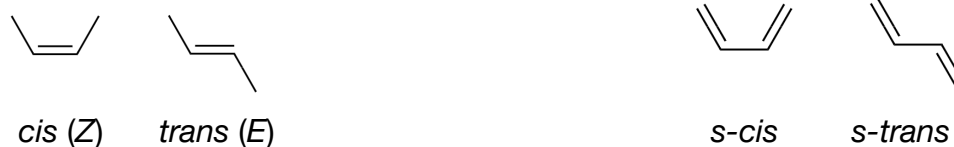


16.2.2. Heterocyclic Compounds



16.2.3. Nomenclature of Stereoisomerism Using Cahn-Ingold-Prelog (CIP) Convention

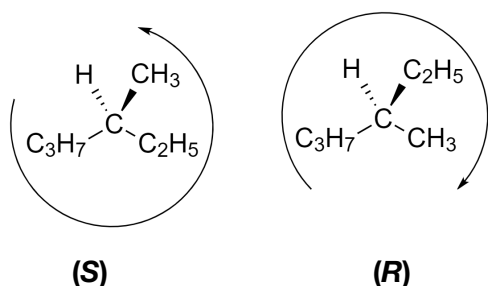
Geometric Isomerism



When alkenes are hetero-substituted, priority is assigned by the highest atomic number of the nearest neighbouring atom (**not** the group as a whole).

- The *trans* isomer is more stable than the *cis* isomer. They do not interconvert.
- The *s-trans* isomer is more stable than the *s-cis* isomer. They may interconvert.

Optical Isomerism



For chiral centres with four different substituents in sp^3 (tetrahedral) geometry, where the priority is assigned by the highest atomic number of the nearest neighbouring atom (**not** the group as a whole) when the lowest substituent (H in above example) is facing directly away from view.

anticlockwise priority

clockwise priority

Other conventions include:

- **D/L:** similarity to glyceraldehyde. D: anomeric hydroxyl group on the right of Fischer projection.
- **+/-:** + slows down right-handed (clockwise, from receiver) circularly polarised light, and vice versa.

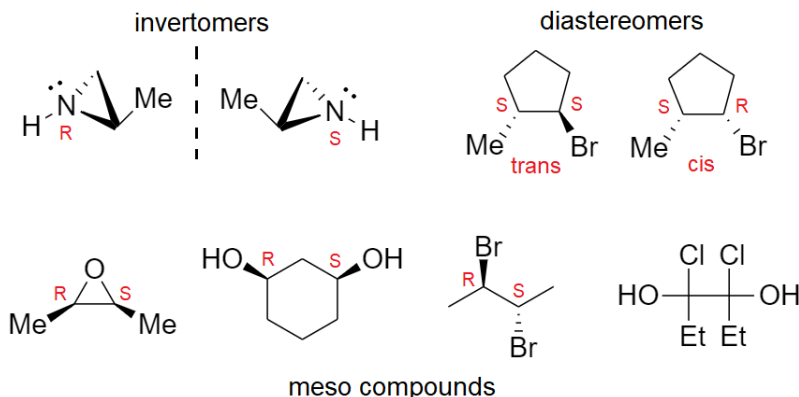
Specific optical rotation, $\alpha_{\lambda}^{(T)}$ [$\text{deg ml g}^{-1} \text{dm}^{-1}$] = $\frac{\Delta\theta [\text{deg}]}{c [\text{g ml}^{-1}] \times L [\text{dm}]}$, depends on temperature and wavelength.

Enantiomers rotate plane-polarised light in opposite directions (optically active).

Diastereomers: multiple stereocenters.

cis: same stereochemistry; *trans*: opposite stereochemistry.

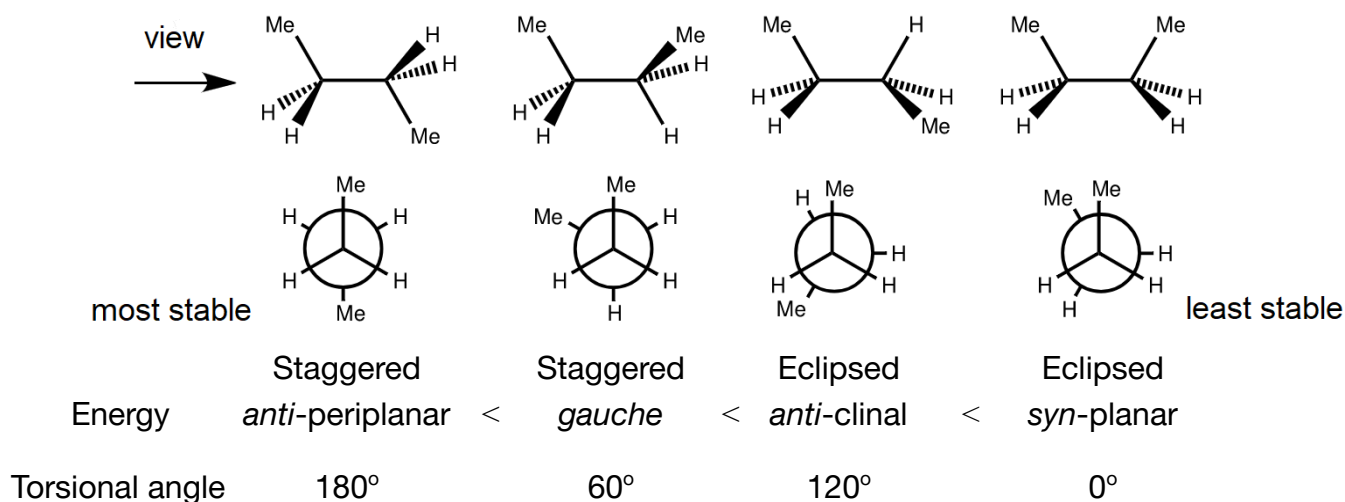
Invertomers: constrained N-centres.



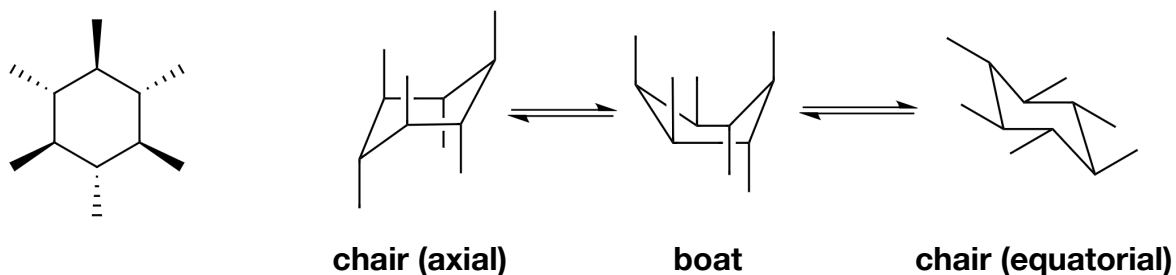
Meso compounds: both *R* and *S*, with a plane of symmetry (not chiral; inactive).

16.2.4. Nomenclature of Conformational Stereoisomerism

Newman Projections of the Rotamers of Butane



Bond-Line Structures of the Conformations of Cyclohexane

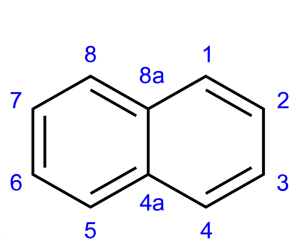


Hashed bonds are drawn downwards. Wedged bonds are drawn upwards.

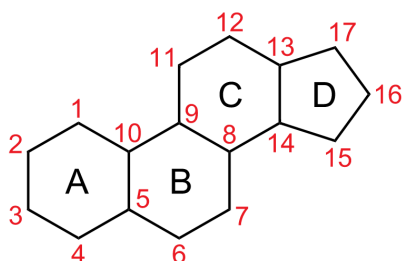
The relative position (axial / equatorial) of all substituents is swapped in a chair ring flip.

The stability of the three conformations depend on substituents: the more stable conformation minimises axial-axial interactions.

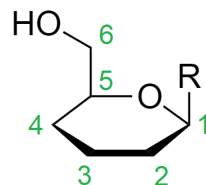
16.2.5. Numbering System for Specific Cyclic and Polycyclic Compounds



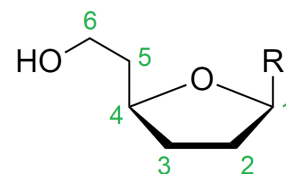
naphthalene



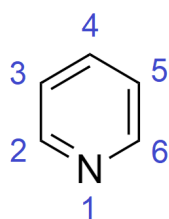
steroid



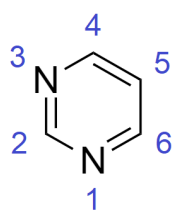
pyranose sugar



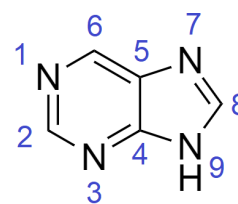
furanose sugar



pyridine



pyrimidine base



purine base

16.2.6. Nomenclature of Bicyclic and Spiro Compounds

Numbering of Bicyclic Compounds:

- Begin numbering from one bridgehead along the **longest** path to the 'other' bridgehead.
- Continue numbering from the 'other' bridgehead along the next longest paths.

Numbering of Spiro Compounds:

- Begin numbering in the smaller ring, adjacent to (not at) the spiro carbon.
- Continue numbering around the other ring.

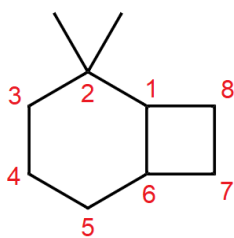
Naming:

- Count the total number of carbon atoms in the ring system, giving the root name.
- Find all unique paths between the bridgeheads, counting the number of carbons (x, y, z) between the bridgeheads.
- The name is then either

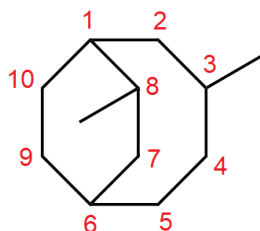
“bicyclo[$x.y.z$]alkane” (where $x \geq y \geq z \geq 0$)

or “spiro[$x.y$]alkane” (where $2 \leq x \leq y$)

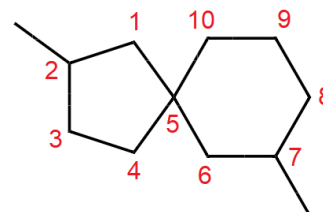
Examples:



2,2-dimethyl-
bicyclo[4.2.0]octane



3,8-dimethyl-
bicyclo[4.2.2]decane

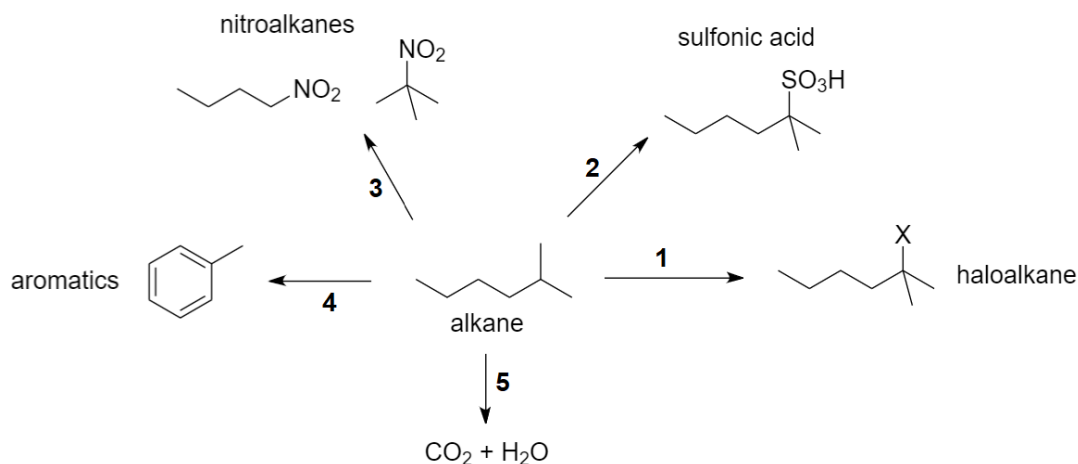


2,7-dimethyl-
spiro[4.5]nonane

16.3. Synthetic Organic Chemistry

16.3.1. Reactions of Hydrocarbons and Aliphatic Haloalkanes

Alkanes:



1: Halogenation. Reagents: X_2 (Cl_2 or Br_2), UV light ($h\nu$). Mechanism: free radical substitution.

Regioselectivity: $3^\circ > 2^\circ > 1^\circ$. Rate: $\text{Br} > \text{Cl}$.

2: Sulfonation. Reagents: oleum (conc. H_2SO_4 (g), *in situ* $\text{H}_2\text{S}_2\text{O}_7$), 400°C . Regioselectivity: $3^\circ > 2^\circ > 1^\circ$.

Only used for higher alkanes (carbon numbers $n \geq 6$).

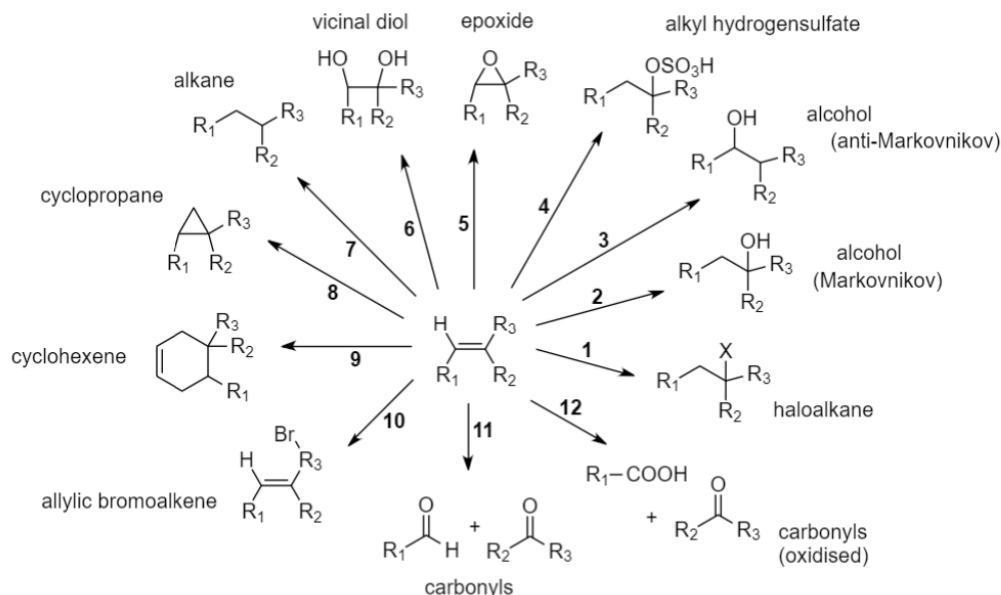
3: Nitration. Reagents: HNO_3 (g), 400°C . Forms a mixture of products by breaking all combinations of C-C and C-H bonds and replacing them with C- NO_2 .

4: Aromatisation. Reagents: Cr_2O_3 , Al_2O_3 cat, 600°C . Mechanism: cyclisation (reforming) then dehydrogenation. n -hexane \rightarrow benzene; n -heptane \rightarrow toluene.

5: Combustion (complete oxidation). Heat in air. Excess O_2 gives pure CO_2 and H_2O . Limiting O_2 gives incomplete combustion to C, CO, CO_2 , H_2O and some amount of the unburned hydrocarbons.

For reactions on alkanes used in the petrochemical industry, see Section 14.4.1.

Alkenes:



1: Hydrohalogenation or Dihalogenation. Reagents: **HX or X₂ in dry ether.** Mechanism: electrophilic addition. Rate: HI > HBr > HCl. Follows Markovnikov and peroxide rules.

2: (a) Acid catalysed hydration or (b) oxymercuration-demercuration. Reagents: **(a) H₂O, H₂SO₄ (aq) cat. or (b) 1) Hg(OAc)₂ (aq); 2) NaBH₄, NaOH.** Mechanism: electrophilic addition.

3: Hydroboration-oxidation. Reagents: **1) BH₃ or Sia₂BH or 9-borabicyclo(3.3.1)nonane (9-BBN), tetrahydrofuran (THF); 2) H₂O₂, NaOH, H₂O.** Mechanism: Step 1 involves addition of H and BHR' across the C=C bond. Regioselectivity: Anti-Markovnikov. Stereoselectivity: *syn* addition of H and OH.

4: Hydrogen sulfate formation. Reagents: **conc H₂SO₄.** Mechanism: electrophilic addition. Can be hydrolysed to the alcohol when heated. Regioselectivity: Markovnikov's rule. Stereoselectivity: *anti* addition of H and OSO₃H.

5: Epoxidation ((b): Prilezhaev reaction). Reagents: **(a) 1) Cl₂ + H₂O (in situ HClO); 2) NaOH or (b) RCO₃H (peroxy acid), dichloromethane or (c) for ethene only: O₂, Ag cat.** Mechanism: intramolecular S_N2. **(a)** forms a chlorohydrin intermediate. **(b)** also produces the carboxylic acid RCOOH.

6: Syn oxidation. Reagents: **(a) KMnO₄, cold NaOH (aq) (Baeyer's reagent) or (b) OsO₄, N-methylmorpholine N-oxide (NMO), NaHSO₄.**

7: Syn hydrogenation. Reagents: **H₂ (g), Ni / Pt / Pd-C cat, 50 °C.** Mechanism: heterogeneous catalysis.

8: Simmons-Smith cyclopropanation. Reagents: **Zn(Cu), CH₂I₂.** Mechanism: I-CH₂-ZnI carbenoid. Releases ZnI₂.

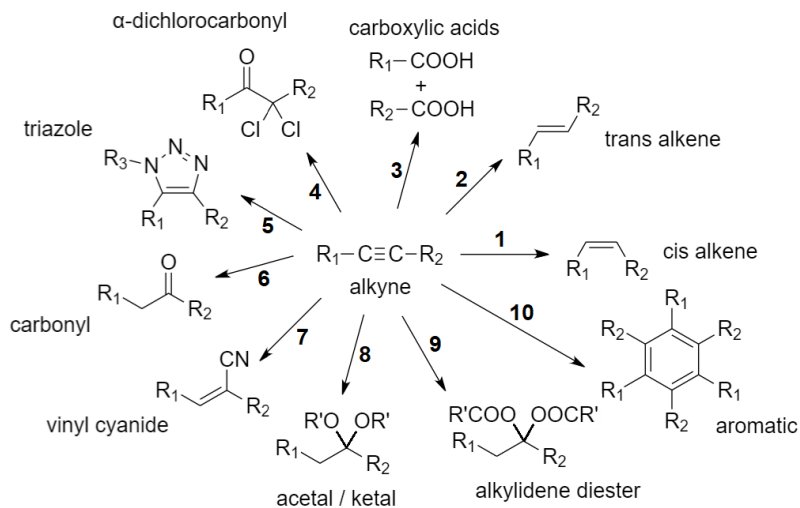
9: Diels-Alder cycloaddition. Reagents: **buta-1,3-diene, heat.** For more information, see Section 16.3.13.

10: Wohl-Ziegler reaction (allylic bromination). Reagents: **N-bromosuccinimide (NBS), (PhCOO)₂, CCl₄.**

11: Ozonolysis. Reagents: **1) O₃ (CCl₄); 2) Zn or dimethyl sulfide (DMS), H₂O.** Using H₂O₂ in step 2) gives R-COOH instead of R-CHO.

12: Oxidative cleavage. Reagents: **KMnO₄, hot conc H₂SO₄.**

Alkynes:



1: Partial syn hydrogenation. Reagents: H_2 (g), Pd-CaSO_4 cat., quinoline (Lindlar's catalyst). Mechanism: poisoned heterogeneous catalysis.

2: Birch reduction (partial anti hydrogenation). Reagents: Na (s), NH_3 (l) (in situ NaNH_2). Terminal alkynes ($\text{R}_2 = \text{H}$) stop at $\text{R}_1-\text{C}\equiv\text{C}^- \text{Na}^+$, which can undergo C-C bond-forming S_{N} reactions. Using Cu^+ or Ag^+ in this case forms similar alkynide salts.

3: Oxidative cleavage. Reagents: O_3 / KMnO_4 . Terminal alkynes ($\text{R}_2 = \text{H}$) give $\text{H}_2 + \text{CO}_2$ due decomposition of formic acid (HCOOH).

4: Condensation. Reagents: $\text{HCl} + \text{H}_2\text{O}$ (in situ HClO). Regioselectivity: R_1 more sterically bulky than R_2 .

5: Huisgen cycloaddition (Click chemistry). Reagents: R_3-N_3 (azide), copper(I) cat e.g. Cu_2O . Mechanism: [3+2] cycloaddition. Also forms the other isomer. Faster rate of reaction when alkyne is strained (SPAAC) e.g. cyclooctyne or benzyne.

6: Oxymercuration. Reagents: H_2O , HgSO_4 , H_2SO_4 . Mechanism: nucleophilic addition. Keto-enol tautomerism occurs. If terminal alkyne, ketone is favoured. Alkynes form π compounds with heavy metal ions (Hg^{2+} , Pb^{2+} , Ba^{2+}).

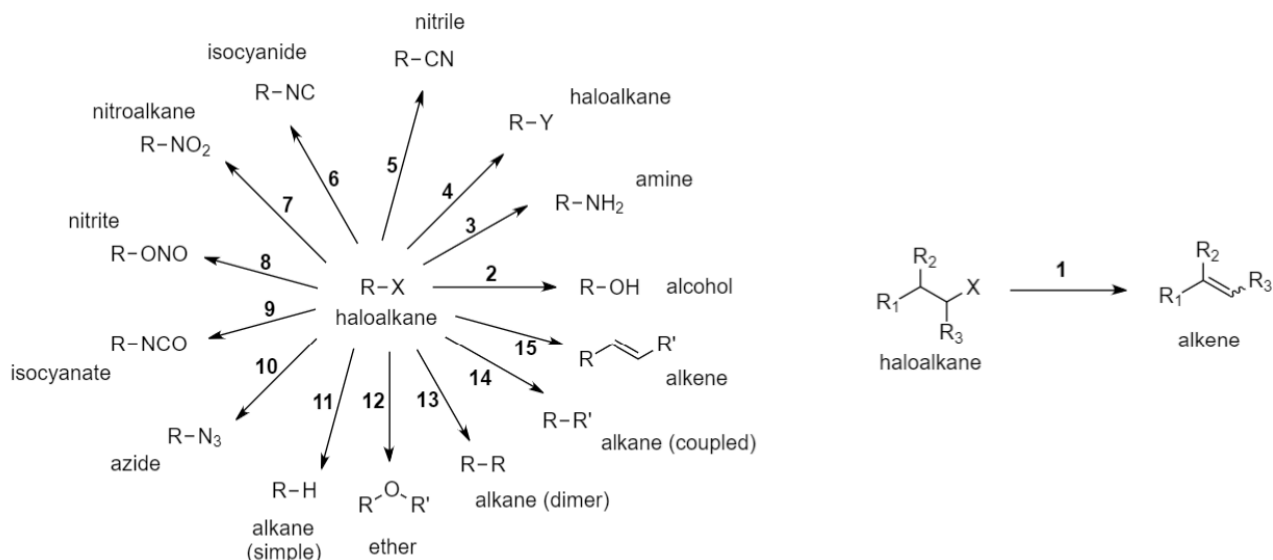
7: Nitrile addition. Reagents: $\text{Ba}(\text{CN})_2$. Mechanism: nucleophilic addition.

8: Acetal formation. Reagents: 1) $\text{R}'\text{-OH}$ (2 mol eq), HgSO_4 , heat; 2) H_2O ; 3) heat. Mechanism: 1) forms a vinyl ether. 2) hydrolyses to an alcohol and aldehyde. 3) forms the acetal.

9: Ester formation. Reagents: $\text{R}'\text{-COOH}$ (2 mol eq), HgSO_4 . Mechanism: nucleophilic addition. Using 1 mol eq $\text{R}'\text{-COOH}$ gives the vinyl (mono)ester.

10: Aromatisation (Alkyne trimerisation). Reagents: red hot iron tube, 600°C or rhodium(I) catalyst e.g. $\text{RhCl}(\text{PPh}_3)_3$ for intramolecular aromatisation. Mechanism: [2+2+2] cycloaddition. Acetylene \rightarrow benzene; propyne \rightarrow 1,3,5-methylbenzene. Impractical as shown due to excessive side reactions. Can be done using a compound with three alkyne bonds separated by 3-4 C's intramolecularly to form polycyclic compounds.

Haloalkanes:



1: Elimination. Reagents: **conc. NaOH, ethanol, heat**. Mechanism: elimination. Rate: $I > Br > Cl > F$; $3^\circ > 2^\circ > 1^\circ$.

2: Alcohol formation. Reagents: **dil NaOH (aq)**. Mechanism: nucleophilic substitution. Regioselectivity: Markovnikov's rule. Stereoselectivity: *Anti*-addition of H and OH. Rate: $I > Br > Cl > F$.

3: Hoffmann ammonolysis. Reagents: **NH₃, ethanol, heat in sealed tube**. Mechanism: nucleophilic substitution. Forms 2°, 3° and 4° ammonium salt if haloalkane is in excess.

4: (a) Finkelstein reaction (Y = I > Br > Cl) or (b) Swartz fluorination (Y = F). Reagents: **(a) HY, acetone or (b) AgF / SbF₃, dimethylsulfoxide (DMSO)**.

5: Nitrile formation. Reagents: **KCN, ethanol, heat**. Mechanism: nucleophilic substitution.

6: Isocyanide formation. Reagents: **AgCN**. Mechanism: nucleophilic substitution (AgCN more covalent than KCN).

7: Nitroalkane formation. Reagents: **AgNO₂**. Mechanism: nucleophilic substitution.

8: Alkyl nitrite formation. Reagents: **NaNO₂**. Mechanism: nucleophilic substitution.

9: Isocyanate formation. Reagents: **NaOCN**. Mechanism: nucleophilic substitution.

10: Azide formation. Reagents: **NaN₃**. Mechanism: nucleophilic substitution.

11: Reduction. Reagents: **LiAlH₄ in dry ether**. Non-selective.

12: Williamson ether synthesis. Reagents: **R'OH + Na (in situ R'ONa)**. Mechanism: nucleophilic substitution.

13: Wurtz coupling. Reagents: **Na, ether**.

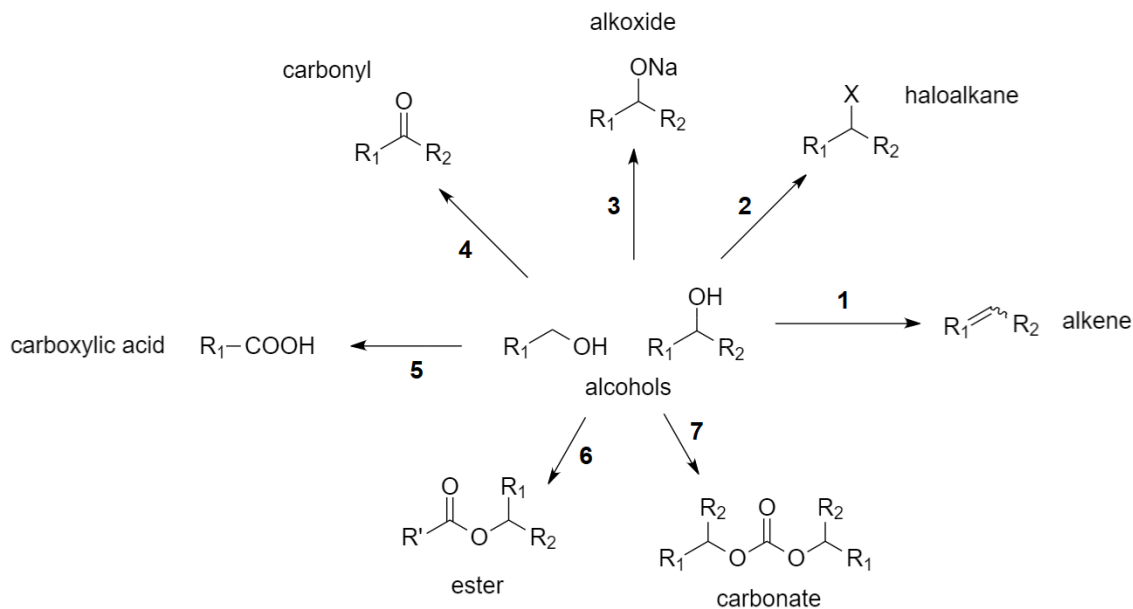
14. (a) Corey-House synthesis or (b) Grignard reaction or (c) Alkynide coupling or (d) Suzuki reaction or (e) Stille cross-coupling. Reagents: **(a) 1) Li + CuI; 2) R'-X (organic pseudohalide) or (b) R'-MgBr (Grignard reagent) or (c) R''-C≡C-Na (alkynide salt, where R'' = R''-C≡C-) or (d) R'-BY₂, Pd⁰ cat or (e) R'-SnBu₃, Pd cat.**

Mechanism: **(a)** 1) forms the complex Gilman reagent $Li^+ [R-Cu-R]^-$. 2) also forms RCu and LiX; **(b)** Releases MgBrX; **(c)** R''-C≡C-Na can be made from terminal alkynes with NaNH₂.

15. Heck reaction. Reagents: **Pd⁰ cat, base**. Releases HX. Mechanism: palladium cross-coupling catalytic cycle.

16.3.2. Reactions of Oxygen-Containing Organic Compounds

Alcohols:



1: Dehydration. Reagents: **conc. H_2SO_4 / $POCl_3$ / Al_2O_3 / P_2O_5 / ThO_2 / MoO_3 / Cu cat, heat.** Mechanism: elimination. Follows Zaitsev's rule. Stereoselectivity: trans alkenes favoured.

2: Halogenation. Reagents: **HX / PX_3 / PX_5 / $SOCl_2$, pyridine.** Mechanism: nucleophilic substitution. Forms a carbanion intermediate.

3: Neutralisation. Reagents: **Na (s).** Mechanism: Lewis acid-base reaction. Releases H_2 (g) as effervescence.

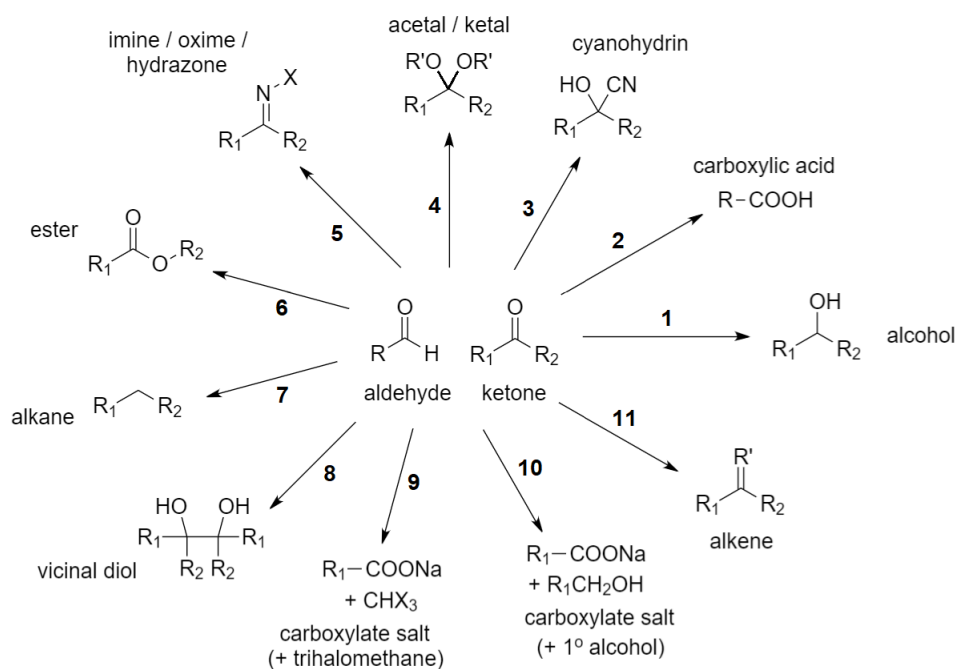
4: (a) Jones oxidation or (b) Oppenhour oxidation or (c) Dess-Martin oxidation or (d) Swern oxidation. Reagents: **(a) CrO_3 or $K_2Cr_2O_7$, H_2SO_4 (Jones reagent or similar chromates) / PCC (pyridinium chlorochromate) / PDC (pyridinium dichromate) or (b) Cu , $300\text{ }^\circ C$ / $(iPrO)_3Al$, heat or (c) DMP (Dess-Martin periodinane) or (d) 1) $(COCl)_2$ (oxalyl chloride), $DMSO$; 2) Et_3N .** Produces: 1° : aldehyde, requires distillation. 2° : ketone. 3° : unreactive without harsh oxidative cleavage. Partial oxidation; avoids complete oxidation of aldehydes.

5: Complete oxidation. Reagents: **excess $K_2Cr_2O_7$ + conc. H_2SO_4 / $KMnO_4$ / CrO_3 + H_2O , heat.** 1° only, requires reflux to oxidised intermediate aldehyde.

6: Fischer esterification. Reagents: **$R'-COOH$, H_3O^+ cat.** Releases H_2O by condensation.

7: Phosgenation. Reagents: **$COCl_2$ (phosgene).** Releases HCl . Forms chloroformate intermediate ($ROCOCl$).

Carbonyls (Aldehydes and Ketones):



1: (a) Non-selective reduction or (b) Grignard reaction or (c) Meerwein-Ponndorf-Verley reduction (MPV reduction). Reagents: **(a)** $NaBH_4$ / $LiAlH_4$ (less selective), **dry ether then NaOH**, or **(b)** R_3-MgBr , or **(c)** $(iPrO)_3Al$, **heat**. Reaction **(a)** can form 1° / 2° alcohols, **(b)** can form 3° alcohols.

2: Oxidation. Reagents: $K_2Cr_2O_7$, **conc. H_2SO_4** or $CrO_3 + H_2O$ (Jones reagent), **heat** or $KMnO_4$, or $AgNO_3$, NH_4OH (Tollen's reagent). Oxidises aldehydes only.

3: Cyanohydrin formation. Reagents: $NaCN$, HCl (aq) (in situ HCN). Mechanism: nucleophilic addition. Alternatively, using $NaHSO_3$ gives a bisulfite ($HO-C-SO_3Na$). Variation: α -aminonitrile formation, using NH_3 and HCN , which can be used to form amino acids by acid hydrolysis (Strecker amino acid synthesis).

4: Acetal / ketal formation. Reagents: $R'-OH$. 1 mol eq \rightarrow hemiacetal/hemiketal; 2 mol eq \rightarrow acetal/ketal; $R' = H$ (water) \rightarrow hydrate (geminal diol). Cyclic acetals form with diols. Mechanism: nucleophilic addition.

5: (a) Imine or (b) oxime or (c) hydrazone formation. Reagents: **(a)** $R-NH_2$ or **(b)** hydroxylamine (NH_2OH) or **(c)** hydrazine (N_2H_4). Mechanism: nucleophilic addition.

6: Baeyer-Villiger oxidation. Reagents: $R'CO_3H$ (peroxy acid: e.g. *meta*-chloroperoxybenzoic acid (m-CPBA)). Forms lactones (cyclic esters if using a cyclic ketone). Regioselectivity: R_2 more sterically bulky than R_1 .

7: (a) Wolff-Kischner reaction or (b) Clemmensen reduction or (c) Mozingo reaction. Reagents: **(a)** N_2H_4 , KOH or **(b)** $Zn(Hg)$ (zinc amalgam), **conc. HCl** or **(c)** 1) dithiol e.g. propane-1,3-thiol; 2) H_2 , Raney Ni. Mechanism: **(a)** hydrazone intermediate; **(b)** carbenoid mechanism; **(c)** 1) forms the cyclic dithioacetal. 2) $Ra-Ni$ irreversibly becomes nickel sulfide.

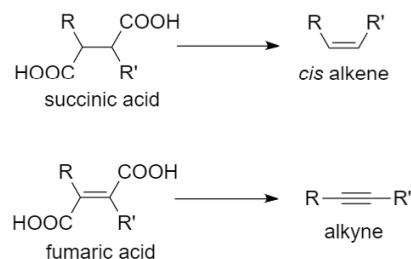
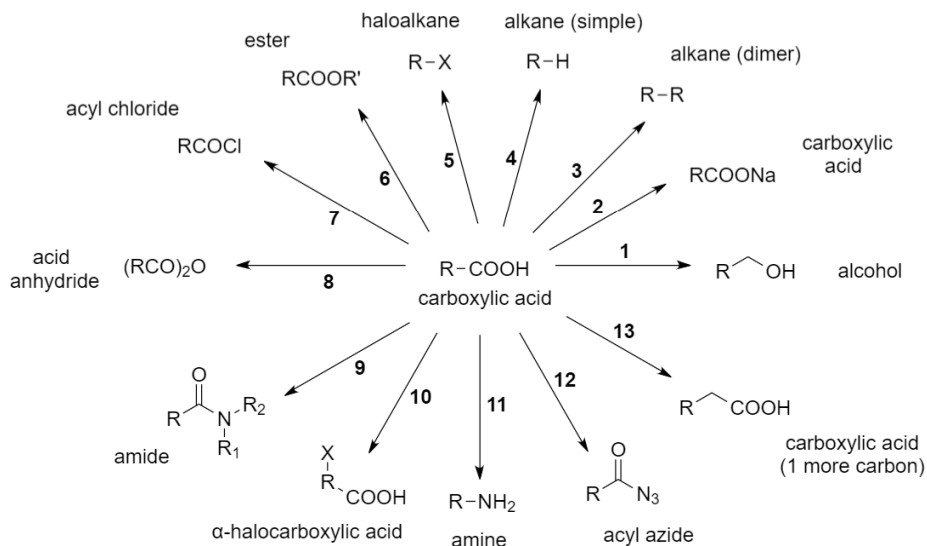
8: Pinacol radical coupling. Reagents: Mg (s) then H_3O^+ . Stereoselectivity: the two $-OH$ groups end up *syn* to each other. Mechanism: the intermediate complex has $C^*-O-Mg-O-C^*$.

9: Haloform reaction. Reagents: X_2 , $NaOH$ (in situ $NaXO$) ($X = Cl, Br, I$). Methyl ketones only. Releases CHX_3 .

10: Cannizzaro reaction. Reagents: $NaOH$. Non-enolisable aldehydes only. Mechanism: nucleophilic acyl substitution.

11: (a) Wittig reaction or (b) McMurry reaction ($R' = R_1-C-R_2$) or (c) Peterson olefination ($R' = R_3-C-H$). Reagents: **(a)** $Ph_3P + R'-Br$ (haloalkane) then base (Wittig reagent) or **(b)** $TiCl_4$, THF , $LiAlH_4$ (Ti^{2+} intermediate) or **(c)** 1) $Me_3Si-C(X)-R_3 + Mg/Li$; 2) acid or base. In **(a)**, R' must be 1° or 2° . In **(b)**, R' is identical to R_1-C-R_2 (the alkene is coupled). Stereoselectivity: **(a)** If $R' =$ alkyl, alkene is *cis*. If $R' =$ ester/ketone, alkene is *trans*. Mechanism: The Wittig reagent is an ylide (1,2-dipolar zwitterion), whose carbanion attacks the carbonyl; **(b)** uncontrolled (sterics). **(b)** can also work intramolecularly with amides or esters to form heterocycles; **(c)** In Step 2, acid yields *cis*, while base yields *trans*.

Carboxylic Acids:



1: Reduction. Reagents: NaBH_4 then NaOH or LiAlH_4 in dry ether (less selective).

2: Neutralisation. Reagents: NaOH / KOH .

3: Kolbe electrolysis. Reagents: 1) NaOH (aq); 2) electrolysis, collect at anode. Mechanism: decarboxylates to release CO_2 then fuses the α C in two alkyl radicals together. Forms the higher alkane at the anode. Variation:

3': Biradical Kolbe electrolysis of dicarboxylic acids. Reagents: 1) NaOH , 2 eq., 2) electrolysis with (a) for cis: Ni or (b) for trans: Na (s) + NH_3 (l) (in situ NaNH_2 ; Birch conditions). If the dicarboxylic acid has $\text{C}2=\text{C}3$ (e.g. fumaric acid, $\text{HOOC}-\text{C}=\text{C}-\text{COOH}$) then the alkyne is formed.

4: Decarboxylation. Reagents: soda lime (CaO , NaOH), heat. Releases CO_2 .

5: (a) Hunsdiecker reaction or (b) Kochi reaction. Reagents: (a) 1) AgF ; 2) X_2 , CCl_4 or (b) $\text{Pb}(\text{OAc})_4$, LiX .

6: Fischer esterification. Reagents: $\text{R}'\text{OH}$, H_3O^+ cat. Using $\text{R}'\text{-SH}$ (thiol) instead gives a thioester (RCOSR').

7: Acyl chloride formation. Reagents: SOCl_2 (thionyl chloride) or PCl_3 or PCl_5 , pyridine solvent.

8: Acid anhydride formation. Reagents: R-COCl or P_2O_5 . Mechanism: S_N then elimination.

9: Amide formation. Reagents: $\text{R}_1\text{-NH-R}_2$, heat or dicyclohexylcarbodiimide (DCC). Mechanism: S_N then E.

10: Hell-Volhard-Zelinsky reaction (HVZ reaction). Reagents: 1) $\text{P} + \text{X}_2$; 2) H_2O . Can react with ammonia to form amino acids.

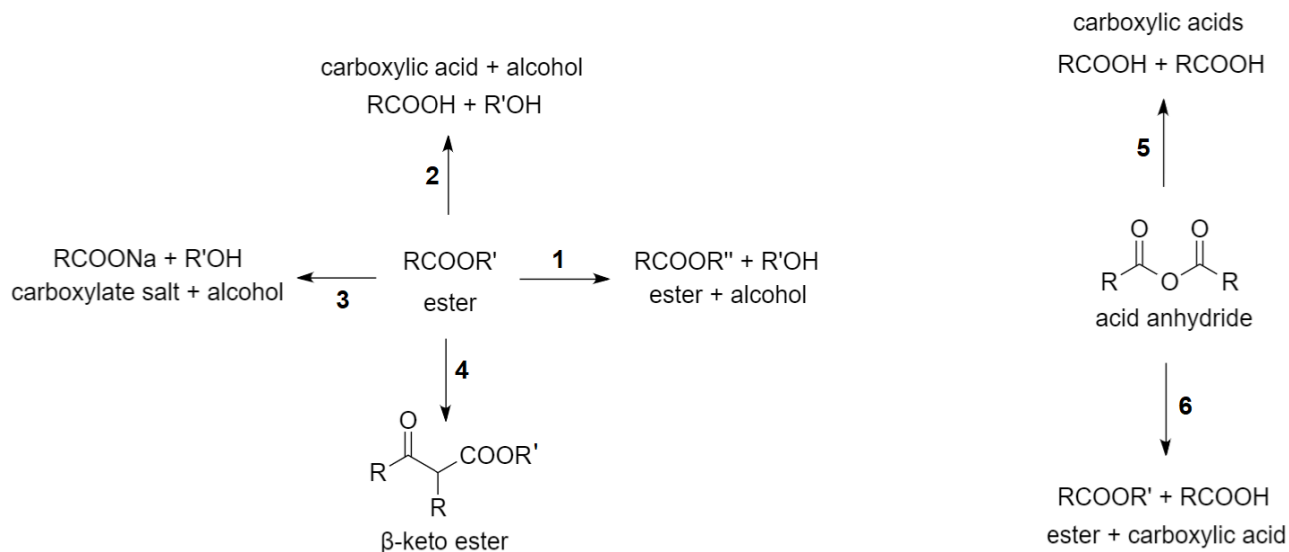
11: Schmidt reaction. Reagents: hydrazoic acid (HN_3), cold conc H_2SO_4 . Releases CO_2 and N_2 .

Mechanism: forms an isocyanate intermediate.

12: Acyl azide formation. Reagents: 1) N_2H_4 (hydrazine); 2) HNO_2 (nitrous acid) or diphenylphosphoryl azide (DPPA). Mechanism: 1) forms the acyl hydrazine (R-CO-NH-NH_2). 2) forms the acyl azide. DPPA forms the acyl azide directly.

13: Arndt-Eistert reaction (homologation). Reagents: 1) SOCl_2 ; 2) CH_2N_2 (diazomethane), ether; 3) Ag^+ cat, H_2O , dioxane. Mechanism: Wolff rearrangement of the intermediate diazoketone via the ketene. Using $\text{R}'\text{OH}$ or $\text{R}'\text{NH}_2$ in Step 3 results in the ester $\text{RCH}_2\text{COOR}'$ or amide $\text{RCH}_2\text{CONHR}'$ respectively. Can be used to convert α -amino acids to β -amino acids with protection.

Esters and Acid Anhydrides:



1: Transesterification. Reagents: $\text{R}''\text{-OH}$.

2: Acid hydrolysis. Reagents: H_2O , HCl (aq) cat. Equilibrium.

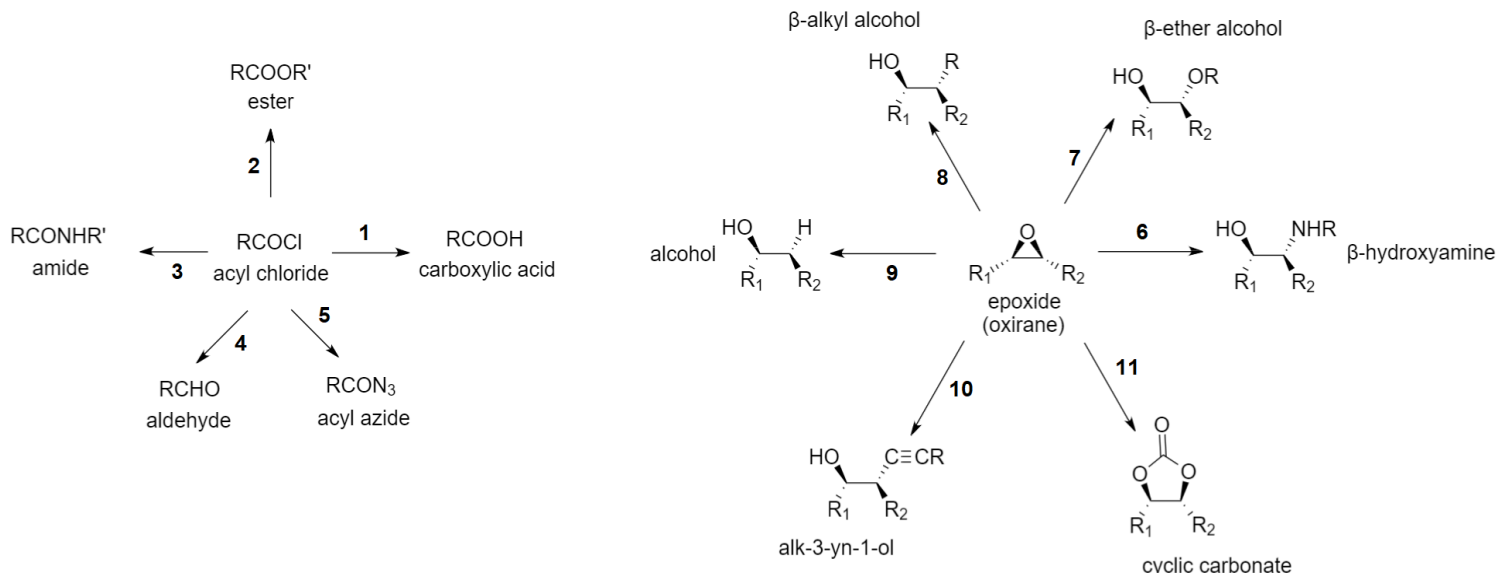
3: Base hydrolysis / saponification. Reagents: H_2O , NaOH (aq) .

4: (a) Claisen condensation or (b) Dieckmann rearrangement (intramolecular). Reagents: **1) $\text{R}'\text{ONa}$, ethanol;** **2) H_3O^+ .** Mechanism: enolate chemistry. Can use two different esters for cross-Claisen condensation. The $\text{R}'\text{ONa}$ alkoxide base must match the R' group in the ester to avoid product mixtures due to trans esterification.

5: Hydrolysis. Reagents: H_2O , **pyridine solvent.** Using H_2O_2 instead forms a peroxy acid $\text{RCO}_3\text{H} + \text{RCO}_2\text{H}$.

6: Esterification. Reagents: $\text{R}'\text{OH}$.

Acyl Chlorides (Acid Chlorides) and Epoxides



1: Hydration. Reagents: H_2O . Releases HCl as effervescence.

2: Esterification. Reagents: $\text{R}'\text{OH}$, *pyridine solvent*. The pyridine neutralises the acid.

3: Schotten-Baumann reaction (amidation). Reagents: $\text{R}'\text{NH}_2$, H_2O , Et_2O .

4: Rosenmund reduction. Reagents: H_2 (g), Pd-BaSO_4 cat, *quinoline (Rosenmund catalyst)*. Mechanism: poisoned heterogeneous catalysis. Selective for acyl chlorides.

5: Acyl azide formation. Reagents: NaN_3 or Me_3SiN_3 .

6: Amine addition by (a) Acid or (b) base catalysed epoxide ring opening. Reagents: RNH_2 (amine), CH_3NO_2 solvent, (a) acid or (b) base. Stereoselectivity: Anti-addition of -OH and -NHR. Regioselectivity: (a) steric hindrance $\text{R}_2 > \text{R}_1$; (b) steric hindrance $\text{R}_1 > \text{R}_2$.

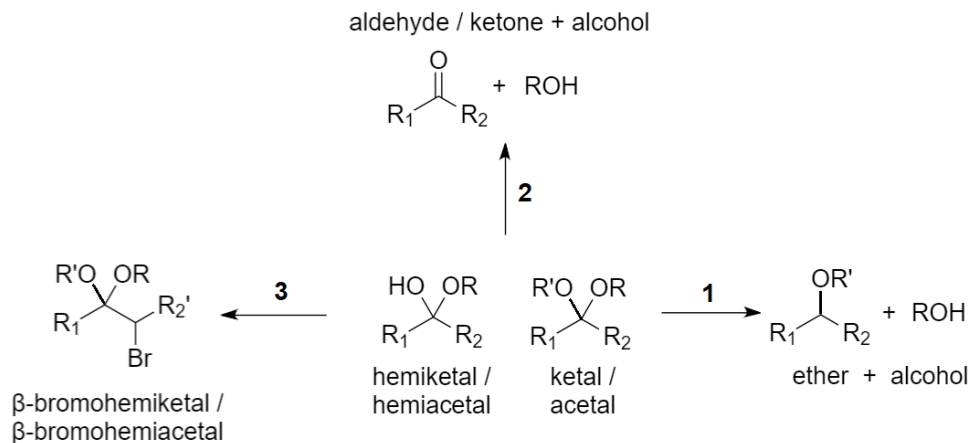
7: Alcohol addition by base catalysed epoxide ring opening. Reagents: ROH , base. Anti addition of -OH and -OR.

8: Grignard reaction. Reagents: R-MgBr , H_3O^+ . Anti addition of -OH and -R.

9: Reduction. Reagents: LiAlH_4 , *dry ether*, H_3O^+ . Anti addition of -OH and -H.

10: Alkylidene addition. Reagents: $\text{R}'\text{-C}\equiv\text{C}^- \text{Li}^+$ (alkylidyne), H_3O^+ . Mechanism: nucleophilic addition. Anti addition of -OH and -C-C \equiv C-R.

11: Cyclic carbonate formation. Reagents: CO_2 , Zn / Al / *ammonium-based catalyst*. Organic carbonates are useful for carbon storage (green chemistry) and as electrolytes in LiPo batteries.

Acetals and Ketals:

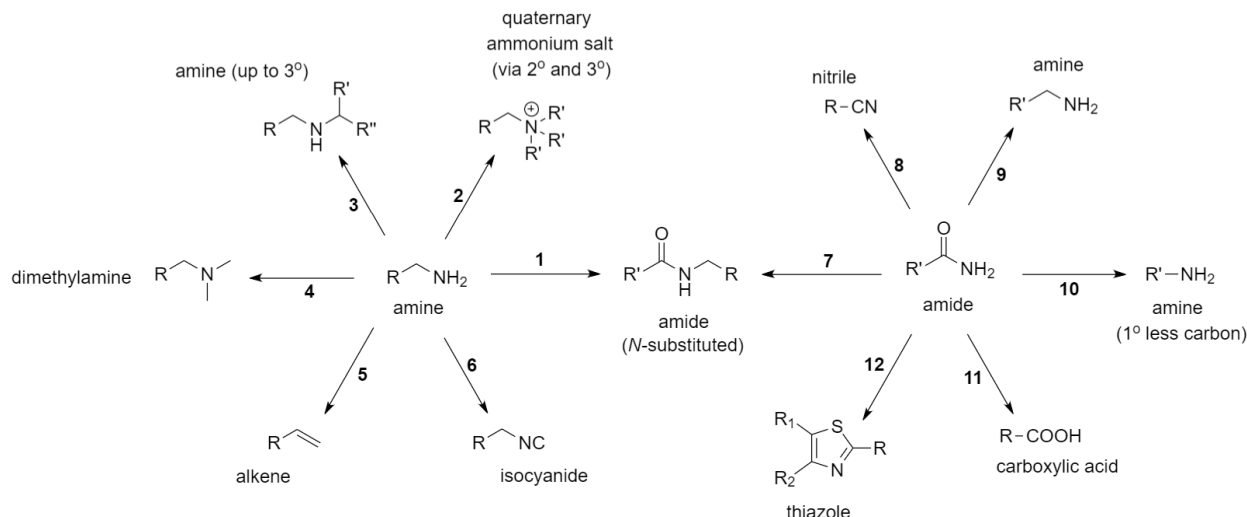
1: Reduction. Reagents: **diisobutylaluminium hydride (DIBAL-H)**. Note that LiAlH_4 does **not** reduce acetals/ketals, allowing e.g. ethane-1,2-diol to be used to protect aldehydes/ketones during reduction (forms a cyclic acetal).

2: Acid hydrolysis. Reagents: H_3O^+ . Used for de-protecting.

3: β -Halogenation ($\text{R}_2 = \text{R}_2' - \text{CH}_2 -$). Reagents: $\text{Br}_2 (\text{l})$. Mechanism: protons adjacent to acetal are slightly acidic.

16.3.3. Reactions of Nitrogen-Containing Organic Compounds

Amines and Amides:



1: Amidation. Reagents: **(a) R'COOH, heat or (b) R'COCl, pyridine or (c) (R'CO)₂O, pyridine.**

Mechanism: nucleophilic addition-elimination.

2: Hoffman ammonolysis / alkylation. Reagents: **excess R'-X**, via the 2° and 3° amines.

3: Reductive amination. Reagents: **R'-CO-R'' (carbonyl), NaBH₃CN.** Mechanism: imine/iminium intermediate.

4: Eschweiler-Clarke reaction. Reagents: **CH₂O, HCOOH.** Mechanism: imine/iminium intermediate. Releases CO₂.

5: Hoffman elimination. Reagents: **1) excess MeI; 2) Ag₂O, H₂O, heat, vacuum.** Mechanism: Step 1 forms the quaternary trimethylammonium salt, Step 2 is thermal decomposition of the hydroxide salt. Regioselectivity: anti-Zaitsev (forms the **least** substituted alkene).

6: Carbylamine reaction. Reagents: **CHCl₃, KOH (ethanolic chloroform).** Mechanism: dichlorocarbene (:CCl₂) forms as an intermediate.

7: Alkylation. Reagents: **R'-X.**

8: Dehydration. Reagents: **SOCl₂ or POCl₃ or P₂O₅, pyridine, distil.** Requires primary amide. Releases SO₂ + HCl.

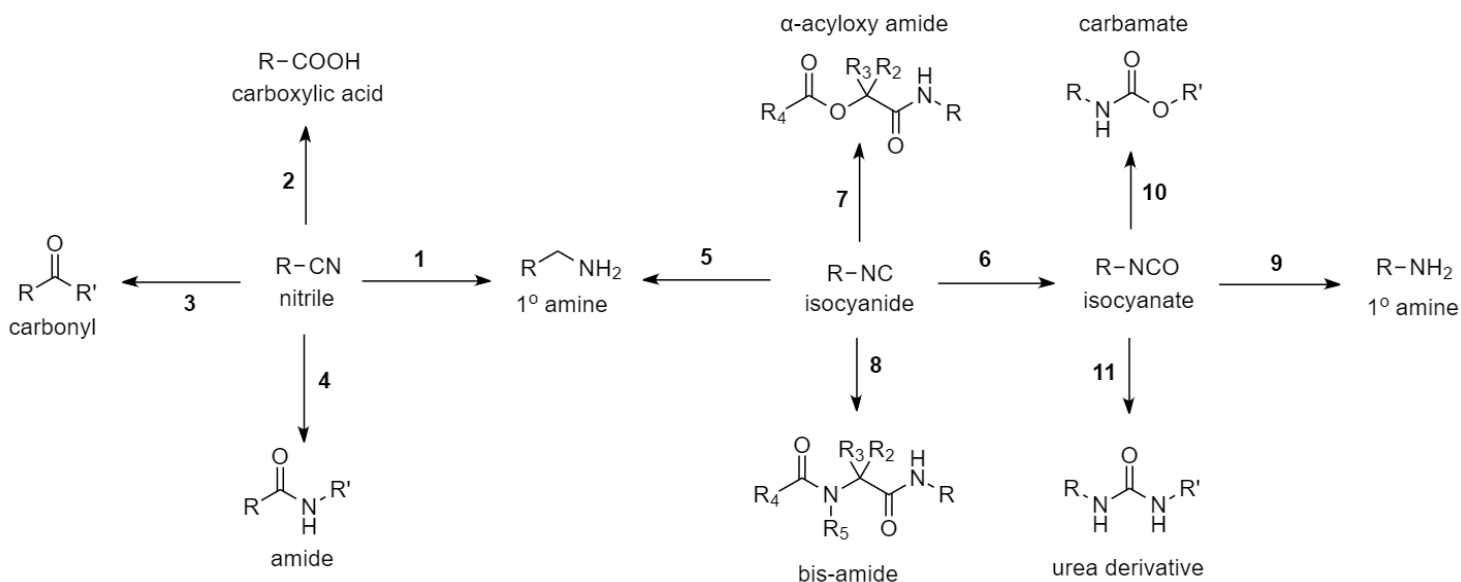
9: Reduction. Reagents: **LiAlH₄, dry ether.** Can be used to form 3° amines from *N,N*-disubstituted amides.

10: Hoffman degradation / rearrangement / bromoamide synthesis. Reagents: **1) Br₂ + NaOH (in situ NaBrO); 2) H₂O.** Mechanism: 1) generates NaBrO, which forms the intermediate isocyanate. 2) adds water to give a carbamic acid which loses CO₂ to give the amine.

11: Acid hydrolysis. Reagents: **H₂O, H₂SO₄.** Releases NH₃ (or amine if substituted).

12: Hantzsch thiazole synthesis. Reagents: **1) anisole (CH₃-O-C₆H₅; methoxybenzene) + P₂S₅ (Lawesson's reagent); 2) α-haloketone (R₁-CHX-CO-R₂), heat.** Mechanism: Lawesson's reagent converts C=O to C=S (thioamide). 2) forms the ring, releasing HX and H₂O. For other heterocycles, see Section 16.3.9.

Nitriles, Isocyanides and Isocyanates:



1: Reduction. Reagents: $LiAlH_4$ then H_2O . Mechanism: $LiAlH_4$ forms the dianion $[R-C-N]^{2-}$. Water forms the primary amine. Also can be used with nitroalkanes i.e. $R-CH_2NO_2 \rightarrow R-CH_2NH_2$.

2: Oxidation. Reagents: H_2SO_4 (aq), heat. Mechanism: forms an amide intermediate.

3: Grignard reaction. Reagents: $R'MgX$, H_3O^+ . Also works with HCN to form aldehydes.

4: Ritter reaction. Reagents: $R'OH$ (alcohol), H_3O^+ . Works best for 3° alcohols. Mechanism: alcohol is eliminated to give the carbocation, which is attacked by the nitrile. Any species which generates a carbocation can be used e.g. alkenes, epoxides. Stereoselectivity: *syn* addition. Extensions can be used in enantioselective organocatalysis.

5: Reduction. Reagents: $LiAlH_4$ then H_2O . Mechanism: $LiAlH_4$ forms the dianion $[R-C-N]^{2-}$. Water forms the primary amine.

6: Oxidation. Reagents: $HgCl_2$, H_2O . Releases Hg (l) and HCl. Forms the isocyanate.

7: Passerini reaction. Reagents: R_4-COOH (carboxylic acid), $R_2-C(O)-R_3$ (ketone).

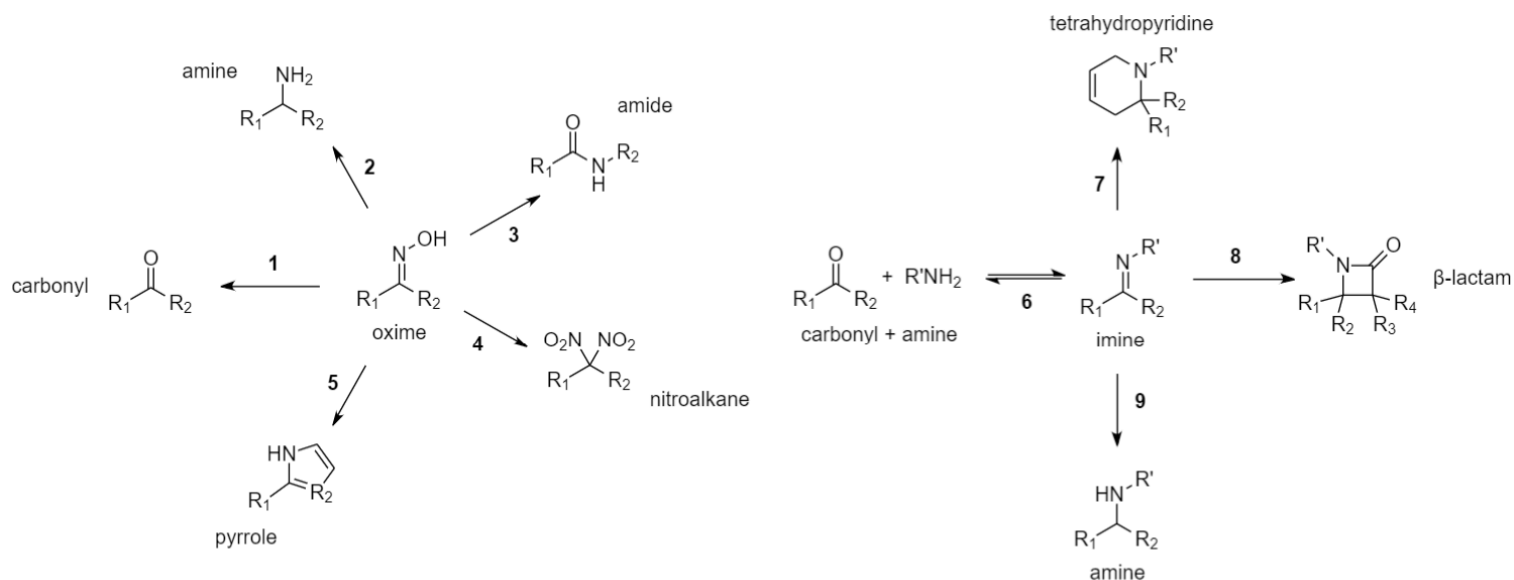
8: Ugi reaction. Reagents: R_4-COOH (carboxylic acid), $R_2-C(O)-R_3$ (ketone), R_5-NH_2 (amine).

9: Hydration. Reagents: H_2O . Mechanism: nucleophilic addition.

10: Alcoholysis. Reagents: $R'OH$. Mechanism: nucleophilic addition.

11: Ammonolysis. Reagents: $R'NH_2$. Mechanism: nucleophilic addition. Forms a urea derivative.

Oximes, Imines and Hydrazones:



1: Hydrolysis. Reagents: H_2O . Occurs naturally (equilibrium).

2: Reduction. Reagents: NaBH_4 or LiAlH_4 or H_2 / Ni .

3: Beckmann rearrangement. Reagents: H_2SO_4 or SOCl_2 or PCl_5 (aq) cat.
Cyclic oximes give lactams with +1 ring number. Orientation depends on oxime E/Z.

4: Ponzio reaction. Reagents: N_2O_4 .

5: Cyclisation. Reagents: C_2H_2 (acetylene).

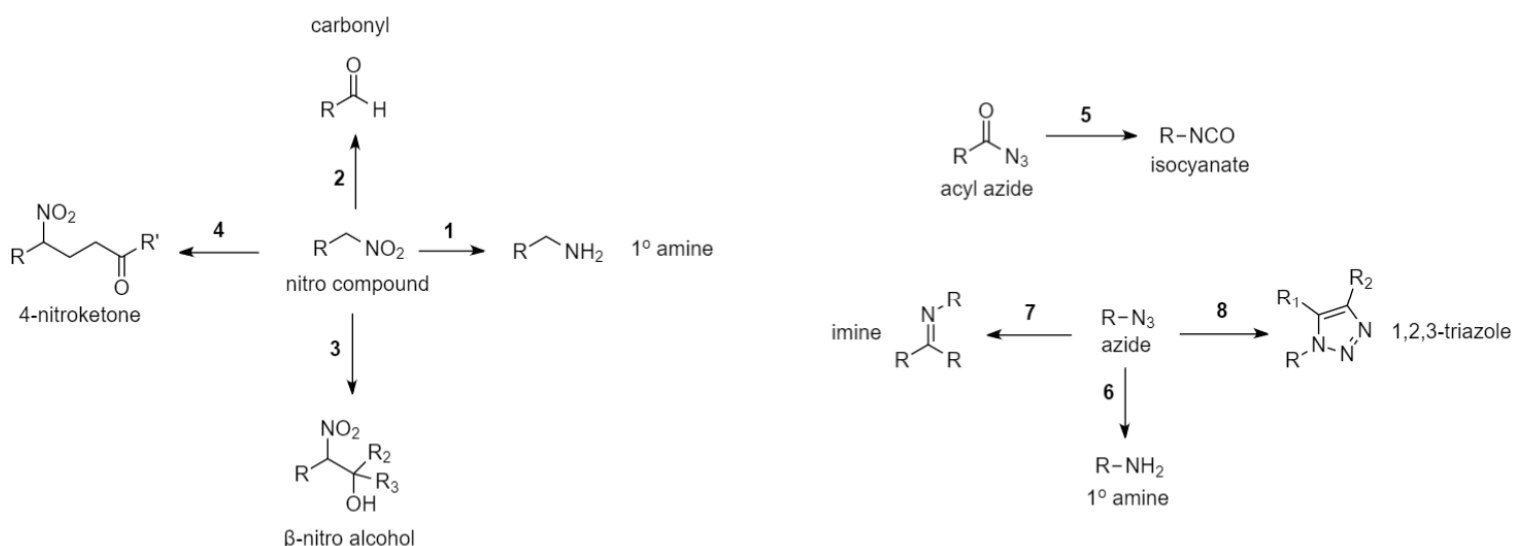
6: Hydrolysis. Reagents: H_2O . Occurs naturally (equilibrium).

7: Hetero Diels-Alder reaction. Reagents: buta-1,3-diene. Mechanism: [4+2] cycloaddition.

8: Staudinger synthesis of β -lactams. Reagents: $\text{R}_3\text{-C(=O)-R}_4$ (ketene). Mechanism: [2+2] cycloaddition.

9: Reductive amination. Reagents: H_2 (high pressure) / Pd.

Nitroalkanes, Azides and Acyl Azides:

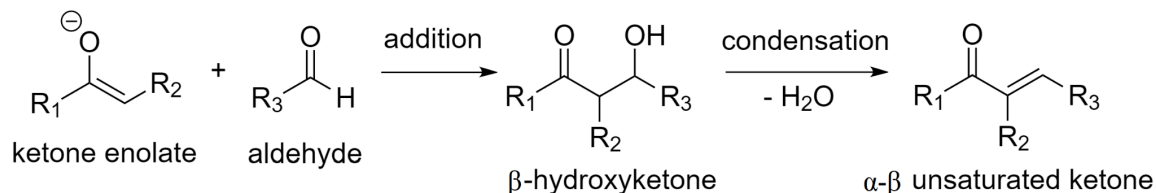


- Reduction.** Reagents: H_2 / Pd or Sn / HCl or LiAlH_4 (non-selective, forms azo compound with nitrobenzene).
- Nef reaction.** Reagents: 1) OH^- ; 2) H_3O^+ . Releases N_2O . Mechanism: Step 1 forms a nitronate salt intermediate.
- Henry reaction (nitroaldol reaction).** Reagents: OH^- . This product can be eliminated to a nitroalkene, reduced to a β -amino alcohol or oxidised to an α -nitro carbonyl.
- Michael addition (umpolung).** Reagents: $\text{CH}_2=\text{CH-C(O)R}'$ (α - β unsaturated ketone), base then acid. The nitro compound acts as the Michael donor, with a carbanion at the α position. If R is an acidic and base is in excess then the product can undergo intramolecular aldol reaction to a cyclopentenone (like a Robinson annulation).
- Curtius rearrangement.** Reagents: heat (thermal decomposition).
- Staudinger reaction.** Reagents: 1) PPh_3 ; 2) H_2O . Mechanism: Step 1 forms the ylide $\text{Ph}_3\text{P=NR}$.
- Aza-Wittig reaction.** Reagents: 1) PPh_3 ; 2) R_2CO (ketone).
- Huisgen cycloaddition.** Reagents: $\text{R}_1\text{-C}\equiv\text{C-R}_2$ (alkyne), heat or Cu or Ru cat. A good click reaction.

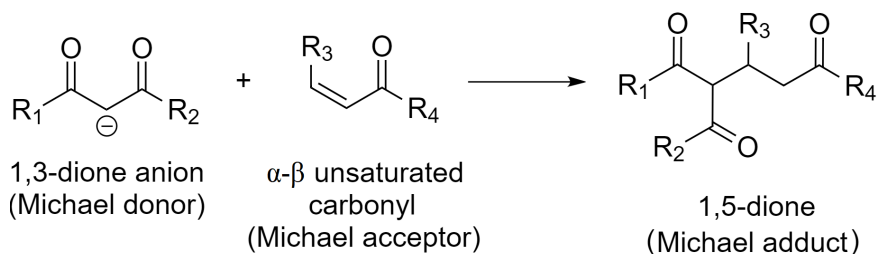
16.3.4. Reactions Involving Enolate Chemistry

Some reactions of carbonyls proceed via enol (carbonyl + acid) or enolate (carbonyl + base) chemistry. Common bases are NaOH, KOH, Ba(OH)₂.

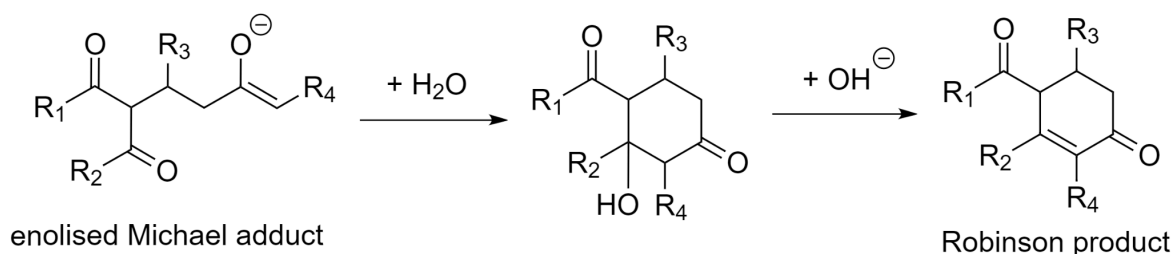
Aldol Reaction: using enolate form (if enol form, aldehyde is protonated; same products):
Cross-aldol products may form with multiple reacting carbonyls, such as in:



Michael Addition: the dione anion can be formed with 1,3-dione + base:

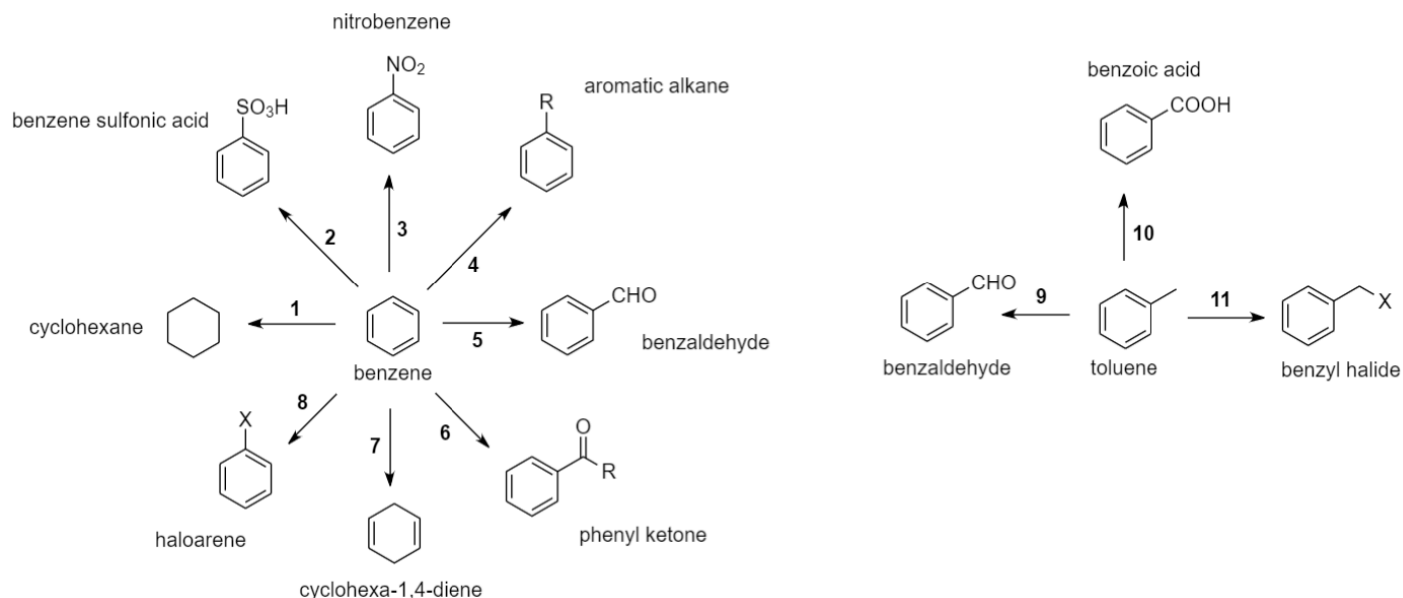


Robinson Annulation: a Michael addition followed by an intramolecular aldol reaction, possible if excess base is present:



16.3.5. Reactions of Aromatic Compounds

Benzene and Toluene:



1: Hydrogenation. Reagents: H_2 (3 mol eq.), Ni cat, $300\text{ }^\circ\text{C}$, 30 atm. Requires harsher conditions than regular hydrogenation since benzene is resonance stabilised.

2: Sulfonation. Reagents: SO_3 , conc H_2SO_4 , reflux.

3: Nitration. Reagents: conc HNO_3 and H_2SO_4 (aq), $30\text{ }^\circ\text{C}$. At higher temps, 1,3- and 1,3,5- compounds form.

4: Friedel-Crafts alkylation. Reagents: R-Cl (haloalkane) + AlCl_3 cat.

5: Gatterman-Koch reaction. Reagents: $(\text{CO}$ or $\text{HCN}) + \text{HCl}$.

6: Friedel-Crafts acylation. Reagents: R-COCl (acyl chloride) + AlCl_3 cat.

7: Birch reduction. Reagents: Na, NH_3 , EtOH solvent. Mechanism involves radical anion formation due to presence of the electride salt $[\text{Na}(\text{NH}_3)_x]^+ \text{e}^-$. Regioselectivity: protonation occurs at the *ortho* and *para* positions, with ERGs favouring the *ortho* position and EWGs favouring the *para* position.

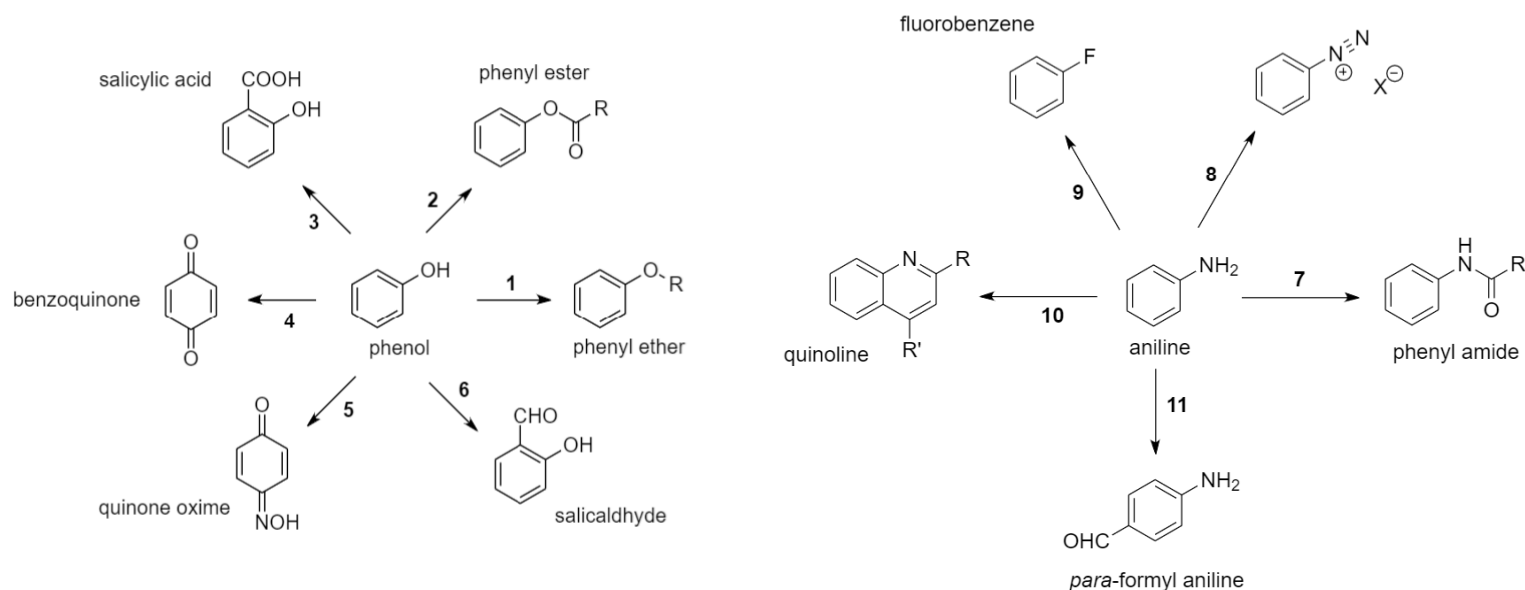
8: Halogenation. Reagents: X_2 , FeX_3 ($\text{X} = \text{Cl} / \text{Br}$) or I_2 , CuBr_2 ($\text{X} = \text{I}$). Fluorination ($\text{X} = \text{F}$) is uncommon.

9: Étard reaction. Reagents: CrO_2Cl_2 (chromyl chloride).

10: Oxidation. Reagents: KMnO_4 . Requires at least one C-H bond on the sp^3 carbon. Will break off any further C-C bonds to give the benzoic acid.

11: Aliphatic halogenation. Reagents: X_2 , UV. Mechanism: free-radical substitution.

Phenol and Aniline:



1: Williamson synthesis. Reagents: **1) Na or OH⁻; 2) RX**. For anisole (PhOMe), use 2) **DMS (dimethyl sulfate)**, which releases phenyl hydrogensulfate.

2: Esterification. Reagents: **RCOOH** or **RCOCl** or **(RCO)₂O**, **pyridine** or **NaOH**.

3: Kolbe reaction (ortho carboxylation). Reagents: **1) Na; 2) CO₂, high pressure; 3) H₃O⁺**.

4: Oxidation. Reagents: **Na₂Cr₂O₇**. The quinones can be reduced back to the hydroquinones with **SnCl₂**.

5: Nitrosation. Reagents: **HNO₂, 0 °C**. Mechanism: the oxime tautomerises with the nitroso phenol (HO-Ar-N=O) via proton transfer.

6: Reimer-Tiemann reaction. Reagents: **CHCl₃, NaOH**. Mechanism: carbylamine mechanism, forms dichlorocarbene (:CCl₂) as an intermediate.

7: Amidation. Reagents: **RCOOH** or **RCOCl** or **(RCO)₂O**, **NaOH** or **pyridine**.

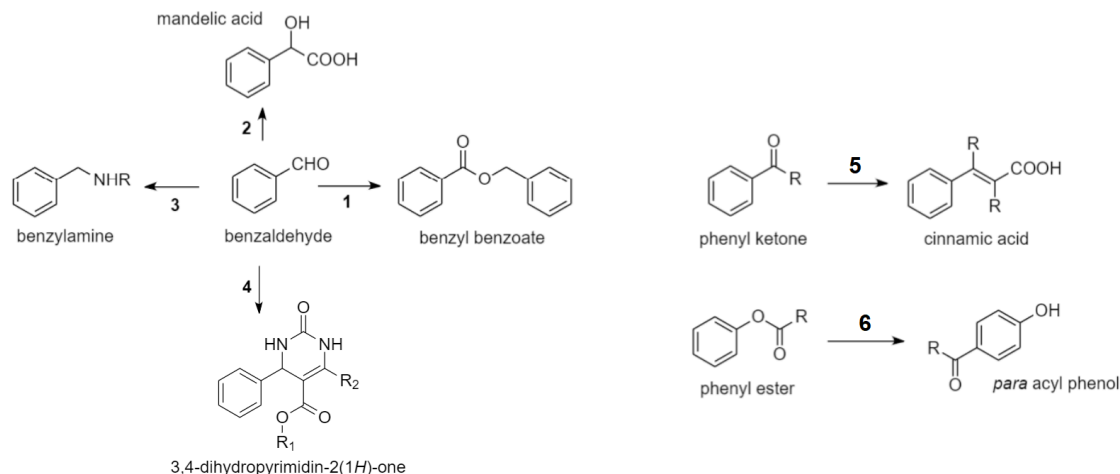
8: Diazotisation. Reagents: **NaNO₂, H₃O⁺, 0 °C**. The resonance structure (Ph-N=N⁺) may bond to neighbouring rings by **S_NAr**.

9: Balz-Schiemann reaction. Reagents: **1) NaNO₂, H₃O⁺; 2) HBF₄ or HPF₆ or HSbF₆, heat**. Mechanism: 1) forms the diazonium salt. 2) displaces the counter anion which thermally decomposes.

10: Combes quinoline synthesis. Reagents: **R-CO-CH₂-CO-R' (1,3-diketone) then H₃O⁺**. Mechanism: First, N: attacks a carbonyl, which rearranges by proton transfers. The C=O⁺H carbocation is attacked by the benzene ring.

11: Vilsmeier-Haack reaction. Reagents: **1) DMF, POCl₂; 2) H₂O**. Can also start with various other electron-rich species e.g. alkenes (styrene → cinnamaldehyde) or α-methylene groups.

Benzaldehyde, Phenyl Ketones and Phenyl Esters:



1: Cannizzaro reaction. Reagents: **conc NaOH (aq)**. Mechanism: disproportionation to benzyl alcohol and benzoic acid which then react in esterification.

2: Mandelic acid synthesis. Reagents: **1) HCN; 2) H₂O (2 mol eq)**. Mechanism: Step 1 forms the hydroxynitrile which is hydrolysed in Step 2 to the carboxylic acid. Forms a α -hydroxycarboxylic acid.

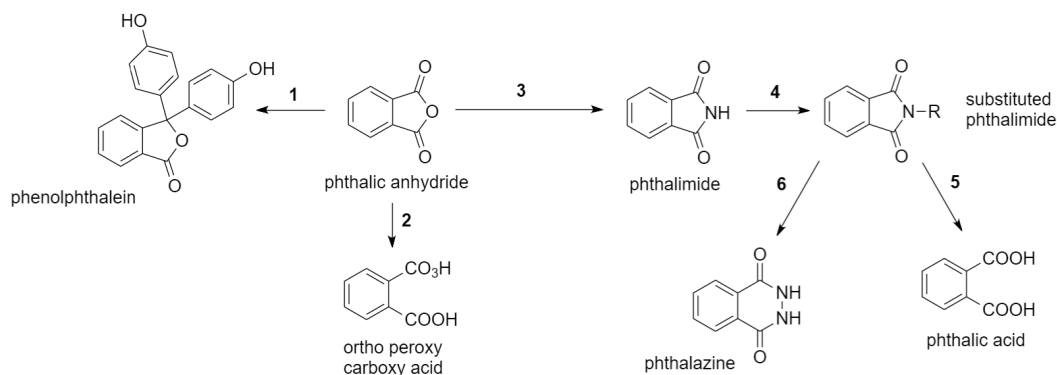
3: Reductive amination. Reagents: **RNH₂, H₂ / Ni cat.**

4: Biginelli reaction. Reagents: **R₂-C(O)-CH₂-COOR₁ (β -keto ester), CO(NH₂)₂ (urea)**. Forms a dihydropyrimidinone. Enantioselectivity at C4 can be induced using a chiral proline catalyst.

5: Perkin condensation. Reagents: **(R'Ac)₂O (acid anhydride), NaOAc**. Mechanism: aldol condensation. Also forms the carboxylic acid R'-CH₂-COOH. If reagent is Ac₂O (acetic anhydride) then R = R' = H.

6: Fries rearrangement. Reagents: **HF or AlCl₃ or BF₃ or TiCl₄ (CS₂)**.
 Regioselectivity: kinetic product (< 60 °C) → para; thermodynamic product (> 160 °C) → ortho.

Phthalic Anhydride and Phthalimide:



1: Phenolphthalein synthesis. Reagents: **phenol (2 mol eq)**;

2: Ring-opening with peroxide. Reagents: **H₂O₂**.

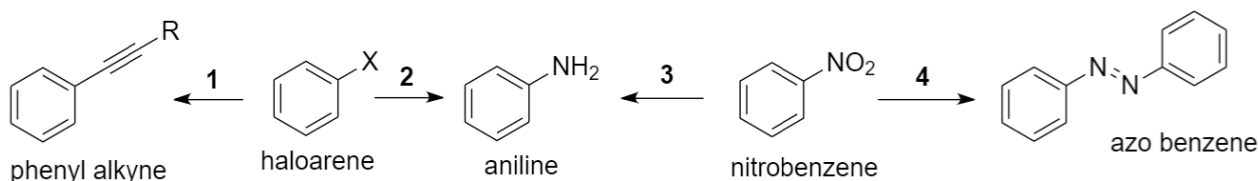
3: Phthalimide synthesis. Reagents: **NH₃ or (NH₃)₂CO₃ or urea**;

4: Gabriel's phthalimide synthesis. Reagents: **KOH, RI**;

5: Hydrolysis of phthalimide. Reagents: **H₂O**.

6: Gabriel's amine synthesis. Reagents: **N₂H₄ (hydrazine)**. Releases the amine R-NH₂.

Haloarenes and Nitrobenzene:



1: Sonogashira reaction. Reagents: $\text{R}-\text{C}\equiv\text{CH}$ (terminal alkyne), $\text{Pd}(\text{PPh}_3)_4$ cat., CuI , Et_3N , THF.

Can also start with a vinylic haloalkene.

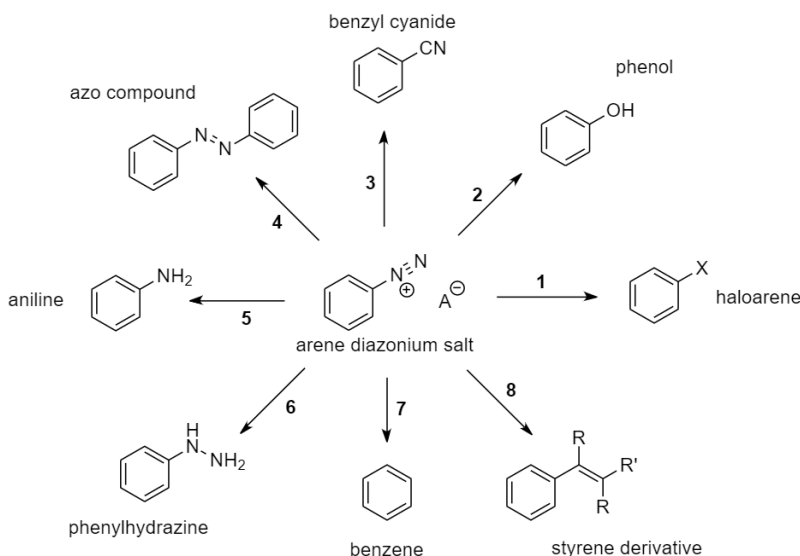
2: Aniline formation. Reagents: Na , NH_3 (l), -30°C . Benzyne mechanism ($\text{S}_{\text{N}}\text{Ar}$).

Elimination gives an aryne intermediate.

3: Reduction. Reagents: H_2 , Pd-C or Zn / Sn / Fe.

4: Azo coupling. Reagents: Zn, NaOH (MeOH).

Arenediazonium Salts:



1: Sandmeyer reaction to haloarene. Reagents: HBF_4 , heat ($\text{X} = \text{F}$), CuCl ($\text{X} = \text{Cl}$) or CuBr ($\text{X} = \text{Br}$) or KI ($\text{X} = \text{I}$).

2: Sandmeyer reaction to phenol. Reagents: H_2O , (H_2SO_4 or Cu_2O), heat

3: Sandmeyer reaction to benzonitrile. Reagents: CuCN .

4: Azo coupling. Reagents: benzene (or other aromatics), NaOH. Azobenzenes can photoisomerise, with higher frequency (UV) light favouring *cis*, lower frequencies (light) favouring *trans*. Substituted benzenes are *para*-directed. Larger aromatics (e.g. 2-naphthol) give colourful dyes.

5: Reverse diazotisation. Reagents: Zn, HCl.

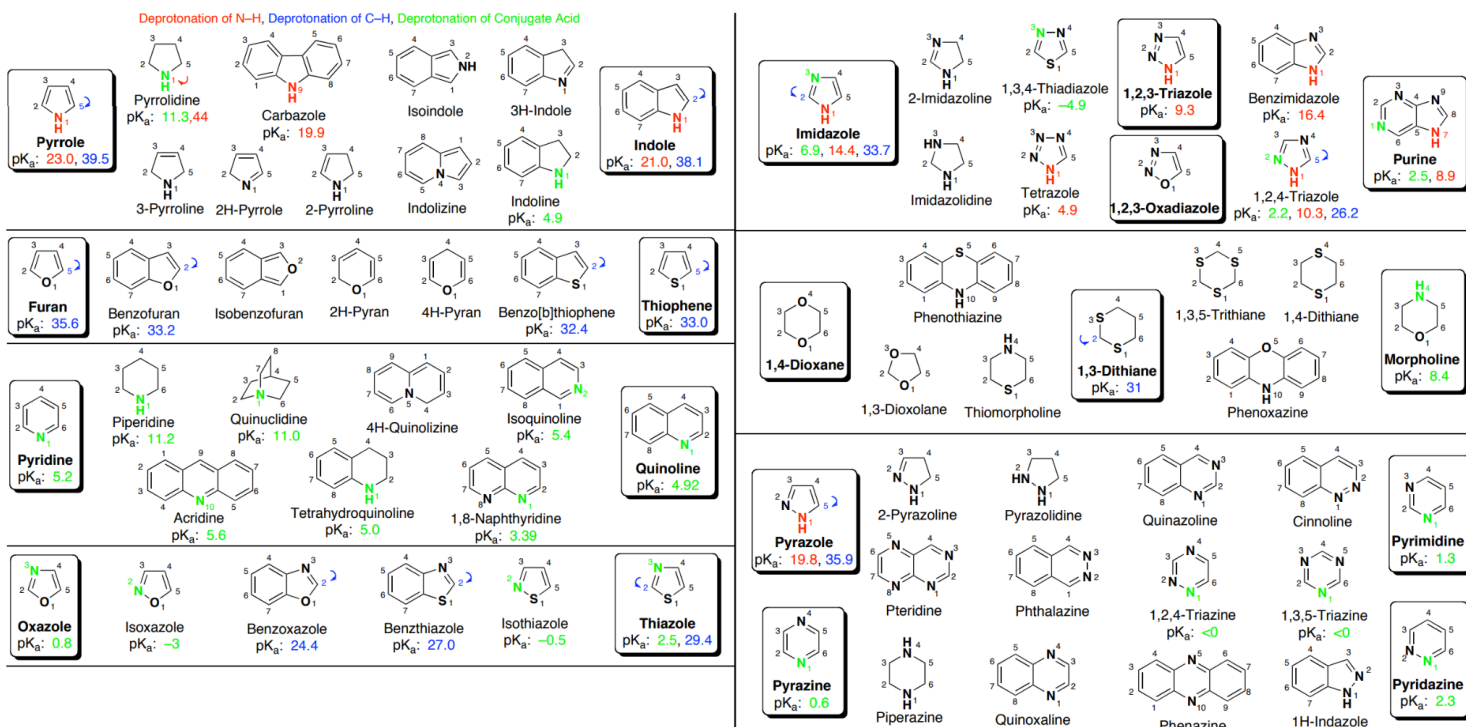
6: Phenylhydrazine formation. Reagents: SnCl_2 , HCl or NaSO_3 , NaOH (aq)

7: Reduction. Reagents: H_3PO_2 .

8: Meerwein arylation. Reagents: $\text{R}-\text{CH}=\text{CRR}'$ (alkene). R' is an EWG.

16.3.6. Heterocyclic Aromatic Compounds

Names, numbering and ionisation of heterocyclic organic compounds:

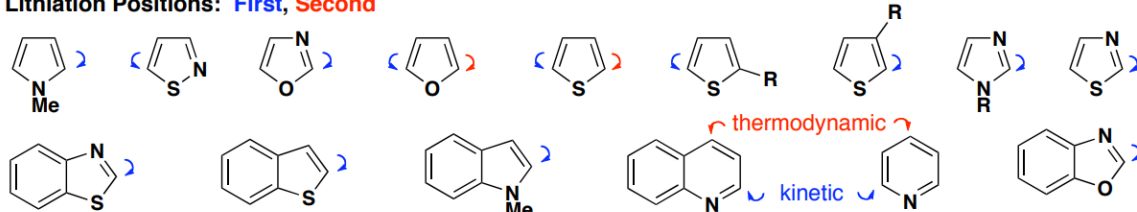


Regioselectivity in heterocyclic systems: sites of lithiation and electrophilic substitution

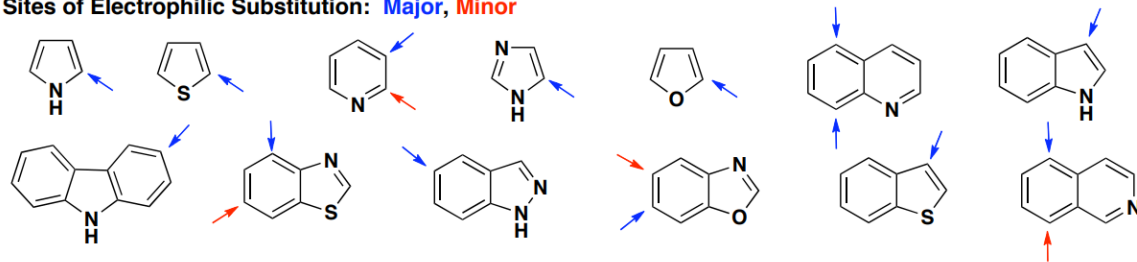
Effects of Substitution on Pyridine Basicity:

		Me	^t Bu	NH ₂	NHAc	OMe	SMe	Cl	Ph	vinyl	CN	NO ₂	CH(OH) ₂
	2-position	6.0	5.8	6.9	4.1	3.3	3.6	0.7	4.5	4.8	-0.3	-2.6	3.8
	3-position	5.7	5.9	6.1	4.5	4.9	4.4	2.8	4.8	4.8	1.4	0.6	3.8
	4-position	6.0	6.0	9.2	5.9	6.6	6.0	3.8	5.5	5.5	1.9	1.6	4.7

Lithiation Positions: First, Second

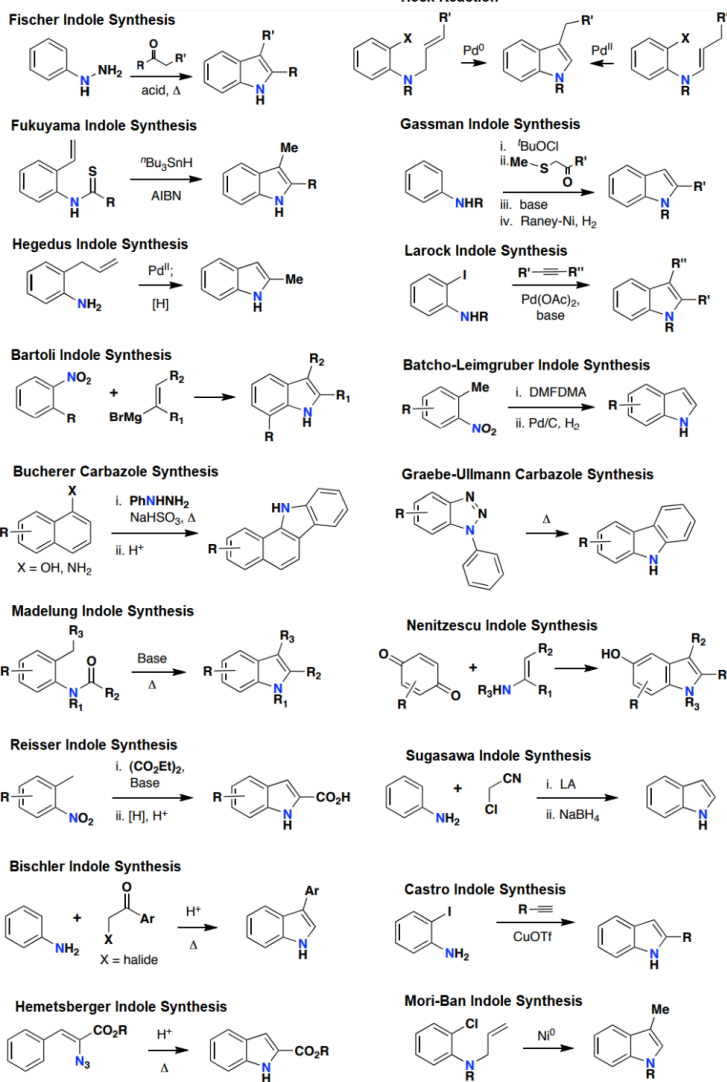


Sites of Electrophilic Substitution: Major, Minor

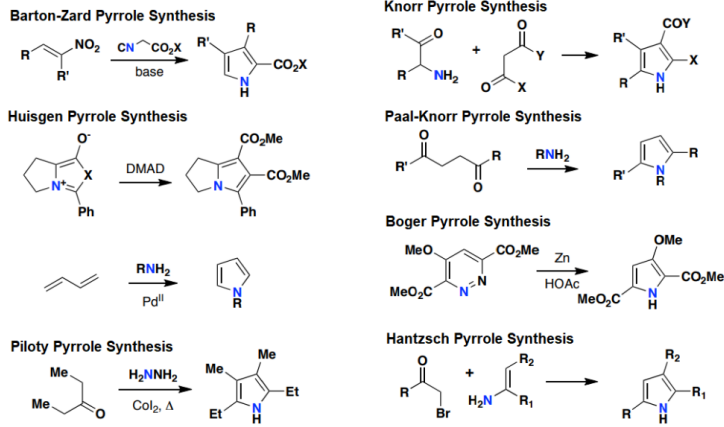


Synthesis of Heterocycles (Indoles, Carbazoles, Pyrroles, Thiophenes, Oxazoles and Isoxazoles):

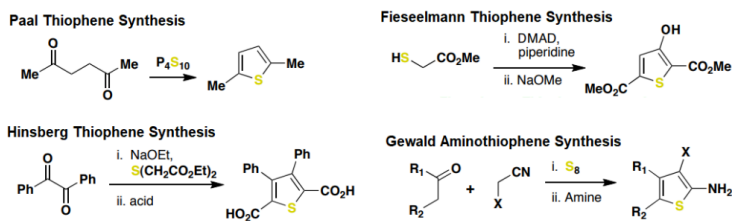
Synthesis of Indoles and Carbazoles:



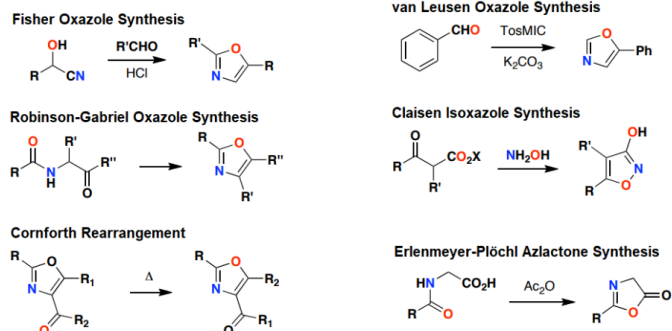
Synthesis of Pyrroles:



Synthesis of Thiophenes:



Synthesis of Oxazoles and Isoxazoles:

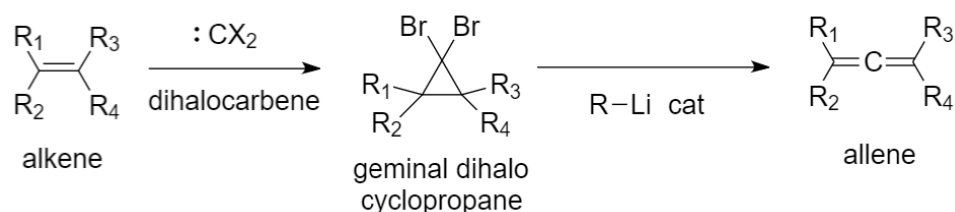


16.3.7. Other Miscellaneous Reactions

This section outlines reactions which cannot be easily classed as converting a single functional group into another. For pericyclic reactions such as the heteroatomic Diels-Alder reaction, the Cope rearrangement, the oxy-Cope rearrangement, the Claisen rearrangement, and more, see Section 16.1.8.

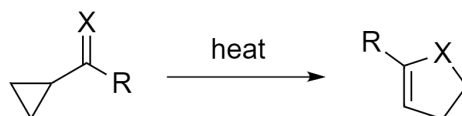
Doering-LaFlamme allene synthesis: forms cumulated dienes (allenes).

The second step is called the Skattebøl rearrangement.

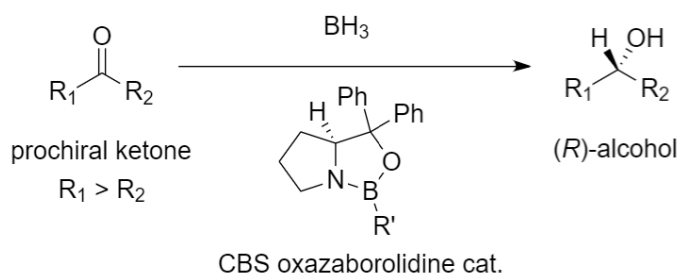


Vinylcyclopropane Rearrangement: forms cyclopentenes or heterocycles.

X = CH₂ / O / NH.

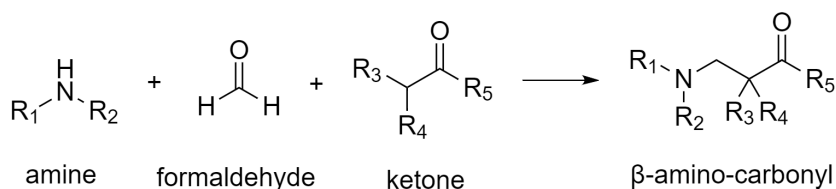


Corey-Itsuno Reduction (CBS Reduction): enantioselective reduction of prochiral ketones.



Mannich Reaction: multi-component addition.

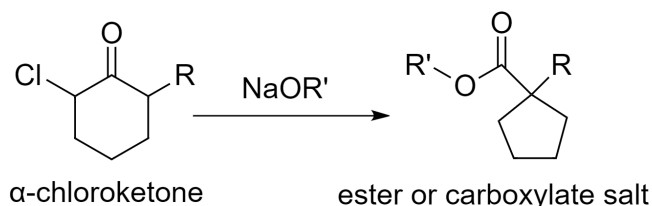
Can use a chiral proline catalyst to carry out an asymmetric transformation.



Favorskii Rearrangement: ring contraction.

Using NaOH instead of NaOR' gives the carboxylate salt instead.

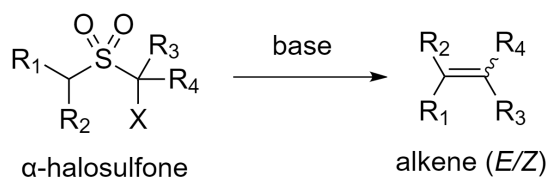
Forms a spiro or bicyclic cyclopropanone intermediate.



Peterson Olefination: alkene formation from α -halosulfones.

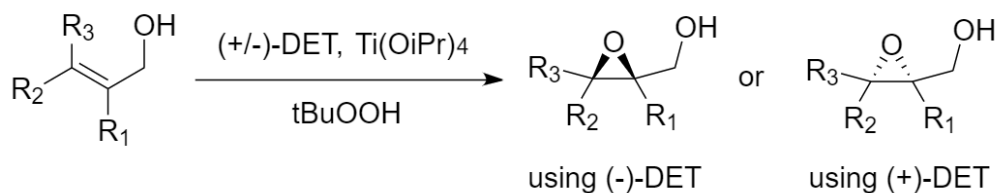
Forms a thiirane dioxide intermediate which extrudes SO_2 by cheletropic reaction.

The α -halosulfone can be made by α -halogenating an organic sulfide (thioether) (e.g. with NBS) followed by oxidation with mCPBA. Often used in cyclic systems (e.g. tetrahydrothiophene dioxides) to enforce stereoselectivity by ring strain (e.g. to form cyclobutenes).



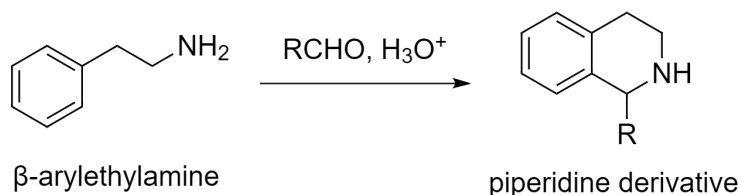
Sharpless Epoxidation: enantioselective epoxide formation from α -hydroxyalkenes.

DET is diethyltartrate, using either (*S,S*) = (-) or (*R,R*) = (+). tBuOOH is *tert*-butyl hydroperoxide, the oxidising agent.

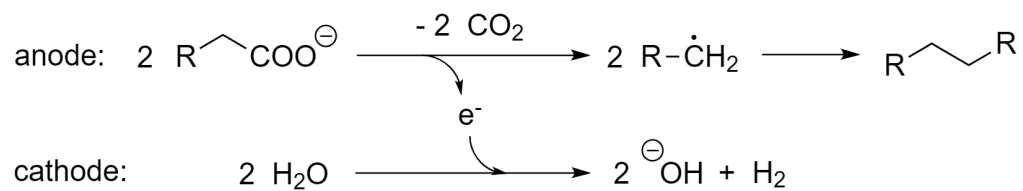


Pictet-Spengler Reaction: ring closure of β -arylethylamines with aldehydes.

Electron-rich aromatic rings work best e.g. indoles, pyrroles, 3,4-dimethoxyphenyls.



Kolbe Electrolysis: an electrosynthesis reaction. Electrolysis of aqueous carboxylate salts forms free radicals at the anode after decarboxylation, which can react to form either dimer or intramolecular C-C bonds.



For 1,4-dicarboxylates, the radical termination step is intramolecular and forms an alkene.

16.4. Analytical Methods in Chemistry and Molecular Biology

16.4.1. Flame Tests for Metals in Inorganic Compounds

Metals can be identified by dipping a nichrome wire (e.g. an inoculation loop) into an aqueous solution of their salt and holding it into a Bunsen burner flame on high heat.

The electrons in heated metal ions are thermally excited to higher orbitals, which then undergo relaxation, releasing light at characteristic wavelengths (colours). This is applied quantitatively in **flame emission spectroscopy** to identify the ions from their line spectrum.

Li^+ lithium deep brick-red	Na^+ sodium intense yellow	K^+ potassium lilac	Rb^+ rubidium red-violet	Cs^+ caesium blue-violet		
Ca^{2+} calcium orange-red	Sr^{2+} strontium red	Ba^{2+} barium pale green	Ra^{2+} radium crimson	Cu^{2+} copper blue-green	$\text{Fe}^{2+}/\text{Fe}^{3+}$ iron yellow-orange	Zn^{2+} zinc light blue-green
B^{3+} boron bright green	In^{3+} indium indigo	Pb^{2+} lead blue-white	As^{3+} arsenic light blue	$\text{Sb}^{3+}/\text{Sb}^{5+}$ antimony light green	$\text{Se}^{2+}/\text{Se}^{4+}$ selenium blue	

Some metals which produce white (or silvery) flame tests such as magnesium (very bright), aluminium, beryllium, cobalt, chromium, hafnium, nickel, tin (blue-white), and titanium. Zinc and lead are also sometimes reported as white.

Flame tests may alternatively be carried out using the borax bead test (see Section 15.4.3).

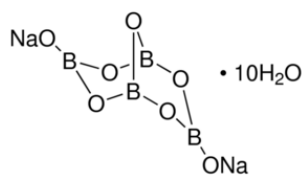
The variation in the colours of fireworks is based on the same principle as the flame test. In a firework, a fuel (black gunpowder: 75% KNO_3 + 15% charcoal + 10% sulfur) and oxidiser (chlorates and nitrates) are used with a dextrin binder to heat the powdered metal salt and produce coloured light.

16.4.2. Test-Tube Reactions for Inorganic Compounds

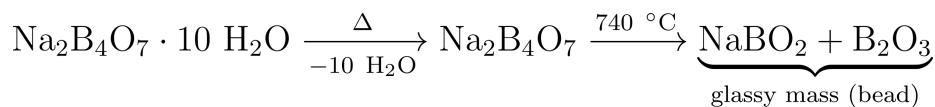
Analyte (testing for)	Procedure	Positive result	Notes
hydrogen (H ₂)	Hold a lit splint into a test tube.	'Squeaky pop' sound heard.	Hydrogen is combusted in air.
carbon dioxide (CO ₂)	Bubble through limewater (Ca(OH) ₂ (aq)).	Limewater turns cloudy (increased turbidity).	Cloudiness is due to formation of a solid suspension of CaCO ₃ .
ammonia (NH ₃)	Hold damp red litmus paper into the test tube.	Litmus paper turns blue.	Ammonia is alkaline.
chlorine (Cl ₂)	Hold damp blue litmus paper into the test tube.	Litmus paper bleached to white.	HCl + HClO bleach mixture formed.
sulfates (SO ₄ ²⁻)	Add dilute HCl (aq) then barium chloride solution (BaCl ₂ (aq)).	White precipitate of insoluble BaSO ₄ formed.	The acid neutralises carbonate ion impurities which would give false positive.
carbonates (CO ₃ ²⁻)	Add dilute HCl, collect gas and pump into limewater.	Limewater turns cloudy (increased turbidity) due to release of CO ₂ .	HCl liberates CO ₂ from carbonates.
chlorides (Cl ⁻)	Add dilute nitric acid (HNO ₃) then silver nitrate solution (AgNO ₃ (aq)).	White precipitate formed, soluble in dilute ammonia.	The acid neutralises ions which could give false positives. Forms AgCl; dissolves in NH ₃ .
bromides (Br ⁻)	Confirm colour by testing solubility in dilute and concentrated ammonia (NH ₃).	Cream precipitate formed, soluble in concentrated NH ₃ .	Forms AgBr; dissolves only in concentrated NH ₃ .
iodides (I ⁻)	(Note: AgF is water soluble so it gives no precipitate).	Yellow precipitate formed, insoluble in concentrated NH ₃ .	Forms AgI; insoluble in NH ₃ .
ammonium ions (NH ₄ ⁺)	Add dilute NaOH and warm gently. Hold in damp red litmus paper.	Litmus paper turns blue.	Reaction forms ammonia and water.

16.4.3. Borax Bead Test for Identification of Metals

Boric anhydride reacts with many metal salts to form coloured metaborates.



The beads are formed by holding borax into a Bunsen flame:



The bead (on the end of an inert metal wire) is then dipped into a sample, which partially adheres to the bead. The bead is then held in the **reducing (lower)** part and then in the **oxidising (upper)** part of the Bunsen flame, and the colours are observed in each case.

Element	Oxidising flame		Reducing flame
	Hot	Cold	Hot / Cold
Chromium	yellow-red	green	green
Manganese	violet	violet	colourless
Nickel	yellow-brown	red-brown	grey
Copper	green-blue	green-blue	red-brown
Cobalt	blue	blue	blue
Iron	yellow-red	pale yellow	green

16.4.4. Colours of Common Period 3 Transition Metal Ion Solutions

Aqueous ions (metal-aquo complexes) $[\text{M}(\text{H}_2\text{O})_6]^{a+}$ in various oxidation states:

Sc	Ti	V	Cr	Mn	Fe	Co	Ni	Cu	Zn
	+2	+2	+2	+2	+2	+2	+2	+2	+2
+3	+3	+3	+3	+3	+3	+3	+3	+3	
	+4	+4	+4	+4	+4	+4	+4		
	+5	+5	+5	+5	+5	+5			
			+6	+6	+6				
				+7					

Some of these may be reported differently.

Solid phase compounds often have different colours to their aqueous phases. Most salts are colourless when anhydrous, only showing colour in aqueous solution.

Some compounds may also differ in colour to those shown above due to field splitting by ligands (see CFT in Section 15.4.4).

(Ti³⁺: lilac, V²⁺: lilac, V³⁺: green, V⁴⁺: light blue, V⁵⁺: yellow, Cr²⁺: dark blue, Cr³⁺: green, Cr⁶⁺: orange, Mn²⁺: very pale pink, Mn⁷⁺: deep purple, Fe²⁺: pale green, Fe³⁺: pale yellow, Co²⁺: pink, Co³⁺: dark yellow, Ni²⁺: green, Cu²⁺: dark blue, all others are colourless.)

16.4.5. Qualitative Determination of Organic Compounds by Test-Tube Reactions

Analyte (testing for)	Procedure	Positive result	Notes
Alkenes	Add bromine water.	Bromine water decolourised.	Br ₂ is removed from the water by reaction to form dibromoalkanes.
Haloalkanes	Warm with NaOH in 1:1 water-ethanol, test for halide ion using AgNO ₃ / HNO ₃ (aq) then NH ₃ .	White (Cl) / Cream (Br) / Yellow (I) ppt formed.	NaOH converts to alcohol and releases the halide ion.
Alcohols (1° and 2°)	Mix with acidified potassium dichromate (K ₂ Cr ₂ O ₇ / H ⁺). Heat and distil products.	Colour changes from orange to green.	Cr ⁶⁺ reduced to Cr ³⁺ .
Alcohols (all)	Add ceric ammonium nitrate solution [Ce(NH ₄) ₂ (NO ₃) ₆].	Colour changes from amber to red.	Ligand substitution: forms [Ce(NO ₃) ₄ (ROH) ₃].
Aldehydes (also: α-hydroxyketones, hemiacetals and all reducing sugars)	Add Tollens' reagent.	Silver mirror formed.	Ag ⁺ reduced to Ag.
	Add Fehling's solution or Add Benedict's reagent.	Blue solution turns to brick-red precipitate.	Cu ²⁺ reduced to Cu ⁺ .
Carbonyls (aldehydes and ketones)	Add Brady's reagent (methanol + acidic 2,4-DNPH; 2,4-dinitrophenylhydrazine)	Forms orange precipitate.	
Carboxylic acid	Add NaHCO ₃ or Na ₂ CO ₃ .	Effervescence.	Acid liberates CO ₂ .
1° amines	Add dilute NaOH and benzene sulfonyl chloride (PhSO ₂ Cl). Observe reaction then add HCl. (Hinsberg's test)	No initial change; insoluble precipitate forms with HCl.	Sulfonamide product has acidic hydrogen so soluble only in alkali.
2° amines		Precipitate forms; does not dissolve in HCl.	Sulfonamide product has no acidic hydrogen so insoluble in alkali.
3° amines		Precipitate forms; dissolves in HCl.	No reaction; forms soluble ammonium salt.
Aromatic amines	Add NaNO ₂ + HCl then 2-naphthol.	Bright red-orange insoluble precipitate formed.	Diazonium salt undergoes diazotisation.

16.4.6. Qualitative Determination of Biochemical Compounds by Test-Tube Reactions

Analyte (testing for)	Procedure	Positive result	Notes
Reducing sugars as α -hydroxyketones	Tollens' test Add Tollens' reagent.	Silver mirror formed.	Ag^+ reduced to Ag.
	Fehling's test or Benedict's test Add Fehling's solution or Add Benedict's reagent.	Blue solution turns to brick-red precipitate.	Cu^{2+} reduced to Cu^+ .
Carbohydrates	Molisch's test Add 1% alcoholic solution of 1-naphthol, then add conc H_2SO_4 .	Violet ring forms at the interface of the two layers.	The carbohydrate is dehydrated to an aldehyde by the acid, which reacts with the phenol to form the coloured product.
Starch	Iodine starch test Stain with iodine.	Turns dark blue / black.	I_3^- (triiodide) complexes in amylose helices.
Proteins	Biuret test Add alkaline CuSO_4 (aq).	Turns from pale blue to violet.	Cu^{2+} complexes with peptide CONH bonds.
	Ninhydrin test Boil with aqueous ninhydrin (2,2-dihydroxyindane-1,3-dione).	Turns blue-violet.	Protein is hydrolysed, amino acids react.
	Xanthoproteic test Add concentrated HNO_3 .	Turns yellow.	Benzene rings on aromatic groups (Tyr, Trp or Phe) are nitrated.
	Millon's test Add mercuric nitrate in nitric acid (HgNO_3 , HNO_3).	White precipitate forms.	Reacts with the phenolic group in tyrosine.
Glycosamino-glycans	Use Alcian blue stain.	Stains blue.	Often used to test cell tissues.

For spectrometric methods, see Section 16.4.5.

16.4.7. Infrared (IR) Spectroscopy

IR spectroscopy involves recording the transmittance of infrared radiation through a sample. Molecular bonds have characteristic absorbance ‘peaks’ at corresponding energies.

- Wavenumber k [cm^{-1}] = $\frac{10^4}{\text{wavelength } [\mu\text{m}]}$,
- Energy E [eV] = 1.9662×10^{-5} [eV cm] $\times k$ [cm^{-1}]

Bond	Wavenumber / cm^{-1}
N – H (amines)	3300 – 3500
O – H (alcohols)	3230 – 3550
C – H	2850 – 3300
O – H (acids)	2500 – 3000
C \equiv N	2220 – 2260
C = O	1680 – 1750
C = C	1620 – 1680
C – O	1000 – 1300
C – C	750 – 1100

16.4.8. Fourier Transform IR and Raman Band Correlation Data (Sorted Ascending)

In case of disagreement between the here and the IR table in Section 16.4.1, the table below should be considered more accurate.

Wave-number (cm ⁻¹)	Assignment	Intensity	Wave-number (cm ⁻¹)	Assignment	Intensity
100 - 210	lattice vibrations	strong	1625 - 1680	C=C	very strong
150 - 430	metal-O	strong	1630 - 1665	C=N	very strong
250 - 400	C-C (aliphatic)	strong	1690 - 1720	urethane	moderate
295 - 340	Se-Se	strong	1710 - 1725	aldehyde	moderate
425 - 550	S-S	strong	1710 - 1745	ester	moderate
460 - 550	Si-O-Si	strong	1730 - 1750	aliphatic ester	moderate
490 - 550	C-I	strong	1735 - 1790	lactone	moderate
505 - 700	C-Br	strong	1740 - 1830	acid anhydride	moderate
550 - 790	C-Cl	strong	1745 - 1780	acyl chloride	moderate
580 - 680	C=S	strong	2020 - 2100	isothiocyanate	moderate
630 - 1250	C-C (aliphatic)	moderate	2070 - 2250	alkyne	strong
670 - 780	C-S	strong	2080 - 2150	Si-H	moderate
720 - 800	C-F	strong	2090 - 2170	isonitrile	moderate
800 - 950	C-O-C	weak	2100 - 2170	thiocyanate	very weak
910 - 960	COOH acid dimer	weak	2110 - 2160	azide	moderate
990 - 1100	aromatic rings	strong	2200 - 2230	aromatic nitrile	moderate
1010 - 1095	Si-O-C	weak	2200 - 2280	diazonium salt	moderate
1010 - 1095	Si-O-Si	weak	2220 - 2260	nitrile	moderate
1020 - 1225	C=S	strong	2230 - 2270	isocyanate	very weak
1025 - 1060	sulfonic acid	very weak	2290 - 2420	P-H	very weak
1050 - 1210	sulfonamide	moderate	2530 - 2610	thiol	strong
1050 - 1210	sulfone	moderate	2680 - 2740	aldehyde	weak
1120 - 1190	Si-O-C	weak	2750 - 2800	N-CH ₃	weak
1145 - 1240	sulfonic acid	very weak	2770 - 2830	CH ₂	strong
1315 - 1435	carboxylate salt	moderate	2780 - 2830	aldehyde	weak
1320 - 1350	nitro	very strong	2790 - 2850	O-CH ₃	weak
1355 - 1385	C-CH ₃	weak	2810 - 2960	C-CH ₃	strong
1365 - 1450	aromatic azo	very strong	2870 - 3100	aromatic C-H	strong
1405 - 1455	CH ₂	weak	2880 - 3530	OH	weak
1405 - 1455	CH ₃	weak	2900 - 2940	CH ₂	strong
1450 - 1505	aromatic ring	moderate	2980 - 3020	CH=CH	strong
1535 - 1600	nitro	moderate	3010 - 3080	terminal =CH ₂	strong
1540 - 1590	aliphatic azo	moderate	3150 - 3480	amide	moderate
1550 - 1610	heteroatomic ring	strong	3150 - 3480	amine	moderate
1550 - 1700	amide	strong	3200 - 3400	phenol	weak
1600 - 1710	ketone	moderate	3210 - 3250	alcohol	weak
1610 - 1740	carboxylic acid	moderate	3250 - 3300	alkyne	very weak

16.4.9. ^{13}C NMR Spectroscopy

NMR provides information on molecular structure and connectivity by analysing the relaxation of spin- $\frac{1}{2}$ nuclei, which possess an intrinsic magnetic moment, in the presence of a magnetic field.

General Principle of Nuclear Magnetic Resonance (NMR) Spectroscopy

- In the presence of an external magnetic field, spin $\frac{1}{2}$ nuclei align with or against the field. These two alignments have different nuclear energy levels.
- When RF (radio wave, M range) electromagnetic radiation is incident on the nuclei, they undergo transitions between the two states at resonant frequencies.
- The difference in resonant frequencies between a given nucleus and a standard is dependent on interactions in the chemical environment, and is reported as the chemical shift δ in ppm.

Organic molecules contain ^{13}C at an average abundance of 1.1%. In proton-decoupled ^{13}C NMR spectra, splitting does **not** occur, and the integration ratio does **not** indicate atom count. In very high resolution ^{13}C NMR, splitting can be observed ($n + 1$, where n is the number of attached hydrogens to the carbon).

Type of carbon	Group	δ (ppm)	Type of carbon	Group	δ (ppm)
$\text{R}_3\text{-C-C-R}_3$	alkyl	5 - 40	$\text{R}_2\text{C=CR}_2$	alkene	90 - 150
R-C-Cl or Br	haloalkane	10 - 70	RCN	nitrile	110 - 125
RCOCR_3	carbonyl	20 - 50	C_6H_6	benzene / aryl	110 - 160
RCNR_2	amine	25 - 60	RCOR	ester, carboxylic acid	160 - 185
R_3COR	alcohol, ether, ester	50 - 90	RCOR	aldehydes, ketones	190 - 220

16.4.10. Proton (^1H) NMR Spectroscopy

The compound under study is immersed in a deuterated solvent (e.g. heavy water (D_2O), deuterated chloroform (CDCl_3) or CD_3CN) as the $\text{D} = ^2\text{H}$ nucleus has no spin, or proton-free solvent (e.g. CCl_4), and the NMR is conducted against a TMS standard.

Proton NMR Chemical Shifts

Type of proton	Group	δ (ppm)	Type of proton	Group	δ (ppm)
RCH_3	methyl	0.7 - 1.2	ROCHR_2	ether	3.1 - 3.9
RNH_2	amine	1.0 - 4.5	RCH_2Cl or Br	haloalkane	3.1 - 4.2
ROH	alcohol	1.0 - 5.0	RCOOCHR_2	ester	3.7 - 4.1
RSH	thiol	1.0 - 5.0	$\text{R}_2\text{C=CHR}$	alkene	4.5 - 6.0
R_2CH_2	alkyl (2°)	1.2 - 1.4	C_6H_6	aryl / benzene	6.5 - 8.0
R_3CH	alkyl (3°)	1.4 - 1.6	RCHO	aldehyde	9.0 - 10.0
RCOCHR_2	carbonyl	2.1 - 2.6	RCOOH	carboxylic acid	10.0 - 12.0

NH, OH and SH peaks are often broad and the sample must be very dry for them to show.

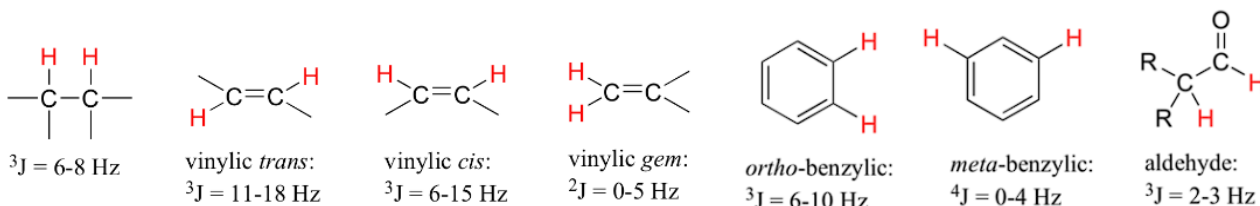
Chemical shifts of groups near electronegative atoms are shifted downfield (larger δ) due to deshielding.

Integration Ratio: peak area is proportional to number of H-atoms in an identical environment. This is sometimes shown on the spectrum as an accumulating curve (integration ratio = step size).

Splitting: high-resolution NMR can show peak splitting when H-atoms on adjacent atoms are present

Number of peaks in a split = $n + 1$ (n : number of H atoms bonded to adjacent atoms). Types of peaks: Singlet ($n = 0$), doublet ($n = 1$; 1:1), triplet ($n = 2$; 1:2:1), quartet ($n = 3$; 1:3:3:1), quintet ($n = 4$, 1:4:6:4:1), etc.

J -coupling constant, $^mJ_{ab}$: difference in frequency (in Hz) between peaks due to proton environments a and b , separated by m bonds. The values of J for some proton configurations are:



H atoms bonded to O, N, etc typically do **not** split due to proton exchange through hydrogen bonds, unless the temperature is low (e.g. if $T \leq 0^\circ\text{C}$ then O-H **does** contribute to splitting).

Species undergoing dynamic equilibrium on the NMR frequency timescale will display noisy spectra due to the Heisenberg uncertainty principle, as well as exchange peak broadening.

The protons on benzene rings are shifted further ($\delta \sim 7.3 \text{ ppm}$) than on vinyl alkenes due to aromatic ring current deshielding.

16.4.11. NMR Spectroscopy with Other Nuclei (^{15}N , ^{19}F , ^{31}P , ^{129}Xe)

16.4.12. Advanced NMR Spectroscopy (DEPT, COSY, HSQC and HMBC)

16.4.13. UV/Vis Spectrophotometry

Absorbance: $A = -\log_{10} \frac{I}{I_0}$ (I : initial intensity, I_0 : measured intensity)

Beer-Lambert law: $A = \epsilon bc$ and $I = I_0 e^{-\epsilon bc}$ half intensity at $bc = \frac{\ln 2}{\epsilon}$

(ϵ : solvent molar absorptivity (molar extinction coefficient), b : path length, c : concentration)

The molar absorptivity varies significantly with wavelength, so the wavelength must be specified when reporting (e.g. $A_{240} \rightarrow \lambda = 240 \text{ nm}$). In the visible range, the technique is called colourimetry.

Protein Assays: spectrophotometry is often used for quantitative determination of proteins (e.g. enzymes, antibodies, antigens) by addition of a colourimetric reagent and measuring UV/Vis absorbance at a fixed wavelength:

- **Biuret Assay:** add Biuret's reagent. The solution turns violet as Cu^{2+} in the reagent complexes with peptide bonds. Measure A_{540} .
- **Lowry Assay:** add alkaline CuSO_4 (aq) followed by the Folin-Ciocalteu reagent. The solution turns blue. Measure A_{750} .
- **Bradford Assay:** add the dye 'Coomassie brilliant blue G-250'. The solution turns blue. Measure A_{600} .
- **BCA Assay / Smith Assay:** add Biuret's reagent followed by bicinchoninic acid (BCA). The solution turns violet. Measure A_{560} .

Cofactor Assays: Enzymatic reaction kinetics can be assessed by tracking the concentration of a cofactor (e.g. NADH: A_{260} or A_{340}) over time.

16.4.14. Immunological Assays for Selective Quantitative Determination of Proteins

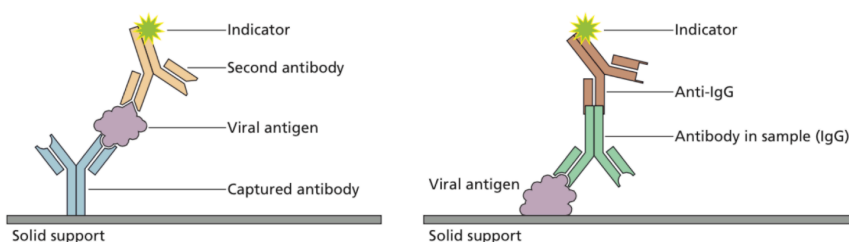
Immunological assays are used to determine the amount of a specific protein present in a sample, typically applied to antibodies, antigens or hormones in biofluids.

Enzyme-Linked Immunosorbent Assay (ELISA): detects antibodies or antigens

(A) Sandwich ELISA for antigen (Ag) detection: 1) Ag-specific mAbs are immobilised on a solid support. 2) Ag-containing solution is added. 3) After washing, a second (detection, enzyme-conjugated) mAb specific to a different Ag epitope is added.

(B) Indirect ELISA for antibody (Ab) detection: 1) Antigens for the target antibody are immobilised on a solid support. 2) Ab-containing solution is added. 3) After washing, a second (detection, enzyme-conjugated) mAb specific to the constant region of the target Ab is added.

Then, a chromogenic/fluorogenic enzyme-specific substrate is added, which is cleaved by the conjugated enzyme to produce a colorimetric or fluorescent signal.



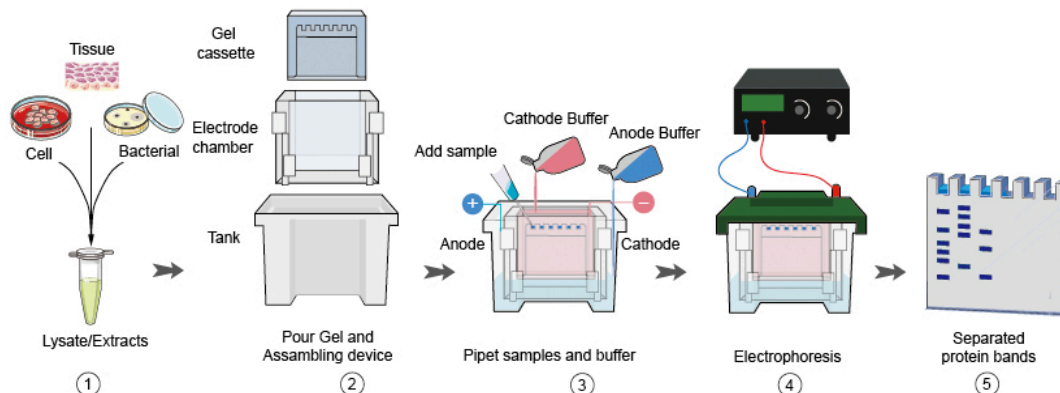
(A) Detecting antigens (e.g. viral) **(B) Detecting antibodies (e.g. IgG)**

Western Blotting (Immunoblotting): separates mixtures of proteins

First, 2D gel electrophoresis (carried out in two steps) produces the electropherogram:

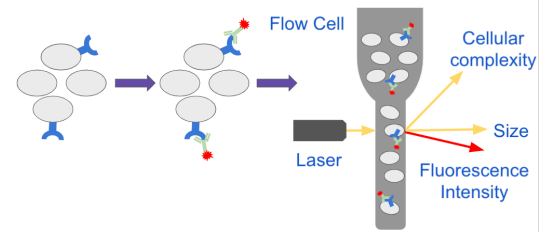
- **Isoelectric Focussing (IEF):** pH gradient and electric field applied in one direction, giving separation by isoelectric point.
- **SDS-PAGE:** proteins are denatured with surfactant (SDS), and migration by applied electric current applied in perpendicular direction in polyacrylamide gel gives separation by molecular weight.

The protein spots are then transferred to a gel, and the sandwich ELISA principle is applied.



Flow Cytometry: measures antigen expression on cells

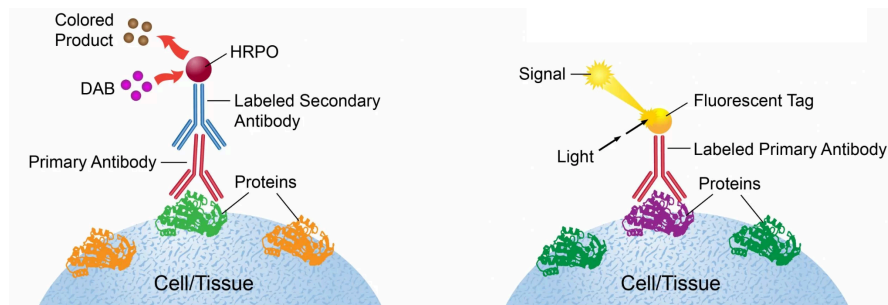
Cells expressing a particular antigen (Ag) are suspended in PBS (phosphate-buffered saline) and labelled with fluorophore-conjugated antibodies (Ab) for the target Ag. The cell solution is loaded into a flow cytometer where it passes a laser in a single-file stream. The detector measures the fluorescent response from cells with the Ag.



Immunocytochemistry (ICC) / Immunofluorescence (IF): identifies intracellular proteins.

Cells containing a particular protein are immobilised and permeabilised with Triton X-100. To prevent non-specific antibody binding, a solution of bovine serum albumin (BSA) is added to bind all surface antigens, and washed. A primary antibody for the target protein is added, and a secondary indicator antibody (binds to the constant region of the primary Ab) is added.

The indicator Ab is conjugated to a fluorophore (for IF: fluorescent microscopy) or enzyme (for ICC: chromogenic staining, by adding DAB substrate (3,3'-diaminobenzidine) to form a coloured product).



Immunocytochemistry (ICC)

Immunofluorescence (IF)

Immunohistochemistry (IHC) uses the same method as ICC, but is applied to a whole biological tissue rather than a cellular solution.

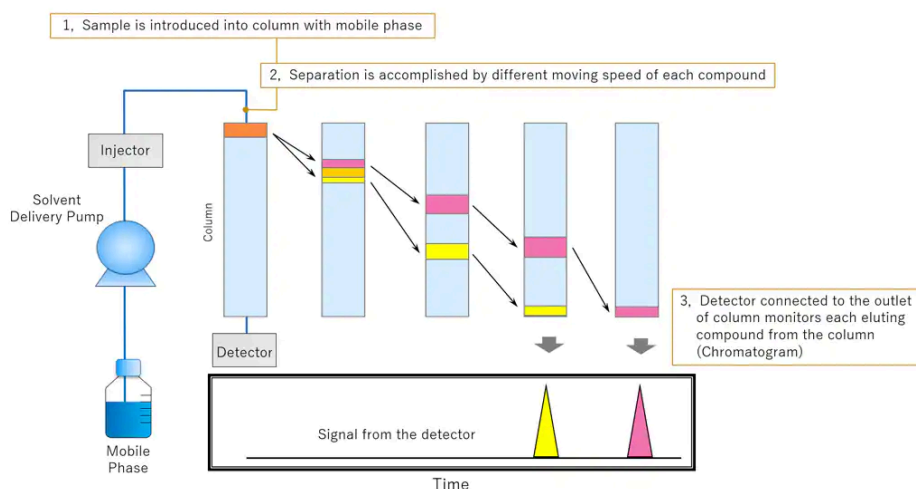
16.4.15. Chromatography for Simple Organic Molecules

Thin-layer chromatography (TLC): separation is based on relative affinity to a mobile phase (solvent) and a stationary phase (adsorbate/substrate).

The analyte can be located by spraying the chromatogram with a developing agent (e.g. ninhydrin) or viewing under blacklight (UVA light). The retention factor R_f is the ratio of the distance travelled by an analyte to the distance travelled by the solvent front.

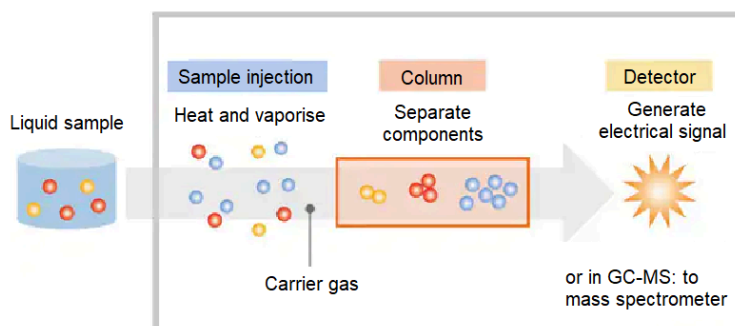
High-Performance Liquid Chromatography (HPLC):

A column is packed with porous silica beads. Analytes adhere to the silica to different extents resulting in different retention times. Automated systems for column chromatography enable high precision and quantitative determination of the components of a mixture. A variation is supercritical fluid chromatography (SCF), which uses supercritical CO_2 as the solvent.



Gas Chromatography (GC):

A liquid mixture is evaporated in an oven and injected into a carrier gas which acts as the solvent, and is transported through a long coil-shaped pipe. The separated components arrive at the detector and can be analysed for their mass (GC-MS).



Dead time (holdup time): time taken for the eluent (unretained solvent) to reach the detector.

16.4.16. Chromatography for Protein Separation and Purification

Ion Exchange Chromatography (IEC): separates proteins by isoelectric point

The chromatography column is chosen to be either:

- Anionic exchanger: uses a positive (cationic) column (e.g. DEAE-C, diethylaminoethyl cellulose) to bind negatively charged proteins ($\text{pH} \gg \text{pI}$).
- Cationic exchanger: uses a negative (anionic) column (e.g. CMC, carboxymethyl cellulose) to bind positively charged proteins ($\text{pH} \ll \text{pI}$).

For further separation, a pH gradient over time (anionic: high \rightarrow low pH; cationic: low \rightarrow high pH), or a salt (NaCl or Na_2SO_4) concentration gradient over time (R_f increases with concentration and charge) can be applied to the eluent. As elution occurs, determination of protein concentration is recorded in real-time by UV/Vis spectrophotometry.

Hydrophobic Interaction Chromatography (HIC): separates proteins by hydrophobicity.

Addition of salt exposes hydrophobic sections of the protein (salting out) which can bind to the hydrophobic column.

Affinity Chromatography: separates recombinant (tagged) proteins.

The column contains adsorbent ligands for affinity tags that can be added to recombinant proteins. Common fusion tags, corresponding column adsorbents and eluents include:

Fusion tag	Affinity adsorbent	Elution with
glutathione-S-transferase (GST)	glutathione	glutathione
protein A	IgG	free IgG (competitive elution; cleaves the tag)
maltose binding protein	amylose	maltose
6xHis tag	nickel-NTA agarose (immobilised metal affinity chromatography, IMAC)	imidazole or histidine
epitope tag (e.g. FLAG tag)	anti-FLAG mAbs	free FLAG
strep-II tag	streptavidin	biotin (vitamin B ₇)
CBD intein	chitin	DTT (cleaves the tag)

Tags can also be cleaved by engineering the protein with a protease recognition site upstream of the tag, then adding the protease to the eluted protein.

Size Exclusion Chromatography (SEC) / Gel Filtration (GF): separates proteins by size.

Large molecules (proteins) run through the column without fractionation, while smaller molecules are adsorbed more. This can also be used to separate salts from protein (desalting), or as a final 'polish' step in purifying a protein solution.

16.4.17. Mobility of Amino Acids in Thin-Layer Chromatography (TLC)

The table shows the R_f values of some amino acids for TLC with a silica stationary phase and a variety of polar mobile phases. Solvent compositions are given in v/v %.

M_1 : ethylene glycol

M_2 : ethanol

M_3 : acetone

M_4 : ethanol/ethylene glycol (1:1)

M_5 : ethanol/ethylene glycol (7:3)

M_6 : ethanol/ethylene glycol (3:7)

M_7 : ethanol/ethylene glycol/acetone (5:3:2)

M_8 : ethanol/30% aq. ethylene glycol/acetone (5:3:2)

M_9 : ethanol/50% aq. ethylene glycol/acetone (5:3:2)

M_{10} : ethanol/70% aq. ethylene glycol/acetone (5:3:2)

M_{11} : ethanol/70% aq. ethylene glycol/acetone (5:3:1)

M_{12} : ethanol/70% aq. ethylene glycol/ethyl acetate (5:3:3)

Amino acids	Mobile phases (M)											
	M_1	M_2	M_3	M_4	M_5	M_6	M_7	M_8	M_9	M_{10}	M_{11}	M_{12}
Leucine	0.98	0.14	0.01	0.91	0.71	0.92	0.77	0.82	0.82	0.75	0.87	0.87
Isoleucine	0.97	0.21	0.01	0.92	0.72	0.92	0.76	0.81	0.81	0.77	0.85	0.81
Phenyl alanine	0.99	0.26	0.01	0.90	0.74	0.90	0.78	0.81	0.88	0.78	0.88	0.89
Tyrosine	0.97	0.22	0.02	0.92	0.75	0.91	0.80	0.83	0.86	0.77	0.90	0.88
Alanine	0.93	0.14	0.01	0.90	0.54	0.91	0.66	0.67	0.70	0.70	0.77	0.68
Lysine	0.97	0.06	0.01	0.27	0.07	0.31	0.60	0.10	0.08	0.11	0.08	0.07
Proline	0.92	0.10	0.01	0.75	0.47	0.76	0.36	0.45	0.46	0.53	0.58	0.58
Serine	0.94	0.14	0.01	0.88	0.61	0.91	0.59	0.65	0.70	0.71	0.75	0.68
Glutamic acid	0.95	0.17	0.01	0.70	0.68	0.77	0.54	0.47	0.41	0.58	0.64	0.49
Methionine	0.92	0.10	0.01	0.84	0.68	0.89	0.69	0.72	0.75	0.66	0.85	0.81
Arginine	0.92	0.07	0.01	0.24	0.05	0.28	0.09	0.10	0.06	0.05	0.07	0.05
Histidine	0.92	0.11	0.01	0.79	0.40	0.85	0.55	0.64	0.48	0.16	0.66	0.54
Tryptophan	0.99	0.14	0.01	0.83	0.77	0.89	0.63	0.83	0.88	0.78	0.88	0.83

16.5. Polymers and Biochemistry

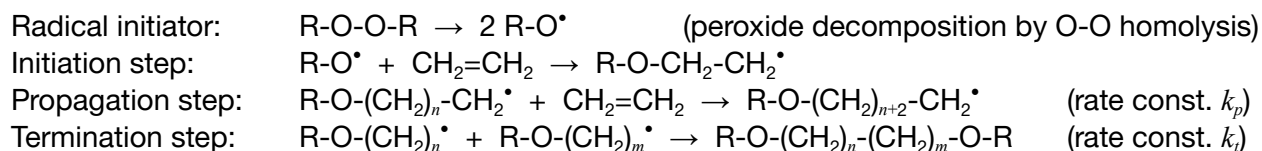
16.5.2. Addition Polymerisation

Addition polymerisation typically proceeds by a free-radical mechanism. The initiator may be a radical (e.g. from homolysis of a peroxide), an ion (superacids / alkyllithium), or an organometallic complex (coordination polymerisation: Ziegler-Natta catalysts).

Free Radical Initiators: produces free radicals used to carry out the initiation step

- Peroxides ($R-O-O-R \rightarrow 2 R-O^{\bullet}$): e.g. hydrogen peroxide (H_2O_2), benzoyl peroxide ($(PhCOO)_2$, BPO)
- Azo compounds ($R-C-N=N-C-R \rightarrow 2 R-C^{\bullet} + N_2$): e.g. α, α' -azobis(isobutyronitrile) (AIBN)
- Redox initiators: e.g. $R-C-OOH + Fe^{2+} \rightarrow R-C-O^{\bullet} + OH^- + Fe^{3+}$
- UV light (photolysis) and/or heat (thermolysis) can also induce radical initiator breakdown.

Free-Radical Polymerisation: using ethene \rightarrow polyethene as an example



Total number of molecules: $N = N_0(1 - p)$ (p : conversion ratio)

Mean degree of polymerisation (mean chain length): $\overline{DP} = \frac{N_0}{N} = \frac{1}{1-p}$

Conditions of Free-Radical Polymerisation Reactions

Polymerisation can be done in bulk (no contamination), in suspension (e.g. water with stabiliser), in solution (e.g. $scCO_2$) or in emulsion (micelles act as microvesicles). Bulk polymerisation results in an increased viscosity with chain growth. Due to decreased Brownian motion, the termination step can become kinetically impeded, leading to rapid reaction rate increase, temperature rise and gelation (autoacceleration; Trommsdorff effect):

$$r_p = k_p [M] \left(\frac{f k_d [I]}{k_t} \right)^{1/2} \quad (M: \text{monomer}, I: \text{initiator}, f: \text{radical formation efficiency of initiator})$$

During the propagation steps, head-to-tail orientation is most common due to steric effects (single repeating unit). Stereochemistry is typically random (atactic) unless temperature is low. Chain transfer reactions, in which the oligomer radical moves, can create branched polymers. Disproportionation or reaction with initiators will produce side product impurities.

Monomers with allylic hydrogens (e.g. propene, isobutene) are unable to undergo free-radical polymerisation due to chain transfer of the allylic H. Polymerisation of dienes can form cyclic repeating units or crosslinks (for thermosets). Conjugated dienes can form 1,2-, *cis*-1,4- or *trans*-1,4- polymers.

16.5.3. Condensation Polymers, Photopolymers and Copolymers

Condensation Polymerisation

Condensation polymerisation involves the joining of different monomers and the elimination of a small molecule (e.g. H₂O, HCl).

Common pairs of functional groups: di(acyl chloride) + dicarboxylic acid → polyester, dicarboxylic acid + diol → polyester, diamine + di(acyl chloride) → polyamide.

Typical reaction: $n \text{HOOC-R}_1\text{-COOH} + n \text{HO-R}_2\text{-OH} \rightarrow [-\text{OOC-R}_1\text{-COO-R}_2-]_n + (2n - 1) \text{H}_2\text{O}$

Photopolymerisation

Photopolymerisation typically proceeds as free-radical addition polymerisation, although the free-radical initiator is generated using ultraviolet radiation ($h\nu$). Photopolymerisation is often autocatalytic, since the resulting polymeric regions of the reacting mixture have higher refractive index, which in turn guides more light into the region, amplifying the rate of polymerisation in those regions.

Stereolithography (vat photopolymerisation; 3D inkjet printing) uses lasers of UV radiation to cure sections of a liquid photosensitive monomer-oligomer mixture (SLA resin) into the solid polymer state. It can also be used to induce cross-linking of reactive side groups or terminal groups.

Copolymerisation

The use of multiple monomers to generate a polymer with variation in the chain structure (a copolymer, as opposed to a homopolymer). In a block copolymer, monomer types are the same for large sections of the polymer, but alternate. Copolymers may also be branched (graft polymers, dendrimers).

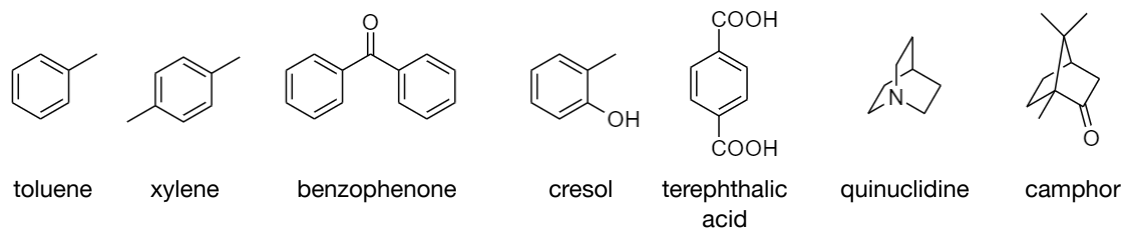
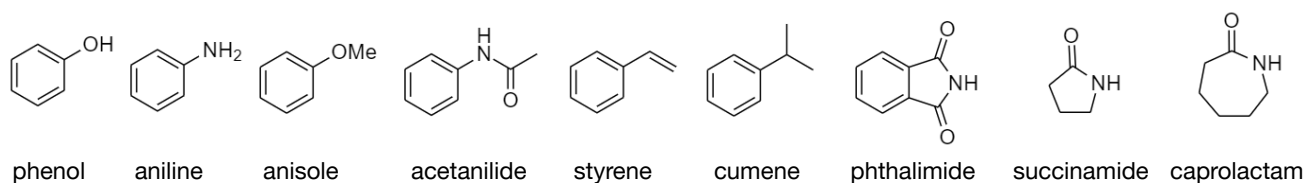
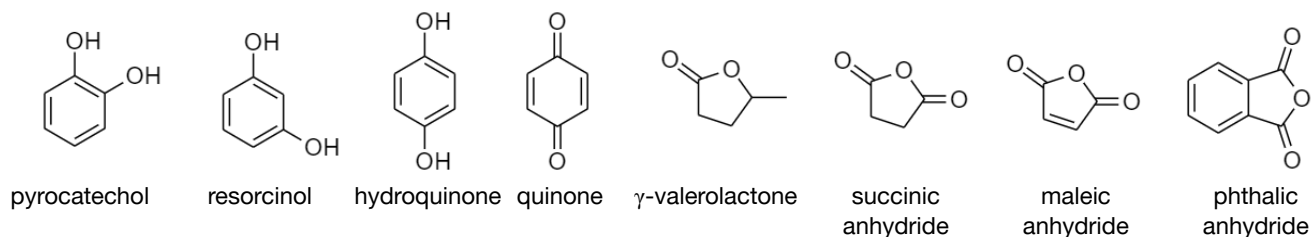
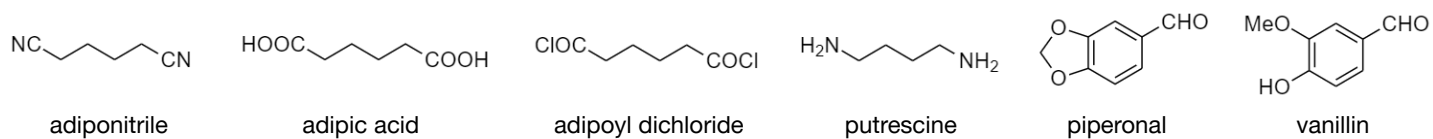
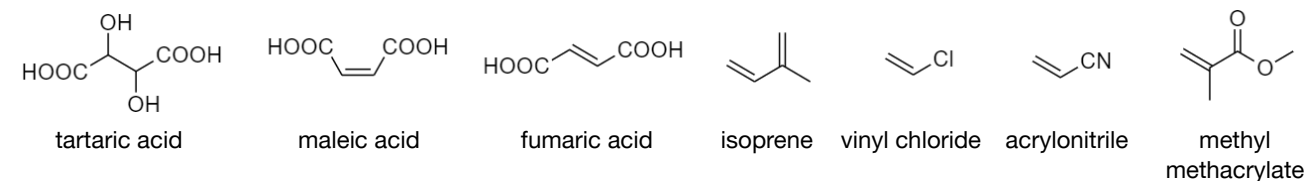
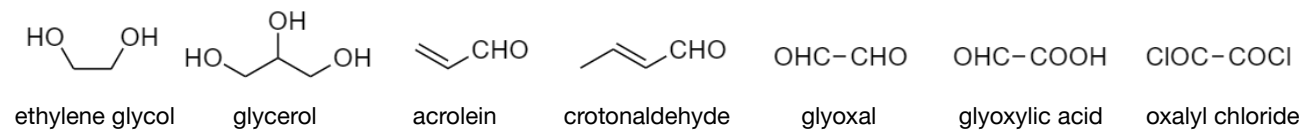
Synthetic Biopolymers

Bacteria can be gene-edited to secrete useful polymers (bioplastics) e.g. polyhydroxybutyrate (PHB) and polydiketoenamine (PDK), or to synthesise enzymes that can synthesise the monomers for a new polymer. These polymers are also typically biodegradable and highly recyclable, although their mechanical properties are typically less optimal than those derived from traditional methods.

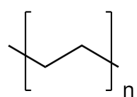
Enzymes have also been found to degrade synthetic plastics into monomers (e.g. PETase into ethylene glycol and terephthalic acid). These enzymes are often mutations of e.g. cutin hydrolases, where the active site is enlarged to permit hydrolysis of bulky condensation polymers. The metabolites can be used to make new materials (upcycled plastics) or degraded further into useful chemicals. Some bacteria can also break down per-/polyfluoroalkyl substances (PFAS, 'forever chemicals').

16.5.4. Common Names of Synthetic Precursors and Reagents

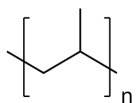
Small molecule alcohols, aldehydes and carboxylic acids:



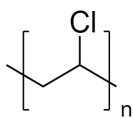
16.5.5. Structures of Some Common Polymers



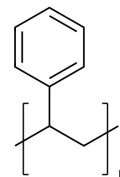
polyethylene (PE)



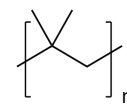
polypropylene (PP)



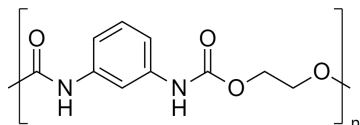
polyvinyl chloride (PVC)



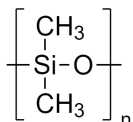
polystyrene (PS)



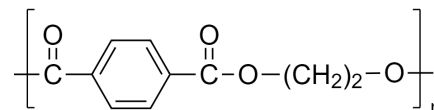
polyisobutylene



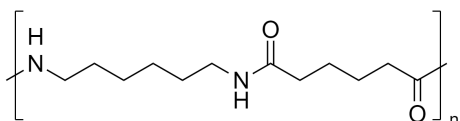
polyurethane



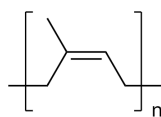
silicone



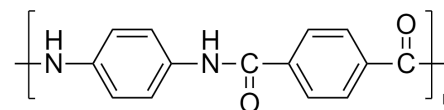
polyethylene terephthalate (PET) / terylene / dacron



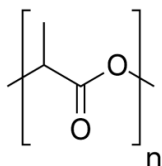
Nylon 6,6



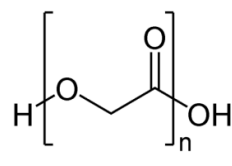
natural rubber (polyisoprene)



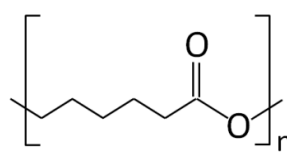
kevlar



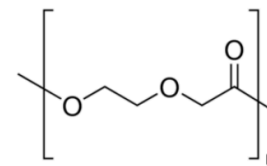
poly(lactic acid) (PLA)



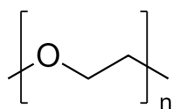
poly(glycolic acid) (PGA)



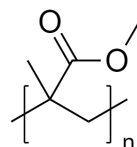
polycaprolactone (PCL)



poly trimethyl carbonate (PTMC)



poly(ethylene glycol) (PEG)



poly(methyl methacrylate) (PMMA)

16.5.6. Sugars and Carbohydrates

Monosaccharides: consists of one sugar unit (no glycosidic bonds: cannot be hydrolysed).

Sugars based on open-chain group (C_n epi- means the epimer (opposite stereochemistry) at carbon n)

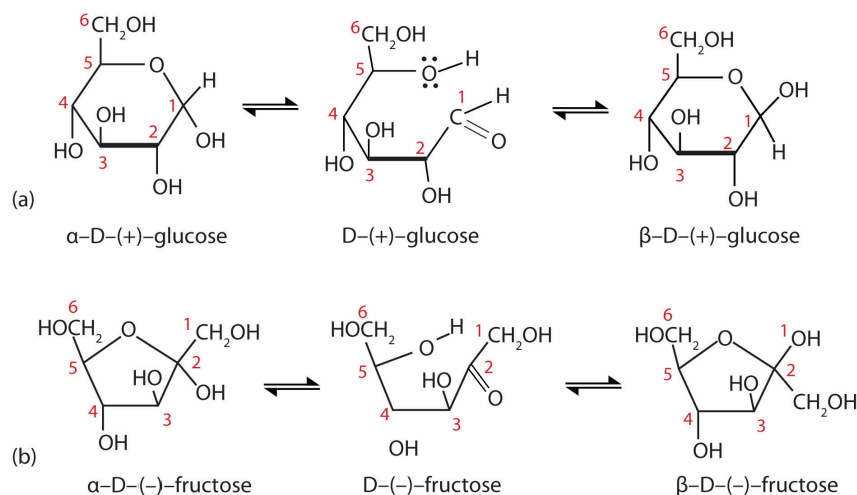
- Trioses (3 C): glyceraldehyde, dihydroxyacetone
- Tetroses (4 C): threose (Thr), erythrose (C_2 epi-Thr)
- Aldopentoses (5 C): ribose (Rib), arabinose (C_2 epi-Rib), xylose (C_3 epi-Rib), lyxose (C_2 epi-Xyl)
- Ketopentoses (5 C): ribulose (Rbu), xylulose (C_3 epi-Rbu)
- Aldohexose (6 C): glucose (Glu), mannose (C_2 epi-Glu), allose (C_3 epi-Glu), galactose (C_4 epi-Glu)
- Ketohexose (6 C): fructose (Fru), psicose (C_3 epi-Fru), sorbose (C_5 epi-Fru)

Monosaccharides exist in two different crystalline forms, α and β (anomers), which differ in stereochemistry at C_1 (the anomeric carbon). There is an equilibrium between the cyclic hemiacetal/hemiketal forms with the open-chain forms, with the ring typically being predominant.

The D and L convention refers to chemical similarity with glyceraldehyde, while the + and - convention shows the direction of specific optical rotation. These may differ from each other, as well as from the standard *R* and *S* convention.

Deoxy sugars have carbon atoms with no hydroxyl groups e.g. 2-deoxyribose (Section 16.5.9).

Macrolides are biomolecules composed of a ~15-membered lactone ring with deoxy sugars bonded to it by glycosidic bonds, and are used as bacteriostatic antibiotics.



Monosaccharides undergo various reactions due to their aldehyde/ketone and alcohol groups:

- Oxidation with e.g. Tollens' reagent, Fehling's solution (forms brick-red ppt), Br_2 (aq) ($CHO \rightarrow COOH$) or conc. HNO_3 ($-CH_2OH$ and $-CHO \rightarrow 2 -COOH$)
- Reduction with e.g. HI ($-CHO \rightarrow -CH_3$, $-OH \rightarrow -H$) or $Na(Hg) + H_2O$ ($-CHO \rightarrow -CHOH$)
- Sugar oxime formation with NH_2OH (hydroxylamine) or sugar cyanohydrin formation with HCN
- Acetylation with e.g. CH_3COCl ($-COH \rightarrow -OOCCH_3$)
- Osazone formation with e.g. $PhNHNH_2$ (phenylhydrazine) ($CHO, 1^\circ -COH \rightarrow -C=NNHPh$)

Oligosaccharides

Oligosaccharides can be disaccharides (2 sugars), oligosaccharides (3-10 sugars). Monosaccharides can form oligosaccharides by condensation reactions at C1 and C4 (forming glycosidic C-O-C bonds). They can be acid-hydrolysed to the constituent monosaccharides by boiling in acidified alcoholic solution.

- **Sucrose:** α -glucose + β -fructose with (Glu C1 - Fru C4)
- **Maltose:** α -glucose + α -glucose with (Glu C1 - Glu C4)
- **Lactose:** β -galactose + β -glucose with (Gal C1 - Glu C4)
- **Raffinose:** α -galactose + α -glucose + α -fructose (Gal C1 - Glu C6; Glu C1 - Fru C4)

Polysaccharides (glycans)

Polysaccharides are longer and are not considered sugars (they are not sweet in taste).

Particular polysaccharides and derivatives:

- **Starch:** polymer of α -glucose with 1,4 links (**amylose**) and 1,6 crosslinks (**amylopectin**)
- **Cellulose:** polymer of β -glucose with 1,4 links
- **Xanthan gum:** cellulose with C3-substituted trisaccharide of β -glucose derivatives
- **Glycogen:** same as starch with more crosslinks (like amylopectin, with even more branching)
- **Dietary Fibre:** carbohydrates which cannot be absorbed or metabolised in the body
- **Glycosaminoglycans:** repeating disaccharides with carboxylic acid/sulfate/ether/amine/amide/phosphate at the C2, C4 and/or C5 positions. Examples: heparin, chondroitin, keratan (sulfates), hyaluronic acid.
- **Lipopolysaccharides:** glycans substituted with fatty acids ('lipid A') and O-linked oligosaccharides (antigen).

These derivative polysaccharides are often important components of biological cell walls/organelle membranes and can form complex structures in solution (Section 16.5.7, Section 17.2.1.)

Iodine starch test: stain with iodine. In the presence of starch, it will turn dark blue/black, due to the complexing of I_3^- (triiodide) in amylose helices.

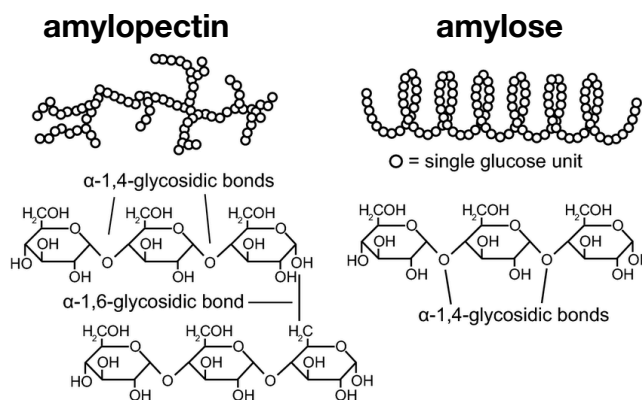
Reducing and Non-Reducing Sugars

All reducing sugars undergo mutarotation (anomers interconvert to an equilibrium mixture) in aqueous solution (but not in the solid state) due to formation of the open-chain structure.

- All monosaccharides are reducing.
- Free reducing groups (aldehyde, α -hydroxyketone or hemiacetals) also indicate reducing sugars.
- If reducing groups are bonded, then the resulting disaccharide is non-reducing.

Tests for reducing sugars: Tollens' / Fehling's / Benedict's reagents (Section 15.4.3).

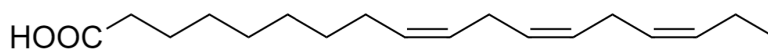
Test for any carbohydrate: Molisch's test (add 1-naphthol, H_2SO_4 : purple ring forms at interface)



16.5.7. Lipids (Fats and Oils)

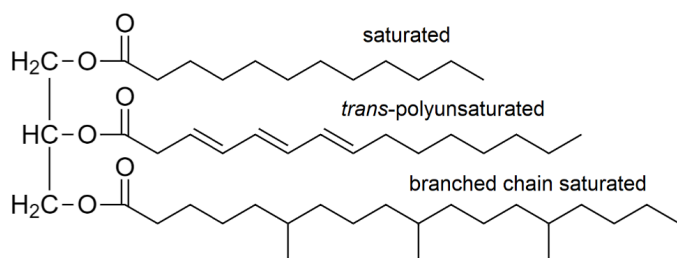
Lipids are typically amphiphilic long-chain molecules. Fats are solid lipids, oils are liquid lipids, at room temperature. The chain of a lipid may be saturated (C-C bonds only) or unsaturated (has C=C bonds: mono = 1, poly = more); which in turn may be *cis* or *trans*.

Fatty acids: a single hydrophilic -COOH head with an alkyl tail.

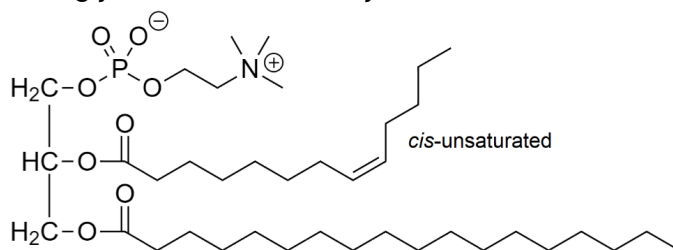


- Omega-3 fatty acid: a polyunsaturated *cis*-fat with a C₃=C₄ bond (counting from the end), with various beneficial health effects including supporting growth of the brain.

Triglycerides and Phospholipids: the ester product of glycerol with three fatty acids.



Triglyceride

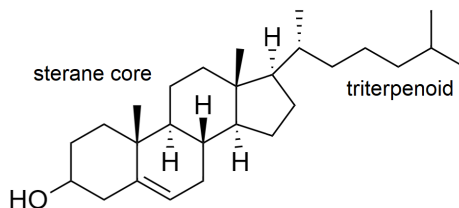


Phospholipid

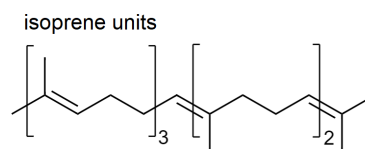
- Saponification: base hydrolysis of triglycerides to fatty carboxylate salts and glycerol. Fatty carboxylate salts form micelles in solution and can be used as anionic surfactants.
- Transesterification with methanol produces methyl esters (biodiesel) and glycerol.
- Monounsaturated fat: a chain with only one C=C bond.
- Partial hydrogenation of vegetable oils can convert *cis* bonds to *trans*, producing *trans*-fats.
- *Trans*-fats are harder to break down due to denser intermolecular packing, as well as promoting accumulation of low-density lipoprotein (LDL, 'bad') cholesterol in the body.
- Phospholipid: one chain is replaced by a substituted phosphate. Can form micelles in water and inverse micelles in organic solvent, and together can form phospholipid bilayers and/or liposomes.

Other Types of Lipids:

- Steroids, sterols and steranes: four fused rings with alkyl side chains, e.g. cholesterol, gonane.
- Triterpenoids: hydrocarbons of repeating isoprene units e.g. squalene, squalane.
- Sphingolipids: long-chain aliphatic amino alcohols. e.g. sphingosine, sphingomyelin, ceramide.



Cholesterol: a triterpenoid steroid.



Squalene: a triterpenoid hydrocarbon oil.

For the carbon numbering convention of the polycyclic steroid system, see Section 16.2.5.

16.5.8. Proteins

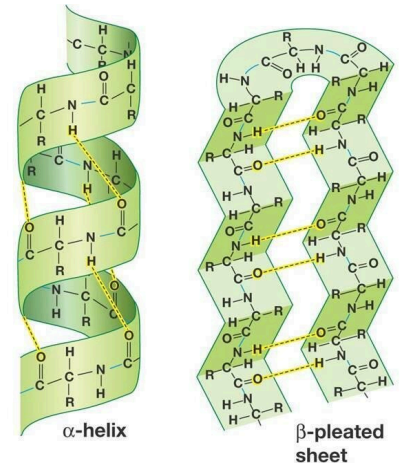
Proteins are linear sequences of amino acid residues, linked by peptide (-CONH-) bonds. Smaller units may be dipeptides (two linked amino acids), oligopeptides (less than ~10 linked amino acids) or polypeptides (a larger chain, ~100 linked amino acids). Amino acids may also form cyclic oligopeptides which is a common motif for antibiotics.

Primary Structure: the amino acid sequence comprising the protein.

- The C-terminus (end with the -COOH group) corresponds to the 5' end of RNA.
- The N-terminus (end with the -NH₂ group) corresponds to the 3' end of RNA.
- In biology, proteins are formed by translation of RNA from 5' to 3'.
- The peptide bonds are planar, delocalised and resist hydrolysis at pH 7 / 25 °C ($k \sim 10^{-10} \text{ s}^{-1}$)

Secondary Structure: the localised structures which arise due to interactions (typically hydrogen bonds) between the backbones of amino acid residues.

- **α -helix:** a right-handed spiral formed due to backbone coaxial C=O...H-N bonds.
- **β -pleated sheet:** a folded sheet formed due to backbone transverse C=O...H-N bonds.
- **Turns:** β -turns, γ -turns and β -hairpins.



Tertiary Structure: the wider-range structures which arise due to interactions between the side chains of primarily-distant amino acid residues which determine the folding pattern.

- **Disulfide bridge:** a covalent -S-S- bond formed due to oxidative folding of cysteine. These may also form when thiol side groups (in antioxidants e.g. glutathione) neutralise reactive oxygen species (ROS: e.g. peroxides) and free radicals in the body. Releases H₂.
- Ionic bonds / Salt bridge: ionic attractions between formally charged side chains.
- Lactam bridge (synthetic only): intramolecular amide bond formation between adjacent residues containing -COOH and -NH₂ side chains. Can stabilise α -helices.

Quaternary Structure: the assembled form of a protein in its biophysiological environment.

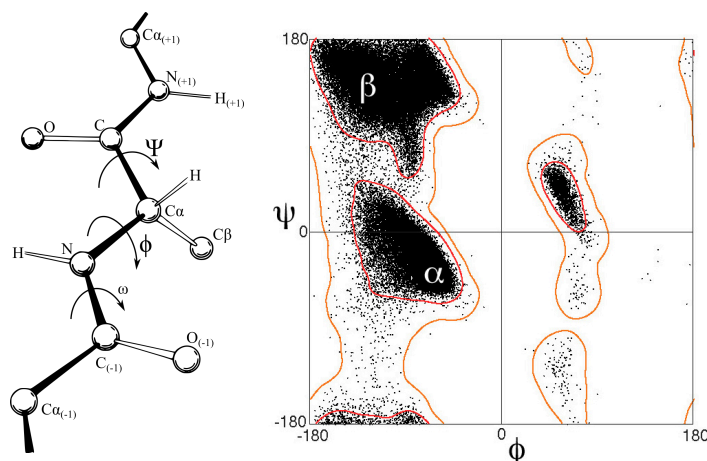
- Complexes: interactions with cofactors such as nucleic acids and prosthetic groups.
- Oligomers: interactions with protein chains on a different protein subunit.

Protein shape: proteins may be globular (round) or fibrous (elongated). Only globular proteins have functional (enzymatic) roles, while fibrous proteins are typically structural (e.g. keratin, collagen for connective tissue and actin, myosin for muscle fibres).

Anfinsen's dogma: the hypothesis/postulate that the tertiary structure of small polypeptides depends only on the primary structure, independent of environment conditions. In general, proteins have several free energy minima across a range of conformational folding patterns, but the equilibrium conformation is the unique lowest energy thermodynamically stable form. Exceptions include the 'intrinsically disordered proteins' and 'circadian oscillator proteins'.

Ramachandran plot: shows the energetically feasible regions of folding conformations (in terms of the amino acid backbone dihedral torsional angles (ψ , ϕ) due to steric effects. Angle ω is always 180° due to the planarity of the amide bond. Analysis of 3D protein structure yields a kernel density plot in (ψ , ϕ) space.

The dihedral angles of amino acid residues in right-handed α -helices (α) and beta-sheets (β) occupy different regions in the Ramachandran plot. Left-handed α -helices occupy the island region with $\phi > 0$.



Protein water solubility: when in water, hydrophobic residues tend to be found closer to the centre of the protein, while polar and/or charged residues are found interacting with water on the surface. The presence of salt ions in the water influences the stability (solubility) of the secondary and tertiary structures of the protein according to the Hofmeister series (lyotropic series). From **promoting salting out (decreases solubility, strengthens solute-solute interactions)** to **promoting salting in (increases solubility, weakens solute-solute interactions)**:

Salt anions:

$\text{Cit}^{3-} > \text{PO}_4^{3-} > \text{SO}_4^{2-} > \text{Tar}^{2-} > \text{HPO}_4^{2-} > \text{CrO}_4^{2-} > \text{Ac}^- > \text{OH}^- > \text{HCO}_3^- > \text{F}^- > \text{Cl}^- > \text{Br}^- > \text{NO}_3^- > \text{I}^- > \text{SCN}^- > \text{ClO}_4^- > \text{ClO}_3^-$

Salt cations:

$\text{Al}^{3+} > \text{Mg}^{2+} > \text{Ca}^{2+} > \text{Ba}^{2+} > \text{Li}^+ > \text{Na}^+ > \text{K}^+ > \text{NH}_4^+ > \text{Rb}^+ > \text{Cs}^+ > \text{Gua}^+$

(Cit: citrate, Tar: tartrate, Ac: acetate, Gua: guanidium)

The effect of the anion typically dominates over the effect of the cation, if they compete.

It is generally observed that **kosmotropic ions (promote ordering of the water structure)** and **chaotropic ions (promote disordering of the water structure)** correlate with **salting out** and **salting in** respectively, but the predictive power and underlying mechanistic validity of making this connection is uncertain. 'Hydrotropic ions' can solubilise proteins even more than chaotropic ions, and using surfactants more still, by unfolding (destabilising, and often denaturing) the protein to break up aggregate particles and form a stabilised colloid (Section 14.3.9). At high protein content, the solution may form a hydrogel (Section 16.5.11).

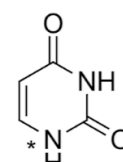
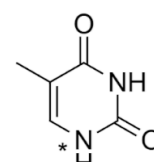
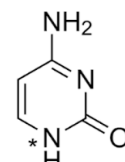
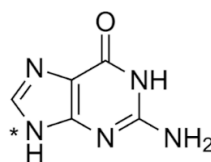
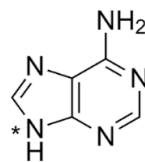
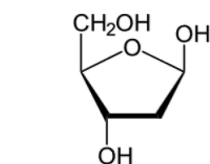
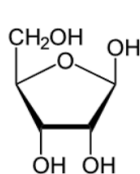
Glycoconjugation of Proteins (Glycosylation): addition of polysaccharide chains to proteins

Glycoproteins are made of proteins and carbohydrates, in which amino acid side chains form either glycosidic bonds (O-linkage, e.g. from Ser, Thr, Tyr) or peptide bonds (N-linkage, e.g. from Asn, Arg) with the C1 position on a sugar (forming an oligosaccharide / polysaccharide side chain). The glycan chains are typically relatively short and branched.

Proteoglycans are made of proteins and glycosaminoglycans (GAGs: Section 16.5.7, 16.5.9), again using either glycosidic (O-linkage) or amide bonds (N-linkage) to attach them to the protein structure. Enzymes can also substitute -OH groups for -OSO₃H (sulfate, by sulfonation) on the GAG chain. There are typically multiple GAG chains per protein, and they are long and linear.

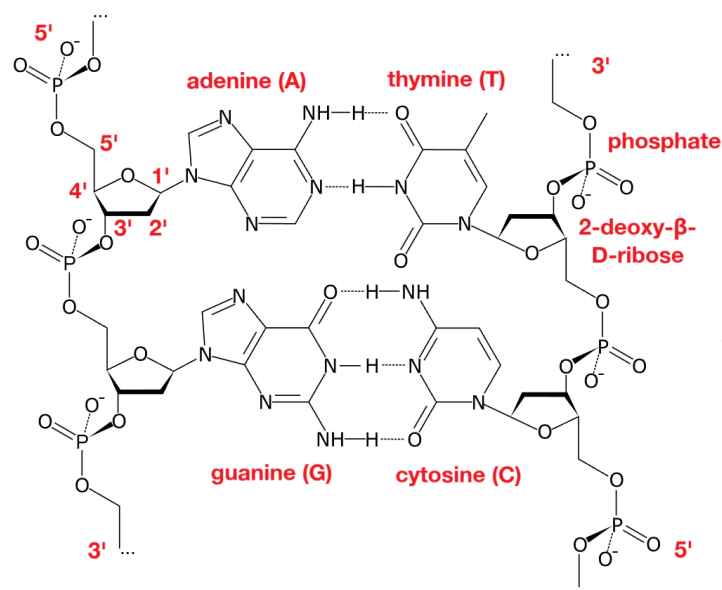
Biuret test for proteins: add alkaline CuSO₄ → turns **violet** due to Cu²⁺-CONH complexing.

16.5.9. Nucleobases, Nucleotides, DNA and RNA

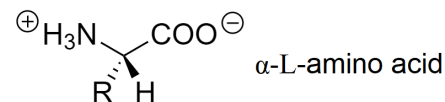


β -D-ribose β -D-2-deoxyribose adenine (A) guanine (G) cytosine (C) thymine (T) uracil (U)
(furanose sugars, Haworth projection) (purine nucleobases) (pyrimidine nucleobases)

- In DNA (shown right) and RNA, nucleobases are bound to sugars by a bond at the anomeric carbon, in which the 1-hydroxyl group (on the sugar) and the amino group (shown above with the starred *N) condense to lose H₂O.
- Sugars are bound to phosphate groups at the 3'- and 5'-hydroxyl groups, forming condensation polymers.
- A single nucleotide consists of a phosphate, pentose sugar, and a nucleobase. A nucleoside is a sugar and nucleobase.
- In life, the negative charges due to the phosphate groups are balanced by counterions (e.g. Mg²⁺) in transport and by protonated amino groups in lysine side chains on histone proteins in chromosomes (Section 17.2.2).
- DNA is a right-handed double helix of paired nucleotides. β -D-2-deoxyribose is the sugar. Complementary base pairings are A-T (2 H-bonds) and G-C (3 H-bonds).
- RNA is a right-handed single helix of nucleotides. β -D-ribose is the sugar. Base conversions in the transcription of DNA to RNA are A \rightarrow U, T \rightarrow A, G \rightarrow C, C \rightarrow G.



16.5.10. Amino Acids: Structures and Biochemical Data



Amino Acid (A-Z)			Side group, R	M_r	RNA codons	pK_a	pK_b	pK_x	pI
Alanine	Ala	A	-Me	89.1	GCX	2.34	9.69	-	6.00
Asparagine	Asn	N	-CH ₂ CONH ₂	132.12	AAU, AAC	2.02	8.80	-	5.41
Aspartic acid	Asp	D	-CH ₂ COO ⁻	133.11	GAU, GAC	1.88	9.60	3.65	2.77
Cysteine	Cys	C	-CH ₂ SH	121.16	UGU, UGC	1.96	10.28	8.18	5.07
Glutamic acid	Glu	E	-CH ₂ CH ₂ COO ⁻	147.13	GAA, GAG	2.19	9.67	4.25	3.22
Glutamine	Gln	Q	-CH ₂ CH ₂ CONH ₂	146.15	CAA, CAG	2.17	9.13	-	5.65
Glycine	Gly	G	-H	75.07	GGX	2.34	9.60	-	5.97
Isoleucine	Ile	I	-CH(Me)CH ₂ Me	131.18	AUU, AUC, AUA	2.36	9.60	-	6.02
Leucine	Leu	L	-CH ₂ CH(Me) ₂	131.18	UUA, UUG, CUX	2.36	9.60	-	5.98
Lysine	Lys	K	-CH ₂ CH ₂ CH ₂ CH ₂ NH ₃ ⁺	146.19	AAA, AAG	2.18	8.95	10.53	9.74
Methionine	Met	M	-CH ₂ CH ₂ SMe	149.21	AUG	2.28	9.21	-	5.74
Serine	Ser	S	-CH ₂ OH	105.09	UCX, AGU, AGC	2.21	9.15	-	5.68
Threonine	Thr	T	-CH(Me)OH	119.12	ACX	2.09	9.10	-	5.60
Valine	Val	V	-CH(Me) ₂	117.15	UAC	2.32	9.62	-	5.96
Arginine	Arg	R	-CH ₂ CH ₂ CH ₂ NH-C(=NH ₂)NH ₂ ⁺	174.2	AGA, AGG, CGX	2.17	9.04	12.48	10.76
Histidine	His	H		155.16	CAU, CAC	1.82	9.17	6.00	7.59
Phenylalanine	Phe	F		165.19	UUU, UUC	1.83	9.13	-	5.48
Proline	Pro	P		115.13	CCX	1.99	10.6	-	6.30
Tryptophan	Trp	W		204.23	UGG	2.83	9.39	-	5.89
Tyrosine	Tyr	Y		181.19	UAU	2.20	9.11	10.07	5.66

Red: positively charged; **Blue:** negatively charged; **Orange:** uncharged polar; **Black:** hydrophobic non-polar; Essential amino acid; Aromatic side group.

- M_r values are given in the neutral (zwitterionic) state, in g mol⁻¹.
- In the RNA codon table, 'X' represents **any** of A, U, G or C.
- At low pH, -COO⁻ is protonated, giving net +ve charge. At high pH, -NH₃⁺ is deprotonated, giving net -ve charge.
- pK_a and pK_b are dissociation constants for the main -COOH and -NH₂ groups respectively.
- pK_x is the dissociation constant for any ionisable side groups (-OH, -SH, -COOH, -NH, -NH₂).
- pI is the isoelectric point, given by $pI \approx (pK_a + pK_b) / 2$ (assumes equal acid and base strengths).
- Selenocysteine (R = -CH₂SeH) and pyrrolysine are special amino acids sometimes incorporated at stop codons.

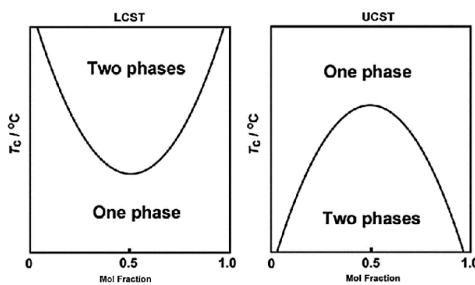
16.5.11. Polyelectrolytes and Hydrogels

Polyelectrolyte: a polymer in which the polymer chains contain formally charged groups, with counterions present in the interstitial medium. Most biopolymers (e.g. proteins, glycosaminoglycans, DNA & RNA) are polyelectrolytes.

- Polyanions ($-\text{COO}^-$, $-\text{SO}_3^-$, $-\text{OSO}_3^-$, $-\text{CSS}^-$, $-\text{OPO}_3^{2-}$): anions on the polymer chain.
- Polycations ($-\text{NH}_3^+$, $=\text{NH}_2^+$, $-\text{NR}_3^+$, $-\text{PR}_3^+$): cations on the polymer chain.
- Polyampholytes: the polymer chain is zwitterionic (both anionic and cationic).

If the number of charged groups is low, there may be microphase separation in which hydrophobic sections of the polymer cluster between regions of high charge density.

Responsive materials: polyelectrolytes conformation is sensitive to the environment.



Temperature changes: induces a phase change between the sol (two-phase, liquid) and gel (one-phase, solid, cross-linked).

Lower critical solution temperature hydrogels (LCST) and upper critical solution temperature hydrogels (UCST) have different phase diagrams in water (shown left), with the type depending on the hydrophobicity/hydrophilicity.

pH changes: presence of H^+ or OH^- can neutralise chain groups and cause aggregation.

- **Anionic** hydrogels swell in basic conditions ($\text{pH} > \text{pK}_b$)
- **Cationic** hydrogels swell in acidic conditions ($\text{pH} < \text{pK}_a$)

Light intensity changes: may induce conformational change e.g. azo compound *trans* \rightarrow *cis*, acting like a switch. Use of light can also induce cross linking (in e.g. methacrylates with an initiator), solidifying the gel state into a more rigid structure.

Hydrogels: a solid network of hydrophilic crosslinked polymer chains in water. Hydrogels applied in technology (e.g. bioinks for 3D printing, Section 17.4.17) are often derived from biopolymers. Hydrogels swell in water but do not dissolve. Hydrocolloids do dissolve and form a gel, independent of temperature. Some polymers commonly used in hydrogels are: (UCST, LCST, variable, anionic, cationic, nonionic)

- **Natural:** agarose, alginate, chitosan, gelatin, collagen, hyaluronan, fibrin, matrigel
- **Synthetic:** PEG diacrylate (PEGDA), modified cellulose, methacrylated gelatin (GelMA), pluronic F127

Protein-based hydrogels (e.g. gelatin) can be made mechanically stiffer by addition of kosmotropic anions (e.g. citrate) (Section 16.5.8) during gel formation, due to promoted protein agglomeration.

By combining responsive hydrogels with functional materials (e.g. MoS_2 monolayers, Section 8.6.6), mechanical responses (actuation) can be induced from a variety of stimuli (e.g. light, pH, heat).

~ LN, 2024